Glutamate receptors in the spinal cord with emphasis on the dorsal horn

by

Gergely György Nagy, M.D.

A thesis presented for the degree of Doctor of Philosophy
in the Faculty of Biomedical and Life Sciences,
Division of Neuroscience & Biomedical Systems,
University of Glasgow

July 2004

IBLS, Spinal Cord Group
University of Glasgow

SUMMARY

Glutamate is the principal excitatory neurotransmitter throughout the CNS, including the spinal cord. It acts on ionotropic (iGluR) and metabotropic glutamate receptors. Three iGluR families have been identified by the development of more-or-less selective agonists: N-methyl-D-aspartate (NMDA), alpha-amino-3-hydroxy-5-methyl-4-isoxazole propionic acid (AMPA) and kainate receptors. Both AMPA (GluR1-4) and NMDA (NR1, NR2A-D) receptors have been detected in the spinal cord and these play a major role in physiological processes such as fast excitatory transmission, synaptic plasticity and neuronal development. In addition, they have also been implicated in pathological conditions including neuropathic pain and neurodegenerative disorders. However, very little is known about the synaptic distribution of these receptors in the spinal gray matter. This is because conventional immunocytochemical techniques, generally used to investigate the location of proteins in the CNS, fail to detect these subunits at synapses due to the presence of an elaborate protein meshwork associated with the postsynaptic membrane, which masks synaptic receptors. Postembedding immunocytochemistry on freeze-substituted, Lowicryl-embedded material is a technique which has been used exclusively for the detection of synaptic AMPA and NMDA receptors. This project initially set out to use this method to examine these receptors on neurons of the adult rat spinal cord, with emphasis on their involvement in the sensory processing of the dorsal horn.

With antibodies against the GluR1, GluR2/3, NR1, NR2A and NR2B subunits, heavy labelling was observed at many asymmetrical synapses and where the plane of section was perpendicular to the cleft, most of the immunogold particles were associated with the postsynaptic density. To examine the receptor expression pattern of selected cell populations a new method was developed which involved the combination of postembedding electron microscopy with immunofluorescence and confocal microscopy. However, during the course of this study heavy immunogold labelling of dense-cored vesicles (dcvs) inside axonal boutons was observed with all NMDA antibodies. Several studies have found iGluRs in primary afferent terminals in the spinal gray matter and these are thought to function as presynaptic receptor. In order to determine whether gold particles found over dcvs corresponded to presynaptic receptors in transit, immunogold reactions were carried out on transgenic mice which lacked the NR2A subunit. Surprisingly, not only did the dcv labelling remain in these knock-out animals, but there was also a significant synaptic labelling. This suggested that the postembedding

immunogold labelling observed with the NR2A antibody was non-specific. Since the labelling patterns were similar with other NMDA antibodies this cast doubts on the validity of the postembedding method for detecting NMDA receptors.

In a search for alternative techniques for the detection of synaptic receptors, an antigen unmasking method, initially developed by Watanabe et al. (1998), was adopted and used to reveal both AMPA and NMDA receptors. This involved subjecting the spinal cord sections to limited proteolytic digestion with pepsin. Following pepsin treatment punctate immunostaining was observed with antibodies against various iGluRs.

Of the four AMPA subunits examined, GluR1 showed the most restricted distribution, with immunoreactive puncta being very frequent in lamina II, and present at lower density in other dorsal horn laminae. In the ventral horn puncta immunostained for GluR1 were rarely seen. A large number of GluR2-immunoreactive puncta were present throughout the grey matter, with the strongest labelling in laminae I and II. The staining pattern for GluR3 was similar to that for GluR4. In both cases immunoreactive puncta were densely distributed throughout the ventral horn and the deeper regions of the dorsal horn, with much weaker labelling in laminae I and II. It was confirmed that the puncta seen after antigen unmasking corresponded to receptors at synapses, since a great majority of them were apposed to various types of glutamatergic axon and with electron microscopy on pepsin-treated sections the reaction product was associated with the postsynaptic aspect of synapses. Colocalization studies showed that GluR2 was present at virtually all AMPA-containing synapses in all laminae examined. Another major finding was that GluR1 was preferentially associated with primary afferent terminals.

Functional studies were also carried out to determine whether morphologically detectable changes involving synaptic AMPA receptors occurred in response to peripheral noxious stimulation. Following intradermal capsaicin injection a rapid phosphorylation of synaptic GluR1 subunits at the Ser845 site was detected and this is apparently the first immunocytochemical demonstration of plastic changes at glutamatergic synapses *in vivo*.

The distribution of NMDA receptors on pepsin treated sections was investigated using antibodies against NR1, NR2A and NR2B subunits. NR1-immunoreactive puncta were widespread in all laminae, while NR2A and NR2B showed a differential distribution. NR2A was expressed at highest levels in lamina III and at much lower levels elsewhere, with the immunostaining being weakest in lamina IIo. NR2B was present at high levels in laminae I-II, and gradually decreased towards the ventral horn. The synaptic expression of all NMDA subunits examined was weaker in the ventral horn than in the dorsal horn. A majority of NMDA-immunoreactive puncta were also labelled for GluR2 suggesting that

these represented receptors at glutamatergic synapses. In addition, the NR2A immunostaining completely disappeared in the NR2A knock-out mice. In the dorsal horn approximately half and one-third of GluR2-immunoreactive puncta were immunoreactive for NR1 and NR2A or NR2B, respectively. This indicates that NMDA receptors are selectively expressed by a subset of neurons or selectively targeted to certain synapses.

In summary, the results of the present study indicate that antigen unmasking is suitable for detecting synaptic AMPA and NMDA receptors. The differential distribution of certain iGluR subunits stress the need for further studies to determine which subunits are associated with particular neuronal populations in the spinal cord. In addition, the finding that phosphorylation of GluR1 subunits at glutamatergic synapses *in vivo* can be revealed by immunocytochemistry provides a novel approach for investigating central sensitization and other forms of synaptic plasticity in specific neuronal circuits throughout the CNS.

ACKNOWLEDGEMENTS

I should like express my gratitude to my supervisor Prof. Andrew Todd for his continuous support, help and encouragement during my studies. His optimism, enthusiasm, experience and positive personality created an inspiring atmosphere and ensured that I greatly enjoyed doing research in his laboratory. In addition, his constructive criticism and useful suggestions were invaluable during the writing up of my results. I could not have wished for a better supervisor. I also appreciate the help I have received from my co-supervisor, Prof. David Maxwell. It was not only a pleasure, but also an honour to work in their group.

I would like to thank particularly to Christine Watt and also to Robert Kerr and Margaret McGill for their excellent technical help and assistance. I am also grateful to Dr. David Andrew for his help with the statistics, to Dr. David Hughes and Dr. Robert Hartley for their helpful advice regarding the preparation of the thesis and to Dr. Erika Polgár for her support before and during my studies.

Prof. Masahiko Watanabe and Dr. Masahiro Fukaya from Hokkaido University, Japan were very kind to give expert advise on antigen unmasking and generously provided the NR2A knock-out animals and various iGluR antibodies, while Prof. Ole Petter Ottersen from University of Oslo, Norway made it possible for me to visit his laboratory and learn postembedding immunocytochemistry.

Last, but not least I would like to thank to my father and mother for backing my decision to come to Glasgow and for providing moral support and encouragement throughout my studies.

DECLARATION

I declare that the work presented in this thesis is my own (except where otherwise stated) and it has not been submitted previously for any higher degree.

LIST OF ABBREVIATIONS

ALS	amyotrophic lateral sclerosis
AMPA	α-amino-3-hydroxy-5-methyl-4-isoxazole propionic acid
ATPA	(RS)-s-amino-3(3-hydroxy-5-tert-butylisoxazol-4yl)propanoic acid
BNPI	brain specific sodium-dependent inorganic phosphate transporter
CCD	charge coupled device
CGRP	calcitonin gene-related peptide
ChAT	choline acetyltransferase
CNS	central nervous system
CTb	cholera toxin B
Cy5	cyanine 5-18
DRG	dorsal root ganglia
EM	electron microscope or electron microscopy
ENK	enkephalin
EPSC	excitatory postsynaptic current
EPSP	excitatory postsynaptic potential
ER	endoplasmic reticulum
FITC	fluorescein isothiocyanate
GABA	γ-aminobutyric acid
GKAP	guanylate kinase-associated protein
GluR1-pS845	GluR1 phosphorylated at the serine^{845} residue
HSA	human serum albumin
IB4	*Bandeiraea simplicifolia* isolectin B4
iGluR	ionotropic glutamate receptor
KA	kainate
LTD	long term depression
LTP	long term potentiation
mGluR	metabotropic glutamate receptor
NeuN	neuron-specific nuclear protein
NK1	neurokinin 1
NMDA	N-methyl-D-aspartate
NOS	nitric oxide synthase
NPY	neuropeptide Y

NT	neurotensin
PA	parvalbumin
PAD	primary afferent depolarization
PB	phosphate-buffer
PBS	phosphate-buffered saline
PBST	phosphate-buffered saline with Triton
PCR	polymerase chain reaction
PI	propidium iodide
PKA	protein kinase A
PKC	protein kinase C
PLC	phospholipase C
PSD	postsynaptic density
RR	Rhodamine Red-X
RT-PCR	reverse transcriptase polymerase chain reaction
SNI	spared nerve injury
SOM	somatostatin
SP	substance P
TBST	Tris-buffered saline with Triton
TSA	tyramide signal amplification
VGLUT	vesicular glutamate transporter
VIP	vasoactive intestinal polypeptide

TABLE OF CONTENTS

FIGURES AND TABLES

Chapter 1

General introduction and aims: Glutamate and its receptors in the spinal cord with emphasis on the dorsal horn

GENERAL INTRODUCTION

Glutamate is the main excitatory neurotransmitter throughout the central nervous system (CNS). In the past fifty years, glutamatergic systems have been extensively studied, but despite the huge amount of accumulated experimental data, we still know very little about the role of glutamate and glutamate receptors in the neuronal circuits of the spinal cord. Spinal glutamatergic systems are involved in acute and chronic pain and certain neurodegenerative disorders. Therefore knowledge of glutamatergic circuits not only has theoretical significance, but is also of major interest for physicians, surgeons and pharmacologists. In addition, information on these systems could have practical implications for patients suffering from any of these disorders.

This chapter deals with the characteristics of glutamatergic systems in the CNS, with emphasis on the dorsal horn of the spinal cord. Information about synthesis, transport, release and uptake of glutamate and the structure, function and distribution of glutamate receptors is crucial for understanding their role in sensory processing and locomotion. Therefore first some basic information about glutamate and it receptors is discussed and summarized, then a more detailed review is provided on glutamatergic systems and glutamate receptors in the spinal cord.

HISTORICAL OVERVIEW

In 1933, Dusser de Barrenne developed a method of applying substances directly to the brain or spinal cord of live animals with microelectrophoresis. His technique was widely used in the 1950s to study the behavioural changes and electrical responses induced by administration of different compounds. A large number of substances, mainly isolated from brain, were tested and by the end of the decade it was well established that glutamate had an excitatory effect (Curtis et al, 1959) on a wide range of neurons. Interestingly, due to the ubiquitous nature of its effect (Curtis et al., 1959, 1960), its high concentration in brain extracts (Krebs et al, 1949), its general involvement in other metabolic pathways (Krebs, 1935) and its excitotoxicity (Olney et al., 1970), it was not until the early 1970s that glutamate was accepted as a neurotransmitter. This was facilitated by the discovery of specific agonists and antagonists, which led to the revision of the previously widely accepted "non-specific action theory" of glutamate. Subsequent pharmacological studies indicated that glutamate actually acts on more than one receptor. Meanwhile, these initial studies have attracted more and more neurobiologists to the area of excitatory amino acid research, so it is not surprising that during the following 20 years a highly sophisticated

system was revealed. The cloning of various types of glutamate receptor in the early 1990s led to the production of subunit-specific antibodies and to the construction of polynucleotides suitable for *in situ* hybridization and PCR, which further facilitated the research into glutamatergic systems in the CNS. When functional glutamate receptors were found in extra-neuronal tissues, the scope of research widened. Glutamate receptors were detected in bone, keratinocytes, pancreas, megakaryocytes, lung, heart, liver, kidney, stomach, intestine, thymus, taste buds and testis (Skerry and Genever, 2001).

GLUTAMATE AS A NEUROTRANSMITTER

Glutamate, as one of the 20 main amino acids, is involved in protein synthesis, detoxification, energy supply and metabolism in virtually every cell. At the same time it has a further key role in the CNS as the most important fast acting excitatory neurotransmitter. How can such an ubiquitous molecule be used for neurotransmission without the signal to noise ratio being degraded? Its overall concentration in brain tissue is 10 mM, with the vast majority being stored intracellularly, mainly in glial cells and glutamatergic terminals (where its concentration can be up to 45 mM). The extracellular glutamate concentration is very low (2-3 μM), and the several thousand-fold concentration gradient across the plasma membrane assumes the existence of an efficient uptake system as well as a barrier that prevents glutamate entering the CNS from the blood vessels. The relative impermeability of the blood-brain barrier to glutamate and the lack of net uptake from the blood indicates that glutamate must be produced in the brain (Hertz et al., 1999).

Synthesis, transport and release of glutamate in the CNS

Neurons and astrocytes are both involved in maintenance of the glutamate pool in glutamatergic boutons and in the elimination of released transmitter (Hertz et al., 1999). Both cell types are capable of glutamate production by either the hydrolysis (deamination) of glutamine or the transamination of α-ketoglutarate (2-oxoglutarate). The vast majority of α-ketoglutarate derives from the degradation of glucose, the only nutrient in the tricarboxylic acid cycle that is present in the systemic circulation in high concentrations and can readily cross the blood-brain barrier. Via α-ketoglutarate, glutamate can also enter the intermediary metabolism to produce energy.

Glutamate produced in the neuronal cell body is taken up into 35-50 nm small, round vesicles (Iliakis, 1996) by a highly specific, Mg^{2+}-dependent active transport system. The driving force is mainly the membrane potential component of an electrochemical proton gradient generated by a Mg^{2+}-activated vacuolar ATPase (Ozkan and Ueda, 1998).

Three vesicular glutamate transporters (VGLUTs) have recently been identified and cloned, and this has a major importance in neurobiology research as these can be used to identify glutamatergic neurons in the CNS (Takamori et al., 2000; Fremeau et al., 2001; Herzog et al., 2001; Varoqui et al., 2002; Todd et al., 2003). A previously known, brain specific sodium-dependent inorganic phosphate transporter (BNPI) has been found on synaptic vesicle membranes and was shown to be responsible for packing glutamate into these vesicles by using the proton gradient generated by the vacuolar ATPase, thus BNPI was named VGLUT1 (Bellocchio et al., 1998, 2000). Following neuronal activity BNPI/VGLUT1 is also expressed in the plasma membrane of glutamatergic neurons (Bellocchio et al., 1998), where it transports phosphate into the cytoplasm (Ni et al., 1994). This phosphate can then activate the phosphate-activated glutaminase, an enzyme found in glutamatergic neurons that is responsible for deaminizing glutamine into glutamate (Najlerahim et al., 1990). Shortly after the identification of BNPI as VGLUT1, a differentiation-associated sodium-dependent inorganic phosphate transporter (DNPI) (Aihara et al., 2000), was identified as VGLUT2 (Takamori et al., 2001; Varoqui et al., 2002). Based on screening of cDNA libraries, Takamori et al. (2002) described VGLUT3, which shares sequence homology and functional relationship with the two other VGLUTs (Gras et al., 2002). VGLUTs transport 500-5000 glutamate molecules into individual vesicles reaching a glutamate concentration of 60-200 mM (Fonnum et al., 1998).

Upon reaching the axon terminal, action potentials activate Ca^{2+}-channels on plasma membranes of neurons, and the subsequent Ca^{2-}-entry is responsible for the action potential-exocytosis coupling (Turner, 1998). Various presynaptic receptors acting directly or indirectly, can either facilitate or inhibit glutamate release through three major mechanisms: firstly influencing the kinetics of Na^{-} and K^{-} channels, secondly modifying the amount of Ca^{2+} available in the terminal, and thirdly regulating the intracellular cascade that leads to the exocytosis of vesicles (Nicholls, 1998). The release of the contents of one single vesicle is enough to produce a 1 mM rise in the glutamate concentration within the synaptic cleft which is sufficient to activate the ionotropic receptors in the postsynaptic density (Clements et al, 1992).

Uptake of released glutamate from the extracellular space and its recycling

To avoid the degradation of signal to noise ratio and to prevent the necrosis of neurons caused by the excitotoxic effect of glutamate, the released amino acid has to be rapidly removed. Since no significant extracellular metabolism of glutamate occurs, this is accomplished by the fast uptake of glutamate into glial cells and neurons (Balcar and

Johnston, 1972). Two major groups of proteins (together with some minor ones, for review see Bonanno and Raiteri, 1994) act as glutamate transporters on the plasma membranes (Danbolt, 2001): the high affinity sodium and potassium coupled transporters or excitatory amino acid transporters (EAAT 1-5) and the low affinity glutamate transporters.

Glutamate taken up by neurons can either be reused as a transmitter, or used in general cellular metabolism. However not all glutamate is taken up by neurons; in fact glial cells are responsible for a major proportion of glutamate uptake. This glutamate is converted to glutamine with the enzyme glutamine synthetase, found within the CNS only in glial cells. Glutamine, unlike glutamate, can readily cross the cell membrane and after leaving the astrocytes it is taken up by neurons, where it is deaminated back to glutamate by members of the glutaminase enzyme family. Thus glutamate is constantly released by neurons, taken up by glial cells and returned to neurons as glutamine, in a cycle, which is called the glutamate-glutamine cycle (Kvamme, 1998).

GLUTAMATE RECEPTORS

A number of different glutamate receptors have been identified and cloned. These are not only responsible for fast transmission of propagating action potentials from one cell to another, but they also play a role in more complex cellular mechanisms such as synaptic plasticity and excitotoxicity. These in turn are involved in both physiological (learning, memory) and pathological conditions (e.g. neuropathic pain, epilepsy, amyotrophic lateral sclerosis). Glutamate receptors can be divided into two major groups: ionotropic receptors (iGluRs) which form fast acting, ligand-gated ion channels and G-protein coupled metabotropic receptors (mGluRs) which have complex, long-lasting intracellular actions through a variety of signal transduction molecules and second messengers.

Ionotropic glutamate receptors (iGluRs)

Three ionotropic glutamate receptor families have been identified by the development of more-or-less selective agonists: N-methyl-D-aspartate (NMDA), alpha-amino-3-hydroxy-5-methyl-4-isoxazole propionic acid (AMPA) and kainate receptors (KA). All receptors form homo- or heteromers made up of one or more type of subunits. It is widely accepted that individual subunits will only assemble with other ones from their own family, but in spite of the numerous pharmacological, molecular biological and biophysical experiments the exact composition of native receptor complexes is not precisely known. Initially there were debates about whether the complexes are tetra- or pentamers, but recently, following the purification of GluR2 subunits a tetrameric

stoichiometry was suggested (Safferling et al., 2001). It is clear that the subunit composition of a single receptor-complex determines its electrophysiological and pharmacological properties. Six gene families (1 for AMPA, 2 for KA and 3 for NMDA receptors), with sequence homology within each family, encode the different type of iGluRs. Each gene (altogether at least 16 genes) is responsible for the synthesis of a single subunit, but post-transcriptional (alternative splicing, RNA editing) and post-translational (glycosylation, phosphorylation, palmitoylation) modifications further increase the number of structural variants. Ionotropic glutamate receptor subunits have a generally similar tertiary structure: 900-1400 amino acids form a 95-163 kDa macromolecule, with three transmembrane domains (M_1, M_3, M_4), an extracellular N- and an intracellular C-terminal (Fig. 1.1). A cytoplasm-facing re-entrant membrane loop (M_2) between M_1 and M_3 forms the inner pore of the cation channel, while the ligand-binding domain is a clam-shell-like pocket formed partly by the extracellular N-terminal domain (S_1) and partly by the M_3-M_4-loop (S_2). The N-terminal region also contains biding sites for allosteric modulators (Zn^{2+}, H^+, polyamines) and glycosylation sites, while the extracellular loop between M_3 and M_4 contains an RNA splice variant which has a role in receptor desensitization. The cytoplasmic C-terminal incorporates important phosphorylation sites and biding sites for anchoring proteins (PDZ domains). For reviews on the structure and function of iGluRs see Ozawa et al. (1998), Bigge (1999), Dingledine et al (1999), Burnashev and Rozov (2000), Cull-Candy et al. (2001), Franciosi (2001), and Lerma et al. (2001).

AMPA-receptors

Currently four AMPA receptor subunits are known (GluR1-4) and these can form homo- or heteromers. Each subunit has at least 2 splice variants (flip or flop), based on the presence or absence of a 38 amino acid segment within the M_3-M_4-loop. In addition, GluR2 and GluR4 subunits have other, long (GluR2L, GluR4) or short (GluR2S, GluR4c) splice variants in the C-terminal region. In the case of GluR2-4, structural variants also arise from mRNA editing, so altogether 30 AMPA subunit variants exist with different primary structures (Burnashev and Rozov, 2000). Theoretically, more than 100,000 different AMPA complexes can be assembled from these different subunits/variants. It remains a question whether different subunits can freely form complexes or not. Wenthold et al. (1996) used immunoprecipitation studies to show that hippocampal CA1 and CA2 pyramidal neurons mainly contain heteromeric GluR2/GluR1 or GluR2/GluR3 complexes, but GluR1/GluR3 and homomeric GluR1 complexes were also found in small amounts. It is now also clear that multiple AMPA receptor subtypes can coexist in the same neuron

Figure 1.1 Schematic drawing illustrating the tertiary structure of an iGluR subunit, in this case GluR1. The receptor protein has three transmembrane domains (*M1, M2, M4*). The inner pore of the channel is formed by an intracellular re-entrant membrane loop (*M2*). Part of the large extracellular N-terminal domain (*S1*) and part of an extracellular loop connecting M3 and M4 (*S2*) form the ligand-binding site. In the M3-M4 loop, an alternatively spliced 38 amino acid segment can either be present (Flip form) or absent (Flop form). The intracellular C-terminal domain can be phosphorylated and in the case of a GluR1 subunit the most important phosphorylation sites are the two serine residues at position 845 and 831.

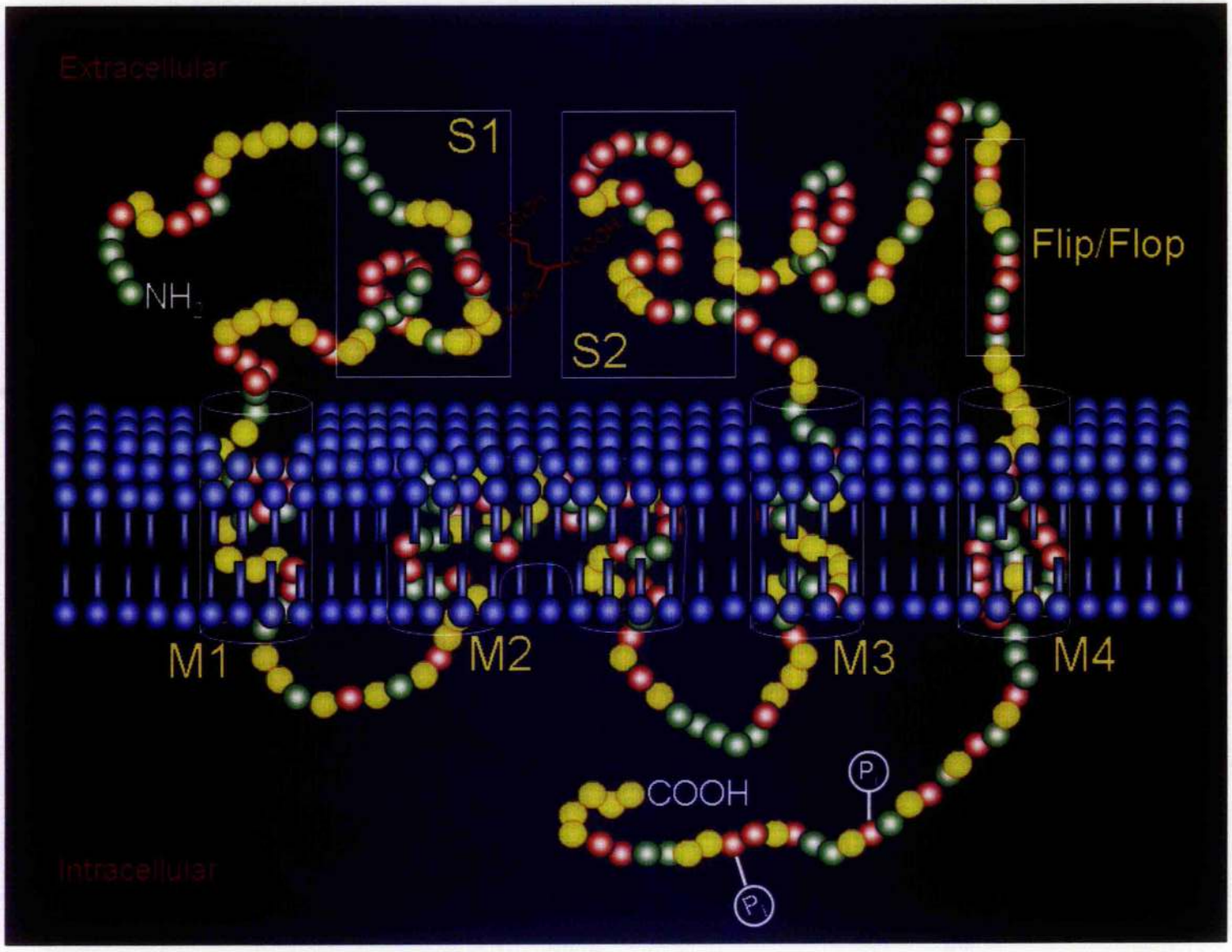
Extracellular
S1
S2
Flip/Flop
NH2
M1
M2
M3
M4
COOH
Intracellular

(Washburn et al., 1997) and the subunit composition may influence subcellular membrane targeting within the same cell (Rubio and Wenthold, 1997). However, not all neurons express all four AMPA subunits. In mammalian CNS GluR1-3 subunits are widely expressed, but GluR4 is mainly restricted to cerebral cortex, hippocampus, dentate gyrus, olfactory bulb and spinal cord (Petralia and Wenthold, 1992). Although most studies have focused on neuronal expression, there is also convincing evidence that astrocytes and oligodendrocytes have functional AMPA receptors which are activated by the synaptically released transmitter. Astrocytes and oligodendrocytes mainly contain GluR1/GluR4 and GluR1/GluR3 subunits respectively (Verkhratsky and Steinhauser, 2000).

AMPA receptor channels are mainly responsible for rapid excitatory synaptic transmission. Their characteristic feature is the fast opening (1-4 ms) and closing (2-14 ms) kinetics upon application of agonists. Activation of flip variants with glutamate is 4-5 times more effective than that of flop (Sommer et al., 1990), while flop variants have a 2-4 fold faster and more complete desensitization kinetics (Mosbacher et al., 1994). AMPA receptors are principally permeable to K^+ and Na^+ ions, but certain regions express AMPA receptors with substantial Ca^{2+}-conductance. Homomeric GluR1, GluR3 or GluR4 complexes have Ca^{2+}-permeability, but homomeric GluR2 or heteromeric complexes of GluR2 with any other subunit lack Ca^{2+}-conductance. Based on these electrophysiological findings, it is assumed that most AMPA receptor complexes within the CNS contain the GluR2 subunit. Further investigations led to the discovery that a single arginine (R) residue [which replaces a glutamine (Q) as a result of mRNA editing (Q/R editing)] in the M_2 membrane re-entrant hairpin loop of the GluR2 subunit is responsible for the prevention of Ca^{2+} (and other divalent cation) permeation (Burnashev et al., 1992). Q/R editing also results in a decrease of single channel conductance. It has to be noted, that the activation of Ca^{2+}-inpermeable AMPA receptors may also lead to Ca^{2+}-influx, via voltage-dependent Ca^{2+} channels. However, due to the different spatiotemporal distribution of the subsequent Ca^{2+}-currents, this may have different consequences from the activation of ligand-gated Ca^{2+} channels (NMDA receptors or Ca^{2+}-permeable AMPA receptors).

AMPA receptors are not static components of the postsynaptic density of asymmetric synapses but have the potential to enter, leave and then possibly reenter the synapse either in a constitutive or inducible manner. In the latter case, various events such as NMDA receptor activation can lead to the internalization or membrane insertion of AMPA receptors. AMPA complexes that contain a subunit with a long C-terminal tail (GluR1, GluR4, GluR2L) require activity for synaptic delivery, while receptors that contain subunits with only short C-terminal tails (GluR2S, GluR3, GluR4c) constitutively

cycle into and out of the synapse. The regulated distribution and redistribution of AMPA receptors are thought to play a major role in synaptic plasticity (Bredt and Nicoll, 2003), although it is widely believed that these long-term changes in synaptic strength are initiated by the activation of NMDA receptors (see below). In the hippocampus and cerebellum, long term depression (LTD) is correlated with AMPA internalization while long term potentiation (LTP) is associated with the recruitment of AMPA receptors into the synaptic membrane. Due to its possible involvement in synaptic plasticity, AMPA receptor trafficking has been extensively studied. Stargazin, a membrane protein, has been found to play a crucial role in the surface expression of AMPA subunits. Other, mainly PDZ scaffold proteins such as neuronal activity-regulated pentraxin (NAPR), synapse associated protein 97 (SAP97), glutamate receptor interacting protein 1 (GRIP1), GRIP2/ABP (AMPA-receptor binding protein) and protein that interacts with C kinase (PICK-1) stabilize the receptors in the synapse. It is likely that AMPA receptors enter the postsynaptic density following exocytosis to non-synaptic regions and they are endocytosed after drifting laterally from the postsynaptic density (Passafaro et al., 2001). This could be related to the fact that AMPA receptors are fairly often seen at the lateral edge of some (Kharazia et al., 1996, 1997; Bernard et al., 1997; Matsubara et al., 1996), but not all synapses (Sassoe-Pognetto and Ottersen, 2000). It is also interesting that in the hippocampus (Takumi et al., 1999; Racca et al., 2000) and cortex (Kharazia and Weinberg, 1999) there is a correlation between the length of the synapse and the level of AMPA receptor expression. Synapses with smaller active zones fairly often lack AMPA receptors, therefore they are thought to be functionally silent (Nüsser et al., 1998; Racca et al., 2000). The synaptic expansion of these silent synapses may lead to AMPA receptor recruitment and this could play a role in the development of long term potentiation (Kullmann, 1994; Isaac et al., 1995; Liao et al., 1995). There are three forms of AMPA receptor endocytosis: a constitutive form, which is rapid and results in an apparent turnover of surface receptors, a regulated form, which is dependent on the rise in intracellular Ca^{2+} as a signal and involves a great number of proteins (protein kinase C, calcineurin, arrestin, AP2, clathrin etc) and an activity independent form, which does not require Ca^{2+} (Carroll et al., 2001).

Kainate receptors

Kainate receptors in many ways resemble AMPA receptors, thus it is not surprising that these two families are often described together as AMPA-KA receptors or non-NMDA receptors. Our knowledge on the function and distribution of kainate receptors is less abundant than that of either AMPA or NMDA receptors. This is mainly due to the lack of

specific antibodies and the only recently solved difficulties in differentiating them from GluR1-4 receptors on the basis of their pharmacology. Even early radioligand binding studies distinguished low and high affinity kainate binding sites, which later turned out to represent the two subtypes of KA receptors, GluR5-7 and KA1-2, respectively. GluR6-7 have 2 splice variants, whereas GluR5 has 4. For GluR5 and GluR6 the number of different subunits is further increased by mRNA editing (one site for GluR5, three for GluR6). To date altogether 28 kainate receptor proteins are known with different primary structure. GluR5-7 may form homomeric complexes, but they can also co-assemble with KA1 or KA2, which on the other hand cannot form functional receptors on their own.

Although *in situ* hybridization and radioligand binding studies have demonstrated that KA receptors are widely expressed throughout the CNS, the expression patterns of the various subunits are heterogeneous. The dorsal root ganglion (DRG) cells, the subiculum, the septal nuclei, some cortical areas and the Purkinje cells of cerebellum contain large quantities of GluR5 mRNA. GluR6 is mainly expressed in the cerebellar granule cells, in the CA3 region of the hippocampus, in the dentate gyrus and in the striatum, while GluR7 mRNA is found at highest levels in the cortex, in the striatum and in the inhibitory neurons of the molecular layer of the cerebellum. The expression of KA1 is mostly restricted to the CA3 region of the hippocampus, however lower levels can be found in other areas, such as dentate gyrus, amygdala and entorhinal cortex. KA2 is ubiquitous throughout the CNS. Due to difficulties in producing selective antibodies, the available data on the immunohistochemical localization of kainate receptors is limited. The investigations which have been undertaken to date have shown KA receptor immunoreactivity both presynaptically in axons and also in postsynaptic membranes (Petralia et al., 1994a).

The electrophysiological properties of KA receptors depend greatly on their subunit composition. Most recordings have been performed on heterologous expression systems, so little is known about the native receptors. They are principally permeable to K^+ and Na^+ ions, but certain splice variants also display Ca^{2+}- and Cl-fluxes. Rapid desensitization and slow recovery is one of the most characteristic features of KA receptors.

NMDA receptors

As in case of the other two iGluRs, a number of different subunits have been identified for NMDA receptors. The most ubiquitously expressed is NR1, which exists in 8 different splice variants (Table 1.1) based on its three regions for alternative splicing: amino terminal N_1-cassette, and carboxy terminal C_1- and C_2-cassettes (Zukin and Bennett, 1995). Splicing out the C_2-cassette, results in the loss of the first stop codon of the NR1

gene, and causes the expression of a distinct amino acid sequence, the C_2'-cassette. Two other gene families encode the four NR2 subunits (NR2A-D) and the two NR3 subunits (NR3A-B). All of these apart from NR2A have splice variants. Although Moriyosi et al. (1991) initially reported that NR1 subunits can assemble to functional homo-oligomers, nowadays it is widely accepted that unlike AMPA and KA receptors, NMDA subunits do not form homomeric complexes. NR1 subunits must be assembled with at least one NR2 to form functional receptors (Ishii et al., 1993), while NR3 subunits probably have regulatory functions within the complex (Ciabarra et al., 1995; Chatterton et al. 2002; Matsuda et al., 2002). Immunoprecipitation studies of native receptors show that different NR2 subunits and various isoforms of NR1 can coexist in one receptor assembly. Subunit composition has an effect on the physiological, biochemical and pharmacological properties of the receptor (see below).

Name of splice variant	N_1-cassette (exon 5)	C_1-cassette (exon 21)	C_2-cassette (exon 22)
NR1-1a or NR1 1	-	+	+
NR1-1b or NR1 2	+	+	+
NR1-2a or NR1 3	-	-	+
NR1-2b or NR1 4	+	-	+
NR1-3a or NR1 5	-	+	-
NR1-3b or NR1 6	+	+	-
NR1-4a or NR1 7	-	-	-
NR1-4b or NR1 8	+	-	-

Table 1.1. Terminology of various splice variants of the NR1 subunit

NMDA NR1 is found throughout the CNS, with the highest concentrations in the pyramidal cells of CA1-3 region of the hippocampus, the granule cells of the dentate gyrus, the granule, Purkinje and Golgi cells of the cerebellum, layer 2,3,5 of the cerebral cortex, sensory and motor neurons in the spinal cord and dorsal root ganglia (Brose et al., 1993, Petralia et al., 1994b, 1994c). NMDA NR2 subunits are also abundantly found in the mammalian brain. Each has a characteristic distribution, although they overlap with each other. Northern blot and *in situ* hybridization studies revealed prominent NMDA NR2A expression in the cerebral cortex, hippocampus, olfactory areas, thalamic nuclei, cerebellar cortex and some brainstem regions. NMDA NR2B is widely expressed in telencephalic and thalamic regions, NMDA NR2C is largely restricted to the granular layer of the cerebellum, while NMDA NR2D can be found mainly in diencephalic and lower brainstem areas (Ishii et al., 1993). Immunocytochemical studies using a polyclonal antibody reacting with both NMDA NR2A and NR2B subunits found similar distribution of

immunoreactivity to that of NMDA NR1, but cerebellar Purkinje cells showed a less intense labelling (Petralia et al., 1994b). NR3A is mainly expressed during development and its levels decrease sharply after the second postnatal week (Ciabarra et al., 1995; Wong et al., 2002). NR3B is expressed highly in pons, midbrain, medulla, and the spinal cord, but has low levels in the forebrain and the cerebellum (Matsuda et al., 2002).

NMDA receptors are responsible for the slow component of the excitatory postsynaptic potential (NMDA EPSP) recorded upon activation of the appropriate neurons. With their "nonlinear computational" properties they also play a major role in synaptic plasticity. They not only open more slowly than AMPA or KA receptors, but also have longer desensitization kinetics. The deactivation is fastest for NR1/NR2A complexes, slower for NR1/NR2B or NR1/NR2C complexes and slowest for NR1/NR2D channels. The ion channel formed by the NMDA receptor complex has a high conductance for Na^+, K^+ and Ca^{2+} ions (MacDermott et al., 1986), although the presence of of NR3 in NMDA receptors dramatically reduces the Ca^{2+}-permeability of the complex (Perez-Otano et al., 2001; Matsuda et al., 2002; 2003). Influx of Ca^{2+}, unlike that of Na^+ or K^+, not only has an effect on the membrane potential, but also acts as a second messenger and can trigger intracellular biochemical cascades leading to changes in the synaptic strength. Another distinct feature of NMDA receptors, besides Ca^{2+}-permeability, is the voltage dependent blockage at resting membrane potential by physiological concentrations of extracellular Mg^{2+} ions (Mayer et al., 1984). A single asparagine residue in the M_2 domain of the receptor protein seems to be mainly, but not solely responsible for both of these properties. Membrane depolarization decreases the effectiveness of the Mg^{2+}-block on channel conductance, while hyperpolarisation increases it. The Mg^{2+}-block on NMDA receptor complexes formed by NR1/NR2A or NR1/NR2B subunits exhibits a stronger voltage dependence than that on receptors composed of NR1/NR2C or NR1/NR2D subunits. A third prominent characteristic of NMDA receptors is the obligatory need for glycine as a co-agonist for channel opening (Larson et al., 1988). Interestingly, when NR3A or NR3B co-assembles with NR1, the receptor complex forms excitatory glycine receptors that are unaffected by glutamate or NMDA (Chatterton et al., 2002). D-alanine and D-serine have also been identified as co-agonists (Brugger et al., 1990). Several pharmacological agents, some of which are used routinely in human pharmacotherapy, have been developed that affect NMDA receptor function (Table 1.2) by acting on one of four possible sites: the glutamate/NMDA recognition site, the glycine binding site, the intra-ion-channel binding site and an allosteric modulatory site (Sucher et al., 1996).

Drug	AMPA				NMDA				
	GluR1	GluR2	GluR3	GluR4	NR1	NR2A	NR2B	NR2C	NR2D
L-glutamate	+				+				
L-aspartate					+				
glycine					+				
D-serine					+				
spermine					+				
AMPA	+								
NMDA					+				
2-amino-3-(3-hydroxy-5-phenyl-4-isoxazolyl) propionic acid (APPA)	+								
2-amino-3-(3-carboxy-5-methyl-4-isoxazolyl propionic acid (ACPA)	+								
5-fluorowillaridiine	+								
β-N-methylamino-L-alanine	+								
GYKI 53655, GYKI 52466, GYKI 53405 (2,3-benzodiazepines)	-								
6-cyano-7-nitroquinoxalin-2,3-dione (CNQX)	-								
Joro spider toxin		-							
dextromethorphan, dextrorphan					-				
memantine					-				
amantadine					-				
ketamine					-				
dizlocipine (MK-801)					-				
phencyclidine (PCP)					-				
4-(3-phosphonopropyl)piperazin-2-carboxylic acid (CPP)					-				
2-amino-5-phosponovalerate (APV)					-				
2-amino-5-phosphonoheptanoate (APH)					-				
5,7-dichlorokynurenic acid (DCKA)					-				
ifenprodil							-		
CP101,606							-		
Ro 25-6981							-		

Table 1.2 Table showing the most important AMPA and NMDA receptor agonists (+) and antagonists (-).

The distribution of NMDA receptors within glutamatergic synapses has been extensively studied with the postembedding immunogold method. In the brain regions examined, subunits were concentrated at the postsynaptic membrane of asymmetrical synapses (Bernard and Bolam, 1998; Valtschanoff et al., 1999, Racca et al., 2000). The gold particles representing NR1 subunits accumulated in the centre of the active zone (Kharazia and Weinberg, 1997), while this was not the case for NR2 (Valtschanoff et al., 1999). The density of labelling for NR1 was independent of synaptic size (Takumi et al., 1999; Kharazia and Weinberg, 1999), indicating that the number of NMDA receptors at a given synapse is proportional to the size of the postsynaptic density. NMDA and AMPA receptors have been shown to colocalize in the same synapse (Kharazia et al., 1996; He et al., 1998; Racca et al., 2000), although a number of synapses only contained functional NMDA receptors. The latter are thought to correspond to silent synapses (see above) as for these glutamate release under normal circumstances does not depolarize the postsynaptic membrane, due to the Mg^{2+}-block of the NMDA receptors.

The anchoring of NMDA receptors to the PSD is the subject of extensive research. It involves a large number of recently identified membrane proteins including postsynaptic density protein 95 (PSD95, also known as synapse associated protein 90, SAP90), PSD93 (also known as chapsyn110), SAP102, guanylate kinase-associated protein (GKAP), dynein, Shank, neuronal nitric oxide synthase (nNOS), α-actinin, tubulin, spectrin, neuroligin, calmodulin, CaM kinase II. Many of these have enzymatic activity (e.g. PSD-95 with guanylate kinase activity), while others link the receptors to the cytoskeleton (e.g. α-actinin). It is clear, that these proteins not only cluster the receptors to the postsynaptic density, but also play a role in their trafficking, function, regulation and in synaptic plasticity (e.g. Kennedy, 1997). PSD-95 seems to be the most important anchoring protein in NMDA clustering, because it can form a bridge between the receptor subunits and other membrane proteins. Electron microscopic immunocytochemical studies have shown that PSD-95 has a similar cellular and subcellular localization to NMDA receptors (Valtschanoff et al., 1999; Aoki et al., 2001), but it has still not been proved that PSD-95 is present at every NMDA receptor containing synapse.

Metabotropic glutamate receptors (mGluRs)

Although mGluRs were not investigated during the course of this study, a brief overview is provided here. There are eight different subtypes of metabotropic glutamate receptors (mGluR1-8), of which mGluR1, mGluR4 and mGluR5 have additional splice variants. These are G-protein coupled receptors (GPCRs) and do not form ion channels.

They all belong to the seven transmembrane domain containing GPCR superfamily. They contain 854-1179 amino acids, and share 40% sequence homology with each other. Their unusually large extracellular N-terminal domain contains the glutamate binding site, while the intracellular C-terminal domain plays a role in anchoring and signal transduction. It also contains phosphorylation sites for functional regulation. A mainly hydrophobic core region of 250 amino acids contains the seven transmembrane domains (m1-7), which are interconnected by extra- and intracellular loops. The first (i1) and third (i3) intracellular loops are highly conserved, suggesting they are responsible for G-protein activation, while in the case of mGluR1, i2 and i4 are responsible for phospholipase C (PLC) coupling.

Based on their amino acid homology, pharmacology and second messenger system, mGluRs are classified into three subgroups (I-III). Group I mGluRs (mGluR1/mGluR5) are activated by quisqualate and use the PLC signaling pathway. mGluR2 and mGluR3, which belong to group II, are activated by dicarboxycyclopropyl glycine (DCG-IV) and are negatively coupled to the adenylate cyclase enzyme. Group III mGluRs, which consist of mGluR4, 6, 7, 8, and activated by L-2-amino-4-phosphonobutyrate (L-AP4), and like those of group II, are also negatively coupled to adenylate cyclase. Glutamate binding to group I mGluRs leads to the activation of PLC, which catalyses the hydrolysis of phosphatidil-inositol-4,5-diphosphate to inositol-1,4,5-triphosphate (IP_3) and diacyl-glycerol (DAG). IP_3 opens Ca^{2+}-channels on the endoplasmatic reticulum, while DAG activates protein kinase C (PKC). Activation of group II and III mGluRs leads to the inhibition of protein kinase A (PKA) through decreased levels of cAMP.

Different groups of metabotropic glutamate receptors show a distinct subcellular segregation. In general group I mGluRs are usually found at somatodendritic domains, at the peripheral parts of postsynaptic densities ("perisynaptic location") and they have excitatory effects on the neurons. They contribute to the regulation of synaptic plasticity. Group II and III mGluRs on the other hand, are mainly located presynaptically and they have an inhibitory effect on the presynaptic terminal, negatively regulating the release of glutamate or GABA. The following reviews discuss the characteristics of mGluRs in detail: Ozawa et al. (1997), Shigemoto and Mizuno, (2000), De Blasi et al. (2001).

THE FUNCTIONAL NEUROANATOMY OF THE SPINAL CORD

The spinal cord is evolutionary the most ancient part of the CNS, and is of fundamental importance in receiving and processing sensory information and relaying it towards higher CNS regions. It plays a vital role in integrating basic motor functions, executing voluntary movements orchestrated by the brain and in regulating autonomic

body functions. In anatomical terms the spinal cord is a very complex neuronal network of intrasegmental and intersegmental propriospinal neurons and projection cells, which communicate with the periphery of the body through afferent and efferent connections and with higher brain regions through ascending and descending projections. The morphological, neurochemical and functional complexity of these neuronal circuits in the spinal cord are often underestimated, even by neurobiologists dealing with higher CNS regions. For detailed description on spinal cord anatomy see Willis and Coggeshall (1991).

Instrinsic neurons and cytoarchitectural lamination

Cell bodies located in the gray matter of the spinal cord belong to local interneurons, projections cells, motoneurons or efferent autonomic preganglionic neurons. Several anatomical terms exist to describe the exact location of these nuclear groups, but the most satisfactory and widely accepted terminology is based upon the cytoarchitectural lamination of the spinal cord initially described in cat by Rexed (1952, 1954, 1964), and subsequently adopted for other species (e.g. Molander et al., 1984, 1989). The spinal gray matter is divided into ten layers: laminae I-VI and VIII-IX correspond to the dorsal and ventral horns respectively, while the intermediate gray matter is lamina VII and the area around the central canal (central gray matter) is lamina X. The great majority (>95%) of spinal cord neurons are interneurons and functionally these can be inhibitory or excitatory.

Primary afferents

Electrical responses evoked by external and internal mechanical, chemical and thermal stimuli are conveyed to the dorsal horn by primary afferent fibres. Cell bodies of these primary sensory neurons are located in the DRG and give rise to axons which bifurcate into a peripheral and a central branch. The former innervate somatic (skin, muscles, joints) and visceral (blood vessels, heart, lungs etc.) organs, while the latter terminate in the spinal cord (or brainstem) and form synapses with second-order intrinsic neurons or motoneurons. Peripheral nerve fibres show distinct functional, morphological and electrophysiological properties; therefore they can be classified in several ways. The most widely used classification, based on conduction velocity, fibre diameter and certain electrical properties, distinguishes A- (Aα, Aβ, Aδ, Aγ), B-, and C-fibres. Primary afferents can belong to the Aα, Aβ, Aδ and C groups (e.g. Lynn and Carpenter, 1982). Aα/Aβ-afferents are large, myelinated fibres (4-12 μm) with high conduction velocity. They mainly belong to cutaneous low threshold mechanoreceptors which arborize in a band extending from the inner part of lamina II (IIi) to lamina IV or to proprioceptive muscle spindle and Golgi tendon organ afferents which terminate in laminae IV-VII and

the ventral horn. Aδ-afferents are thinly myelinated, smaller calibre fibres (1-4 μm) conducting with an intermediate velocity. Low-threshold mechanoreceptive Aδ-fibres innervate hair follicles and terminate in lamina IIi, while those responding to high intensity noxious stimulation form synapses mainly in lamina I, although a minority penetrate deeper into the dorsal horn and end in lamina V. Visceral afferents are usually very thinly myelinated, slowly conducting fine fibres and these terminate throughout the dorsal horn. C-fibres are very thin (<1 μm), unmyelinated fibres with very low conduction velocity. These belong to somatic and visceral nociceptors, thermoreceptors, low threshold mechanoreceptors and together with the Aδ-fibres mainly terminate in laminae I-II. However scattered C-fibre terminals can be found deeper in the dorsal horn. Unmyelinated cutaneous afferents can be divided into two major groups based on their neurochemical characteristics and their sensitivity for different neurotrophins. Peptidergic C-fibres usually contain CGRP together with various other neuropeptides, they are sensitive to nerve growth factor (NGF) and express the high-affinity neurotrophin receptor, trkA. Non-peptidergic C-fibres, lack neuropeptides, they are sensitive to glial cell line-derived neurotrophic factor (GDNF), express the receptor tyrosine kinase enzyme (RET), have fluoride-resistant acid phosphatase (FRAP) activity and strongly bind a lectin (IB4), derived from a plant, *Bandeiraea simplicifolia*. Peptidergic C-fibres mainly terminate in lamina I and the outer part of lamina II (IIo), while non-peptidergic ones arborize in the central part of lamina II. The postsynaptic targets of peptidergic C-fibres include projection neurons in lamina I, as well as a population of projections cells in laminae III and IV with dendrites that pass dorsally to the superficial laminae.

Primary afferent terminals in the dorsal horn generally have simple synaptic arrangements, although some form complex structures known as glomeruli. A synaptic glomerulus consists of a central terminal formed by the primary afferent, and this is surrounded by several profiles. The peripheral profiles can either be axons forming axo-axonic synapses with the primary afferent or they can be dendrites, which are postsynaptic to the central terminal. Some of the dendrites belong to GABAergic neurons (Todd, 1996) and form reciprocal axo-dendritic/dendro-axonic synapses with the primary afferent. Ribeiro-da-Silva and Coimbra (1982) described two types of synaptic glomerulus in the rat dorsal horn. Type I glomeruli belong to non-peptidergic C-fibres and are mainly present in the middle part of lamina II (Ribeiro-da-Silva, 1994). These have scalloped terminals, densely packed clear vesicles of variable size, dark axoplasm and few mitochondria. The central bouton typically receives a single axo-axonic synapse from a peripheral axon (Ribeiro-da-Silva, 2003). Central terminals of type II glomeruli belong to Aδ D-hair

afferents (Réthelyi et al., 1982) and are located slightly more ventrally, in lamina IIi and the outer portion of lamina III (Bernardi et al. 1995). These have loosely packed clear vesicles of uniform size, light axoplasm and many mitochondria. The central terminal often receives large numbers of axo-axonic synapses.

Ascending projections from the spinal cord

Action potentials arriving via primary afferent fibres are usually received by spinal interneuronal systems which relay the information towards supraspinally projecting neurons after a complex processing, although direct monosynaptic connections to projection cells also exist. Cell bodies of projection neurons are mainly located in lamina I and laminae III-VI. The axons belonging to many of these projection cells cross the midline, travel in the ventral or lateral funiculi of the white matter (anterolateral system) and carry mechanoreceptive, nociceptive and thermal sensory information to various areas of the brainstem and diencephalon. This is subsequently transmitted to the telencephalon where, as a result of still poorly understood integrative neuronal activity, pain, touch-pressure, and heat sensation is generated from the sensory information. In humans the main termination of the anterolateral system is the thalamus, while in rats only a small proportion of the fibres that originate from laminae I, III and IV arborize in this region; instead they mainly project to the periaqueductal gray matter, the lateral parabrachial area, the medullary reticular formation and the nucleus of the solitary tract. The cerebellum is involved in receiving spinal ascending fibres (spinocerebellar tracts) related to proprioceptive input, but this information is not consciously perceived, instead it is concerned with the coordination of somatic motor activity, equilibrium and the regulation of muscle tone. Other ascending tracts from the rat dorsal horn include the post-synaptic dorsal column (PSDC) pathway and the spinocervical tract. It should be noted that the majority of primary afferents responsible for vibration and kinaesthetic sense, two-point discrimination and tactile localization have ascending branches that travel in the posterior white columns and terminate in the gracile or cuneate nuclei.

Descending projections to the spinal cord

Several brain regions send descending pathways to the spinal cord, and these influence the activity of neurons or primary afferents in a neurochemically complex way. Descending systems are involved in motor function, in modulating sensory processing particularly in antinociception, and in autonomic regulation. They mainly originate in the telencephalon and brainstem, although neurons located in the diencephalon and cerebellum also send fibres to the spinal cord. An important projection to the spinal cord is the

corticospinal tract, which transmits information responsible for voluntary movements. It terminates mainly in laminae III-VII, with scattered terminals in the superficial laminae and ventral horn. Several descending pathways (tectospinal, rubrospinal, vestibulospinal, reticulospinal, interstitiospinal, fastigiospinal), responsible for the regulation of muscle tone, righting and posture reflexes, originate in the brainstem or cerebellum and terminate in laminae V-IX. Some of these form direct synaptic contacts with α- or γ-motoneurons, while others activate local interneurons. There are substantial monoaminergic projections from various brainstem nuclei to the spinal cord. These fibres can also contain various neuropeptides and are very important in antinociception, but also play a role in locomotion and autonomic regulation. Serotonin-containing fibres originate from several groups of neurons in the brainstem (B1-3, B5, B7 and B9) and terminate in all spinal laminae, but mainly in laminae I-IIo and the ventral horn. Similarly cell bodies of noradrenergic axons that project to the spinal cord are located in cell groups of the medulla or pons (A1-2, A5-7) and innervate neurons throughout the dorsal and ventral horns.

This complex neuronal system uses a great variety of neurotransmitters and neuromodulators to achieve its role in regulating body functions and serving as a central processing unit between the periphery and the brain. Although the most important and wide-spread excitatory transmitter is glutamate, up until very recently it was not known exactly what proportion and types of spinal neurons were glutamatergic. Even less was known about the exact cellular, subcellular, synaptic and subsynaptic localization of the glutamate receptors, although their presence and role in physiological and pathological conditions has been demonstrated by several studies (Fundytus, 2001).

GLUTAMATERGIC SYSTEMS IN THE SPINAL CORD

Glutamate as a neurotransmitter in the spinal cord

Curtis and Watkins (1960) were the first to describe the excitatory effect of glutamate on spinal cord neurons, and following biochemical, pharmacological, electrophysiological and immunocytochemical studies (e.g. Biscoe et al., 1976; Jessell et al. 1986; Wanaka et al., 1987; De Biasi and Rustioni, 1988) it is now widely accepted that glutamate is the major excitatory transmitter in the spinal cord. Earlier studies investigating excitatory amino acid transmitters in the CNS used autoradiography to detect the uptake and axonal transport of radioactive D-aspartate in neurons or immunocytochemistry to reveal accumulation of glutamate in axon terminals (transmitter pool). These studies established that glutamate is the main transmitter in all (or virtually

all) primary afferent terminals (De Biasi and Rustioni, 1988; Rustioni and Weinberg, 1989; Broman, 1993, 1994b; Todd and Spike, 1993). Glutamate is also used by most ascending (Broman, 1994a) and some descending projections. Glutamatergic ascending systems include the spinothalamic (Ericson et al., 1995), spinocervical (Kechagias and Broman, 1995) and spinocerebellar tracts (Ji et al., 1991). The corticospinal (Rustioni et al., 1982; Giuffrida and Rustioni, 1989) and rubrospinal tracts (Beitz and Ecklund, 1988), and at least some of the tectospinal (Moony et al., 1990), reticulospinal (Brodin et al., 1994) and monoaminergic descending projections (Sorkin et al., 1993; Fung et al., 1994a 1994b; Hökfelt et al., 2000a) are also glutamatergic.

It has been shown that a majority of spinal cord interneurons do not contain GABA, are not enriched with glycine, and are thus unlikely to be inhibitory interneurons (Todd et al., 1990, 1991, 1993). However, it has been difficult to prove that these cells were glutamatergic. Autoradiography is not optimal for colocalization studies, while glutamate antibodies are not suitable for detecting cell bodies of glutamatergic neurons (Ottersen and Storm-Mathisen 1984; Yingcharoen et al., 1989; Walberg et al., 1990) since the metabolic pool of glutamate in cell bodies of non-glutamatergic neurons is sufficiently large to give a significant level of immunostaining. This makes it impossible to distinguish between glutamatergic and non-glutamatergic cell bodies using antibodies against glutamate. With the postembedding immunogold method, glutamate antisera can be used to detect the accumulated glutamate in excitatory terminals (De Biasi and Rustioni, 1988; Maxwell et al., 1990a, 1990b; Todd et al., 1993, 1994), however it is difficult to identify these boutons as belonging to axons of local interneurons. Previous studies had demonstrated that some intrinsic neurons use glutamate as a neurotransmitter (e.g. Rustioni and Cuenod, 1982; Antal et al., 1991). However, until the recent discovery of VGLUTs (see above) as suitable immunocytochemical markers for glutamatergic axons, the difficulties in identifying glutamatergic spinal interneurons had hampered our understanding of the neuronal circuitry in the spinal cord.

Todd et al. (2003) were the first to carry out a detailed survey of VGLUT1 and VGLUT2 in the spinal cord. They found that terminals of local interneurons expressing markers which are usually not found in GABA- or glycine-immunoreactive cells contained VGLUT2, and were thus likely to be glutamatergic. Their study also showed that myelinated primary afferents contained VGLUT1, but not VGLUT2, and that inhibitory interneurons lacked both VGLUTs. Surprisingly, although unmyelinated C-fibres are also glutamatergic (Broman et al., 1993), they lacked VGLUT1 and were either unstained or

very weakly stained with a VGLUT2 antibody. Landry et al. (2003) showed that C-fibres also did not contain VGLUT3, suggesting that these fibres use a different VGLUT.

Ionotropic glutamate receptors in the spinal cord

AMPA receptors

mRNAs for all four subunits of the AMPA receptor have been identified in the spinal cord with *in situ* hybridization, but the level of expression for each subunit varied between laminae and there are some discrepancies between the results of different studies (Furuyama et al., 1993; Henley et al., 1993; Tölle et al., 1993, 1995b; Jakowec et al., 1995b; Shibata et al., 1999). The expression of GluR2 is strongest in the superficial laminae of the dorsal horn. Furuyama et al. (1993) found that strongly labelled cells formed a dense plexus in lamina II and the outer part of lamina III, while Tölle et al. (1993) reported that GluR2 mRNA was evenly expressed throughout laminae I-III. GluR2 expression was moderate in the deeper laminae of the dorsal horn and in the ventral horn (Furuyama et al., 1993). GluR1 mRNA levels were highest in laminae I and IIo (Tölle et al., 1993), moderate in laminae IIi and III and low in the ventral horn (Furuyama et al. 1993). In contrast, the expression of GluR3 and GluR4 was high in the ventral horn, while in the dorsal horn only occasional cells contained moderate levels of GluR3 mRNA and the expression of GluR4 was found to be extremely low (Furuyama et al., 1993). Tölle et al. (1995b) investigated the distribution of "Flip" and "Flop" splice variants in the rat lumbar spinal cord and found that in the dorsal horn the predominant mRNAs were GluR1 and GluR2 "Flip" while in the ventral horn the most abundant forms were GluR2 "Flip", GluR3 "Flip" and "Flop" and GluR4 "Flop".

Immunocytochemical studies at light and electron microscopic levels have also been carried out with antibodies against AMPA subunits (Tachibana et al., 1994; Jakowec et al., 1995a; Popratiloff et al., 1996, 1998a; Morrison et al., 1998; Spike et al., 1998) and the results of these studies were broadly similar to those obtained with *in situ* hybridization. However there is some controversy regarding the pattern of GluR1 and GluR2 expression by motoneurons (see below). Light microscopic immunocytochemistry with the various antibodies showed labelling of cell bodies and proximal dendrites, which is likely to represent subunits in transit. AMPA subunits located at asymmetrical synapses could not be revealed generally, as these sites appear to become inaccessible to antibodies during chemical fixation (see below). Another problem with these studies was that due to the lack of specific antibodies, the GluR2 and GluR3 subunits could not always be distinguished. This is because most antibodies directed against GluR2 cross-react with

GluR3 due to the considerable sequence homology between the C-terminals of these two subunits. Using antibodies against GluR1 and GluR2/3, Popratiloff et al. (1996) showed that GluR2/3 staining was substantial in the superficial dorsal horn, being strongest in lamina IIi, while GluR1 was concentrated in laminae I and IIo. GluR2 or GluR2/3 immunostaining has been found in neurons in other parts of the gray matter including lamina IX, while there is general agreement that adult motoneurons do not express GluR1 (Jakowec et al., 1995a; Popratiloff et al., 1996; Morrison et al., 1998; Engelman et al., 1999). However there have also been reports that motoneurons have GluR1 (Pellegrini-Giampietro et al., 1994; Virgo et al., 1996; Temkin et al., 1997; Williams et al., 1997; Bar-Peled et al., 1999; Shibata et al., 1999) or lack GluR2 subunits (Williams et al., 1997; Bar-Peled et al.,1999; Del Cano et al., 1999; Shaw et al., 1999). GluR4-immunoreactive cells were present in all laminae except I-II.

Although synaptic iGluRs are masked following fixation, using postembedding immunocytochemistry Popratiloff et al. (1996, 1998a) showed clustering of gold particles, representing GluR1 and GluR2/3 subunits, over the postsynaptic density, postsynaptic membrane and cleft of certain asymmetrical synapses in the dorsal horn. Presynaptic profiles could be identified as being of both primary afferent and interneuronal origin. Synapses formed by both types of synaptic glomeruli were labelled, but to a different extent. Synapses formed by type I glomeruli were predominantly GluR1-positive, while those formed by type II glomeruli were more often GluR2/3-immunoreactive. As expected, labelling was not observed over symmetrical synapses, which are likely to have been predominantly inhibitory. Morrison et al. (1998) and Ragnarson et al. (2003) used the postembedding method to examine AMPA receptors in the ventral horn. Morrison et al. found that the percentage of GluR2-labelled synapses and the number of gold particles at individual synapses did not differ between dorsal and ventral horn. Ragnarson et al. provided evidence that synapses on motoneurons possessed GluR2/3 and GluR4 subunits, but not GluR1, suggesting that chemical transmission at Ia synapses is mediated through GluR2/3 and GluR4 receptors.

The high level of GluR2 expression in the dorsal horn suggests that many of the AMPA receptor complexes in this region are impermeable to Ca^{2+}. However, using Ca^{2+}-sensitive indicator dyes, Reichling and MacDermott (1993) demonstrated that a small population of neurons in laminae I and IIo express significant levels of Ca^{2+}-permeable AMPA receptors. Ion permeability studies (Goldstein et al., 1995; Nagy et al., 1994; Engelman et al., 1997, 1999) and pharmacology (Gu et al., 1996) were also used to demonstrate the presence of these receptors in the dorsal horn. Many dorsal horn neurons

co-express Ca^{2+}-permeable and impermeable AMPA receptors (Goldstein et al., 1995, Gu et al., 1996, Vandenberghe et al., 2001). GluR1- and GluR2-expressing dorsal horn neurons were neurochemically characterized by Spike et al. (1998). Using preembedding and postembedding immunocytochemistry they showed that 52% of GluR1-immunoreactive neurons were GABA-immunoreactive, 26% were GABA- and glycine-immunoreactive and 22% did not contain either of these inhibitory transmitters. On the other hand 96% of the neurons immunostained for GluR2/3 were not GABA- or glycine-immunoreactive. Five markers were used to characterize the GluR1- and GluR2-immunoreactive neurons further. Neurotensin (NT) and somatostatin (SOM) are mainly associated with excitatory interneurons, while parvalbumin (PA), nitric oxide synthase (NOS) and choline acetyltransferase (ChAT) are generally found in inhibitory neurons. Double-immunofluorescence and confocal microscopy showed that virtually all NT- and SOM-immunoreactive cells were GluR2/3-immunoreactive, but were not stained for GluR1, whereas parvalbumin was always colocalized with GluR1 but usually not with GluR2/3. Approximately half of the NOS-expressing cells were labelled with either the GluR1 or the GluR2/3 antibody, and all of the ChAT-immunoreactive cells tested were immunoreactive for GluR1 and GluR2/3. Based on these results the authors concluded that GluR1 subunits are mainly associated with inhibitory neurons and GluR2 with excitatory ones. The presence of GluR1, but not GluR2 in cell bodies of parvalbumin-immunoreactive neurons makes it likely that at least some of these inhibitory neurons express Ca^{2+}-permeable AMPA receptors. This is consistent with the results from cortical structures, where Ca^{2+}-permeable AMPA receptors were restricted to subpopulations of GABAergic interneurons (Kharazia et al., 1996; Racca et al., 1996). In addition, Stanfa et al. (2000), reported facilitation of C-fibre evoked responses in dorsal horn neurons, by Joro spider toxin, a selective antagonist of Ca^{2+}-permeable AMPA receptors. They concluded that functional Ca^{2+}-permeable AMPA receptors within the spinal cord were present predominantly within inhibitory pathways. Kainate-induced cobalt loading studies on cultured spinal neurons showed that 59% of GABAergic inhibitory neurones expressed Ca^{2+}-permeable AMPA receptors (Albuquerque et al., 1999). These authors also found these receptors on 77% of NK1-receptor-immunoreactive (presumably excitatory) neurons. Engelman et al. (1999) also reported that a proportion of lamina I NK1-receptor expressing cells possess AMPA complexes with Ca^{2+}-permeability. The role of Ca^{2+}-permeable AMPA receptors in the dorsal horn is poorly understood. These receptors have also been identified on motoneurons in the ventral horn (Carreido et al. 1996, 2000; Vandenberghe et al., 2000a, 2000b, 2001; van Damme et al., 2002; Kawahara et al., 2003), where they have

been implicated in excitotoxicity and neurodegeneration in amyotrophic lateral sclerosis (for review see Strong and Rosenfeldt, 2003).

Although most AMPA receptors are likely to be located at glutamatergic synapses, there is evidence that they are also expressed by primary afferents. Both mRNA for AMPA receptors and the proteins themselves were detected in dorsal root ganglion neurons (Huettner, 1990; Partin et al., 1993; Sato et al., 1993; Tachibana et al., 1994; Chambille and Rampin, 2002; Lu et al., 2002). Using immunocytochemistry at the light and electron microscopic level, Lu et al. (2002) found AMPA receptors in central terminals of primary afferents in the dorsal horn following weak fixation. These are though to represent presynaptic receptors. With immunofluorescence, axonal labelling corresponding to GluR4 or GluR2/4 was mainly found in laminae I and II and was colocalised with IB4-binding (representing non-peptidergic C-fibres). Axonal labelling for GluR2/3 subunits was mainly present in laminae III and IV and appeared to be present in myelinated fibres, which were labelled by transganglionically transported cholera toxin b subunit (CTb). GluR2/3 was also present in terminals of inhibitory interneurons. Immunostaining for GluR1 or GluR2 was very rarely detected in axon terminals or in DRG neurons, suggesting that the GluR2/3 and GluR2/4 antibody labelled presynaptic GluR3 and GluR4 subunits. Lee et al. (2002) demonstrated that activation of presynaptic AMPA receptors caused inhibition of glutamate release from the primary afferent terminals, possibly via primary afferent depolarization (PAD). These findings challenge the traditional view that GABA acting on $GABA_A$ receptors exclusively mediates PAD.

Functionally, AMPA receptors in the dorsal horn have mainly been implicated in acute pain (Nishiyama et al., 1998; Kontinen 2002; Voitenko et al., 2004), although it has also been suggested, that they play a role in central sensitization (Sang et al., 1998; Stanfa and Dickenson, 1999) and in chronic pain of both neuropathic and inflammatory origin (Chaplan et al., 1997; Garry et al., 2003). For a more detailed discussion on the role of AMPA receptors in central sensitization see Chapter 5.

Kainate receptors

Our knowledge about kainate receptors in the spinal cord is very limited, mainly due to the lack of reliable, subunit-specific antibodies. However, it is generally accepted that kainate receptor subunits are not abundant in the cord. *In situ* hybridization studies detected a relatively high level of KA2 subunit and moderate levels of GluR5 (mainly in lamina I) and of GluR7 (in laminae I-II), while GluR6 subunits were not detected (Tölle et al., 1993). Dai et al. (2002) used single cell RT-PCR on cultured rat spinal cord neurons

and found high levels of GluR7 and KA2, moderate levels of GluR5 and low levels of GluR6 and KA1. Adult motoneurons in the ventral horn are thought not to express kainate receptors (Stegenga and Kalb, 2001).

There is evidence to suggest that kainate receptors in the spinal cord are mostly found presynaptically on primary afferent terminals. Agrawal and Evans (1986) reported that kainate depolarized those dorsal root ganglion cells which gave rise to C-fibres, and this was confirmed by Heuttner (1990). Using immunocytochemistry, Petralia et al. (1994a) detected GluR6/7 and KA2 in dorsal root ganglion cells, while other studies have found GluR5 mRNA and protein in primary afferent terminals or DRG cells (Partin et al., 1993; Sato et al., 1993; Woolf and Costigan, 1999). Hwang et al. (2001) carried out a detailed survey of GluR5/6/7 receptors in the superficial laminae of the dorsal horn and found that following weak fixation approximately two-thirds of GluR5/6/7 puncta were in axon terminals. They also reported that 20% and 40% of these puncta colocalised with IB4-binding or with transganglionically transported CTb, respectively. This suggests that despite the evidence from physiological studies (Agrawal and Evans, 1986; Heuttner et al., 1990) presynaptic kainate receptors are not limited to one functional class of primary afferent. A study which combined electrophysiology and pharmacology provided strong evidence that presynaptic kainate receptors can reduce glutamate release from the terminals of fine diameter primary afferents, and thus modulate one of the most important steps of nociceptive information processing (Kerchner et al., 2001b). Lee et al. (2002) concluded that this inhibition is probably also caused by PAD. Behavioural studies are consistent with these findings, showing that a GluR5 agonist (ATPA) has antinociceptive effects in acute pain and hyperalgesic states (Procter et al., 1998; Mascias et al., 2002).

Some of the kainate receptors expressed in the spinal cord are thought to be present on axon terminals of inhibitory interneurons where they are activated by the spillover of glutamate from primary afferent terminals and facilitate GABA or glycine release from these inhibitory terminals (Kerchner et al., 2001a). Presynaptic kainate receptors on inhibitory terminals can be either sensitive or insensitive to ATPA, suggesting that some contain GluR5 subunits, while other lack them.

It is also clear that KA receptors are not restricted to presynaptic sites. Li et al. (1999b) showed that high-intensity stimulation of primary afferent fibers evokes fast, KA receptor-mediated EPSPs in the superficial dorsal. Activation of postsynaptic kainate receptors could enhance the transmission of nociceptive signals, and in addition could play a role in synaptic plasticity (Ruscheweyh and Sandkühler, 2002). These postsynaptic KA receptors are ATPA-insensitive, thus not likely to contain significant levels of GluR5.

Despite these findings, our knowledge about the role of KA receptors in spinal sensory transmission cannot be complete without the development of selective and sensitive antibodies and subsequent immunohistochemical examination.

NMDA receptors

NMDA NR1, NR2 and NR3 subunits have all been detected in the spinal cord. As in the case of the other two iGluRs, these show a differential expression pattern throughout the gray matter, which is further complicated by the presence of different splice variants. Very few studies have used immunocytochemistry to investigate the distribution of NMDA receptors in the spinal cord (and even these have mainly focused on the NR1 subunit) and therefore most of our knowledge comes form *in situ* hybridization experiments.

Moderate to high levels of NR1 subunit mRNAs have been found throughout the spinal cord gray matter with *in situ* hybridization (Furuyama et al., 1993; Tölle et al., 1993; Luque et al., 1994; Shibata et al., 1999). Furuyama et al. (1993) and Kus et al. (1995) reported that the expression of NR1 was much higher in the ventral horn than in the dorsal horn. Tölle et al. (1995a) examined the distribution of different NMDA NR1 splice variant mRNAs in the rat lumbar spinal cord. NMDA NR1-a, NR1-1, NR1-2 and NR1-4 mRNAs were evenly distributed throughout all laminae of the dorsal horn. NMDA NR1-b mRNA was preferentially detected in laminae IIi and lamina III. NMDA NR1-3 was only found at very low levels and was restricted to laminae I and II. Serial sections of single neurons were also examined, and it was reported that one neuron could express multiple splice variants of NR1. Luque et al. (1994) concluded that most neurons in the dorsal horn expressed the NR1-3b isoform. Prybylowski et al. (2001) used cassette-specific antibodies on Western blots to examine the spinal expression of these splice variants and found that 25-35% of the NR1 subunits contained the N_1-cassette, 5% the C_1-, <20% the C_2-, and >80% the C_2'-cassette (Table 1.1). They therefore concluded that the dominant form of the NR1 subunit in adult rat spinal cord were NR1-4a and NR1-4b. Using a polyclonal affinity-purified rabbit antibody directed against the C_2-cassette of NR1 (specific for NR1-1 and NR1-2 splice variants), Popratiloff et at. (1998a) found NR1 labelling in laminae I-IIf of the dorsal horn. Neuropil staining was the densest in laminae I and IIo and got progressively weaker through lamina IIi and lamina III. The prominent staining in lamina II was probably due to the high density of neurons in this lamina. At the electron microscopic level with postembedding immunocytochemistry, gold particles were associated with asymmetrical synapses and they were centered on the PSDs. Profiles associated with primary afferents and with neurons of unknown origin were labelled.

Primary afferent terminals in both types of synaptic glomeruli and fibres with dome-shaped terminals (many of which are of primary afferent origin) all made synapses with NMDA NR1 receptor expressing spinal neurons. In an electron microscopic investigation using preembedding immunocytochemistry, Aicher et al. (1997) reported that NR1 subunits were postsynaptic to SP-containing axon terminals in the superficial dorsal horn.

There were controversial reports about which NR2 subunits are expressed in the gray matter. Tölle et al. (1993) originally only described NR2D mRNA in the lumbar spinal cord, but eventually all NR2 splice variant mRNAs were detected (Luque et al., 1994; Watanabe et al., 1994a; Boyce et al., 1999; Shibata et al., 1999). NR2A mRNA was found in all laminae except lamina II, while NR2B was more or less restricted to the lamina II. Motoneurons are thought to express mRNA for NR2A and NR2D, although contradicting with this, Shibata et al. (1999) found NR2B mRNA in somatomotor neurons. NR2C is expressed in very low levels in small cells, presumably glial cells, scattered around the gray and white matter (Watanabe et al., 1994b; Shibata et al., 1999).

NR3A mRNA is present throughout the dorsal horn, but higher levels were found in laminae II-III than in lamina I (Ciabarra et al., 1995; Wong et al., 2002). Motoneurons in neonatal rats also express NR3A (Abdrachmanova et al., 2000). In contrast, NR3B shows a restricted distribution in the spinal cord. It is present at high levels in somatic motoneurons, much lower levels in visceromotor neurons and appears to be absent from the dorsal horn (Nishi et al., 2001; Chatterton et al., 2002; Matsuda et al., 2002).

As with AMPA and kainate receptors, it has been suggested that NMDA subunits play a role in the regulation of presynaptic transmitter release in the dorsal horn of spinal cord. Shigemoto et al. (1992) and Watanabe et al. (1994b) were the first to describe NMDA NR1 mRNA in rat dorsal root ganglia. Shortly after this Liu et al. (1994) used an affinity purified antibody against a C-terminal peptide of NR1 to detect the protein itself in DRG and primary afferent terminals with Western blot and immunocytochemistry, respectively. It was also reported that the activation of presynaptic NDMA receptors on nociceptive primary afferents facilitated and prolonged glutamate and SP release from these fibres (Liu and Basbaum, 1997; Malcangio et al., 1998). However, this view has recently been challenged by Bardoni et al. (2004), who proposed that presynaptic NMDA receptors actually play a role in the inhibition of glutamate release from terminals.

Several pharmacological, electrophysiological and behavioural studies suggest that NMDA receptors play a major role in acute pain (Raigorodsky et al., 1990; Sakurada et al., 1998). As can be expected from their physiological properties NMDA receptors are not only involved in the "simple" transduction of nociceptive information, but are also

responsible for long term changes in the excitability of spinal cord neurons that are thought to underlie chronic pain states (Dubner and Ruda, 1992; King et al., 1993; Kolhekar et al., 1993; Neugebauer et al., 1994; Baranauskas and Nistri, 1998). Following stimulation of C-fibres, many dorsal horn neurons become increasingly sensitive to various forms of stimulation, a phenomenon termed central sensitisation (Woolf, 1996; Li et al., 1999; Willis, 2002; Ji et al., 2003). The magnitude of this hyperexcitability is related to the activity of C-fibres. Following extensive and prolonged noxious stimulus such as peripheral inflammation, nerve injury, capsaicin or formalin injection, central sensitisation is very prominent and may result in an altered form of sensation, referred to as hyperalgesia or allodynia. Allodynia is defined as pain resulting from normally innocuous stimuli (e.g. touching an inflamed skin region or movement of the arthritic joint), while hyperalgesia is the increased sensation of pain following a noxious stimulus ("pain of being slapped on a sunburnt back"). NMDA receptor antagonists reduce acute pain (Meller et al., 1992), but they also effectively inhibit the central sensitisation, LTP or *c-fos* expression of dorsal horn neurons following nerve-injury, electric stimulation or chemically induced inflammation (Ren et al., 1992a; Mao et al., 1992; Chapmann et al., 1992a; Neugebauer et al., 1993; Ma and Woolf, 1995; Liu and Sandkuhler, 1995; Huang et al., 1999a, 1999b). In addition NMDA receptor antagonists reduce hyperalgesia and allodynia in experimental animals (Ren et al., 1992a, 1992b, 1993; Yamamoto and Yaksh, 1992a, 1992b; Eisenberg et al., 1995; Spraggins et al., 2001) and also provide means of controlling neuropathic pain in humans (Eide et al., 1994; Eisenberg et al., 1994; Bennett, 2000; McCartney et al., 2004). Knock down of spinal NMDA NR1 receptors with anti-sense oligonucleotides or with the injection of adeno-associated virus expressing Cre recombinase into floxed NR1 mice, also reduces NMDA- and formalin-evoked behaviours and prevents the development of central sensitization in dorsal horn neurons (Garry et al., 2000; Yukhananov et al., 2002; South et al., 2003). Taniguchi et al. (1997) found that selective NR2B receptor antagonists have a marked analgesic effect in carrageenan-induced hyperalgesia, without the behavioral side-effects of other, non-selective NMDA receptor antagonists. These results are consistent with the fact that NR2B subunits are preferentially expressed in lamina II, an area of the dorsal horn where C-fibres terminate (Boyce et al., 1999). These findings were later confirmed by other studies, further emphasizing the importance of NR2B subunits in pain (Chazot et al., 2004; Kovács et al., 2004; McCauley et al., 2004). The generation of central sensitisation not only depends on NMDA receptors, but mGluR, AMPA, GABA, NK-1 receptors, neuropeptides and a number of second messengers have also been implicated (Dougherty et al., 1991a, 1991b;

Willis, 2002). It is generally accepted that central sensitisation involves either the phosphorylation of NMDA receptor proteins by PKC and PKA or the long term depolarization of the cell membrane (e.g. by NK1 receptor activation) leading to reduction of the Mg^{2+}-blockade on the NMDA receptor, which then remains increasingly sensitive to glutamate (1992; Baranauskas and Nistri 1997; Bennett 2000; Herrero et al., 2000; Zou et al., 2000, 2002; Begon et al., 2001; Yahspal et al., 2001; Willis, 2002).

Interestingly, there is emerging evidence, that NMDA receptors may also be involved in the inhibition of nociceptive signals. Inoue et al. (2000) found that SP-induced nociception was enhanced in NMDA NR2A knock-out mice, and suggested that this subunit may play an inhibitory role in the "downstream mechanisms" of SP-containing nociceptive primary afferents, possibly through activation of unidentified inhibitory neurons. Zou et al. (2001) provided the first evidence that inhibitory interneurons are activated by NMDA receptors, by showing that in rats an NMDA receptor antagonist attenuated *c-fos* expression in GABAergic neurons in the dorsal horn following intradermal injection of capsaicin. Ahmadi et al. (2003) have recently shown that during high levels of presynaptic activity, glycine released from inhibitory interneurons escapes the synaptic cleft and reaches nearby NMDA receptors by spillover. As glycine is required for full activation of NMDA receptors, they suggested that this spillover may contribute to the development of inflammatory hyperalgesia, and thus the excitation of inhibitory neurons can paradoxically lead to enhanced nociception.

NMDA receptors also play a role in spinal cord development and ventral horn physiology and pathology. Several authors have demonstrated a spatiotemporal change in NMDA receptor expression pattern in mouse and rat spinal cord during development (Hori et al., 1994; Watanabe et al., 1994b; Dunah et al., 1996), while Kalb (1994) showed that blocking NMDA receptors inhibited motoneuron cell body growth and dendritic branching. NMDA binding sites and mRNA for the NR1 and NR2A subunits were markedly decreased in human patients suffering from amyotrophic lateral sclerosis (Virgo et al., 1995; Samarasinghe et al, 1996). Nerve injuries, such as ventral root avulsion or postnatally performed sciatic nerve section, which lead to motoneuron death had similar effects on NMDA subunits in rats (Piehl et al., 1995). It is not clear whether this reduction plays a role in the pathogenesis of the cell death or it is due to the loss of motoneurons. NMDA-mediated acute excitotoxicity has also been described in the spinal cord and neuronal loss is thought to be initiated through mitochondrial Ca^{2+}-overload and the generation of free oxygen radicals caused by the activation of NMDA receptors (Urushitani et al., 2001).

AIMS OF THE STUDY

Despite extensive research, very little is known about the synaptic distribution of iGluRs in the spinal cord and their involvement in particular neuronal circuits. The aim of the investigations presented in this thesis was to examine the expression of AMPA (GluR1-4) and NMDA (NR1, NR2A, NR2B) receptor subunits at glutamatergic synapses in the gray matter of rat lumbar spinal cord using immunocytochemistry at the light and electron microscopic level.

Investigation 1

Aims: (1) to investigate whether somatostatin- and enkephalin-containing interneurons in the dorsal horn are glutamatergic and (2) form synapses that contain AMPA receptors.

Somatostatin and enkephalin are among the most important sensory neuropeptides in the dorsal horn. However, it is still not known whether intrinsic neurons, immunoreactive for these peptides, also use a classical amino-acid transmitter. There is evidence to suggest that that somatostatin-containing interneurons and the majority of enkephalin-containing axon terminals are glutamatergic (Todd et al. 2003). Two different approaches were used to test these hypotheses: (1) triple-labelling immuno-fluorescence and confocal microscopy was carried out to examine whether somatostatin-immunoreactive axon terminals belonging to interneurons express VGLUT1 or VGLUT2; (2) post-embedding immunogold labelling was used on freeze-substituted, Lowicryl-embedded material to reveal GluR1 and GluR2/3 subunits of the AMPA receptors at synapses formed by somatostatin- or enkephalin-immunoreactive axons.

Investigation 2

Aims: (1) to investigate the receptor expression pattern of synapses formed by SP- and CGRP-containing nociceptive primary afferent terminals on to large, NK1-immunoreactive projection neurons and (2) to describe the synaptic distribution of NMDA receptors in the dorsal horn.

NK1-immunoreactive projection neurons in lamina III/IV, with dendrites projecting dorsally to the superficial laminae, receive strong synaptic input from nociceptive primary afferents. These cells are very important in the processing of nociceptive information (Todd 2002). To allow the identification and examination of these neurons, a novel method was developed for combining post-embedding electron microscopy with

immunofluorescence and confocal microscopy. Two representative NK1-immunoreactive cells were selected with the confocal microscope and following freeze-substitution serial ultra-thin sections were cut through the dendritic tree of these neurons and reacted with antibodies against SP, CGRP and various iGluR subunits. The postembedding immunogold technique was also used to reveal NMDA receptors at synapses in the dorsal horn.

Investigation 3

Aims: (1) to investigate the laminar distribution of GluR1-4 subunits of the AMPA receptor at glutamatergic synapses in the spinal cord, (2) to study the colocalization of various AMPA subunits, (3) to examine the relationship of GluR1 and GluR2 to different types of glutamatergic axon, and (4) to determine whether morphologically detectable changes involving synaptic AMPA receptors occur in response to a peripheral noxious stimulus.

To reveal AMPA receptors at synapses the antigen unmasking technique involving limited proteolytic digestion with pepsin was used. To examine the colocalization of various AMPA subunits and their relationship to different types of glutamatergic axon, triple-labelling immunofluorescence was carried out. Boutons belonging to peptidergic and non-peptidergic C-fibres were identified by CGRP-immunoreactivity and IB4-binding, respectively. Myelinated primary afferents were revealed by VGLUT1, while VGLUT2 was used as a marker for terminals of excitatory interneurons. Electron microscopy was used to confirm that the punctate receptor labelling seen after antigen unmasking represented synaptic receptors. To investigate functional changes involving synaptic AMPA receptors, the phosphorylation of GluR1 was examined following the noxious chemical stimulation of the hindpaw with capsaicin.

Investigation 4

Aims: (1) to investigate the laminar distribution of NR1, NR2A and NR2B subunits of the NMDA receptor at glutamatergic synapses in the spinal cord, (2) to study the colocalization of NR1 with NR2A or NR2B and (3) to examine the relationship of these subunits to GluR2.

Antigen unmasking with pepsin was used to reveal NMDA subunits at synaptic sites. To examine colocalization of NR1, NR2A and NR2B with GluR2, or NR1 with NR2A or NR2B dual-labelling immunofluorescence was carried out.

Chapter 2

Detection of synaptic receptors with the postembedding immunogold method and optimization of the technique

A variety of morphological methods have been used during the course of this study. These include immunofluorescence, signal amplification techniques, conventional preembedding electron microscopic immunocytochemistry, postembedding immunogold labelling following freeze-substitution, antigen retrieval, antigen unmasking techniques, combined confocal and electron microscopy, serial sectioning and 3D reconstruction. Some of these methods are widely used in neurobiology research, while others, such as postembedding immunogold labelling are more specialised and used only in a limited number of laboratories. This chapter focuses on the theoretical background and optimization of this specialised method. The remaining techniques are described in the appropriate chapters, while the composition of buffers and other solutions used during the experiments is provided in the Appendix.

DETECTION OF SYNAPTIC GLUTAMATE RECEPTORS WITH THE POSTEMBEDDING METHOD

The proper understanding of neuronal circuits can only be accomplished with the use of accurate and sensitive morphological methods. Immunocytochemistry has been used for a long time to study the localization of proteins in the CNS, including that of iGluRs. However, the detection of receptors at asymmetrical, glutamatergic synapses has been hampered by the fact that antibodies cannot penetrate into the elaborate protein meshworks of the synaptic cleft and post-synaptic density, especially when the proteins are extensively cross-linked as a result of chemical fixation (e.g. Baude et al., 1995). The main approach used to overcome this problem with antibody penetration is postembedding immunocytochemistry. With this technique antibodies only react with antigens protruding from the cut surface of resin embedded ultrathin sections, therefore there is no need for antibody penetration. However, tissue prepared according to conventional EM processing methods is still not suitable for the postembedding immunogold detection of synaptic proteins. This is due to severe unwanted changes in the native state of the tissue, caused by chemicals used during conventional processing (Kellenberger et al., 1992).

Theoretical background

To examine biological material with transmission electron microscopy two main goals have to be achieved: the first is to preserve the tissue in as near to its native state as possible. This is generally accomplished by chemical fixation with cross-linking agents such as formaldehyde (1-4%) and glutaraldehyde (0.05-4%) for the preservation of proteins, and osmium tetroxide for the retention of lipids. The second goal is to make the

tissue hard enough to allow sections, approximately 60-70 nm thick, to be cut with a diamond knife. This is achieved by embedding the tissue in artificial resins which are then polymerised, most commonly by heating. For conventional embedding, generally epoxy-resins are used. Since most EM-resins are hydrophobic, a dehydration step has to be incorporated between fixation and embedding to remove water from the specimen. This involves treating the sections with graded concentrations of ethanol or acetone.

Cross-linking during chemical fixation (especially with high concentration of glutaraldehyde) not only reduces the penetration of antibodies, but also changes the conformation of proteins, which can result in loss of antigenicity. Osmium also dramatically reduces the antigenicity (Phend et al., 1995). Although decreasing the concentration of these fixatives might have a beneficial effect on antigenicity, it is likely to result in poor structural preservation. Dehydration with ethanol or acetone at room temperature and polymerisation of the resin with heat also denature proteins (Iwasa and Kondo 1999). A characteristic feature of epoxy-resins is that they react with the side chains of tissue proteins, thus incorporating the specimen into the three dimensional structure of the plastic. As a result, this makes it more difficult for primary antibodies to bind to the epitopes they were raised against.

These effects result in a major loss of antigenicity and make conventional postembedding immunocytochemistry unsuitable for the detection of synaptic iGluRs. Freeze substitution is a powerful method, which results in excellent ultrastructural preservation and maintains good antigenicity (Baude et al., 1995; Bernard et al, 1997, Matsubara et al., 1996; 1997; Clarke and Bolam, 1998; Nagelhus et al., 1998; Nüsser et al., 1998; Takumi et al., 1999; Racca et al., 2000; Sassoe-Pognetto and Ottersen, 2000). Freeze-substitution with low-temperature embedding has been developed gradually during the past 50 years. The combination of these methods can overcome many of the problems associated with conventional EM techniques (Shiurba, 2001).

Tissue processing for freeze-substitution resembles the conventional processing described above, in that it also consists of fixation (cryoimmobilization), dehydration (substitution, cryosubstitution) and embedding (Parthasarathy, 1995; Kellenberger, 1991; Kiss and McDonald, 1993). Freezing is achieved by the ultra-rapid cooling (10^4°C/sec) of cryoprotected tissue that has been fixed with 4% formaldehyde and a very low concentration of glutaraldehyde (0.1%), to a temperature below -80°C. Rapid cooling immobilizes the cellular water in a noncrystalline (vitrified) state in milliseconds. As the structure of vitrified water is analogous to that of liquid water, cellular components become immobilized in a state similar to their native form. Although several procedures have been

developed to achieve rapid cooling, the most straight-forward is immersion freezing. This involves plunging the specimen into a liquid cryogen at -180°C.

Cryotechniques are not only used for the freezing, but also during dehydration and embedding of the sections. The most effective method for low-temperature dehydration is freeze-substitution, when ice is dissolved by an organic solvent at -90°C. At such low temperatures, organic solvents and lipids in the tissue behave differently than at room temperature. Under these conditions, lipids are not extracted by the organic solvents and therefore the use of osmium for preserving membranes can be avoided. In addition, far less protein denaturation and precipitation occurs during freeze-substitution than during conventional dehydration (Bohrmann and Kellenberger, 2001). Usually anhydrous acetone or methanol is used with or without a mild secondary fixative such as uranyl acetate, tannic acid or potassium permanganate. These compounds are added to the substitution medium to achieve a better preservation of lipids. For low-temperature embedding acrylate-, or acrylate-methacrylate-resins (e.g. Lowicryl HM20, HM23) are used, as they do not react with the side-chains of tissue proteins and also they can be polymerised by UV light instead of heat, at temperatures as low as -45°C.

In summary, immersion freezing followed by freeze-substitution, low-temperature resin-embedding and UV polymerisation result in excellent preservation of ultrastructure and antigenicity. Therefore, this technique has been used in previous studies to examine the exact cellular, subcellular, synaptic and subsynaptic distribution of iGluRs (e.g. Matsubara et al., 1996, 1999; Landsend et al., 1997, Sassoè-Pognetto et al., 2000, 2003).

Optimization of the freeze-substitution protocol

All animal experiments carried out during the course of this project were approved by the Ethical Review Process Applications Panel of the University of Glasgow, and were performed in accordance with the UK Animals (Scientific Procedures) Act 1986. Every measure was taken to minimize the distress, pain or suffering caused to the animals.

To obtain spinal cord tissue, generally adult male Wistar rats were used (200–350 g; Harlan, Loughborough, UK; exceptions are described in the appropriate chapters). Animals were deeply anaesthetized with an intraperitoneal injection of pentobarbitone (1000 mg/kg) and the thoracic cavity was opened through an anterior incision. A needle was inserted into the left ventricle, meanwhile a small incision was made in the right atrium to allow the blood and excess fixative to leave the blood vessels. Animals were first perfused for 5 seconds with mammalian Ringer's solution containing 0.05% lidocaine hydrochloride. Chemical fixation was achieved by perfusing with one of the following

fixatives: (1) 4% formaldehyde in 0.1 M phosphate buffer, pH 7.4, (2) 4% formaldehyde and 0.1% glutaraldehyde in 0.1 M phosphate buffer, pH 7.4 or (3) 4% formaldehyde in 0.2 M acetate buffer, pH 6.0, followed by formaldehyde in 0.2 M sodium carbonate buffer, pH 10.5 (pH shift protocol). The pH shift protocol was tested as it was previously found to enhance the sensitivity of immunogold labelling for aquaporin-4 water channels (Nagelhus et al., 1998). There was no significant difference in the quality of iGluR immunolabelling of tissue processed with the different fixation protocols. Therefore 4% formaldehyde / 0.1% glutaraldehyde was used for the subsequent studies, as this provided the best ultrastructural preservation.

After the transcardiac perfusion an incision was made on the back of the animals, muscles surrounding the dorsal surface of the vertebral column were removed and laminectomy was carried out to expose the spinal cord. The dura mater was carefully opened. Based on the position of the dorsal roots in relation to the 13th rib and the lumbar vertebrae L_1-L_6, lumbar spinal cord segments were identified, cut into blocks and removed.

For freeze-substitution, tissue was postfixed for 4 h in the same fixative and cut into 300-500 µm transverse sections with a Vibratome. Although there are reports that satisfactory freezing is limited to a few micrometers from the surface (Bennett, 1997), other studies have showed that thick sections can be successfully frozen throughout their entire depth. These 300-500 µm sections are relatively easy to handle during processing and are much less fragile than thinner sections. The spinal cord slices were stored overnight in 4% glucose in phosphate buffer (PB) and cryoprotected in increasing concentrations of glycerol (10%, 20% and 30% in PB for at least 30 min each). Cryoprotection is crucial to minimize crystalline ice formation, which would cause disruption to the tissue and seriously compromise the ultrastructure.

Following cryoprotection sections were placed on the head of a metal specimen pin (diameter 3.5 mm) and the excess buffer was removed with a filter paper. The tissue was then rapidly immersed in liquid propane cooled by liquid nitrogen at –196°C using a Leica EM Cryopreparation Chamber (CPC). The temperature of the propane was kept below - 170°C during freezing. Liquid propane was used as a cryogen as it has a higher heat capacity than that of liquid nitrogen and therefore provides faster cooling. In addition, because the boiling point of liquid nitrogen is much lower (–196°C) than that of liquid propane (–42°C), it would vigorously start to boil when the tissue is immersed and the bubbles formed around the tissue would make the cooling less effective.

Frozen sections were removed from the pin and transferred to a Leica EM Automatic Freeze Substitution (AFS) apparatus, where freeze-substitution was carried out

by a modification of the method of van Lookeren Campagne et al. (1991). Sections were immersed in 0.5-1.5% uranyl acetate in anhydrous methanol for 24 h at –90°C. Methanol was chosen as substitution medium because it can substitute specimens in the presence of substantial amounts of water and also the substitution time is much shorter than for acetone. To avoid secondary ice crystal formation, the temperature was gradually (4°C/h) raised to –45°C. Sections were then rinsed three times with anhydrous methanol and infiltrated with graded concentrations of Lowicryl HM20 (methanol:resin 1:3, 1:1, 3:1, for 1 h each, followed by several rinses in pure resin over a 24 h period). The free radical polymerization of Lowicryl is strongly inhibited by the presence of oxygen (Acetarin et al., 1986). To displace any dissolved oxygen, dry nitrogen gas was bubbled through the resin on a fume bench. Lowicryl HM20 is a very volatile liquid, with irritant vapors. To minimize chemical contact, the pre-mixed Monostep Lowicryl was used in some experiments, rather than the Lowicryl kit, where the resin has to be made up from three components. Following infiltration, sections were carefully transferred to moulds for flat embedding. All items that were to be used in the embedding procedure were dried in an oven at 60°C before being used. Although flat embedding proved to be technically more difficult than embedding in closed capsules, this approach was chosen as it allows the transillumination of the blocks and the subsequent identification of particular regions of interest in selected spinal cord laminae. In initial experiments a common problem was the failure of the resin to polymerise after UV irradiation. This was probably caused by oxygen entering the AFS chamber and dissolving in the resin during manipulations. To avoid this, the nitrogen evaporator control was turned to its maximum and the flat embedding moulds and the plastic caps covering them were filled with liquid nitrogen before being inserted into the chamber. Care was taken during these manipulations to avoid any sudden temperature change inside the chamber. Following flat-embedding, moulds were covered with plastic caps and the resin was cured with 360 nm ultraviolet irradiation (48 h at –45°C, 9 h at –45-0°C and 24 h at 0°C).

The 300-500 μm thick resin-embedded transverse spinal cord sections were trimmed and ultrathin sections (generally in the sagittal plane) were cut with a diamond knife. This approach resulted in a 300-500 μm wide strip of tissue, which included all dorsal horn laminae and the ventral horn.

Optimization of the postembedding protocol

During preliminary experiments several postembedding protocols were tested. There were four critical steps or conditions, which clearly increased the sensitivity of

immunogold labelling: (1) etching with a saturated solution of sodium hydroxide in ethanol to remove the resin from the section surface, (2) using a low concentration of NaCl (0.3%) in the buffers, (3) prolonging incubation in primary antibody (>12 hours) at room temperature, and (4) the use of small (10 nm) gold particles coupled to the F_{ab}-fragments of the secondary antibody (Matsubara et al., 1996).

Etching was carried out for 2-3 seconds prior to postembedding incubation and was followed by several rinses in ultra-pure water. Increasing the time for etching above 3 seconds significantly deteriorated the ultrastructural preservation of the tissue. Another drawback of etching was that it caused "wrinkling" of sections and the resulting folds made serial reconstruction very difficult. This "wrinkling" could be reduced if sections were not processed immediately after cutting, but were allowed to dry for several days. Other methods tested for removing the resin from the sections, such as H_2O_2-treatment or incubation in sodium metaperiodate, did not prove to be as effective as etching with sodium ethanolate.

Decreasing the NaCl concentration from 0.9% to 0.3% dramatically increased the sensitivity of the postembedding method, although it also increased background immunolabelling. Using 0.9% NaCl, only occasional synapses were labelled and these contained few gold particles. With 0.3% NaCl both the number of immunoreactive synapses and the number of gold particles/synapse increased. Immunoreactive synapses contained up to 30 gold particles.

The F_c-fragment of antibodies can bind non-specifically to tissue proteins (Arli et al., 1975; Costa et al., 1984). The use of secondary antibodies consisting only of F_{ab}-fragments at least partly avoids this problem. Removing the F_c-portion also reduces the size of the molecule and allows it to gain better access to antigens (Hainfeld and Powell, 2000). Small gold particles have a similar advantage. In addition, small particles do not obscure adjacent antigens and diffuse better to epitopes, thus providing a more sensitive labelling. Although antibodies conjugated to very small gold particles (1-5 nm) are available, these are difficult to visualize without silver intensification, and were therefore not used in this study. Some other aspects of post-embedding immunogold protocols are further described in the appropriate chapters.

Chapter 3

Evidence that somatostatin- and the majority of enkephalin-containing neurons in dorsal horn of rat spinal cord are glutamatergic and form synapses that contain AMPA receptors

INTRODUCTION

A number of neuropeptides have been detected in the dorsal horn of spinal cord (Todd and Spike, 1993) and these play a particularly important role in the spinal processing of sensory information. The release of some lead to the induction of pain, while others have been implicated in the development of analgesia. Somatostatin and enkephalin belong to this latter group, and although several hypotheses emerged, the exact mechanism of their action remains unknown.

Somatostatin was among the first neuropeptides to be discovered in the hypothalamus and it was later revealed that it has a widespread distribution in other brain regions as well (Fitzpatrick-McElligott et al., 1988, Kiyama and Emson, 1990). In the rat spinal cord it was first described by Hökfelt et al. (1975), and nowadays it is considered as one of the most important sensory neuropeptides. There is a line of evidence suggesting its role in nociception. The release of somatostatin hyperpolarizes the cell membrane, directly inhibiting substantia gelatinosa neurons in the adult rat (Murase et al., 1982; Jiang et al., 2003). Intrathecal administration of somatostatin or its agonists increases pain threshold, prevents *c-fos* expression (Ruan et al., 1997), inhibits both the first and second phases of the formalin response (Chapman and Dickenson, 1992b) and causes analgesia both in patients (Penn et al., 1992) and experimental animals (Mollenholt et al., 1988). Finally, somatostatin and its receptors are found in spinal regions thought to be associated with nociceptive processing (Todd and Spike, 1993; Todd et al., 1998; Song et al., 2002). Similarly, the role of enkephalin in analgesia is also well established. Enkephalin, as a member of the opioid peptide family, is an endogenous ligand of the "morphine receptor" (Hughes et al., 1975a, 1975b) and it has been shown to inhibit primary afferent terminals (Pomeranz and Gurevich, 1979) and dorsal horn neurons by causing presynaptic depolarization (Budai et al., 1998) or postsynaptic hyperpolarization (Murase et al., 1982), respectively. In addition, systemic, intrathecal (Tung and Yaksh, 1982) or epidural (Marsh et al., 1999a; 1999b) administration of enkephalin or other opioid agonists or the stimulation of periventricular brain areas (Akil, 1978), such as the periaqueductal gray matter and the nucleus raphe magnus, which give rise to descending projections that activate enkephalin containing spinal interneurons (Glazer and Basbaum, 1984; Miller and Salvatierra, 1998) produce analgesia. Intravenous administration of opioids prevents *c-fos* expression following noxious heat stimulation (Abbadie et al., 1994). Finally, as in the case of somatostatin, enkephalin and its receptors are also found at areas involved in nociceptive processing (Hökfelt et al., 1977; Arvidsson et al., 1995a; Zhang et al., 1998).

Somatostatin is present mainly in axons which form a dense plexus in the superficial laminae (I and II) of the dorsal horn and it is virtually missing from fibres in the deeper layers. Somatostatin-containing axons are thought to be derived from two sources: primary afferents and local interneurons. Axons belonging to each of these populations can be distinguished, as the primary afferents also contain calcitonin gene-related peptide (CGRP), whereas the axons belonging to interneurons do not (Ju et al., 1987; Ribeiro-da-Silva, 1995; Sakamoto et al., 1999). Cells expressing mRNA for somatostatin were found in the dorsal horn with *in situ* hybridization (Kiyama and Emson, 1990), and with immunocytochemistry a number of somatostatin-immunoreactive cell bodies were detected in laminae I and II. These neurons are thought to generate local axonal arbors and give rise to the non-primary, somatostatin-containing axons in this region. The distribution of enkephalin is similar to that of somatostatin (Todd and Spike, 1993). It is also present in axon terminals throughout laminae I and II, with much lower levels in the deeper layers. These boutons are almost exclusively derived from local interneurons; however a few clearly belong to primary afferents (Garry et al., 1989; Zhang et al., 1993) or descending fibers (Hökfelt et al., 1979). With *in situ* hybridization (Ruda, 1982; Harlan et al., 1987) or sensitive immunohistochemical methods (Todd et al., 1992a, 1992b) enkephalin immunoreactive cell bodies are visible mainly in laminae I-III.

Although it is widely accepted that all primary afferent terminals, including those that contain somatostatin and enkephalin, use glutamate as their principal neurotransmitter (Rustioni and Weinberg, 1989; Willis and Coggeshall, 1991; Todd and Spike, 1993; Broman, 1993, 1994b), it is still controversial whether somatostatin- and enkephalin-containing intrinsic neurons also utilize a classical amino-acid transmitter besides the neuropeptide, and if so, which one. Proudlock et al. (1993) found that somatostatin-containing cells are not GABA-immunoreactive, while in a recent study, Todd et al. (2003) showed that 85% of enkephalin-immunoreactive axon terminals expressed VGLUT2, a marker for glutamatergic spinal interneurons (see Chapter 1). These findings raise the possibility that somatostatin-containing interneurons and the majority of enkephalin-containing axon terminals are glutamatergic. To test these hypotheses, two different approaches were used: (1) triple-labelling immunofluorescence and confocal microscopy was carried out with antibodies against somatostatin, CGRP and the two VGLUTs; (2) postembedding immunogold labelling was used on freeze-substituted, Lowicryl-embedded material to reveal GluR1 and GluR2/3 subunits of the AMPA receptors at synapses formed by somatostatin- or enkephalin-immunoreactive axons.

MATERIALS AND METHODS

Animals

Seven adult male Wistar rats (190–300 g; Harlan, Loughborough, UK) were deeply anaesthetized with pentobarbitone (300 mg i.p.) and perfused through the left ventricle with a fixative consisting of 4% freshly de-polymerized formaldehyde (4 rats, for confocal microscopy) or 4% formaldehyde/0.1% glutaraldehyde (3 rats, for electron microscopy). Lumbar spinal cord segments were removed and stored in the same fixative for 4-24 hours, before being processed for light or electron microscopy.

Immunofluorescence staining for light microscopy

L_3-L_5 segments were postfixed for 24 hours and cut into 60 µm transverse sections with a Vibratome. Prior to immunocytochemistry sections were treated with 50% ethanol in distilled water to enhance antibody penetration (Llewellyn-Smith and Minson, 1992). Sections were incubated for three days in a mixture of rabbit anti-somatostatin (Peninsula Laboratories, Belmont, CA, USA, 1:1000), sheep anti-CGRP (Affinity Research Products Ltd., Exeter, UK, 1:5000) and guinea pig anti-VGLUT1 (Chemicon International, Harlow, UK, 1:20000) or VGLUT2 (Chemicon, 1:5000) antibodies in phosphate-buffered saline (PBS) with 0.3% Triton X-100 added as a detergent to increase penetration. To reveal the distribution of enkephalin, sections were incubated in a rabbit anti-enkephalin (Peninsula, 1:1000) antibody for 24 hours. After thorough rinsing, sections were incubated overnight in a cocktail of species-specific secondary antibodies (Jackson Immunoresearch, all raised in donkey, 1:100) conjugated to fluorescein isothiocyanate (for somatostatin), Rhodamine Red-X (for VGLUT1, VGLUT2 or enkephalin) or cyanine 5-18 (Cy5; for CGRP) in PBST. Sections were then rinsed in PBS, mounted in a glycerol-based antifade medium (Vectashield, Vector Laboratories) and stored at -20°C prior to scanning and analysis.

Postembedding immunocytochemistry for electron microscopy

Mid-lumbar spinal cord segments from rats fixed with 4% formaledhyde/0.1% glutaraldehyde were postfixed for 4 h in the same fixative and freeze-substituted as described in Chapter 2. From the blocks serial ultrathin sections were cut with a diamond knife and collected on single-slot Formvar-coated nickel grids. The sections were reacted using a postembedding immunogold method to reveal various neuropeptides or the GluR1 and GluR2/3 subunits of the AMPA receptor. These two GluR antibodies were chosen as GluR1 and GluR2 are the principal AMPA subunits expressed by neurons in laminae I and II (see Chapter 5). For somatostatin containing interneuronal and primary afferent

terminals three serial sections from each animal were reacted as follows: the first grid was incubated in sheep antibody against CGRP (Affiniti, 1:20,000), the second one in rabbit antibody against somatostatin (Peninsula, 1:5,000) and the third in a cocktail of rabbit antibodies against GluR1 (Chemicon, 1:50) and GluR2/3 (Chemicon, 1:80). For enkephalin containing boutons two serial sections were incubated from each animal: the first one with an antibody against enkephalin (Peninsula, 1:10,000), the second one in the cocktail of GluR1 and GluR2/3 antibodies (as described above).

Sections that were to be incubated in GluR1 and GluR2/3 antibodies were initially etched for approximately 3 s in a saturated solution of sodium hydroxide in ethanol to remove the resin from the section surface, while those used to reveal neuropeptides were not etched. Post-embedding immunogold labelling was carried out by incubating sections in the following solutions at 20°C: (1) Tris-buffered saline (0.3% NaCl) containing 0.1% Triton X-100 (TBST) with 50mM glycine (10 min); (2) TBST with 2% human serum albumin (HSA) 10 min; (3) primary antibody diluted in TBST with 2% HSA (overnight); (4) TBST (2x10 min); (5) TBST with 2% HSA (10 min); and (6), goat anti-rabbit F_{ab}-fragment coupled to 10 nm gold particles (British BioCell International, Cardiff, UK) diluted 1:20 in TBST with 2% HSA. Grids were rinsed in ultra pure water and contrasted with aqueous uranyl acetate (10 min) and lead acetate (2 min). Sections reacted with the sheep CGRP antibody were incubated in unlabelled rabbit anti-sheep IgG (Vector Laboratories, Peterborough, UK, 1:200) for 2 h before immunogold labelling.

Analysis of immunofluorescence

To examine the colocalization of VGLUT1 or VGLUT2 with somatostatin in primary and non-primary axons (distinguished by the presence or absence of CGRP labelling), two triple-labelled sections from each animal were scanned with a BioRad confocal laser scanning microscope (MRC1024) using a 60x oil immersion lens. Twelve optical sections were collected from an approximately 140 µm wide strip covering laminae I-III of the dorsal horn with a z-separation of 0.5 µm. It was found that neither somatostatin, nor CGRP ever colocalized with VGLUT1 and that the expression of VGLUT2 in CGRP-containing fibres was so low, that it was very difficult to distinguish immunoreactive and immunonegative boutons (see below). These were therefore not quantitatively analysed. The colocalization of VGLUT2 with somatostatin in CGRP-lacking (interneuronal) axon terminals was quantitatively analysed using Neurolucida for Confocal image analysis software (MicroBrightField Inc., Colchester, VT, USA). From each animal 100 boutons (50 from each section scanned) that were immunoreactive for

somatostatin (green), but lacked CGRP (blue) were selected. Following the selection of the axon terminals, it was noted whether these contained VGLUT2 (red). Boutons were only included in the study if they were fully contained within the 12 optical sections.

Analysis of immunogold labelling

Grids were viewed with a Philips CM100 transmission electron microscope. On grids reacted with each of the three neuropeptide antibodies, boutons were only considered as immunoreactive if they contained eight or more gold particles and these were located over dense-cored vesicles. The density of background labelling with the neuropeptide antibodies was determined for each section analysed by counting gold particles that were not associated with dense-cored vesicles or located in immunolabelled axon terminals in 20 randomly selected fields each of 1 μm^2. These background values were 0.52–0.71/μm^2 for CGRP, 0.85–1.23/μm^2 for somatostatin and 1.13-2.41/μm^2 for enkephalin. Because dense-cored vesicles have a diameter of approximately 0.1 μm (cross-sectional area of 0.008 μm^2), the presence of a single gold particle over a dense-cored vesicle corresponds to a density of approximately 130 particles/μm^2, which is more than 50-times the highest background value measured. Sections reacted with somatostatin or enkephalin antibodies were initially examined and immunoreactive axon terminals forming one or more synapses were selected. Each axon terminal selected for further analysis was given an individual number, and high (13500x), medium (4200x) and low (750x) magnification digital images were saved to a computer using the CCD camera connected to the EM. The low power image served as a map and the numbers marking the exact locations of different boutons were inserted using image editing software (CM-Prof 2.10.220, Soft-Imaging Software GmbH). With the aid of a relocation software (Remote XY Control, PW6472, Version 1.0; Philips Analytical, Electron Optics) and the map, somatostatin-immunoreactive terminals were relocated on the adjacent section reacted for CGRP, and the presence or absence of CGRP immunoreactivity in the bouton was noted. Boutons were classified as CGRP-negative if they had dense-cored vesicles in their axoplasm, but these contained no gold particles representing CGRP. The somatostatin- or enkephalin-immunoreactive boutons were then identified on the serial section reacted with GluR1 and GluR2/3 antibodies, and those at which a synapse was still visible were included in the sample. Using this approach, 45 boutons that were somatostatin-immunoreactive but lacked CGRP (9–21 from each experiment), 27 axon terminals that were both somatostatin- and CGRP-immunoreactive (between 7 and 10 from each experiment) and 57 that were enkephalin-immunoreactive (17-22 from each experiment) were selected and analysed. It is possible that some of the

somatostatin-immunoreactive boutons that were not CGRP-immunoreactive contained CGRP that was not detected with the postembedding method. However, it is highly unlikely that this would have been a common occurrence, as somatostatin-immunoreactive boutons in the superficial dorsal horn that lack CGRP greatly outnumber those which also contain CGRP (Sakamoto et al., 1999). In addition, the level of CGRP–immunogold labelling was high (up to 50 gold particles per individual dense-cored vesicle) in boutons that were identified as immunoreactive. Digital images of all of the boutons analysed on each grid were captured, and in some cases these were also photographed. For each synapse, with the aid of image analysis software (Zeiss KS400 Image Analysis System), gold particles representing GluR1 and GluR2/3 were counted within 50 nm of the postsynaptic membrane, or within 50 nm of a line drawn along the centre of the synapse if this was sectioned obliquely. This distance was chosen as Nagelhus et al. (1998) found that the density of gold particles labelling membrane proteins reached background levels 50 nm from the membrane. This distance probably reflects the size of the immunoglobulin molecules interposed between the antigen and the gold particle (Matsubara et al., 1996), together with the distance the receptors extend from the lipid bilayer into the postsynaptic density. Synapses at which two or more gold particles were present were counted as immunoreactive, whereas those with a single particle were treated as equivocal.

Antibodies

The affinity purified antibodies against the GluR1 and GluR2/3 subunits of the AMPA receptor were raised in rabbits against the corresponding C-terminal 13 amino-acid segment of the rat GluR1 and GluR2 subunits. The GluR1 antibody was shown not to cross-react with any of the other AMPA subunits, while due to the significant sequence homology between the C-terminus of GluR2 and GluR3, the GluR2/3 antibody also recognize GluR3, but not GluR1 or GluR4 (manufacturer's specifications). Both of these antibodies have been successfully used previously with light and electron microscopic immunocytochemistry, including post-embedding immunogold on freeze-substituted, Lowicryl embedded material (e.g. Matsubara et al., 1996, 1999; Propratiloff et al., 1996, 1998; Bernard et al., 1997, 1998; Takumi et al., 1999; Ragnarson et al., 2003). The Met-enkephalin antibody shows 3% cross-reactivity with Leu-enkephalin and none with dynorphin (manufacturer's specification). CGRP and somatostatin antibodies were raised against corresponding rat peptides and were shown not to cross-react with other neuropeptides such as Substance P, VIP, NPY etc. (manufacturers' specification). The guinea pig VGLUT1 and VGLUT2 antibodies were raised against an unspecified 19 and

18 amino acid sequence of the corresponding rat proteins, respectively. These were shown to label the same axons as the well-characterized rabbit VGLUT1 and VGLUT2 (Synaptic Systems, Germany) antibodies, raised against known sequences (Todd et al., 2003).

RESULTS

Immunofluorescence and confocal microscopy

The staining patterns for VGLUTs and the neuropeptides were identical to those reported previously in other studies (e.g. Ju et al., 1987; Sakamoto et al., 1999; Varoqui et al., 2002; Todd et al., 2003). CGRP labelling was very strong in lamina I and IIo, with scattered boutons elsewhere in the dorsal horn (Fig. 3.1c). Somatostatin immunostaining was similar, but immunoreactive boutons were also numerous in lamina IIi (Fig. 3.1b) and besides the axon terminals, cell bodies were also labelled, mainly in lamina IIi (Fig. 3.2a). As expected, a number of terminals contained both somatostatin and CGRP, while others showed immunoreactivity for only one of these neuropeptides (Fig. 3.2b). Enkephalin-immunoreactivity was also strongest in the superficial laminae (Fig. 3.1a).

Both VGLUT antibodies labelled structures which resembled axonal varicosities. VGLUT1 expression was very sparse in laminae I and IIo, but strong in all deeper laminae (Fig. 3.3a), while VGLUT2 labelling was present throughout the gray matter, although it was particularly strong in the superficial laminae (Fig. 3.3d).

When the colocalization between VGLUTs and the neuropeptides was examined, it was found that VGLUT1 never colocalized with either CGRP or somatostatin, suggesting that somatostatin-containing axon terminals of both primary afferent and interneuron origin lacked this transporter (Figs 3.3a-c; 3.4a-c). Varicosities which contained only somatostatin were strongly labelled with the VGLUT2 antibody (Fig. 3.4d-f) and during the quantitative analysis of one hundred CGRP-lacking, somatostatin-containing boutons that were sampled in each of 3 rats, between 97-98% of these (mean 97.7%) showed immunostaining for VGLUT2. However, boutons that contained both somatostatin and CGRP were consistently either unlabelled or very weakly labelled with the VGLUT2 antibody (Fig. 3.4d-f). The weak labelling in these terminals made it very difficult to differentiate between positive and negative profiles, and therefore the extent of co-localization was not analysed quantitatively.

Postembedding immunogold labelling and electron microscopy

Following freeze-substitution and Lowicryl embedding, the general ultrastructure of the tissue was excellent (Fig. 3.5g). After postembedding immunocytochemistry for somatostatin, CGRP or enkephalin, tissue preservation was still good (Fig. 3.5a-b, d-e, h).

Figure 3.1 Images showing the distribution of methionine-enkephalin (Met-Enk, red, ***a***), somatostatin (Som, green, ***b***) and calcitonin-gene-related peptide (CGRP, blue, ***c***) in transverse sections of mid-lumbar rat spinal cord. Each peptide is present in the superficial dorsal horn, but the distribution of enkephalin and somatostatin is slightly different from that of CGRP. Enkephalin and somatostatin-containing axons are present throughout laminae I and II, while those with CGRP are infrequent in the ventral part of lamina II. Arrows indicate the approximate position of the lamina II/III border. Picture (***a***) comes from a different section than pictures (***b***) and (***c***). Scale bar, 200 μm.

Figure 3.2 Higher magnification views of somatostatin (green) and CGRP (blue) immunoreactivity in the superficial dorsal horn. The image on the left (***a***) shows that besides being in axon terminals, somatostatin-immunostaining is also present in neuronal cell bodies (*arrows*). The right-hand image (***b***) is from a section double-labelled for both peptides: axons of somatostatin-containing interneurons appear green (some are indicated with *arrows*), while those of somatostatin primary afferents (which also contain CGRP) are cyan (some shown with *arrowheads*). Scale bars, 50 μm (left), 10 μm (right).

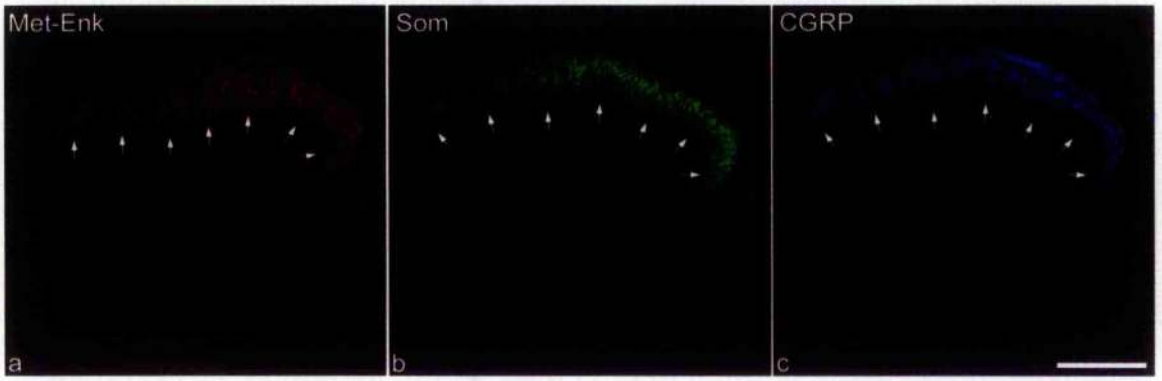
Met-Enk
Som
CGRP
a
b
c

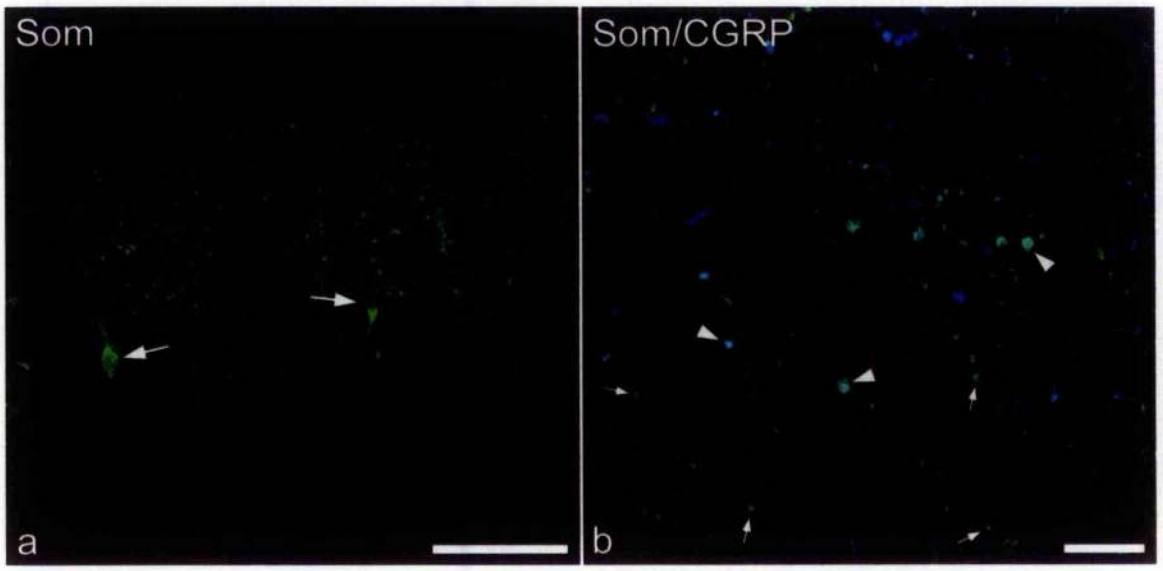
Som
Som/CGRP
a
b

Figure 3.3 Confocal images showing the distribution of VGLUT1 (red, ***a-c***) and VGLUT2 (red, ***d-f***) labelling in the dorsal horn of mid-lumbar rat spinal cord and their relationship with somatostatin (green, ***b, e***) and CGRP (blue, ***c, f***). VGLUT1-labelled axon-terminals are very sparse in the superficial laminae, but numerous in the deeper layers, while VGLUT2 is present throughout the dorsal horn, including laminae I and II. Both neuropeptides are mainly present in laminae I and II, although CGRP is infrequent in the ventral half of the substantia gelatinosa, therefore this region has very sparse labelling on the section stained with VGLUT1 and CGRP antibodies (*c, arrows*). Scale bar, 200 μm.

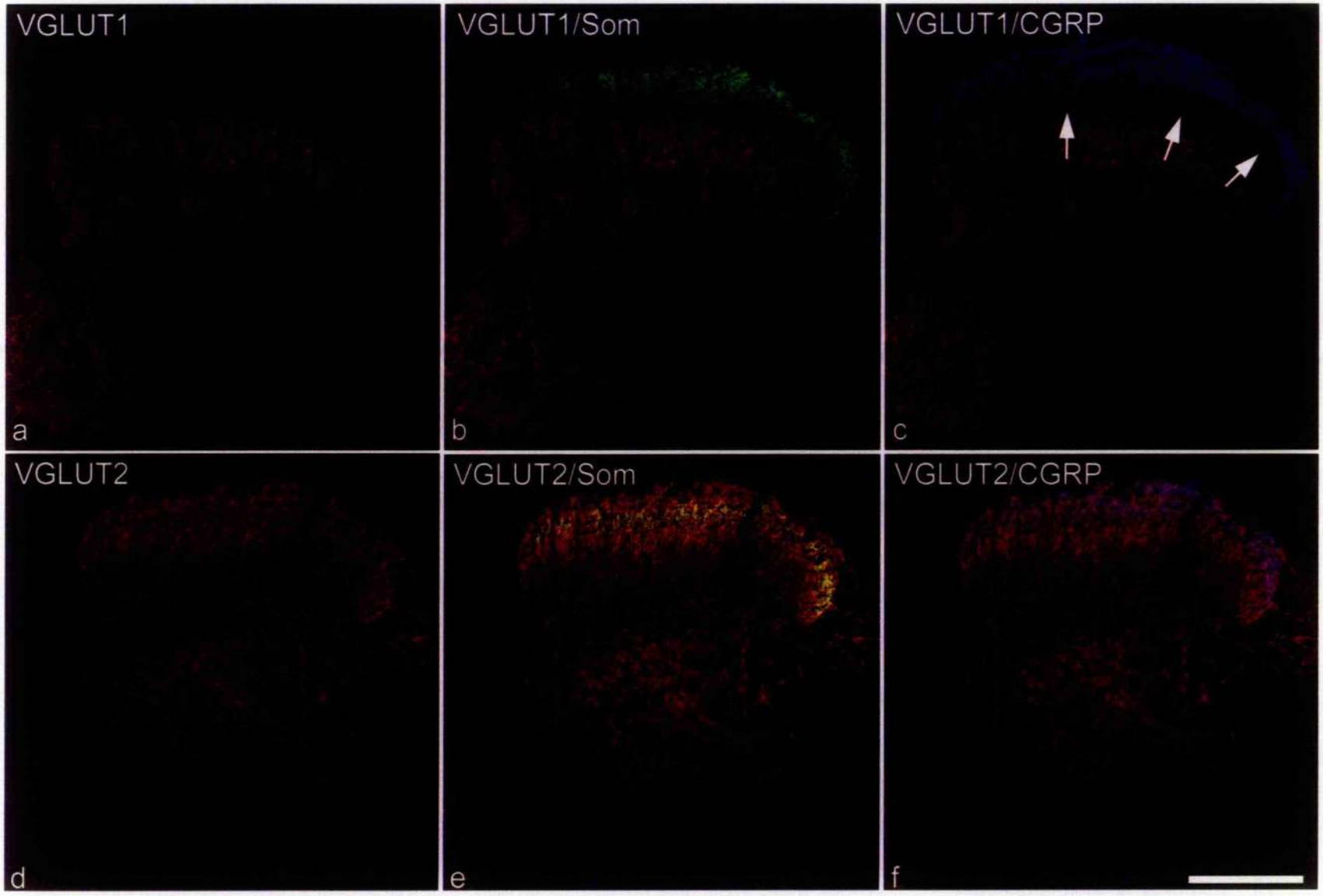
VGLUT1
VGLUT1/Som
VGLUT1/CGRP
a
b
c
VGLUT2
VGLUT2/Som
VGLUT2/CGRP
d
e
f

Figure 3.4 Confocal images showing the relationship between somatostatin (Som, green), CGRP (blue) and VGLUT1 (red; ***b, c***) or VGLUT2 (red; ***e, f***) in single optical sections from lamina II of rat mid-lumbar spinal cord. The panels on the left show the neuropeptides (**a, d**), the ones in the middle represent VGLUT1 or VGLUT2 (***b, e***), while the right pictures show merged images (***c, f***). Again somatostatin-containing boutons that belong to interneurons lack CGRP, so these appear green (***a, d;*** some are marked with *arrows*), while those belonging to primary afferents also express CGRP, so these are cyan (**a, d**; some indicated with *arrowheads*). VGLUT1 is very sparse in the superficial laminae (***b***) and never colocalizes with somatostatin-containing terminals (***c***). For VGLUT2 somatostatin-immunoreactive primary afferents are either very weak (***d, e, f;*** *unlabelled arrowhead*) or negative (***d, e, f;*** *arrowhead with asterisks*), while interneurons generally express high levels of this transporter (***d, e, f;*** *arrows*), so these appear yellow on the merged image. Scale bar, 5 μm.

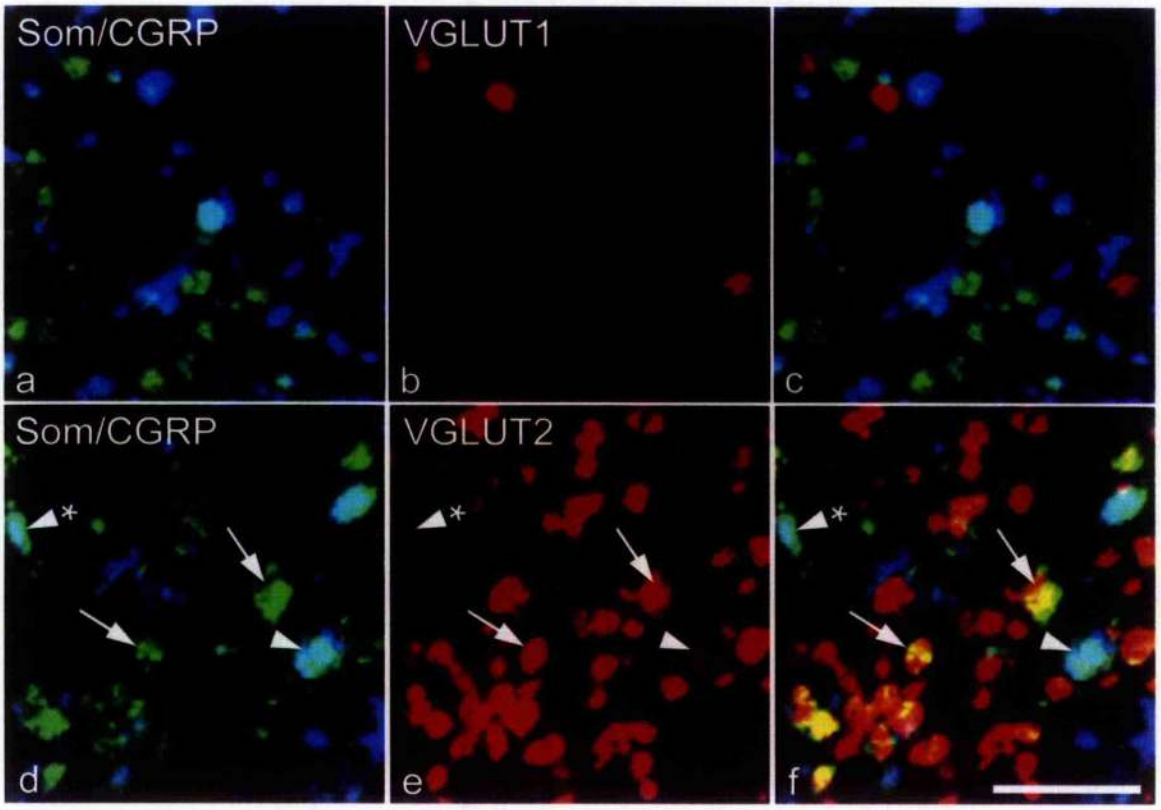
Som/CGRP
VGLUT1
a
b
c
Som/CGRP
VGLUT2
*
*
*
d
e
f

Figure 3.5 Postembedding immunogold labelling on three sets of serial sections from freeze-substituted, Lowicryl embedded rat spinal cord, showing the relationship between neuropeptides and AMPA receptors in the superficial laminae. The axon terminal in the upper row (*a, b, c*) contains several dense-cored vesicles (dcv) and these are somatostatin-immunoreactive (*b*), but lack CGRP (*a*), therefore it is presumably of interneuron origin. Section (*c*) has been reacted with a cocktail of antibodies against the GluR1 and GluR2/3 subunits and the perpendicularly cut asymmetrical synapse contains several gold particles on its postsynaptic density corresponding to AMPA receptors (inset in *c*). The dcv containing profile in the middle row (*d, e, f*) is a primary afferent terminal as shown by its immunoreactivity for both somatostatin (*e*) and CGRP (*d*). It forms two oblique, but clearly asymmetrical synapses. The second, smaller synapse disappears on the section reacted against the AMPA receptors (*f*), but the remaining one contains 21 gold particles (inset in *f*). The bottom row (**g, h, i**) shows a bouton, which forms a curved synapse on a small profile. Section (*g*) has not been postembedding reacted, this therefore demonstrates the general ultrastructure of freeze-substituted tissue after contrasting. In the subsequent section dcvs are immunoreactive for enkephalin (*h*) and again the synapse formed by the axon-terminal is immunolabelled for AMPA receptors (*i*, inset). Scale bar, 0.5 μm.

Fig 3.6 Frequency histograms showing the numbers of gold particles at GluR1/GluR2/3-immunoreactive synapses. Results from boutons that were somatostatin-immunoreactive but lacked CGRP (Som+/CGRP-), that were both somatostatin- and CGRP-immunoreactive (Som+/CGRP+), and that were enkephalin-immunoreactive (M-Enk) are shown on the left, middle and right, respectively.

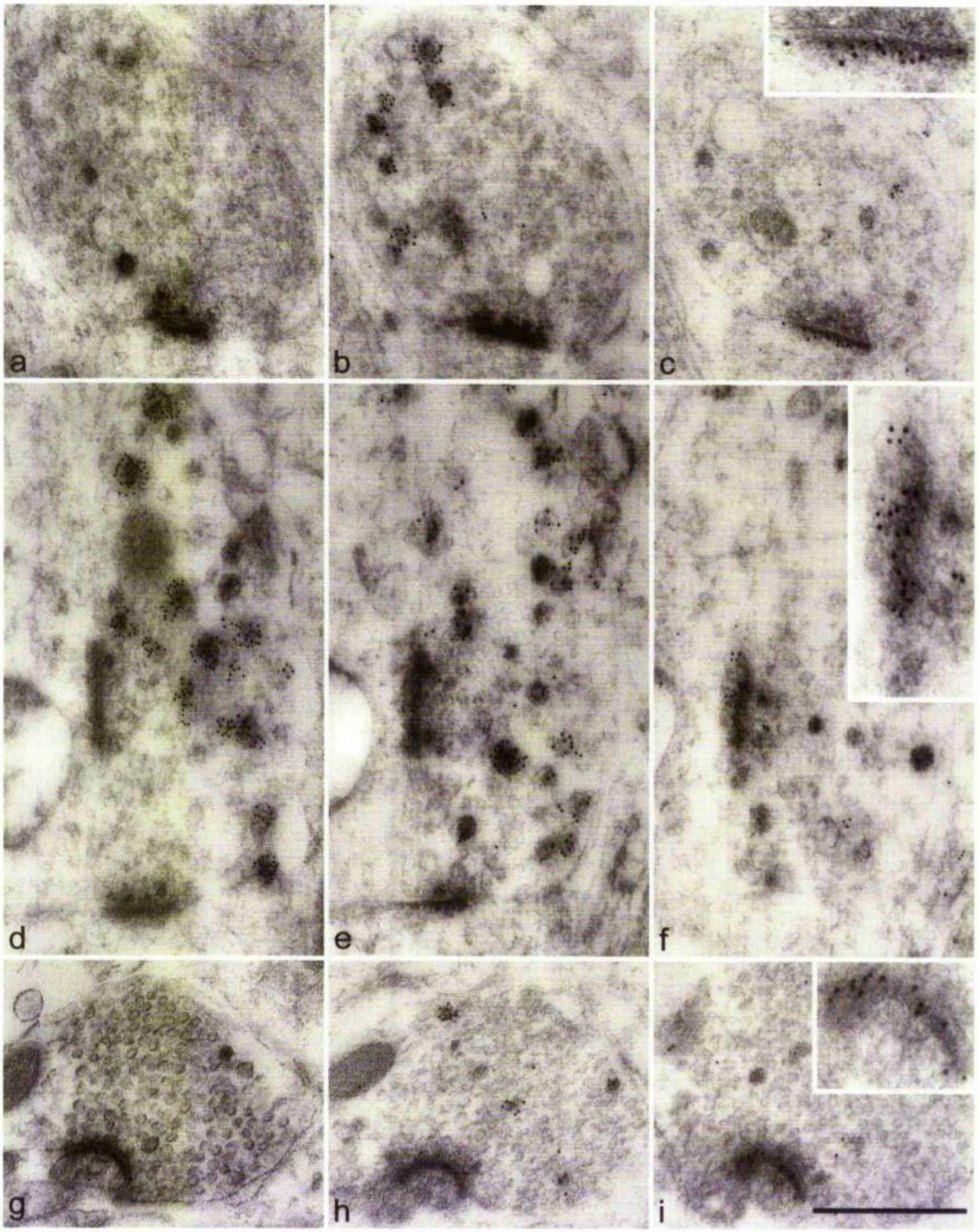
a
b
c
d
e
f
g
h
i

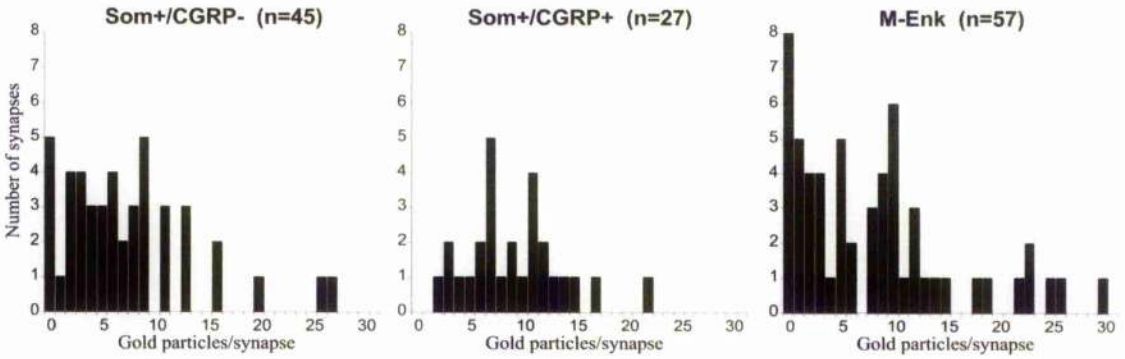
Som+/CGRP- (n=45)
Som+/CGRP+ (n=27)
M-Enk (n=57)
Number of synapses
Gold particles/synapse
Gold particles/synapse
Gold particles/synapse

On sections incubated for the AMPA receptors, the etching with sodium ethanolate slightly compromised the structure, but nevertheless cell organelles and synapses were still clearly identifiable (Fig. 3.5c, f, i, insets). Immunogold particles representing the three neuropeptides were mainly found over dense-cored vesicles in axon terminals (Fig. 3.5b, d, e, h), and there was virtually no background labelling. Somatostatin-immunoreactive boutons formed asymmetrical synapses with their postsynaptic target, while symmetrical synapses were never observed. Enkephalin-containing terminals on the other hand, formed both asymmetrical and symmetrical synapses, although the former greatly outnumbered the latter (only 2 symmetrical were found among 57 synapses examined). In sections reacted with antibodies against the AMPA subunits, immunogold particles were found at many asymmetrical synapses. Where the plane of section was perpendicular to the cleft, most of the particles were associated with the postsynaptic density (Fig. 3.5c, f, i, insets). Immunoreactive synapses contained up to 31 gold particles. Scattered immunogold labelling was visible over cell membranes, and occasionally over mitochondria and dense-cored vesicles. The numbers of gold particles at immunolabelled synapses were similar for each of the sections reacted with GluR antibodies, and the data from each animal were therefore pooled for the histograms in Fig. 3.6.

For the somatostatin-immunoreactive boutons that were not CGRP-labelled, 39 of 45 synapses (87%) were classified as immunolabelled with the GluR antibodies (i.e. they had 2 or more gold particles) (Figs 3.5a-c; 3.6). All 27 of the boutons immunoreactive for both somatostatin and CGRP (Figs 3.5d-f; 3.6) and 44 of 57 (77%) of those formed by boutons containing gold particles for enkephalin (Figs 3.5g-i; 3.6) were GluR-immunoreactive. The two symmetrical synapses formed by enkephalin-immunoreactive boutons had no gold particles corresponding to AMPA receptors.

DISCUSSION

It is generally accepted that all primary afferent terminals, including the neuropeptide-containing ones, are excitatory and use glutamate as a neurotransmitter. It is also well established that certain neuropeptide-containing neurons in the CNS, including some of those in the dorsal horn of spinal cord, also use a classical amino-acid transmitter (glutamate, GABA or glycine) at their axon terminals (Hökfelt et al., 2000b). Somatostatin-immunoreactive interneurons in the superficial dorsal horn do not contain either GABA or glycine, therefore it was suggested that these cells are glutamatergic (Proudlock et al., 1993). Conflicting evidence exists in the literature about the proportion of enkephalin containing neurons that are GABAergic. In an earlier study Todd et al.

(1992b) found that 69% of enkephalin containing cell bodies also contained GABA, which is at odds with their later findings (Todd et al., 2003) showing that 85% of enkephalin-immunoreactive axon terminals expressed VGLUT2.

The results of this study show that virtually all somatostatin-containing intrinsic neurons express VGLUT2 and their axon terminals form asymmetrical synapses, at which AMPA receptors are generally present in the postsynaptic density. These two independent observations strongly suggest that most (if not all) somatostatin-immunoreactive neurons in the dorsal horn of spinal cord are excitatory glutamatergic interneurons. The finding that all somatostatin-containing primary afferents express AMPA receptors at their synapses supports all previous results that primary afferents are glutamatergic. However the observation that these lack either VGLUT1 or VGLUT2 and also fail to express VGLUT3 (Landry et al., 2004; Maxwell et al., unpublished observations) raises the possibility that there is a novel, as yet undiscovered VGLUT expressed by these axons. In support of this, Todd et al. (2003) also found that substance P (SP)- and CGRP-containing and non-peptidergic C-fibres lacked VGLUT1 and were either negative for, or contained very low levels of, VGLUT2.

It was also found that approximately 77% of enkephalin-containing terminals are apposed to AMPA receptor containing synapses, which confirms that the majority of these are indeed glutamatergic as suggested by Todd et al. (2003) who found that most enkephalin-immunoreactive boutons expressed VGLUT2. Asymmetrical synapses where gold particles representing GluR1 and/or GluR2/3 subunits were absent (6 out of 57 for enkephalin and 5 out of 72 for somatostatin) could still belong to glutamatergic terminals, and these could have been false negative results or could correspond to silent synapses, which lack AMPA receptors, but express NMDAs (Nüsser et al., 1998). Only two symmetrical synapses (3.5%) were found on the 57 enkephalin-immunoreactive boutons examined and these lacked AMPA receptors, which suggests that these belonged to inhibitory, presumably GABAergic interneurons. It is likely that previously Todd et al. (1992b) overestimated the proportion of enkephalin-containing neurons that also contain GABA. Colchicine used in earlier studies had revealed many more enkephalin-immunoreactive cells. For example Todd et al. (1992b) found only 10-20 enkephalin-immunoreactive neurons in a 70 μm section, while after colchicine treatment Senba et al. (1988) detected 60 in a 20 μm thick section. In their study Todd et al. avoided the use of colchicine, which is known to change the gene-expression pattern of various cells including neurons (Réthelyi et al., 1991; Koistinaho et al., 1993), and this probably resulted in a decreased detection of enkephalin-containing dorsal horn neurons.

In the light of these findings, the function of somatostatin- and enkephalin-containing interneurons should be re-evaluated. Both neuropeptides have a depressant effect on dorsal horn neurons, and when administered *in vivo* they produce analgesia. Therefore it was suggested that the activation of these interneurons inhibits other cells or axons (Murase et al., 1982; Miller and Salvatierra, 1998; Jiang et al., 2003; Terman et al., 2001). Surprisingly, the findings presented here show that this is not likely to be the only way that these neurons function. The colocalization of enkephalin and somatostatin with an excitatory transmitter, together with the fact that the majority of enkephalin- and somatostatin-containing terminals form synapses at which AMPA receptors are present, suggests that these cells have an excitatory effect on their postsynaptic targets. There is evidence that neuropeptides act through volume transmission (Agnati et al., 1986, 1991, 1995a, 1995b), such that the site of release and the site of action can be quite a distance apart. Therefore, it is likely that the classical amino-acid transmitter and the neuropeptide act on different populations of cells. It could be that glutamate is released at the synapses and exerts its excitatory effect on the postsynaptic neuron (possibly an inhibitory interneuron), whereas enkephalin or somatostatin could be released at extrasynaptic sites and diffuse to various other cells which express the appropriate receptor, resulting in a depressant effect on these neurons (either depolarization on primary afferents or hyperpolarization on dorsal horn excitatory interneurons or projection cells). Another possible functional implication of this colocalization is that glutamate acts as a fast transmitter, while the two neuropeptides are slower with more long-lasting actions (Hökfelt et al., 2000b). In this scenario, the activation of enkephalin- and somatostatin-containing excitatory interneurons could not only have a distinct spatial, but also a distinct temporal effect on dorsal horn interneurons, projections cells and primary afferent terminals. To further complicate matters, glutamate and the neuropeptides could be released following different stimuli. There is evidence suggesting that neuropeptides are only released after high frequency stimulation (Otsuka and Konishi, 1976; Shen et al., 1996; Afrah et al., 2002), while glutamatergic excitatory postsynaptic potentials can be recorded on the postsynaptic cell following a single action potential (Verhage et al., 1991; Nicholls, 1994).

In summary, it is likely that when they are activated, somatostatin- and enkephalin-containing interneurons not only produce analgesia through the release of these neuropeptides, but also play a more complex role in the processing of nociceptive information in the dorsal horn. To understand their exact function, further investigations are needed to identify and neurochemically characterize their postsynaptic targets.

Chapter 4

Detection of NMDA receptors in the rat spinal cord with postembedding immunocytochemistry and non-specific labelling with an antibody against the NR2A subunit

INTRODUCTION

Although it is well-established that NMDA receptors in the spinal dorsal horn are involved in chronic pain states (see Chapter 1), we know very little about their synaptic distribution and involvement in nociceptive circuits. Even less is know about the NMDA (and AMPA) receptor expression pattern of selected cell populations, such as the projection neurons in laminae III and IV that possess the neurokinin 1 (NK1) receptor (a receptor for SP). These cells receive strong synaptic input from nociceptive primary afferents that contain SP and CGRP (Todd, 2002). The lack of knowledge about synaptic NMDA receptors is mainly because conventional immunocytochemical methods fail to reveal ionotropic receptors at synapses, as these are masked by the protein meshworks of the post-synaptic density and synaptic cleft. Post-embedding immunogold labelling following freeze-substitution has been widely used to study the synaptic distribution of receptors (see Chapter 2). The aim of this part of the study was to use this technique to investigate the distribution of NR1, NR2A and NR2B subunits of the NMDA receptors in the dorsal horn. An additional goal was to determine the AMPA and NMDA receptor expression pattern of NK1-immunoreactive neurons at synapses formed by SP- and CGRP-containing nociceptive primary afferents. In preliminary experiments it was found that NK1-receptors are not detectable with the postembedding immunogold method. Although a theoretical alternative would be to use a preembedding technique to reveal these receptors, it was found that preembedding methods are not readily compatible with freeze-substitution. For example the diaminobenzidine (DAB) reaction product that results from immunoperoxidase labelling is not electron dense without osmication, while biotin, avidin, horseradish peroxidase (HRP) or primary antibodies are not recognizable in freeze-substituted sections. An additional requirement for this part of the study was to visualize the 3D structure of individual lamina III/IV NK1-immunoreactive neurons, firstly to confirm the location of their cell bodies, and secondly to allow different parts of their dendritic trees to be examined. Therefore, in order to examine neurons expressing the NK1-receptor, a novel method for combining post-embedding electron microscopy with immunofluorescence and confocal microscopy was developed. However, during the course of this study unexpected immunogold labelling patterns were observed with several NMDA receptor antibodies, which raised questions about the quality and validity of the postembedding method for NMDA receptors. In search for alternative techniques an antigen unmasking method, initially developed by Watanabe et al. (1998), was adopted and used to reveal NMDA receptors at synapses (see also Chapter 6).

MATERIALS AND METHODS

Animals for immunocytochemistry

Five adult male Wistar rats (190–300 g; Harlan, Loughborough, UK), 5 control wild-type mice and 5 transgenic mice in which the NMDA NR2A subunit had been knocked out (Sakimura et al., 1995; generous gifts from Prof. Masahiko Watanabe, Hokkaido University, Japan) were used during this study. Animals were perfused through the left ventricle with a fixative consisting of 4% freshly depolymerized formaldehyde (10 mice for postembedding immunogold or immunofluorescence following antigen unmasking), 4% formaldehyde and 0.1% glutaraldehyde (3 rats, for postembedding immunogold) or 4% formaldehyde, 0.1% glutaraldehyde and 0.2% picric acid (Somogyi and Takagi, 1982) (2 rats for combined confocal and electron microscopy). Lumbar spinal cord segments from all animals, as well as brains from the wild-type and knock-out mice, were removed and stored in the same fixative for 8-24 hours, before being processed for immunocytochemistry. DNA from the transgenic NMDA NR2A lacking mice was extracted before perfusion by a collaborative partner in Japan, and it was confirmed by diagnostic PCR that the NR2A gene was knocked out.

Antibodies

To reveal NR1 subunits of the NMDA receptor, an affinity purified rabbit antibody, raised against a synthetic peptide corresponding to a C-terminal epitope of the rat NR1 protein was used (Chemicon International, Harlow, UK; cat. no. AB1516). It was selective for splice variants NR1-1a-b and NR1-2a-b. No cross-reaction with other glutamate receptor subunits was observed with Western blot analysis. The antibody recognized a single protein band with the molecular weight of 116 kDa, corresponding to NMDA NR1 subunits (manufacturer's specifications). Affinity purified rabbit antibodies against NR2A, and NR2B subunits were generous gifts from Prof. Masahiko Watanabe (Hokkaido University, Japan). These antibodies were raised against synthetic peptides corresponding to the C-terminal residues 1126-1408 of the NR2A subunit, and the C-, or N-terminal residues 1353-1432 (NR2B-C) or 1-48 (NR2B-N) of the NR2B subunit. On immunoblots the NR2A antibody labelled a single protein band with a molecular mass of 175 kDa and no labelling was observed in mice where the NR2A subunit was knocked out (Watanabe et al., 1998). These observations indicate that the NR2A antibody does not cross-react with other NMDA receptor subunits and the 175 kDa band seen on immunoblots represents authentic NR2A subunits. Both the NR2B-N and NR2B-C antibodies labelled a single protein band at 180 kDa. This band was substantially reduced in NR2B (+/-) mice and was

absent in the NR2B knock-out animals, indicating the these antibodies also recognize authentic NR2B subunits and do not cross-react with other PSD proteins (Watanabe et al., 1998). Mouse monoclonal antibody against Neuron-Specific Nuclear Protein (NeuN; Chemicon, cat. no. MAB377; Mullen et al., 1992) has been shown to label only neuronal nuclei in the spinal cord (Todd et al., 1998). The rabbit anti-NK1-receptor antibody was specific for a synthetic peptide corresponding to the C-terminus of the receptor protein (Sigma-Aldrich Inc., Saint Louis, Missouri, USA, product no. 058H4848).

Freeze-substitution and postembedding immunocytochemistry for EM

Mid-lumbar segments of rat or mouse spinal cord were cut into transverse 400 μm thick sections with a Vibratome, cryoprotected and plunge-frozen in liquid propane at −170°C. Freeze-substitution was carried out as described in Chapter 3. From the resin embedded tissue, ultrathin sections were cut with a diamond knife and collected on mesh or single-slot Formvar-coated nickel grids. Sections were etched for approximately 2 s in a saturated solution of sodium hydroxide in ethanol to remove the resin from the section surface (Matsubara et al., 1996). To investigate the distribution of NMDA receptor subunits in the dorsal horn of rat spinal cord, postembedding immunogold labelling was carried out by incubating sections in the following solutions: (1) Tris-buffered saline (0.3% NaCl) containing 0.1% Triton X-100 (TBST) with 50mM glycine (10 min); (2) TBST with 2% human serum albumin (HSA) 10 min; (3) affinity-purified rabbit primary antibodies against NMDA NR1 (1 μg/ml), NMDA NR2A (5.4 μg/ml), NR2B-C (5.2 μg/ml) or NR2B-N (10.6 μg/ml) diluted in TBST with 2% HSA (overnight); (4) TBST (2x10 min); (5) TBST with 2% HSA (10 min); and (6), goat anti-rabbit F_{ab}-fragment coupled to 10 nm gold particles (British BioCell International, Cardiff, UK) diluted 1:20 in TBST with 2% HSA. Grids were rinsed in ultra pure water and contrasted with aqueous uranyl acetate (10 min) and lead acetate (2 min). Incubations were carried out at 20°C, although for some sections reacted against NMDA NR1, an antigen retrieval method with heat treatment was performed. This was achieved by performing the first step of the incubation in a humid chamber in a hot air vented oven at 80°C, 90°C or 100°C.

To compare the NMDA NR2A labelling in wild-type and NR2A knock-out mice, 5 control and 5 transgenic animals were examined with the postembedding method as described above. On 2 wild-type and 2 KO animals quantitative analysis of immunogold labelling was carried out. The effect of increasing the salt concentration in the TBST from 0.3% to 0.6% and 0.9% was also investigated as this could improve the signal/noise ratio by decreasing non-specific labelling. Three ultrathin sections from each animal were

reacted as described above, with TBST containing 0.3%, 0.6% or 0.9% NaCl. One-hundred synapses were selected from each grid from lamina III at a magnification at which the 10 nm gold particles thought to represent the NR2A subunits were not visible. Lamina III was chosen as this is the area which expresses the highest levels of the NR2A subunit in the spinal cord (see Results). Once the synapses were selected, the magnification was increased and the number of gold particles associated with the postsynaptic density was noted. To enable an unbiased assessment of differences in labelling intensity between control and transgenic animals, the investigator was blind to which animal the tissue examined came from and to the NaCl concentration in buffers used during the incubation.

Immunocytochemistry for combined confocal and electron microscopy

For confocal microscopy, mid-lumbar spinal cord segments from two rats were cut into parasagittal, 100 μm thick sections with a Vibratome. This orientation was chosen, because it is optimal for revealing the dorsally projecting dendritic trees of lamina III/IV NK1-immunoreactive cells. Sections were immersed in 50% ethanol for 30 minutes prior to immunoreaction to enhance antibody penetration (Llewellyn-Smith and Minson, 1992). They were then incubated in a cocktail of rabbit anti-NK1 (1:10,000) and mouse anti-NeuN (1:1000) antibodies diluted in phosphate-buffered saline (PBS) for 72 hours on a shaker table at 4°C. Following rinsing in PBS, sections were incubated for 24 hours in species-specific secondary antibodies (Jackson Immunoresearch, all raised in donkey, diluted 1:100) conjugated to FITC for NK1 or cyanine 5.18 for NeuN. Following further rinsing in PBS, sections were incubated in a mixture of propidium iodide (PI, 1:500) and RNAase (1:100) in PBS for 30 minutes at 35°C to reveal cell nuclei (neuronal, glial and endothelial). The RNAase was added to digest cytoplasmic RNA, which would otherwise give cell body labelling with PI. Sections were then mounted with anti-fade medium (Vectashield) and stored at -20°C before being viewed with a confocal microscope.

Dark field digital images were first saved using 4x, 10x and 20x dry lenses. These pictures later served as "maps" for locating and marking the exact position of NK1-immunoreactive neurons, laminar boundaries and landmarks such as blood vessels and myelin bundles. Sections were then scanned with a BioRad confocal laser scanning microscope (MRC1024) using a 20x dry and 40x and 60x oil immersion lenses. Two representative NK1-immunoreactive lamina III/IV cells ("Cell 6" and "Cell 8") were selected in different sections. Low, medium and high power confocal image stacks showing the cell body and dendritic arbor of both neurons, together with the surrounding neuronal and non-neuronal nuclei were saved. These nuclei served as landmarks for the

relocation of the NK1-immunoreactive cells during the EM part of the study. The distance of the selected neurons from the surface of the tissue was also noted.

The two selected sections were then removed from the slides, rinsed in phosphate buffer (PB) containing 4% glucose for 1 hour, cryoprotected and processed for freeze-substitution as described above. There are two critical steps during plunge-freezing at −170°C: (1) the high-speed immersion of the sections into the liquid propane, as due to the impact, the tissue slices can become detached from the pin and lost in the bottom of the cylinder containing the propane; (2) the removal of the sections from the pin following freezing, because at this stage the frozen tissue can break due to handling. To avoid these problems a custom made metal sieve fitted to the bottom of the propane-cylinder was used to retrieve any sections that detached from the pin during immersion freezing. To avoid the disintegration of sections during removal from the pin, 400 µm thick slices were cut from a translucent elastic silicone block with a Vibratome. To provide support these transparent slices were placed on the pin, below the sections. During the freeze-substitution the tissue separated from the Sylgard slices following gentle agitation.

The resin blocks obtained after freeze-substitution were transilluminated with a light microscope and the regions that contained the NK1-immunoractive cells were identified with the aid of the low power dark field and confocal images. The blocks were trimmed to an area that included the selected cells. They were then tilted to an angle that ensured that the plane of the knife was parallel to the surface of the original Vibratome section. Semi-thin serial sections (1 µm) were cut with a diamond knife, mounted on glass slides, counter-stained with toluidine-blue and viewed with light microscopy. Once a depth close to the selected NK1-immunoreactive cell was reached, ultrathin serial sections were cut and collected on Formvar-coated single slot nickel grids. These were then contrasted with aqueous uranyl acetate (10 min) and lead acetate (2 min), and viewed with a Philips CM100 electron microscope. The EM image was compared to the appropriate optical section from the confocal stack, and dendrites of the NK1-immunoreactive cells were relocated by using the neuronal and non-neuronal cell nuclei as landmarks.

Once the neurons were identified, 90 serial sections from Cell 6 and 135 from Cell 8 were collected on either Formvar-coated, single-slot nickel grids or uncoated nickel mesh grids. Grids were then individually numbered. The Formvar coating on the slot grids was generally damaged by the high temperature antigen retrieval method used to enhance the detection of NMDA NR1 subunits. Therefore, although mesh grids are not optimal for examining serial sections (as grid bars can cover the regions of interest), these were used for sections reacted against this subunit. Starting from the third grid, every fifth section

was reacted with an antibody against substance P to identify axon terminals that contained this neuropeptide and formed a synapse with a dendrite of the NK1-immunoreactive neuron. The grids before and after the SP immunolabelled section were reacted with an AMPA or NMDA antibody. The remaining grids were reacted against another iGluR or CGRP, depending on the results obtained from the initial incubations. Boutons were only included in the survey if they were both SP- and the CGRP-immunoreactive and formed a synapse on the section incubated against a particular iGluR subunit. This approach made it possible to determine which iGluRs were expressed on NK1-immunoreactive cells at synapses formed by SP- and CGRP-containing nociceptive primary afferent terminals.

Postembedding incubations were carried out as described above. Sections reacted against the glutamate receptors were etched prior to the immunoreaction, while this step was omitted for the neuropeptides (see Chapter 3). Primary antibodies and their concentrations as follows: (1) rabbit antibody against NMDA NR1 (1 μg/ml), (2) rabbit antibody against NMDA NR2A (5.4 μg/ml), (3) a cocktail of rabbit antibodies against NMDA NR2B-N (10.6 μg/ml) and NR2B-C (5.2 μg/ml), (4) rabbit antibody against GluR1 (1:50), (5) rabbit antibody against GluR2 (1:100), (6) rabbit antibody against GluR 2/3 (1:150) (7) rabbit antibody against GluR4 (1:200), (8) rabbit antibody against SP (1:10,000), and (9) sheep antibody against CGRP (1:20,000). Sections reacted with the sheep CGRP antibody were incubated in unlabelled rabbit anti-sheep IgG (Vector, 1:200) for 2 hours before immunogold labelling.

Initially the SP reacted grids were viewed with the EM. The locations of boutons which formed a synapse with the NK1-immunoreactive neurons were marked on a low (750x) and medium (4,200x) power image obtained using the CCD camera attached to the electron microscope. With the aid of relocation software (Remote XY Control, PW6472, Version 1.0; Philips Analytical, Electron Optics) and the low and medium power images, the selected axon terminals were relocated on the adjacent sections reacted for CGRP or iGluR. The presence or absence of CGRP immunoreactivity in the bouton and the number of gold particles representing glutamate receptors at synapses were noted. With both neuropeptide antibodies, boutons were counted as immunoreactive if they contained eight or more gold particles located over dense-cored vesicles, while they were classified as negative if the profile contained dcvs that had no gold particles representing CGRP or SP. Axon terminals with dense-cored vesicles that had 0-8 gold-particles for SP or CGRP were excluded from the survey. From the relocated terminals high power (17,500x or 24,500x) digital images were saved and in some cases photographs were also taken.

Immunofluorescence staining for light microscopy following antigen unmasking

Lumbar spinal cord segments and cerebella from two wild-type and two NMDA NR2A knock-out mice were cut into 60 μm thick sections with a Vibratome. In order to expose NMDA NR2A receptor subunits at synaptic sites, sections were processed according to an antigen unmasking method involving limited proteolytic digestion with pepsin, as described by Watanabe et al. (1998). A stock solution, containing 100 mg/ml pepsin in distilled water was aliquoted and stored at -70°C, and a fresh aliquot was thawed immediately before pepsin treatment. This stock solution was diluted with pre-warmed 0.2M HCl to make up the pepsin working solution. Pepsin treatment was carried out by incubating sections at 37°C for 30 minutes in double distilled water, followed by 5, 10 or 15 minutes in 0.2M HCl containing 1 mg/ml pepsin (Dako, Glostrup, Denmark) with continuous agitation. The sections were then rinsed (3 × 10 minutes) in PBS with 0.1% Triton X-100 (PBST) and incubated in affinity purified rabbit anti-NR2A antibody (0.05 μg/ml) for 24 hours at 4°C. As the NR2A antibody is not commercially available, to allow its use at a very low concentration, a tyramide signal amplification (TSA) method was generally used to reveal NR2A subunits. Sections were rinsed and incubated for 2 hours at room temperature in biotinylated donkey anti-rabbit IgG (Jackson Immunoresearch, West Grove, PA; diluted 1:500), followed by Streptavidin conjugated to HRP (diluted 1:100, part of TSA kit) for 30 minutes. Amplification was carried out by incubating the sections in tetramethylrhodamine fluorophore stock solution diluted 1:50 in Amplification Diluent according to the manufacturer's instructions (Perkin Elmer, Boston, MA; NEL 702). The amplification time was 7 minutes. Following rinsing, sections were mounted and stored in Vectashield at -20°C. In order to assess the effect of pepsin treatment, some sections that had not been pepsin-treated were also processed in the same bottles.

Cerebellum and spinal cord sections were viewed with a confocal microscope using a 60x oil immersion lens. Representative areas (laminae I-III from the dorsal horn of the spinal cord and the molecular, Purkinje-cell and granular layers of the cerebellum) were scanned from the wild-type and NMDA NR2A knock-out mice using the same laser settings. From the cerebellar folia, where the labelling for NR2A was very strong, low power images were also obtained for illustration, using a 20x dry lens.

RESULTS

Postembedding immunogold labelling for NMDA receptors in the rat spinal cord

The ultrastructural appearance of the tissue following freeze-substitution was good. Membranes were intact and cell organelles were easily identifiable. The etching and the

postembedding reaction moderately decreased the preservation of tissue morphology, nevertheless cell organelles and synapses were still clearly recognizable (Fig. 4.1a-l).

All NMDA receptor antibodies tested in this part of the study gave strong synaptic labelling in the spinal cord. The gold particles representing NR1 subunits were present at asymmetrical synapses throughout the dorsal horn. Where the plane of section was perpendicular to the synaptic cleft, most of the particles were associated with the post-synaptic density. Labelled synapses contained up to 15 gold particles. At the antibody concentration at which synaptic labelling was the strongest, some mitochondria, the heterochromatin of cell nuclei and a proportion of dense-cored vesicles (Fig. 4.2a-b) were also heavily labelled. Occasional gold particles were scattered over non-synaptic membranes. The ten-minute heat treatment before the postembedding incubation dramatically improved the signal/noise ratio for this subunit by increasing the synaptic and reducing the non-synaptic labelling (Fig. 4.1a-d). Heating the sections to 90°C gave a better result than heating to 80°C. Sections treated at 100°C often came off the grid probably due to the bubbles formed in the boiling buffer, and in addition the ultrastructure of these sections was inferior to those for which antigen retrieval was carried out at 90°C. Following heat treatment immunoreactive synapses contained up to 30 gold particles and non-synaptic labelling was almost exclusively restricted to mitochondria and some dense-cored vesicles. Heating did not have a beneficial effect on the other iGluR antibodies.

From the NMDA antibodies used in this part of the study the NMDA NR2A antiserum appeared to give the best synaptic labelling. Immunopositive asymmetrical synapses contained up to 25 gold particles at their postsynaptic density (Fig. 4.1g-h). Synapses in laminae IIi and III were more heavily labelled than those in laminae I and IIo. There was relatively little mitochondrial or extra-synaptic labelling, but dense core vesicles were occasionally very heavily immunoreactive (Fig. 4.2c-d).

Both NMDA NR2B antibodies gave strong synaptic labelling in the dorsal horn, with up to 10 gold particles per synapse. Immunogold particles were also scattered at non-synaptic sites with both antibodies, and some dense-cored vesicles were heavily labelled (Fig. 4.2e-f). Incubating the sections in a cocktail of NR2B-N and NR2B-C antibodies approximately doubled the intensity of the labelling (Fig. 4.1i-l). To enhance synaptic labelling during the combined confocal and EM part of the study these two antibodies were therefore used in a mixture.

Figure 4.1 Electron micrographs showing postembedding immunogold labelling against the NMDA NR1 (*a-d*), NR2A (*e-h*) or NR2B (*i-l*) subunits on freeze-substituted, Lowicryl embedded rat spinal cord. Where the plane of section is perpendicular to the synaptic cleft (e.g. *a*), the 10 nm gold particles representing the receptor subunits are located at the postsynaptic densities of asymmetrical synapses. Immunoreactive synapses contain up to 28 gold particles. Pictures representing NR1 subunits were obtained from sections which were subjected to heat-treatment. Scale bars, 200 nm.

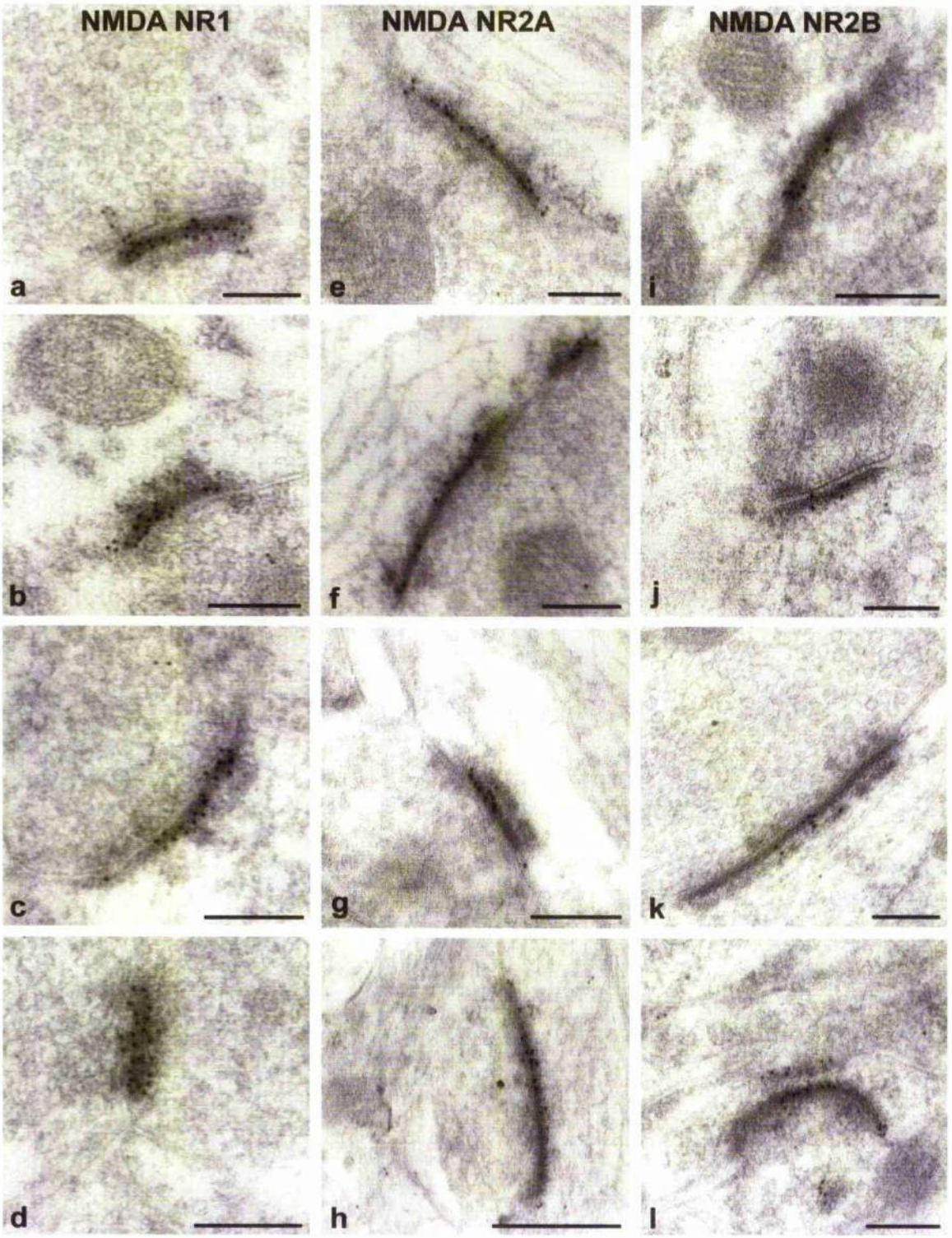
NMDA NR1
NMDA NR2A
NMDA NR2B
a
b
c
d
e
f
g
h
i
j
k
l

Figure 4.2 Electron microscopic images showing dense-cored vesicle labelling in the superficial laminae of rat spinal cord with NR1 (*a-b*), NR2A (*c-d*) and a mixture of NR2B-N and NR2B-C antibodies (*e-f*), revealed with 10 nm gold particles. On each image dense-cored vesicles located inside axon terminals are heavily labelled, with some containing up to 20, 10 nm gold particles. On picture (*b*), a synapse, weakly immunoreactive for NR1, is also visible. Scale bar, 200 nm.

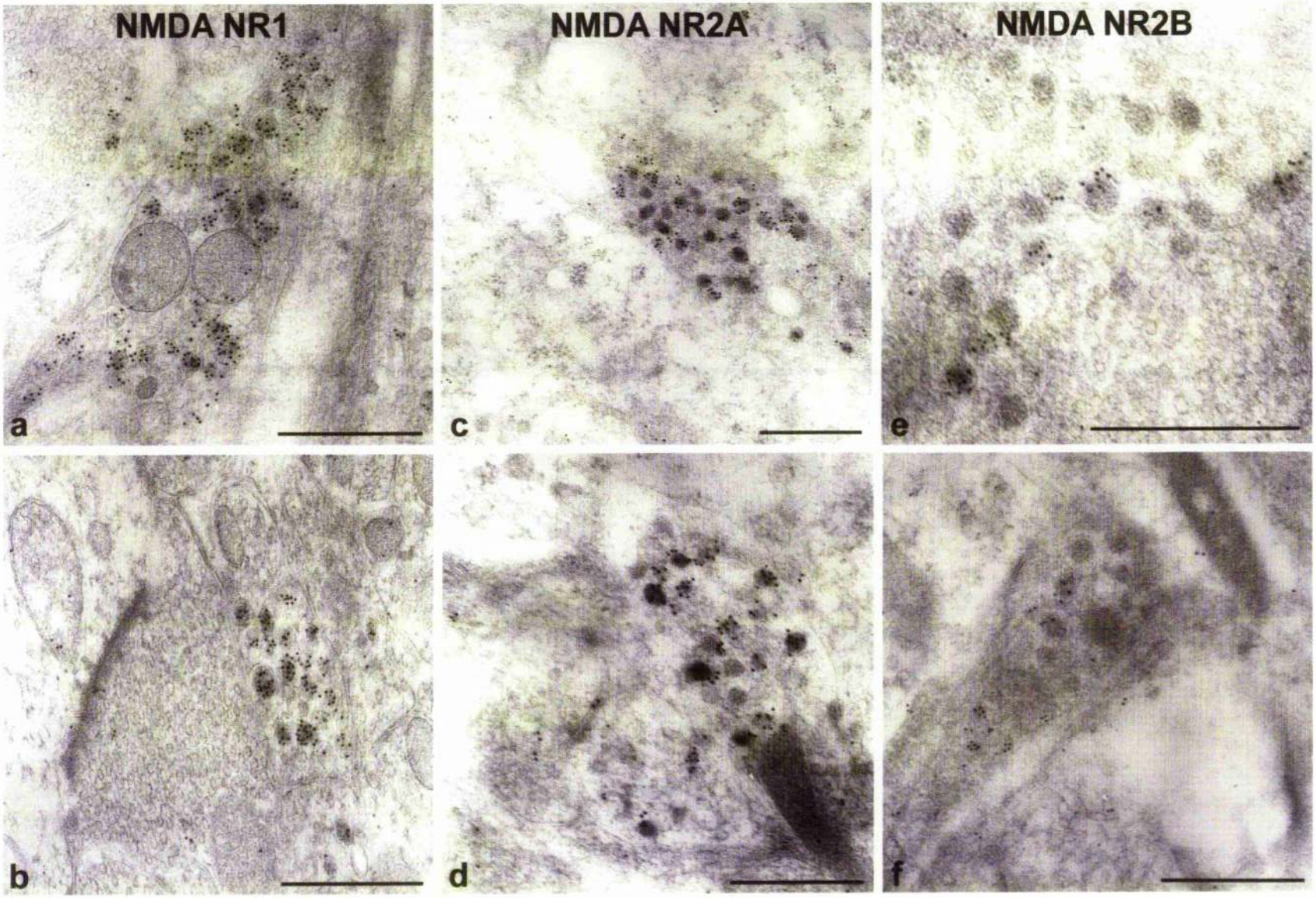
NMDA NR1
NMDA NR2A
NMDA NR2B
a
b
c
d
e
f

Combined confocal and electron microscopic analysis of NK1 cells

The distribution of NK1 receptor expressing cells seen with confocal microscopy was similar to that reported in other studies (Sakamoto et al., 1999). NK1-immunoreactive cell bodies were found in laminae I, III and IV. The neurons selected for analysis were representative examples of the large lamina III/IV NK1-immunoreactive cells that have dendrites projecting dorsally to the superficial laminae (Fig. 4.3a). Neuronal nuclei were stained with both PI and NeuN, while non-neuronal nuclei were only labelled with PI. In neurons weak cytoplasmic labelling against NeuN was often visible (Figs. 4.3c; 4.4a).

With the electron microscope the ultrastructural appearance of the tissue previously subjected to confocal microscopy was slightly compromised. Nevertheless, membranes, cell organelles and synapses were identifiable (Fig. 4.4d-g). On sections reacted with antibodies against either SP or CGRP, gold particles representing the neuropeptides were mainly found over dense-cored vesicles in axon terminals. Several SP-immunoreactive, dense-cored vesicle containing boutons were apposed to the dendrites of the NK1-cells, but these were only analysed if they had gold particles representing CGRP and formed at least one synapse on any of the serial sections reacted against an iGluR (Fig. 4.4). Altogether 42 SP- and CGRP-immunoreactive, (presumed nociceptive primary afferent) axon terminals that formed synapses on grids reacted for an iGluR were identified on the two cells (33 on Cell 8 and 9 on Cell 6). These boutons formed 54 asymmetrical synapses. Gold particles representing all five iGluR subunits examined in this study were found associated with the postsynaptic densities of NK1-positive dendrites. However, the number of particles/synapse and the proportion of labelled synapses varied for the different subunits (Fig. 4.5). Synapses were counted as positive if they were associated with two or more gold particles coding for an iGluR subunit and were considered equivocal if they only had one particle. Out of the 25 synapses found on ultrathin sections reacted for GluR1, 10 were positive, 11 were negative and 4 were equivocal. Of the 17 synapses examined for GluR2, 7 were positive, 7 were negative and 3 were equivocal. Only four synapses could be relocated on grids reacted with the NR1 antibody: 3 were positive and 1 was negative. For NR2A, 21 synapses were found and 3 of these were equivocal, while the remaining 18 were positive. For NR2B out of the 18 synapses, 1 was negative, 1 was equivocal and 16 were positive. The average number of gold particles/synapse was 1.6 for GluR1, 3.3 for GluR2, 2.5 for NR1, 5.6 for NR2A and 5.5 for NR2B. Statistical analysis of the immunogold labelling was not carried out, due to the small sample number.

Serial sections cut through the same synapse and reacted against different iGluR subunits revealed that gold particles corresponding to different subunits could be found on

Figure 4.3 Projected confocal image showing an NK1-immunoreactive neuron (***a, green***), with its cell body located in lamina III and dendrites projecting dorsally to laminae I-II. Several other NK1-immunoreactive dendrites form a plexus in the superficial lamina. Part of the top left dendrite (*box*) is shown at higher magnification at the right (***b-c***). On (***c***) cell nuclei surrounding the selected dendrite are also visible. All nuclei are stained with propidium iodine (red), while NeuN-immunoreactive neuronal nuclei are also stained with Cy5 (blue). Cell nuclei serve as landmarks and three of these are marked with numbers (*1, 2* and *3*). The same area is shown on Figure 4.4 with both confocal and electron microscopy. Scale bars, 10 μm.

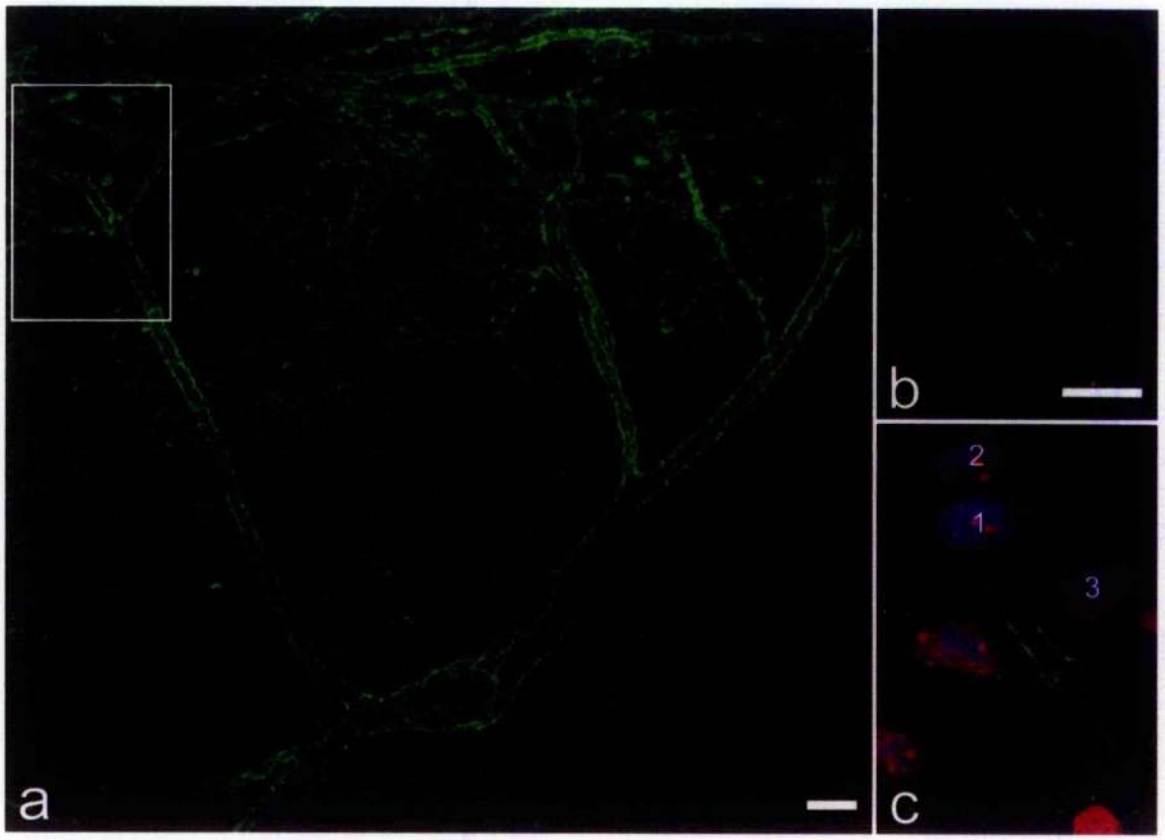
a
b
c
2
1
3

Figure 4.4 Matching confocal and EM images from the same cell (Figure 4.3a-c) are shown in (***a***) and (***b***). On the left image, an NK1-immunoractive dendrite (the same as illustrated on Figure 4.4b-c) forms two branches (*d1* and *d2*). Glial cell nuclei (red) are marked with *asterisks*, while neuronal nuclei (purple) are numbered (*1-5*). There is a faint cytoplasmic NeuN staining (blue) surrounding the neuronal nucleus marked with (*1*). An endothelial cell nucleus (*arrow*) is also visible. The same profiles are present and clearly identifiable on the low power EM picture (***b***). (***c***) shows the box in (***b***) at a higher magnification. The two dendritic branches (*d1* and *d2*) are surrounded by several axon terminals, some of which form synapses. A bouton forming a synapse with the dendrite is visible inside the box. (***d-e***) are serial sections cut through the same bouton and reacted with an antibody against CGRP (***d, g***), SP (***f***) or NR2A (***e***). On the serial sections reacted for the neuropeptides, 10 nm gold particles representing SP or CGRP are located inside dense-cored vesicles, suggesting that the bouton belongs to a nociceptive primary afferent terminal. The synapse formed by this bouton has 21 gold particles representing the NR2A subunit of the NMDA receptor (***e***). (***h***) and (***i***) are higher magnification untilted and tilted images of the synapse from (***e***). On the tilted image (***i***) gold particles are located on the postsynaptic density. Box on (***b***) corresponds to an area of 15.8 x 14 μm. Gold particles are 5 μm. Scale bar, 500 nm.

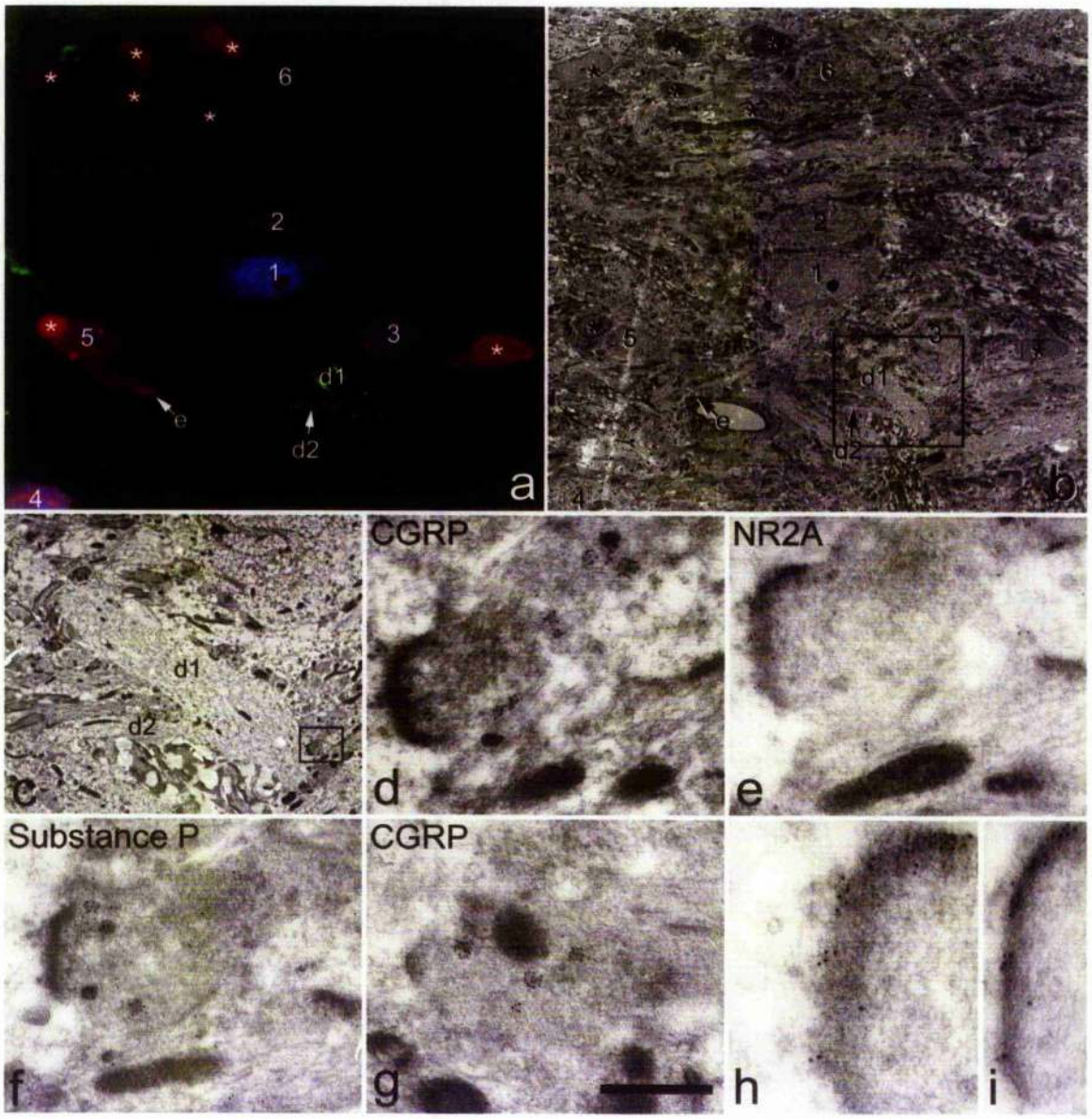
a
b
c
d
e
f
g
h
i
1
2
3
4
5
6
d1
d2
e
CGRP
NR2A
Substance P
CGRP

Figure 4.5 Frequency histograms showing the numbers of gold particles at synapses formed by SP- and CGRP-containing nociceptive primary afferents on NK1-immunoreactive neurons on sections reacted with the GluR1, GluR2, NR1, NR2A and mixture of NR2B-N and NR2B-C antibodies.

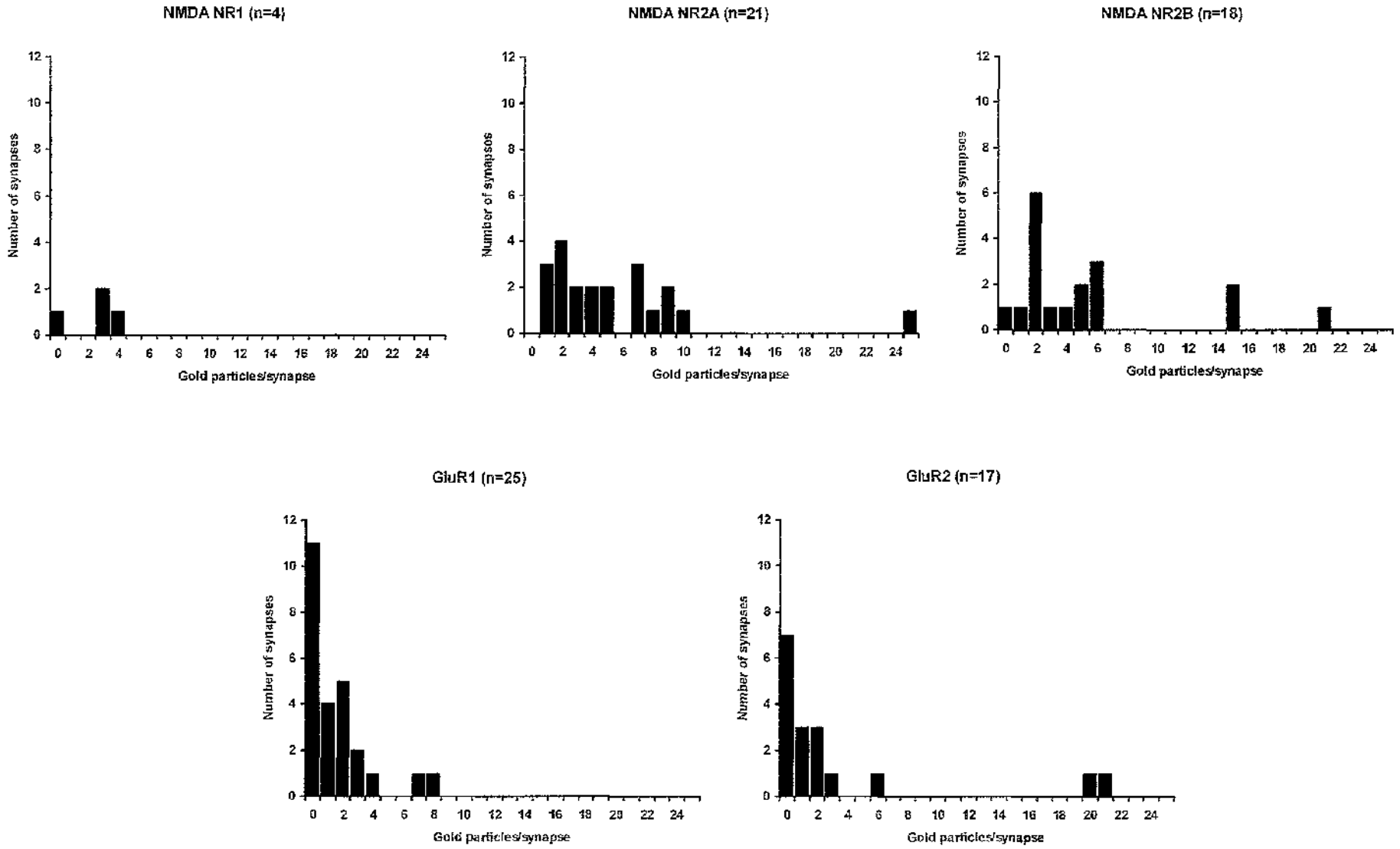
NMDA NR1 (n=4)
NMDA NR2A (n=21)
NMDA NR2B (n=18)
GluR1 (n=25)
GluR2 (n=17)
Number of synapses
Gold particles/synapse

the same synapse. Four synapses were immunoreactive for NR2A and NR2B, one for GluR2 and NR2B, 3 for GluR1 and NR2A, one for GluR1, GluR2 and NR2A, and 2 for NR1 and NR2B.

Immunofluorescence and immunogold study of NMDA NR2A knock-out mice

During the study into the synaptic distribution of NMDA receptors in the dorsal horn, strong dense-cored vesicle labelling was observed inside axon terminals with all NMDA antibodies used (Fig. 4.2a-f). NMDA receptors have been found in primary afferent axon terminals in the spinal gray matter (Liu et al., 1994; Lu et al., 2003), and these are thought to function as presynaptic receptors (see Chapter 1). In order to determine whether gold particles found over dense-cored vesicles corresponded to presynaptic receptors in transit to the membrane or whether these represented non-specific labelling, postembedding immunogold reactions were carried out against NR2A on five wild-type and five NMDA NR2A knock-out mice.

With the postembedding immunogold method wild-type mice showed similar labelling pattern (i.e. dcv and synaptic labelling) to that observed in rats. However, surprisingly, in the knock-out animals not only did the dense-cored vesicle labelling remain (Fig. 4.6d), but there was also significant synaptic labelling (Fig 4.6a-c). Synaptic labelling in the knock-out animals was always weaker than that in the wild-types (Figs. 4.7, 4.8, 4.9). Although not studied systematically, it appeared that in the NR2A knock-out animals, postsynaptic densities of asymmetrical synapses were thinner than in the control mice. A quantitative analysis of the immunogold labelling was carried out to test whether increasing the salt concentration in the TBST from 0.3% to 0.6% or 0.9% could eliminate this apparent non-specific immunolabelling in the knock-out tissue, while leaving the authentic synaptic labelling intact. Increasing the NaCl concentration in the buffers dramatically reduced the intensity of synaptic labelling in both the wild-type and the KO animals. On sections from two wild-type and two NMDA NR2A KO mice incubated in buffers containing 0.3% NaCl the means of the total number of gold particles counted over 100 randomly selected synapses in each animal were 180 (WT) and 84 (KO), respectively. Corresponding numbers for sections incubated in TBST containing 0.6% NaCl were 76 and 28, while for 0.9% salt concentration these numbers were 31 and 12 (Fig. 4.9). The ratio of these means (WT/KO) were 2.1 for 0.3% NaCl, 2.7 for 0.6% NaCl and 2.6 for 0.9% NaCl.

Although diagnostic PCR showed that the NR2A subunit was absent in the knock-out mice (Prof. Masahiko Watanabe, personal communications), antigen unmasking

Figure 4.6 Electron microscopic images showing postembedding immunogold labelling for NR2A subunits at synapses (***a-c***) and dense-cored vesicles (***d***) in mice where the NR2A subunit has been knocked-out. Note the thin appearance of the postsynaptic densities. Scale bars, 200 nm.

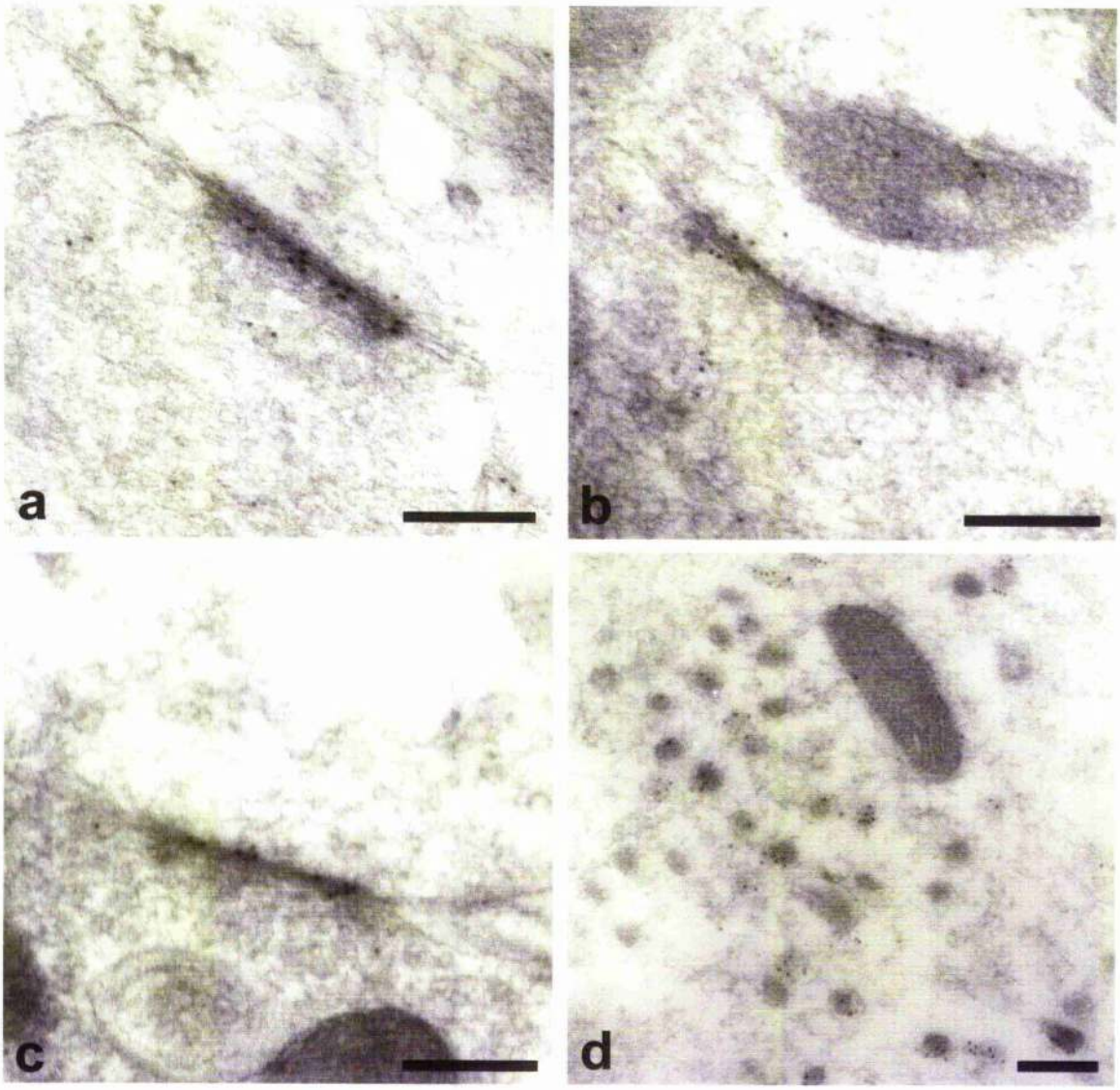
a
b
c
d

Figure 4.7 Frequency histograms obtained after quantitative analysis of NR2A immunogold labelling at synapses in wild-type (*Control 1*, bottom row) and knock-out (*KO 1*, top row) mice using 0.3%, 0.6% and 0.9% NaCl concentrations in the buffers. Data comes from 100 randomly selected synapses form lamina III. Although in the knock-out animal fewer synapses were labelled and the intensity of labelling was generally weaker than in the wild-type, the mutant mouse still showed significant synaptic labelling.

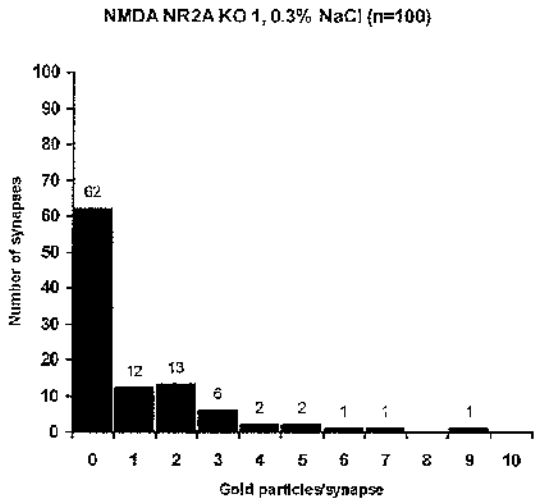
NMDA NR2A KO 1, 0.3% NaCl (n=100)
Number of synapses
Gold particles/synapse
62
12
13
6
2
2
1
1
1

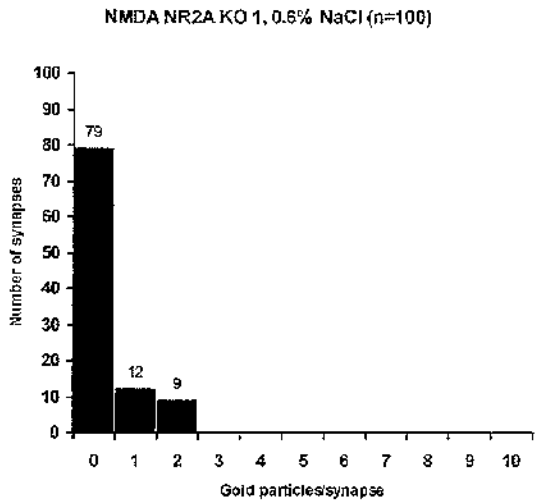
NMDA NR2A KO 1, 0.6% NaCl (n=100)
Number of synapses
Gold particles/synapse
79
12
9

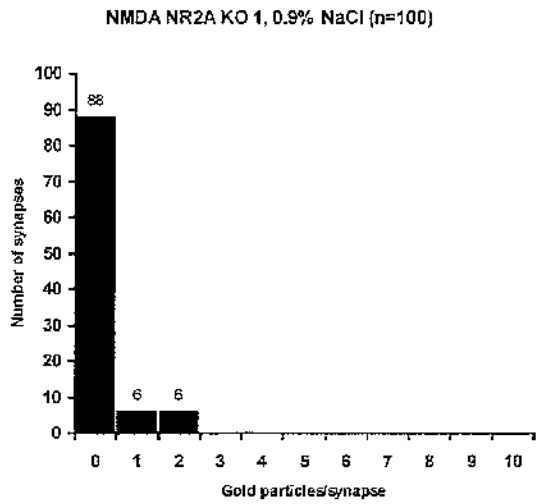
NMDA NR2A KO 1, 0.9% NaCl (n=100)
Number of synapses
Gold particles/synapse
88
6
6

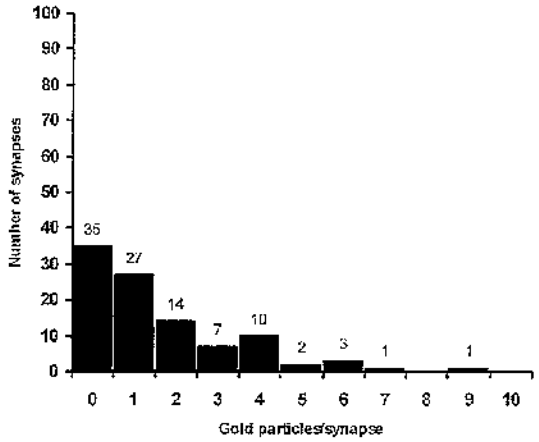
Control 1, 0.3% NaCl (n=100)
Number of synapses
Gold particles/synapse
35
27
14
7
10
2
3
1
1

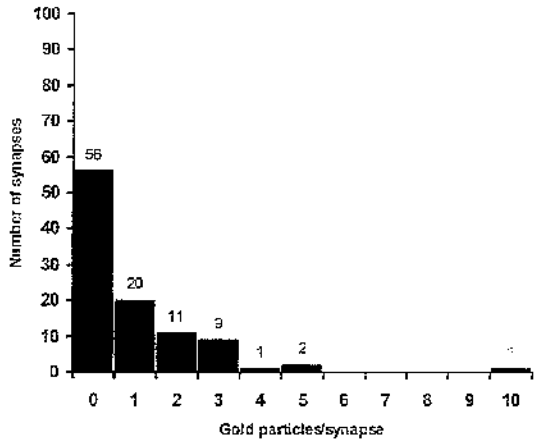
Control 1, 0.6% NaCl (n=100)
Number of synapses
Gold particles/synapse
56
20
11
9
1
2

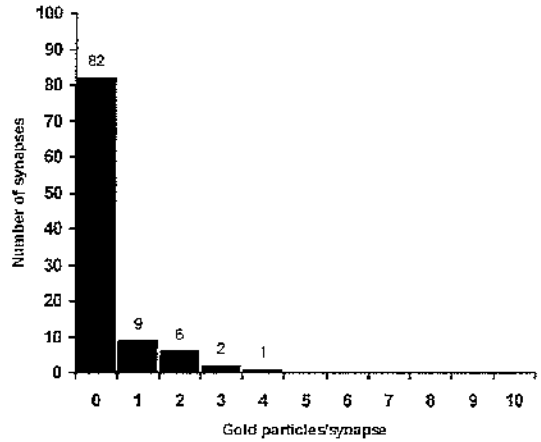
Control 1, 0.9% NaCl (n=100)
Number of synapses
Gold particles/synapse
82
9
6
2
1

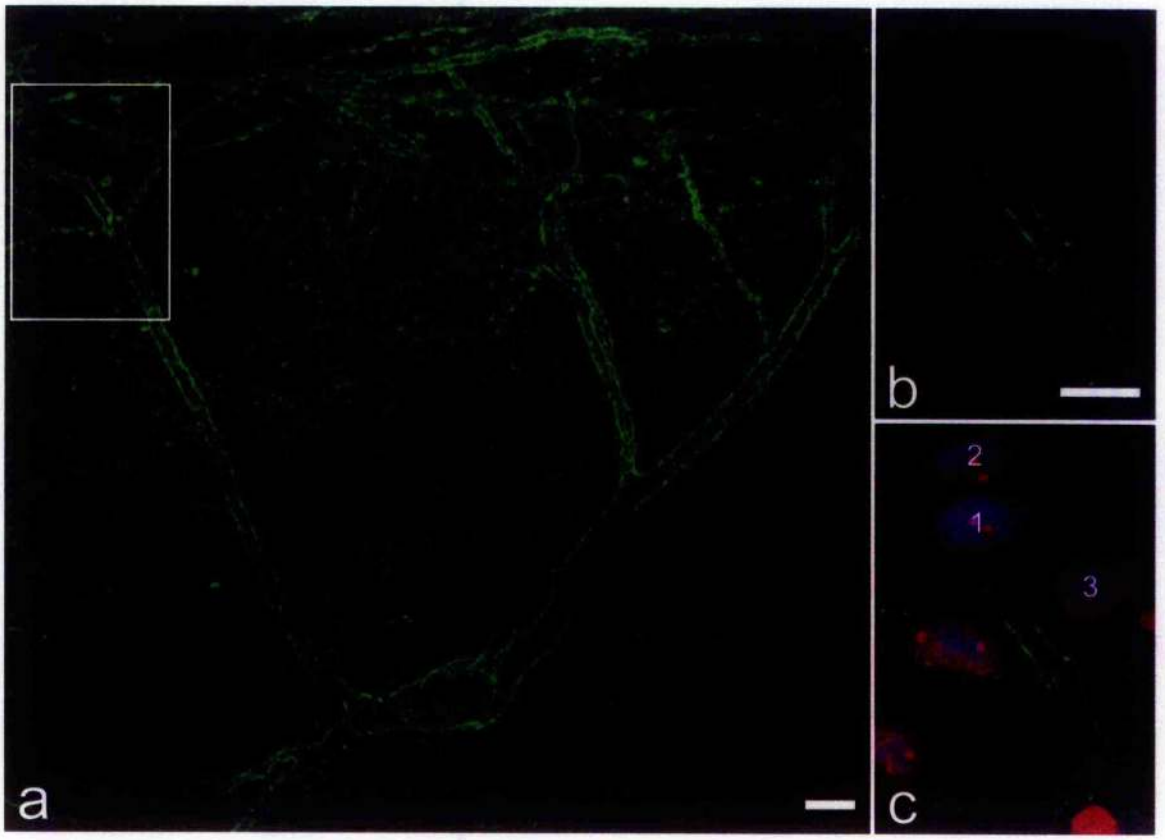
a
b
c
1
2
3

Figure 4.8 Frequency histograms obtained after quantitative analysis of NR2A immunogold labelling at synapses in wild-type (*Control 2*, bottom row) and knock-out (*KO 2*, top row) mice using 0.3%, 0.6% and 0.9% NaCl concentrations in the buffers. Data comes from 100 randomly selected synapses form lamina III. Although in the knock-out animal fewer synapses were labelled and the intensity of labelling was generally weaker than in the wild-type, the mutant mouse still showed significant synaptic labelling.

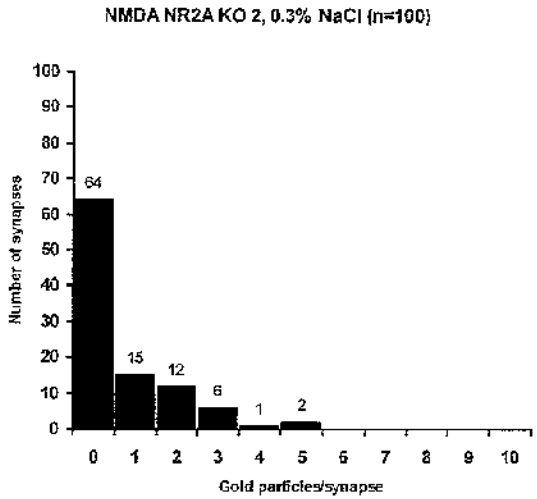
NMDA NR2A KO 2, 0.3% NaCl (n=100)
Number of synapses
Gold particles/synapse
64
15
12
6
1
2

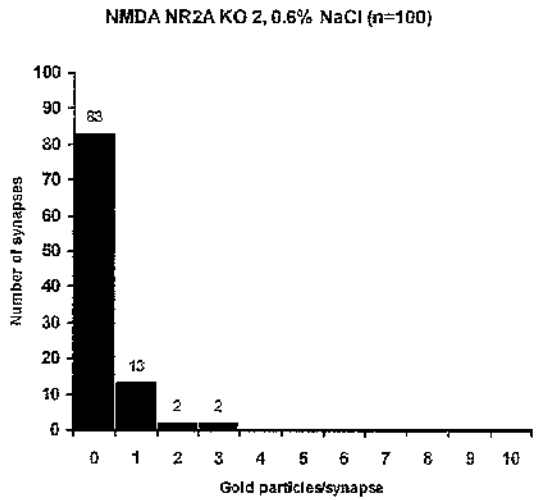
NMDA NR2A KO 2, 0.6% NaCl (n=100)
Number of synapses
Gold particles/synapse
83
13
2
2

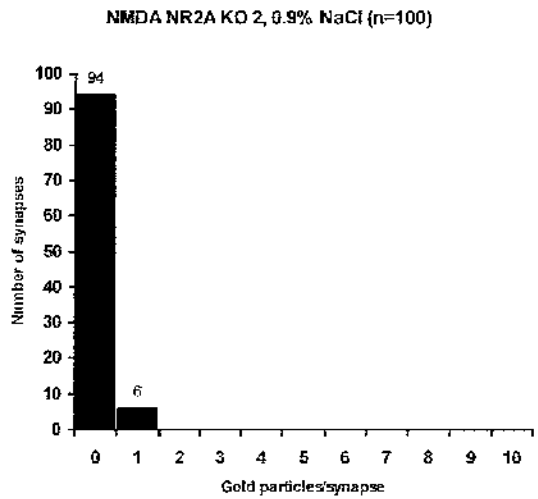
NMDA NR2A KO 2, 0.9% NaCl (n=100)
Number of synapses
Gold particles/synapse
94
6

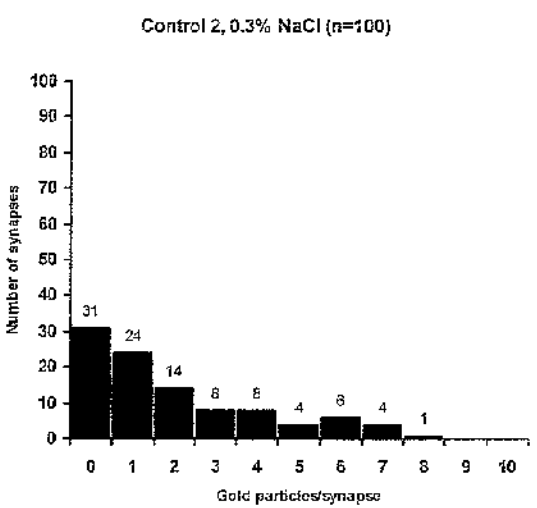
Control 2, 0.3% NaCl (n=100)
Number of synapses
Gold particles/synapse
31
24
14
8
8
4
6
4
1

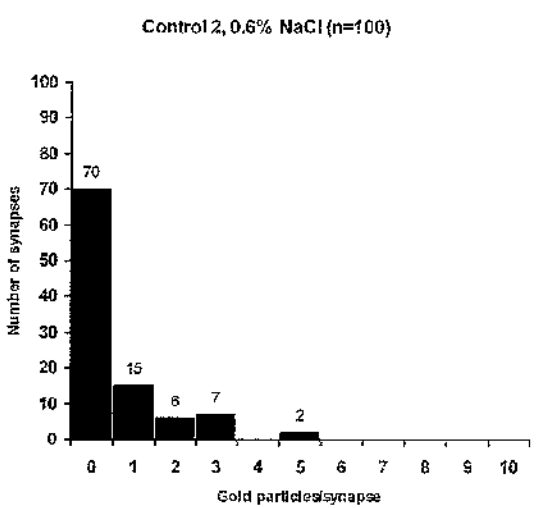
Control 2, 0.6% NaCl (n=100)
Number of synapses
Gold particles/synapse
70
15
6
7
2

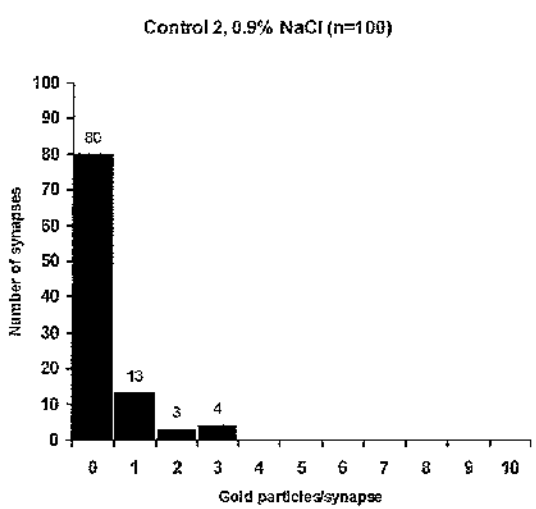
Control 2, 0.9% NaCl (n=100)
Number of synapses
Gold particles/synapse
80
13
3
4

Figure 4.9 Diagram showing the total number of gold particles counted over 100 randomly selected synapses in lamina III of two wild-type (red and light blue) and two NR2A knock-out (pink and dark blue) mice, using the NR2A antibody with various NaCl concentrations in the incubation buffers (0.3%, 0.6% and 0.9%). Increasing the salt concentration reduced the numbers of gold particles at synapses in both the knock-out and the control animals, but did not dramatically increase the ratio of wild-type/knock-out labelling.

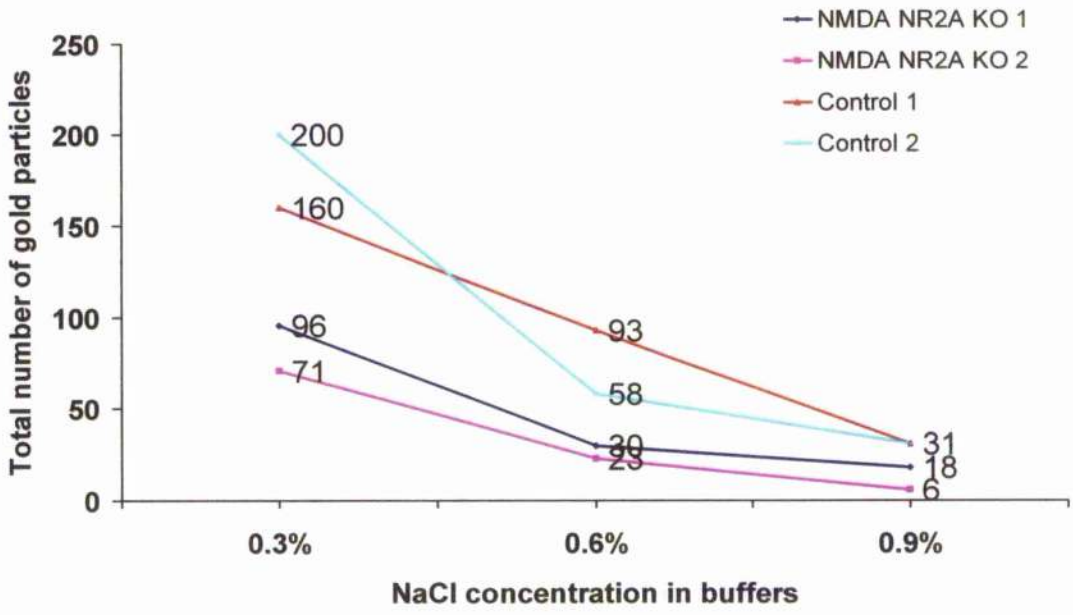
NMDA NR2A KO 1
NMDA NR2A KO 2
Control 1
Control 2
Total number of gold particles
250
200
150
100
50
0
200
160
96
71
93
58
30
23
31
18
6
0.3%
0.6%
0.9%
NaCl concentration in buffers

Figure 4.10 Confocal images of NR2A labelling in the cerebellum and spinal cord following proteolytic digestion in the wild-type (***a-c***) and NR2A knock-out (***d-f***) mice. (***a***) shows heavy labelling in the granular layer of the cerebellum which is completely missing in the corresponding filed from a knock-out animal (***d***). (***b***) and (*e*) show the molecular (*Mo*), Purkinje-cell (*Pc*) and granular (*Gr*) layers of the cerebellum at higher magnification. Labelling in the wild-type is present at mossy fibre synapses. There is a weak non-specific labelling in the Purkinje-cell bodies (*arrowheads*) in both the control and the knock-out animals. Images (***c***) and (***f***) show labelling in laminae II/III of mouse spinal cord. In the wild-type (***c***) there is heavy punctate labelling for NR2A in lamina III, which is almost absent from lamina II. The knock-out spinal cord (***f***) does not show specific labelling. Scale bars, 20 μm.

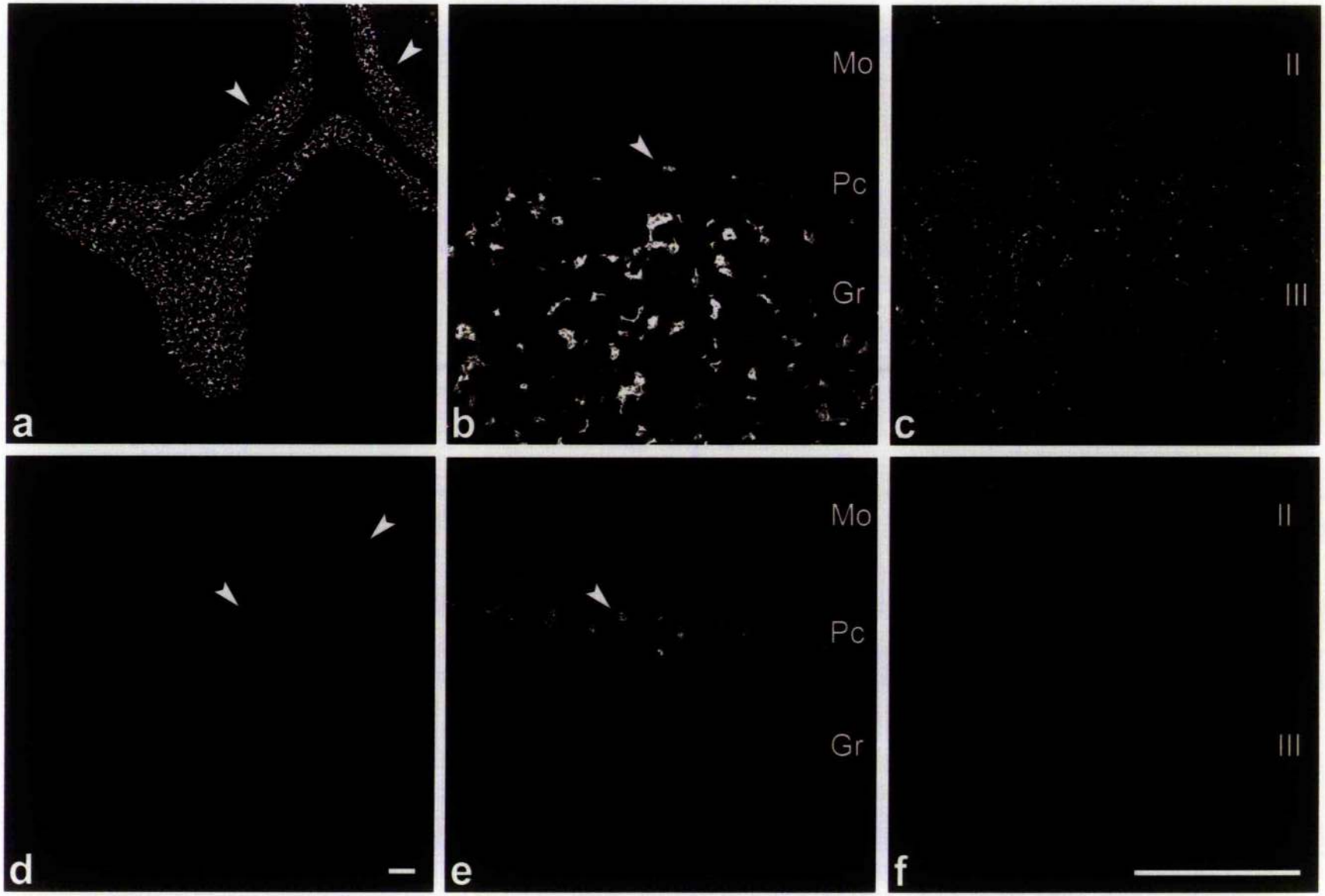
Mo
Pc
Gr
II
III
a
b
c
d
e
f

immunocytochemistry was also performed to confirm this with an independent technique. Sections that had not been treated with pepsin did not show any immunostaining, while after pepsin-treatment a strong punctate immunostaining representing NR2A appeared in the sections from wild-type animals (Fig. 4.10a-c). Punctate labelling was strongest on sections pepsin treated for 10 minutes, while it was weak or absent following proteolytic digestion for 5 minutes. Many of the sections pepsin digested for 15 minutes were damaged, although the ones which remained intact showed punctate labelling. The granular layer of the cerebellum showed a very strong immunoreactivity, which was presumably associated with synapses formed by mossy-fibre terminals (Yamada et al., 2001). No staining was seen in the molecular layer. A faint non-specific immunostaining was observed in the cell bodies of Purkinje-cells in the Purkinje-cell layer (Fig. 4.10a-b). This distribution of NR2A labelling in the cerebellum matched those reported previously by other studies (e.g. Yamada et al., 2001). In the spinal cord of the control animals punctate NMDA NR2A labelling was strongest in lamina III with much lower levels elsewhere, except lamina II, where it was virtually missing (Fig. 4.10c). A few strongly labelled puncta were also visible in lamina I. The NMDA NR2A knock-out mice did not show any immunolabelling, except in the Purkinje-cell layer of the cerebellum, where a faint non-specific staining was seen in the cell bodies, similar to that observed in the control animals (Fig. 4.10d-e).

DISCUSSION

Enhanced immunogold labelling for NR1 following antigen retrieval with heat

Aldehyde fixation, especially with divalent aldehydes like glutaraldehyde creates cross-links between tissue proteins, which mask the epitopes from being recognized by antibodies. Various antigen retrieval techniques, including heating the tissue to 100°C and above, have been used to overcome these difficulties (for reviews see Shi et al., 2000; Hayat, 2002). This approach has also been successfully used previously to increase the level of postembedding immunogold labelling on sections embedded in both epoxy-, and acrylic-resins (Stirling and Graff, 1995; Brorson et al., 1998, 1999a, 1999b, 2001). The finding that incubating the grids at 90°C for 10 minutes increased synaptic labelling and decreased non-synaptic immunogold labelling, suggests that heat reduces the detrimental effects of aldehydes on the antigenicity of synaptic NR1 epitopes. This is probably achieved by breaking up the cross-links formed during fixation, while heating presumably denatures epitopes responsible for non-synaptic and background labelling. The increased sensitivity at synapses and the decreased level of background labelling both contributed to

an improved signal/noise ratio. The fact that heating does not improve the immunogold labelling for the other iGluR antibodies tested suggests, that these receptors are either not extensively cross-linked during fixation, or else that they do not tolerate heat treatment. However, the value of antigen retrieval with heating for the detection of NR1 subunits needs to be reconsidered in the light of subsequent findings with the NR2A antibody on NR2A knock-out mice.

Apparent non-specific immunogold labelling with an NMDA NR2A antibody

Postembedding immunocytochemistry on freeze-substituted tissue has been widely used to study the localization of synaptic proteins (Nüsser et al., 1994, 1995, 1996, 1998; Baude et al., 1995; Bernard et al., 1997; Lujan et al., 1996; Clarke and Bolam, 1998; Gingrich et al., 2004), including the NMDA receptors (He et al., 1998; Racca et al., 2000; Rossi et al., 2002; Kohr et al., 2003; Nyiri et al., 2003) which are usually not detectable with conventional immunocytochemical techniques. In this study, commonly used tissue processing and incubation protocols were employed (Matsubara et al., 1996, 1999; Landsend et al., 1997; Nüsser et al., 1998; Takumi et al., 1999; Sassoè-Pognetto et al., 2000, 2003; Bergersen et al., 2001; He et al., 2001; Rossi et al., 2002; Kohr et al., 2003; Ragnarson et al., 2003; Todd et al., 2003), and these were optimized for the detection of synaptic proteins (etching, overnight incubation at room temperature, 0.3% NaCl in buffers). With this method, dense-cored vesicle and synaptic labelling were observed with a well-characterized, affinity-purified NMDA NR2A antibody in five mice, in which the NMDA NR2A subunit had been knocked out. Diagnostic PCR and immunofluorescence following antigen unmasking confirmed that these animals lacked the NR2A subunit. This suggests that the immunogold labelling observed was non-specific. It is possible to explain the dense-cored vesicle labelling by the fact that the cross-reactivity of the NR2A antibody was tested on Western blots prepared from the PSD fraction of brain homogenates (Watanabe et al., 1998). Therefore, the antibody could react with one or more proteins expressed in dense-cored vesicles and this would remain undetected during specificity tests. However it is not easy to account for the synaptic labelling observed in the transgenic animals. A possible explanation would be that the knock-out mice express a truncated form of the receptor, which is susceptible to proteolytic digestion, thus it is not revealed by immunocytochemistry following antigen unmasking, but remains detectable with postembedding immunogold method. However, this can be ruled out since the NR2A antibody did not give immunolabelling on Western blots prepared from the PSD fraction of NR2A knock-out animals (Watanabe et al., 1998).

The immunogold labelling pattern in the knock-out animals suggests that the NMDA NR2A antibody selectively binds to subcellular compartments with a high protein content, and that this binding is non-specific. Sites with high protein concentration include the heterochromatin of cell nuclei, mitochondria, dense-cored vesicles and postsynaptic densities. Non-specific binding of antibodies to structures with high protein concentration is a well-known phenomenon in immunohistochemistry. It is generally caused by weak ionic forces acting between the antibody and tissue proteins. As early as 1975, Aarli et al. found that the F_c-portion of purified IgG antibody molecules binds to proteins in the CNS. Paasivuo and Saksela (1983) found that F_c-fragments were responsible for the non-specific binding of antibodies to astrocytes in human brain tumors, while Costa et al. (1984) reported that the F_c-fragment of antibodies binds to histone proteins.

Using postembedding immunocytochemistry Josephsen et al. (1999) showed selective, but non-specific labelling of enamel protein-associated compartments by a monoclonal antibody against vimentin. The antibody used in their study was specific for vimentin, and on Western blots it did not stain unfixed enamel proteins. However, following fixation these proteins also became immunoreactive, suggesting that the aldehyde fixation secondarily generated the epitopes responsible for the non-specific immunostaining and immunogold labelling. This implicates the role of the F_{ab}-portion of the IgG molecules involved.

Non-specific labelling of synaptic proteins with the NMDA NR2A antibody appeared to occur with the postembedding method, but not with the antigen unmasking technique or with Western blotting. This raises the possibility that a tissue processing step during freeze-substitution and resin embedding led to the changes in synaptic protein structure, which resulted in the non-specific binding to PSDs. This binding could be mediated by the F_{ab}-fragment of the antibody, because (1) not all asymmetrical synapses were labelled, (2) the non-specific labelling occurred despite blocking with 2% HSA, which is known to block epitopes contributing to background staining and (3) increasing the NaCl concentration in the TBST to compensate for the weak ionic forces usually responsible for background labelling did not significantly change the signal/noise ratio at synapses. However, it is equally possible that the non-specific labelling observed at synapses in the knock-out animals is not against a particular epitope, but only represents selective binding of the antibody to proteins in the PSD. For postembedding iGluR immunogold labelling antibodies are generally used at a much higher concentration (for NR2A 5.4 µg/ml) than for immunofluorescence (for NR2A 0.05-1 µg/ml) or immunoblotting (for NR2A 1 µg/ml). This fact could cause or contribute to the non-

specific binding seen with the NR2A antibody. Regardless of whether the F_{ab}- or F_c-fragments were responsible for the non-specific synaptic labelling observed in this study, these findings draw attention to the fact that antibodies can behave differently under different conditions and this could lead to a serious misinterpretation of the results.

The intensity of synaptic labelling was on average only 2.5 times higher (2.1 for 0.3%, 2.7 for 0.6% and 2.6 for 0.9% NaCl) in the wild-type animals than in the knock-outs. This suggests that at least 40% of the immunogold labelling at synapses seen with the NR2A antibody in control mice was non-specific. In fact, this could be an underestimate, because asymmetrical synapses appeared to be thinner in the transgenic animals. NR2A subunits have a large carboxy-terminal domain (Ikeda et al., 1992) and this region contains interaction sites with other NMDA subunits and a number of synaptic proteins such as PSD95 (Kornau et al., 1995; Kim et al., 1996; Mori et al., 1998; Sprengel et al., 1998). In addition, this region also provides a physical linkage to several intracellular signal-transduction molecules, for example Ca^{2+}/calmodulin-dependent protein kinase II (Omkumar et al., 1996). The loss of NR2A subunits from a region where they are otherwise expressed at high levels could result in the subsequent loss or reduction of other PSD components. Tsunoda et al. (1997) suggested that preventing the interaction of ion channels with their PDZ-domain proteins could decrease the half-life of the signalling molecules. The loss of NR2A subunits and the reduction of other synaptic proteins could thus result in the thinner electron microscopic appearance of the PSD. This might partly account for the weaker labelling observed in the knock-out mice. Some of the synaptic gold particles in the wild-type mice may represent authentic NR2A subunits. However, even if this is the case, such a high non-specific/specific ratio would be unacceptable for the accurate localization of synaptic NR2A subunits.

The labelling patterns seen in rats were similar with all NMDA antibodies tested, particularly in terms of dense-cored vesicle labelling. Therefore the non-specific labelling observed with the antibody against NMDA NR2A subunits raised serious concerns about the validity of the immunogold labelling carried out against the other NMDA receptors in this study. Although it cannot be ruled out that the labelling with the NR1, NR2B-N and NR2B-C antibodies was specific, due to the lethality of NMDA NR1 and NR2B knock-out mice (Kutsuwada et al., 1996; Forrest et al., 1994), the specificity of these other antibodies could not be tested on transgenic animals. It was therefore concluded that the data obtained on the distribution of NR1, NR2A and NR2B subunits in the spinal cord and the NMDA receptor expression pattern of NK1-immunoreactive neurons, could not be considered valid.

These findings raise the question, whether the postembedding method is suitable for detecting synaptic AMPA receptors. There is evidence suggesting that these receptors can reliably be detected with the immunogold technique. For example δ_2-receptor (a synaptic protein structurally related to AMPA and NMDA receptors) antibodies distinguished almost perfectly between the postsynaptic densities of parallel and climbing fibres in the cerebellum (Landsend et al., 1997). AMPA receptors were absent from those Schaffer collateral-commissural synapses of the adult rat hippocampus, which were smaller than 180 nm in length, while they were present at larger ones (Takumi et al., 1999). The AMPA/NMDA receptor ratio for these synapses was a linear function of the postsynaptic density diameter. Matsubara et al. (1996) found that synapses between the inner hair cells and the afferent dendrites in the rat organ of Corti had gold particles representing GluR2/3 and GluR4 subunits of the AMPA receptor, but they lacked GluR1. This lack of GluR1 immunogold signal was not caused by methodological problems since labelling was observed in hippocampal sections processed in an identical way. Ragnarson et al. (2003), found that Ia synapses in the ventral horn of rat spinal cord were very rarely labelled with a GluR1 antibody (<5%), but had other AMPA subunits, while Alvarez et al. (personal communications) has detected high levels of GluR4 in the ventral horn and very low levels in the superficial laminae of the dorsal horn. These findings in the spinal cord are consistent with those obtained with antigen unmasking immunohistochemistry (see Chapter 5). It should also be pointed out that in the present study significant non-synaptic labelling was observed with all iGluR antibodies used, while for example Baude et al. (1995) reported that in the hippocampus immunogold particles representing AMPA receptors were very rarely seen at extrasynaptic membranes and not at all within the spine away from the plasma membrane. These findings therefore suggest that postembedding immunogold can be successfully used to detect AMPARs. However these results show that as with other immunocytochemical techniques, the postembedding immunogold method on freeze-substituted tissue is not free of artefacts. They stress the need for the use of appropriate controls during immunocytochemistry, ideally involving knock-out animals. Controls have to be carried out under conditions identical or closely similar to those used for obtaining the data.

Combination of immunofluorescence and postembedding immunocytochemistry

The original aim of the combined confocal and EM study was to identify three lamina III/IV NK1-immunoreactive neurons and to examine at least 20 synapses formed by SP- and CGRP-containing nociceptive primary afferents for each receptor on each cell.

Due to the concerns with the postembedding detection of NMDA receptors on freeze-substituted tissue this study was aborted less than half way through.

Nevertheless, the combined confocal and electron microscopic method developed for this study could be useful in the future for morphological investigations at the ultrastructural level. This method is especially powerful for (1) identifying and neurochemically characterizing cells with a particular three-dimensional structure or (2) for examining markers which are not detectable by the postembedding immunogold technique.

Antigen unmasking can serve as an alternative for detecting synaptic receptors

Although this study initially set out to examine NMDA receptors in the spinal cord using the postembedding method, it became apparent during the course of the work that the immunogold technique can give non-specific synaptic labelling with NMDA receptors antibodies. However, an important finding of this study has been that antigen unmasking with partial proteolytic digestion can be a suitable alternative to the postembedding immunogold method for detecting synaptic NMDA receptors. In the past, various techniques including heat treatment, microwaving and proteolytic digestion, have been developed by pathologists to reduce the detrimental effect of aldehyde-containing fixatives on antigenicity. These are collectively called antigen retrieval techniques as they aim to recover epitopes cross-linked during fixation (for reviews see Shi et al., 2000; Hayat, 2002). The situation is somewhat different for iGluRs located at asymmetrical synapses as these are not only cross-linked by the fixative, but also masked by the postsynaptic density. For these receptors pepsin treatment is likely to act by partially digesting the proteins of the PSD or synaptic cleft. This presumably exposes proteins that are otherwise hidden. Therefore the term antigen unmasking is used throughout this thesis, because it better describes the mechanism by which pepsin digestion is likely to work. For more details on the theory behind antigen unmasking with pepsin see Chapter 5.

A potential advantage of confocal detection of iGluRs is that it is suitable for examining large number of synapses. However this technique is not appropriate for analysing the subsynaptic distribution of proteins or for differentiation between receptors located in the pre- or postsynaptic membrane. The punctate NR2A labelling found in the spinal cord with this method is almost certainly authentic as it was absent in the NR2A knock-out mice, and also because the laminar distribution matched that reported with *in situ* hybridization for NR2A mRNA (Watababe et al., 1994). For further details concerning NMDA receptors in the spinal cord see Chapter 6.

Chapter 5

Distribution of AMPA receptors at glutamatergic synapses in the rat spinal cord and phosphorylation of GluR1 in response to noxious stimulation revealed with an antigen unmasking method

INTRODUCTION

Despite a number of previous anatomical studies the precise distribution of AMPA receptors at glutamatergic synapses in the spinal cord remains unknown. mRNAs for all four subunits of the AMPA receptor have been identified in the spinal gray matter (see Chapter 1). Although several immunocytochemical studies have also been carried out with antibodies against various AMPA subunits (Tachibana et al., 1994; Jakowec et al., 1995a; Popratiloff et al., 1996, 1998a; Morrison et al., 1998; Spike et al., 1998), it is unlikely that these revealed receptors at excitatory synapses, since these are thought to be inaccessible due to the extensive cross-linking of the elaborate protein meshwork of the synaptic cleft and post-synaptic density that occurs as a result of chemical fixation (see Chapter 2). Popratiloff et al. (1996, 1998a) used a postembedding immunogold method to identify AMPA receptors at synapses formed by primary afferents in the dorsal horn, while Morrison et al. (1998) and Ragnarson et al. (2003) used the same approach to examine GluRs at ventral horn synapses. Postembedding immunogold labelling was also used in Chapter 3 to detect the GluR2/3 and GluR1 subunits at somatostatin- and enkephalin-immunoreactive axon terminals. However, despite these studies, the distribution and colocalization of AMPA subunits at individual synapses and the AMPA receptor expression pattern of various neuronal circuits in the spinal cord remains unknown. In addition the postembedding method for detecting AMPA receptors is relatively insensitive, it is not suitable for examining large numbers of synapses and due to the non-specific labelling patterns observed with the NR2A antibody it cannot be used for determining whether AMPA and NMDA receptors are expressed at the same synapse.

Detection of iGluR subunits at synapses in the spinal cord with confocal microscopy would allow several important and yet unresolved issues to be addressed. These include the occurrence of synapses that lack GluR2, and would thus have exclusively Ca^{2+}-permeable AMPA receptors (e.g. Engelman et al., 1999; Vandenberghe et al., 2001), the possible existence of "silent" synapses that possess NMDA but not AMPA receptors (Li and Zhuo, 1998; Bardoni et al., 1998; Baba et al., 2000), the insertion of AMPA receptors into glutamatergic synapses as a possible mechanism contributing to central sensitization in chronic pain states (Popratiloff et al., 1998a; Ji et al., 2003) and the changes in AMPA expression pattern of synapses during development (Jakowec et al, 1995a, 1995b) or pathological conditions (Mennini et al., 2002; Van Damme et al., 2002; Kawahara et al., 2003, Nagano et al., 2003). In addition, AMPA receptors subunits are significantly different in their physiology, pharmacology and involvement in synaptic plasticity (Dingledine et al., 1999). For example GluR1 subunit-containing AMPA

complexes require activity for synaptic delivery, while those that contain GluR3 constitutively cycle into and out of the synapse (Bredt and Nicoll, 2003). Phosphorylation can also effect the function of AMPA subunits in different ways and this has been reported to play a role in the central sensitization occurring in chronic pain states (Sandkühler, 2000; Fang et al., 2002, 2003; Ji et al., 2003). Knowledge of the subunit composition at synapses in specific neuronal circuits is therefore of fundamental importance for our understanding of synaptic function and plasticity.

In the present study, synaptic AMPA subunits were examined with confocal and electron microscopy, by using the antigen unmasking method based on proteolytic digestion. It has been shown in Chapter 4 that this method is suitable for revealing synaptic receptor subunits in the spinal cord. In this Chapter the first demonstration of the laminar distribution of all four AMPA subunits at synapses in the rat spinal cord is provided and the extent of colocalization between GluR2 and GluR1 or GluR2, GluR3 and GluR4 subunits is also examined. For GluR1 and GluR2 subunits, their relationship to different types of glutamatergic axon was investigated. These two subunits are the most abundant in the dorsal horn, and are thus likely to be present at synapses formed by primary afferents and involved in sensory processing. It is also shown that this method can be used in functional studies, since it was possible to demonstrate phosphorylation of GluR1 at synapses in the superficial laminae in response to noxious stimulation.

MATERIALS AND METHODS

Antibody preparation

Affinity-purified rabbit antibodies against GluR1 and GluR2 (Chemicon) and a monoclonal mouse antibody against GluR2 (Chemicon; cat. no. MAB397; clone 6C4) were all found to give a punctate labelling pattern on sections of spinal cord following antigen retrieval with pepsin treatment. However, other commercially available GluR antibodies did not give acceptable immunostaining with this method. Therefore a rabbit polyclonal antibody against the *C*-terminal amino acid residues 830-862 of the mouse GluR3 (R3C peptide) and a guinea pig polyclonal antibody against amino acid residues 245-273 of the mouse GluR4 (R4N peptide) were generated by a collaborative partner in Japan, as described by Nagy et al. (2004). To test the specificity of these antibodies, Western blotting, dot blotting and immunocytochemistry, using antibodies that had been pre-absorbed with the appropriate synthetic peptides, were carried out. Immunoblots were performed by Dr. Masahiro Fukaya (as described by Nagy et al., 2004). For pre-absorption experiments synthetic peptides (0.2 μg/ml) were added to the primary antibodies. To check

the cross-immunoreactivity of GluR3C antibody to the GluR2 subunit, dot blot assay was performed using C-terminal peptide for GluR2 and GluR3 subunits (R2C and R3C).

Animals for immunocytochemistry

Twelve adult male Wistar rats (220–390 g; Harlan, Loughborough, UK) were deeply anaesthetised with pentobarbitone (300 mg i.p.) and perfused through the left ventricle with a fixative consisting of 4% freshly de-polymerized formaldehyde (10 rats, for confocal microscopy) or 4% formaldehyde/0.1% glutaraldehyde (2 rats, for electron microscopy). To investigate the phosphorylation of GluR1 subunits at glutamatergic synapses following noxious stimulation, three additional adult male Wistar rats were used. These animals received a capsaicin injection (Sigma, Poole, UK; 250 μg dissolved in 25 μl saline containing 7% Tween 80) into the plantar surface of the left hindpaw under general anaesthesia with ketamine and xylazine (73.3 and 7.3 mg/kg i.p., respectively). Rats were maintained under general anaesthesia for 10 minutes after capsaicin injection and then perfused with 4% formaldehyde under terminal pentobarbitone anaesthesia (as described above). Lumbar spinal cord segments from all animals were removed and stored in the same fixative for 8-24 hours, before being cut into transverse 60 μm thick sections with a Vibratome. Sections were immersed in 50% ethanol for 30 minutes prior to immunoreaction to enhance antibody penetration (Llewellyn-Smith and Minson, 1992).

Immunofluorescent detection of GluR1-4

In order to expose AMPA receptor subunits at synaptic sites, sections were processed according to an antigen unmasking method involving limited proteolytic digestion with pepsin, as described by Watanabe et al. (1998). In some experiments glutamatergic axons were identified by using antibodies against the glutamate transporters VGLUT1 and VGLUT2, which are mainly associated with myelinated primary afferents and excitatory interneurons, respectively (Todd et al., 2003). Although unmyelinated (C) primary afferents are glutamatergic (De Biasi and Rustioni, 1988; Broman et al., 1993), it has been found that many of them do not have detectable levels of either VGLUT1 or VGLUT2 (Todd et al., 2003; Landry et al., 2004), and it also appears that these afferents do not contain VGLUT3 (Oliveira et al., 2003; Landry et al., 2004). Peptidergic and non-peptidergic C afferents were therefore identified with antibody against calcitonin gene-related peptide (CGRP) (Ju et al., 1987), and binding of *Bandeiraea simplicifolia* isolectin B4 (IB4) (Silverman and Kruger, 1990), respectively. In preliminary experiments it was found that following antigen unmasking with pepsin immunostaining for CGRP completely disappeared, while staining for VGLUTs and binding of IB4 were reduced near

the surfaces of the Vibratome section, where punctate staining for the GluRs was optimal. Detection of these axonal markers was therefore carried out prior to proteolysis, by using the tyramide signal amplification (TSA) method. This results in deposition of covalently-bound fluorophore (Gross and Sizer, 1959) that was found to be resistant to subsequent pepsin treatment. Pepsin treatment was carried out by incubating sections at 37°C for 30 minutes in phosphate buffered saline (PBS) followed by 10 mins in 0.2M HCl containing 1 mg/ml pepsin (Dako, Glostrup, Denmark) with continuous agitation. The sections were then rinsed (3 × 10 minutes) in PBS. For sections that were processed for immunofluorescence and confocal microscopy, the PBS contained 0.3% Triton-X100.

To investigate whether GluR1- and GluR2-immunoreactive puncta are apposed to various types of glutamatergic axon terminal, spinal cord sections from three rats were incubated for 72 hours at 4°C in one of the following: (1) guinea pig anti-VGLUT1 antibody (Chemicon, diluted 1:200,000 or 1:500,000), (2) guinea-pig anti-VGLUT2 antibody (Chemicon, diluted 1:50,000), (3) a mixture of both guinea pig VGLUT antibodies (at the corresponding concentrations), (4) guinea-pig antibody against calcitonin gene-related peptide (CGRP) (Bachem Ltd, Merseyside, UK, diluted 1:100,000), or (5) biotinylated BS-IB4 (Sigma, 2 μg/ml). Following rinsing they were incubated for 2 hours at room temperature in biotinylated donkey anti-guinea pig IgG (Jackson Immunoresearch, West Grove, PA; diluted 1:500) (except for those sections which were used to detect IB4-binding) and then processed with a TSA kit (tetramethylrhodamine, NEL 702; Perkin Elmer, Boston, MA) as described in Chapter 4. Sections were rinsed three times in PBST, subjected to pepsin treatment (as described previously) and then incubated for 24 hours at 4°C in a cocktail of rabbit anti-GluR1 (1:500) and mouse anti-GluR2 (3.9 μg/ml) antibodies. Following further rinsing, they were incubated for 2-24 hours in species-specific fluorescent secondary antibodies: donkey anti-mouse IgG conjugated to Alexa 488 (Molecular Probes, Eugene, OR; diluted 1:500) and donkey anti-rabbit IgG conjugated to cyanine 5.18 (Jackson Immunoresearch; diluted 1:100). They were then mounted with anti-fade medium (Vectashield, Vector Laboratories, Peterborough, UK) and stored at -20°C.

To examine the relationship between GluR2, GluR3 and GluR4 subunits, triple-labelling immunofluorescence was carried out. Pepsin-treated sections from 3 rats were incubated for 72 hours at 4°C in a mixture of mouse anti-GluR2 (3.9 μg/ml), rabbit anti-GluR3 (GluR3C) (0.41 μg/ml) and guinea-pig anti-GluR4 (GluR4N) (0.76 μg/ml) antibodies. They were then rinsed in PBST and incubated in a mixture of the following species-specific secondary antibodies: donkey anti-mouse IgG conjugated cyanine 5.18 (Jackson Immunoresearch, diluted 1:100) for GluR2, donkey anti-guinea-pig IgG

conjugated to Rhodamine Red (Jackson Immunoresearch, diluted 1:100) for GluR3 and donkey anti-rabbit IgG conjugated to Alexa 488 (Molecular Probes; diluted 1:500) for GluR4. After the incubation sections were mounted in Vectashield and stored at -20°C.

Pre-absorption controls for the GluR3 and GluR4 antibodies were carried out by adding R4N peptide to the GluR4 antibody and R2C or R3C peptide to the GluR3 antibody (10 μg/ml peptide added to 50 μg/ml antibody in each case) and then diluting the antibody to the concentrations given above. To compare the staining obtained with the rabbit and mouse GluR2 antibodies, some sections were treated with pepsin and incubated in a cocktail of these two primary antibodies, followed by appropriate fluorescent species-specific secondary antibodies.

In order to assess the quality of AMPA-immunolabelling on tissue that has not been subjected to antigen unmasking, spinal cord sections that had not been pepsin-treated were also processed for immunofluorescence. These control sections were incubated in either rabbit anti-GluR1 (1:500), mouse anti-GluR2 (3.9 μg/ml), rabbit anti-GluR3 (0.41 μg/ml), or guinea-pig anti-GluR4 (0.76 μg/ml), followed by appropriate fluorescent species-specific secondary antibodies (as described above).

Confocal microscopy and analysis of GluR1-4

To investigate the colocalization of GluR2, GluR3 and GluR4 at immunoreactive synapses, sections reacted with a cocktail of antibodies against these three subunits were analysed. A single, representative section from each of the three animals was scanned through a 60x oil-immersion lens with the Bio-Rad Radiance 2100 confocal laser scanning microscope. Z-series were scanned at 0.3 μm z-separation through the upper 10-15 μm of the section (since penetration of GluR staining was generally limited to this depth), and 5 regions were analysed in each case: laminae I/II, III, IV, V and IX (Molander and Grant, 1984). Confocal image stacks were analysed using the MetaMorph image analysis software (Universal Imaging Corporation). During the selection of immunoreactive puncta for analysis, it was important not to be able to determine the subunit combination of individual puncta. Therefore the three colour channels representing GluR2, GluR3 and GluR4 subunits were initially merged and then combined to produce a monochrome image. One hundred immunoreactive puncta were selected from each region in each animal. To avoid bias towards brighter puncta, a 100-square grid was placed on the image and the punctum that was closest to the lower right corner of each square on the grid was selected on an optical section from near the upper surface of the Vibratome section. The selected

immunoreactive puncta were then examined in the original three-colour image stack and the presence or absence of immunoreactivity for each subunit was determined.

To examine the relationship of GluR1 and GluR2 to various glutamatergic axon terminals, from each of three rats a single section reacted against these subunits and VGLUT1, VGLUT2, CGRP or IB4 was analysed. These sections were scanned through a 60× oil-immersion lens, as described above. VGLUT1- and VGLUT2-immunoreactive boutons were analysed in laminae I, IIo, IIi, III, IV, V and IX. Lamina II was subdivided into inner and outer halves, because VGLUT1 terminals in these two region form functionally distinct populations. Most VGLUT1-immunoreactive boutons in lamina IIi belong to myelinated primary afferents, while those in lamina IIo are not of primary afferent origin (Todd et al., 2003). CGRP- and IB4-immunoreactive axon terminals were analysed in those regions where they were most numerous: laminae I/IIo for CGRP and lamina II for IB4. Confocal image stacks were initially viewed with MetaMorph such that only the axonal marker was visible, and 100 labelled axons were randomly selected from each of the regions to be analysed in each animal. The other two confocal channels were then viewed, and the number of GluR1- and/or GluR2-immunoreactive puncta in contact with each of the selected axonal boutons was determined. The colocalization of GluR1- and GluR2-immunoreactivity in puncta apposed to glutamatergic boutons was also noted.

VGLUT1 and VGLUT2 are thought to label the great majority of glutamatergic terminals in the spinal cord, apart from those belonging to C-afferents (Todd et al., 2003; Landry et al., 2004). To investigate the proportion of GluR2 puncta that were in contact with glutamatergic terminals and are thus likely to represent synaptic receptors, sections that had been reacted with antibodies against both of these transporters, as well as GluR2 were analysed. One section from each of three animals was scanned through a 60x oil-immersion lens and 3 regions were analysed in each case: laminae I/II, laminae III/IV and lamina IX. Image stacks were initially viewed such that only GluR2 staining was visible, and 100 immunoreactive puncta were selected from each region in each animal, by using a 100-square grid (as described above). This approach was used to avoid bias towards selecting clusters of puncta that were found to surround some glutamatergic terminals. The VGLUT staining was then examined, and the proportion of the selected puncta that were in contact with a VGLUT-immunoreactive bouton was determined.

Electron microscopy

iGluRs have been found in primary afferent axon terminals in the spinal gray matter (Lu et al., 2002, 2003), and these are thought to function as presynaptic receptors

(Lee et al., 2002). With confocal microscopy of pepsin-treated sections, AMPA receptor-immunostaining that appeared to be located inside primary afferent boutons was not seen. However, it was possible that some of the punctate labelling apposed to primary afferent terminals represented receptors located in the presynaptic membrane, since the spatial resolution of the confocal microscope is not adequate to allow the distinction between pre- and postsynaptically located proteins. Therefore electron microscopy was carried out to confirm that the punctate labelling seen with GluR1 and GluR2 antibodies after pepsin treatment represented postsynaptic receptors. Sections from the two rats that had been fixed with formaldehyde/glutaraldehyde were treated with 50% ethanol to enhance antibody penetration and with 1% sodium borohydride for 30 mins to reduce the detrimental effects of glutaraldehyde on antigenicity (Kosaka et al., 1986). They were rinsed extensively, treated with pepsin (as described above) and incubated either in rabbit anti-GluR1 (1:2,000) or rabbit anti-GluR2 (1:500) for 72 hours, and in biotinylated donkey anti-rabbit IgG (Jackson Immunoresearch; 1:500) followed by Extravidin-peroxidase conjugate (Sigma, 1:1000) each for 24 hours. The PBS used for diluting these reagents did not contain Triton. Peroxidase was revealed with 3,3'-diaminobenzidine, and the sections were then osmicated (1% OsO_4 for 20 minutes), dehydrated in acetone, embedded in Durcupan between acetate foils and cured for 48 hours at 70°C. A single section from each animal reacted with each antibody was selected, mounted on a stub of cured resin, and trimmed to an area that included laminae I-III of the dorsal horn. Ultrathin sections (silver interference colour) were cut with a diamond knife, collected onto Formvar-coated single-slot grids and stained with lead citrate. For comparison, some Vibratome sections were processed in exactly the same way, except that pepsin-treatment was omitted.

Sections were viewed with a Philips CM100 transmission electron microscope. For the pepsin-treated material, one ultrathin section from each animal reacted with GluR1 and one reacted with GluR2 was examined. The region corresponding to laminae I-III was systematically scanned at high magnification until 50 immunoreactive synapses had been identified on each section, and the location of the DAB reaction product in relation to the synaptic membranes was noted at each immunoreactive synapse. The total area that had been scanned on each section was estimated from the X-Y co-ordinates. During the course of this survey, any immunoreactive vesicle-containing profiles found were also noted. Ultrathin sections from tissue reacted with GluR1 or GluR2 antibodies without pepsin treatment were then viewed (1 from each rat for each antibody), and in each case an area equivalent to that scanned in the corresponding pepsin-treated sections was examined.

Detection of phosphorylated GluR1 subunits

To determine whether immunocytochemically detectable changes involving synaptic AMPA receptors occurred in response to a peripheral noxious stimulus, immunofluorescence labelling was carried out to reveal GluR1 subunits that had been phosphorylated at the Serine 845 site (Roche et al., 1996). Spinal cord sections from three rats that had received capsaicin injection into the left hindpaw (ten minutes before perfusion) were subjected to pepsin treatment and incubated in a mixture of affinity-purified rabbit antibody against GluR1 phosphorylated at Ser845 (GluR1-pS845; Covance, Berkeley, CA; 0.5 μg/ml) and mouse anti-GluR2 (3.9 μg/ml) for 48 hours. Following rinsing sections were incubated in a cocktail of species-specific secondary antibodies raised in donkey and conjugated to biotin (Jackson, diluted 1:500, for GluR1) or Alexa 488 (Molecular Probes, diluted 1:500, for GluR2) for 2 hours. To enhance the immunosignal GluR1-pS845 was revealed by using a TSA kit as described above (tetramethylrhodamine, NEL 702; Perkin Elmer). Following the immunoreaction, sections were rinsed in PBST, mounted in Vectashield and stored at -20°C. The antibody against GluR2 was used in this part of the study to demonstrate that following pepsin-treatment the punctate immunostaining observed with the GluR1-pS845 antibody corresponded to AMPA-containing synapses, since GluR2 was found to be present in virtually all puncta that contain GluR1 (see Results). It was not possible to detect GluR1 and GluR1-pS845 simultaneously, since both antibodies were raised in rabbits.

A single section from each of the three rats was scanned with the confocal microscope using a 60× oil-immersion lens. From each section, three adjacent overlapping fields (each with an area of 155 × 155 μm) from the medial half of laminae I and II of each dorsal horn were scanned with a z-separation of 1 μm. This region was chosen since this is the area where nociceptive primary afferents from the hindpaw terminate, and also because this was the region in which GluR1-pS845-immunoreactivity was observed in the ipsilateral dorsal horn (see Results). For each dorsal horn, the three image stacks were stitched together with Adobe Photoshop 7.0 (Adobe Systems). This resulted in an image (a single optical section) which covered the medial half of the dorsal horn. The region corresponding to laminae I and II was selected for subsequent analysis (using MetaMorph software). The red channel (corresponding to GluR1-pS845) was switched off while this was carried out, to avoid bias in the selection of the optical section or the area that was to be analysed. GluR1-pS845-immunoreactivity was analysed in each of the three optical sections (one from each rat) by setting a threshold for the pixel luminance value that excluded most of the "basal" immunostaining (see below) that was present in the

contralateral (right) dorsal horn. All puncta in each dorsal horn that had at least one pixel exceeding this threshold value were then identified and counted, and the presence or absence of GluR2-immunostaining in these puncta was determined. Because the TSA method involves an enzyme reaction (catalysed by horseradish peroxidase), it is likely that there is a non-linear relationship between the amount of antigen present and the intensity of fluorescence. For this reason, a densitometric approach was not appropriate, and the threshold method was therefore used to determine whether puncta with relatively high levels of GluR1-pS845-immunoreactivity were significantly more numerous on the side ipsilateral to the capsaicin injection.

The affinity purified GluR1-pS845 antibody was raised against a synthetic phosphopeptide corresponding to an sequence that includes the Ser845 residue of the rat GluR1 subunit. On Western blots prepared from rat hippocampus the antibody recognized a single protein band corresponding to a molecular weight of approximately 100kDa, and this labelling was blocked by the phosphopeptide against which it was raised, but not by the dephosphopeptide, indicating that it is specific for the phosphorylated form of GluR1 (manufacturer's specification). Pre-absorption controls for immunocytochemistry were performed by adding either the phosphopeptide used to raise the antibody or the corresponding dephosphopeptide (0.1 μg/ml in each case) to the GluR1-pS845 antibody (0.5 μg/ml) 24 hours before use.

Characteristics of other antibodies

The rabbit antibodies against GluR1 and GluR2 were raised against amino acid sequences corresponding to the C terminal 13 residues (GluR1) and residues 827-842 near the C terminus (GluR2), and are reported to show no cross-reactivity with other GluR subunits (manufacturer's specification). The monoclonal antibody against GluR2 was raised against a peptide sequence corresponding to residues 175-430. It has been extensively characterised and shown to detect GluR2, but not any other AMPA or kainate subunits, in transfected cells (Vissavajjhala et al., 1996). Staining of brain sections with this antibody was blocked by the GluR2 fusion protein, but not by fusion proteins to the corresponding regions of GluR1 or GluR3 (Vissavajjhala et al., 1996). The guinea-pig antibodies against VGLUT1 and VGLUT2 were raised against unspecified sequences corresponding to 19 or 18 amino acids (respectively) from the corresponding rat proteins. It has been previously shown that these antibodies stain identical structures to well-characterised rabbit antibodies against VGLUT1 and VGLUT2 (Todd et al., 2003).

RESULTS

GluR3 and GluR4 antibodies

Although the amino acid sequence for the R4N peptide is specific to GluR4, the sequence used for the R3C peptide has a high level of homology with the corresponding part of the GluR2 subunit, having 20 identical amino acids (Fig. 5.1A). To confirm that the GluR3C antibody did not cross-react with the GluR2 subunit, specificity tests were carried out by means of dot blots, Western blots and immunostaining using pre-absorbed antibodies (Fig. 5.1B-D). Western blots and dot blots were performed by Dr. Masahiro Fukaya (Hokkaido University, Japan), while pre-absorption controls were carried out as part of this study. On dot blots the GluR3 antibody only detected the R3C but not the R2C peptide, indicating that it did not cross-react with the C-terminal region of GluR2 (Fig. 5.1B). In Western blots prepared from the PSD fraction of homogenized mouse spinal cord, the GluR3 and GluR4 antibodies each detected a single protein band with a molecular weight of approximately 98 kDa. The pre-absorption of the GluR3 antibody with the R3C peptide, but not with the R2C peptide and the pre-absorption of the GluR4 antibody with the R4N peptide abolished staining with these antibodies. (Fig. 5.1C). On pepsin-treated spinal cord sections, punctate immunostaining was observed with both antibodies. Again, staining with GluR3 was blocked by pre-absorption with R3C but not R2C peptide, and GluR4 staining was blocked with R4N peptide (Fig. 5.1D). These antibodies are therefore specific for the corresponding subunit.

General appearance of immunofluorescence with GluR1-4 antibodies following antigen unmasking

On pepsin-treated spinal cord sections, punctate staining was seen near the surface of the section (superficial 10-15 μm) with each of the GluR antibodies (Figs 5.2, 5.3). This became progressively weaker deeper in the section, and in the case of both GluR2 antibodies it was replaced by a pattern of cell body labelling identical to that reported with these antibodies on sections not treated with pepsin (e.g. Jakowec et al., 1995a; Popratiloff et al., 1996, 1998a; Spike et al., 1998). The distribution of immunostaining seen with rabbit and mouse GluR2 antibodies was exactly the same, and dual-immunofluorescence labelling with these antibodies revealed that each antibody stained identical structures.

Laminar distribution of AMPA subunits

Of the four AMPA subunits examined, GluR1 showed the most restricted distribution in the spinal cord, with immunoreactive puncta being very frequent in lamina

II, and present at lower density in other dorsal horn laminae. In the ventral horn puncta immunostained for GluR1 were rarely seen (Fig. 5.2). A large number of GluR2-immunoreactive puncta were present throughout the grey matter, with the strongest labelling in laminae I and II (Fig. 5.2). The staining pattern for GluR3 was similar to that for GluR4. In both cases immunoreactive puncta were densely distributed throughout the ventral horn and the deeper regions of the dorsal horn (laminae III-VI), with much weaker labelling in laminae I and II, although a few strongly labelled puncta were seen in this region, particularly in lamina I (Fig. 5.3).

In sections that had not been treated with pepsin, some labelling of cell bodies, and smaller profiles that resembled dendrites, was seen with both the GluR1 and GluR2 antibodies, as described previously (e.g. Jakowec et al., 1995a; Popratiloff et al., 1996, 1998a; Engelman et al., 1999). GluR2-immunoreactive cell bodies were frequent in laminae I-III, while with the GluR1 antibody only scattered neurons were labelled mainly in laminae I-II, but occasionally also in the deeper laminae of the dorsal horn. However, the immunofluorescent staining with the GluR1 and GluR2 antibodies in sections that were not pepsin-treatment was much weaker than that in sections which had undergone antigen unmasking. In addition, puncta similar to those seen after pepsin treatment were not visible in these sections (Fig. 5.4a,b,e,f). The GluR3 and GluR4 antibodies did not stain cell bodies or give punctate labelling in the absence of pepsin treatment (Fig. 5.4c,d,g,h). This therefore suggests that conventional immunocytochemistry without antigen unmasking does not give significant labelling of synaptic AMPA receptors.

Colocalisation of AMPA subunits

This part of the study was mainly carried out to determine whether any AMPA-immunoreactive glutamatergic synapses in the spinal cord lacked GluR2 subunits, and would therefore have exclusively Ca^{2+}-permeable AMPA receptors.

In sections that were labelled with both GluR1 and GluR2 antibodies, it was found that virtually all GluR1-immunoreactive puncta throughout the dorsal horn also showed immunoreactivity for GluR2 (Fig. 5.5a-c), although the relative intensity of immunofluorescence for these two subunits varied considerably between puncta. The extent of colocalisation of these two subunits was investigated in more detail in the analysis of different types of glutamatergic axons (see below).

The relationship between GluR2, GluR3 and GluR4 was examined in triple-labelled sections (Fig. 5.5d-o, Table 5.1). These subunits showed an extensive colocalization throughout the grey matter and this was most prominent in the deep dorsal

Figure 5.1 Characterization of GluR3 and GluR4 antibodies. ***A***, Amino acid sequences showing the C-terminal region of GluR2 and GluR3. Residues which are identical in both subunits are shaded, while the regions used for antibody preparation are boxed (R2C and R3C). *Asterisks* mark the C-terminal end of the protein. ***B***, Dot blot showing that the GluR3C antibody (*Ab*) recognizes the R3C peptide, and it does not cross react with the R2C peptide. ***C***, Western blots prepared from the PSD fraction of spinal cord homogenate using the GluR3C and GluR4N antibodies (*Ab*). Each antibody detected a single protein band at about 98 kDa, and in each case this was blocked by pre-absorption with the corresponding peptide (R3C and R4N). Again, staining with the GluR3 antibody was not blocked by absorption with the R2C peptide. ***D***, Pre-absorption controls for the GluR3 and GluR4 antibodies on pepsin-treated spinal cord sections. Single optical sections were obtained from lamina IX from sections incubated with GluR3 or GluR4 antibodies. Following antigen unmasking both antibodies gave punctate immunostaining (*GluR4N* and *GluR3C*). Pre-absorption of GluR4N antibody with R4N peptide abolished staining (*GluR4N-R4N*). Staining with the GluR3C antibody was blocked by absorption with R3C peptide (*GluR3C-R3C*), but not R2C peptide (*GluR3C-R2C*). Scale bar, 2 μm. Figures ***A-C*** were prepared and kindly provided by Dr. Masahiro Fukaya, from Hokkaido University School of Medicine, Japan.

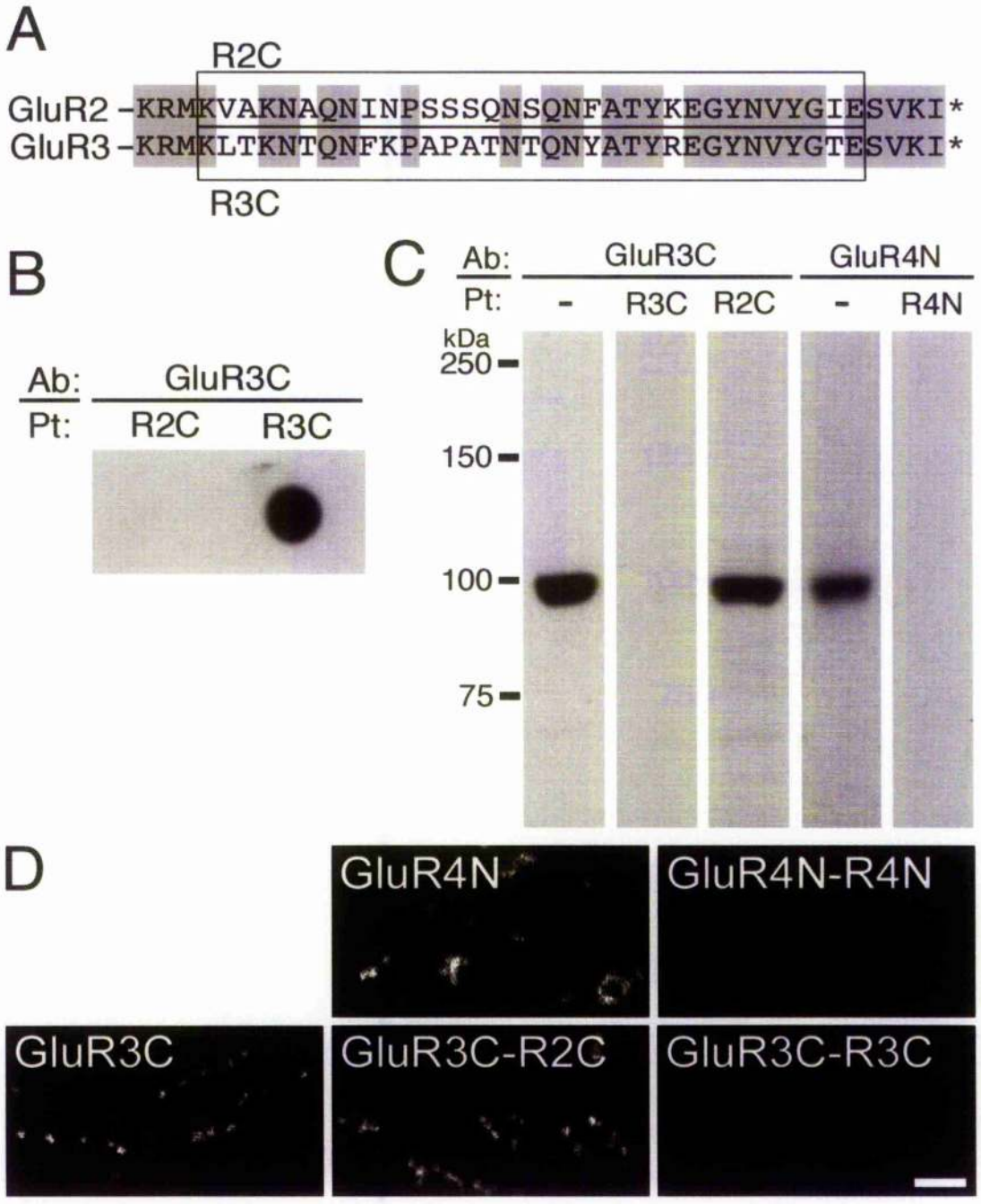
A
R2C
GluR2 -KRMKVAKNAQNINPSSSQNSQNFATYKEGYNVYGIESVKI*
GluR3 -KRMKLTKNTQNFKPAPATNTQNYATYREGYNVYGTESVKI*
R3C
B
Ab: GluR3C
Pt: R2C R3C
C
Ab: GluR3C GluR4N
Pt: - R3C R2C - R4N
kDa
250
150
100
75
D
GluR4N
GluR4N-R4N
GluR3C
GluR3C-R2C
GluR3C-R3C

Figure 5.2 Confocal images of pepsin-treated spinal cord sections showing the distribution of GluR1- and GluR2-immunoreactive puncta. Pictures (***a-b***) correspond to the medial portion of laminae I-III, (***c-d***) to the medial part of laminae IV-V, while (***e-f***) represents lamina IX. GluR2-immunoreactive puncta are distributed throughout the dorsal horn and the ventral horn, but the labelling is strongest in lamina II. GluR1 shows a more restricted distribution. Immunoreactive puncta are numerous in the superficial laminae, present at a lower density in other parts of the dorsal horn, and are virtually missing from lamina IX. All images are projections of three optical sections, scanned at 0.5μm z-separation. Scale bar, 100μm.

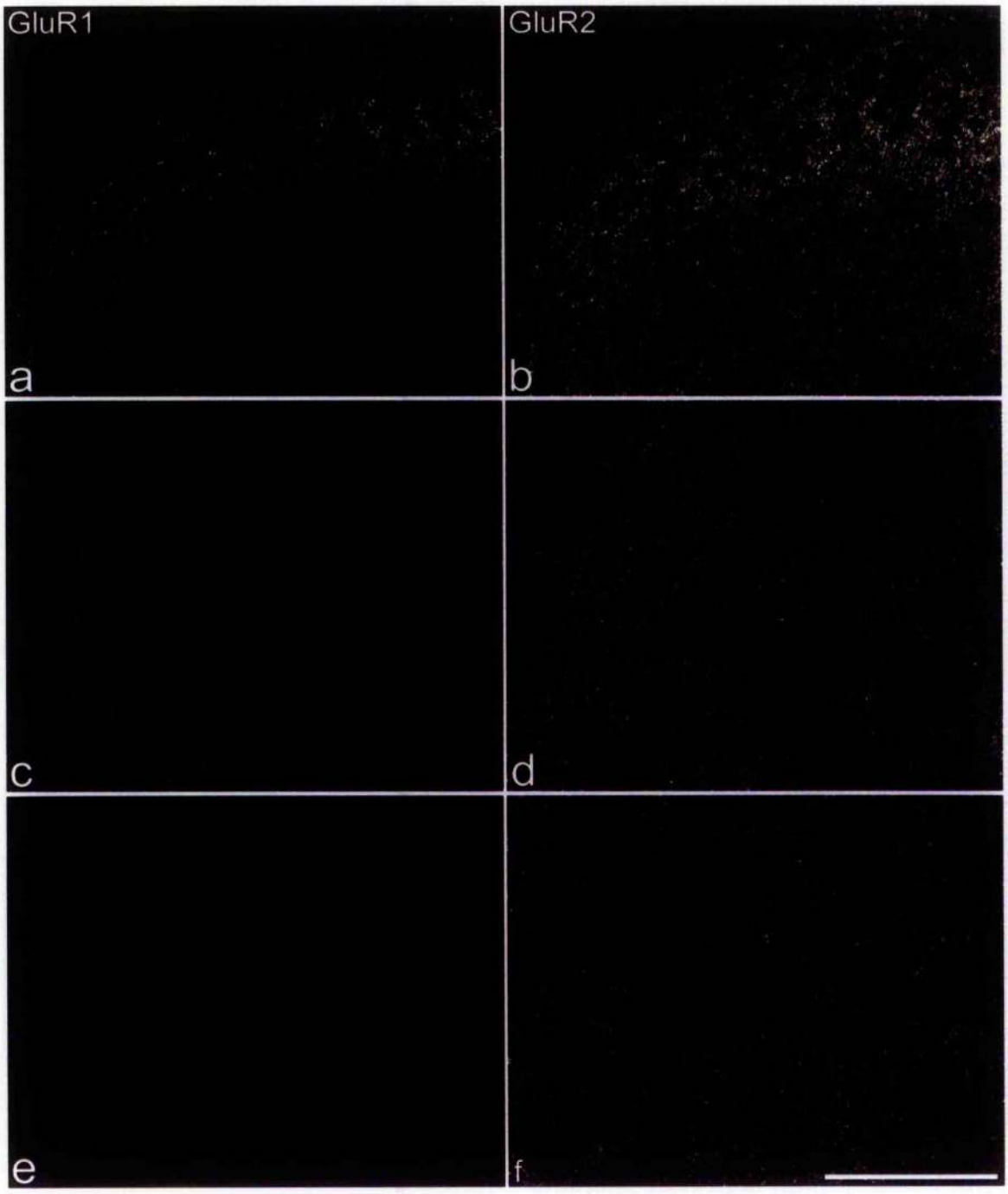
GluR1
GluR2
a
b
c
d
e
f

Figure 5.3 Confocal images of pepsin-treated spinal cord sections showing the distribution of GluR3- and GluR4-immunoreactive puncta. Pictures (***a-b***) correspond to the medial portion of laminae I-III, (***c-d***) to the medial part of laminae IV-V, while (***e-f***) represents lamina IX. With both antibodies immunoreactive puncta are densely distributed throughout the ventral horn and the deeper regions of the dorsal horn, with much weaker labelling in laminae I and II. All images are projections of three optical sections, scanned at 0.5μm z-separation. Scale bar, 100μm.

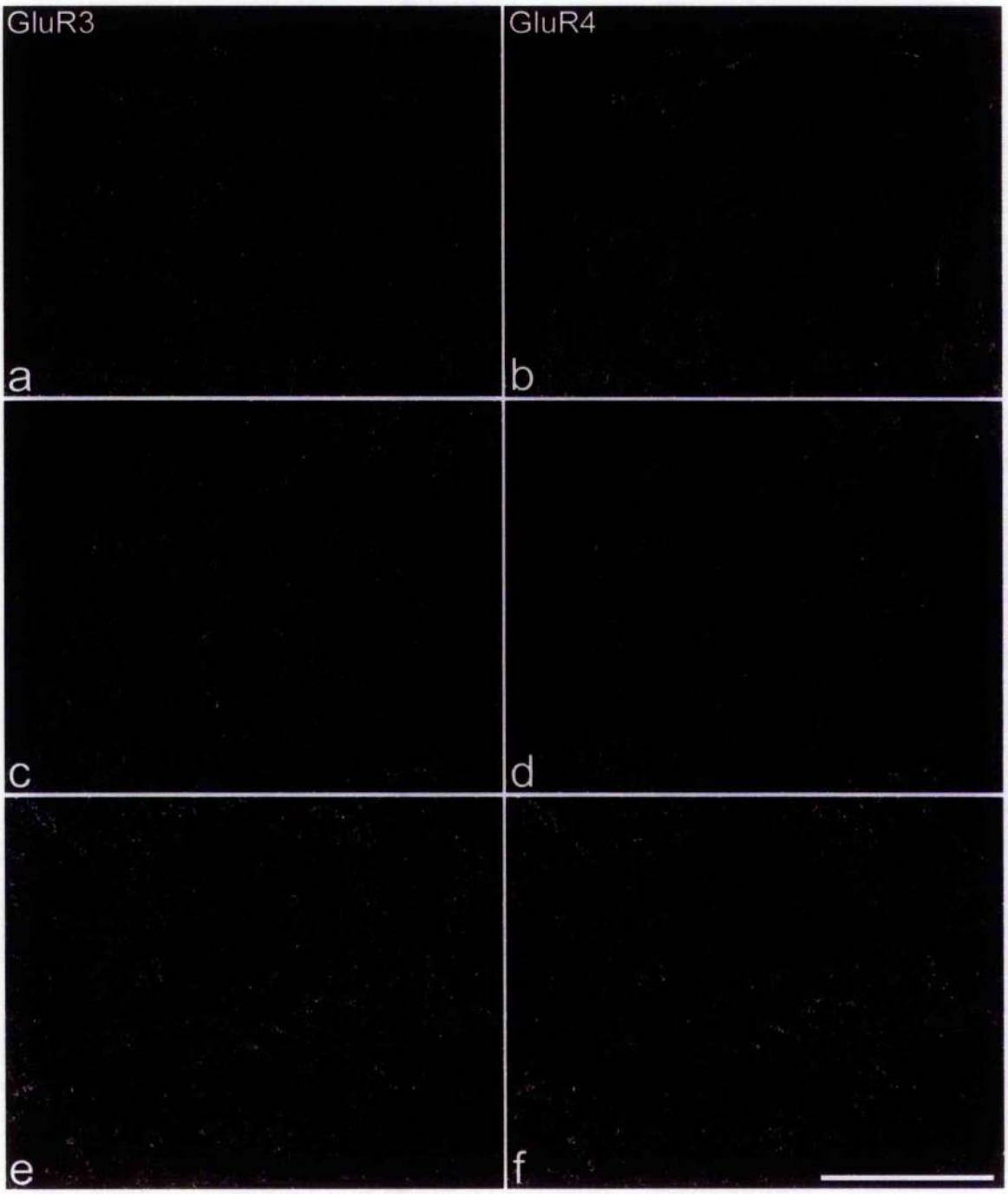
GluR3
GluR4
a
b
c
d
e
f

Figure 5.4 Comparison of immunofluorescent labelling with GluR1-4 antibodies on pepsin-treated (***a-d***) and non-pepsin-treated (***e-h***) sections. Images are single optical sections obtained from lamina II (***a-b, e-f***) or lamina IX (***c-d, g-h***). Each pair was scanned with identical confocal settings. All four antibodies gave strong punctate labelling following antigen unmasking. The GluR3- and GluR4-immunoreactive puncta outline profiles which appear to be dendritic shafts (***c-d***). In sections that had not been treated with pepsin GluR1 and GluR2 antibodies both stained cell bodies, however the labelling of these was so weak that it was either undetectable (GluR1) or barely detectable (GluR2) at confocal settings that clearly revealed punctate staining with these antibodies on pepsin-treated sections. A very faintly GluR2-immunoreactive cell body is visible in (***f***). The GluR3 and GluR4 antibodies did not give immunostaining without antigen unmasking. Scale bar, 2 μm.

Figure 5.5 Colocalisation of various AMPA subunits. (***a-c***) show GluR1 and GluR2 immunostaining in corresponding fields from lamina II. All of the GluR1-immunoreactive puncta are also labelled for GluR2 (appear yellow on the merged image), while there are GluR2-immunoreactive puncta that lack GluR1 (*arrows*). (***d-o***) demonstrate the relationship between GluR2, GluR3 and GluR4 subunits in lamina I (***d-g***), lamina IV (***h-k***) and lamina IX (***l-o***). Nearly all of the immunoreactive puncta in laminae IV and IX are triple-labelled, although the relative intensity of each type varies between puncta. In lamina II GluR3- or GluR4-immunoreactive puncta are also labelled for GluR2, but several puncta are only immunoreactive with the GluR2 antibody (*arrows*). All images show single optical sections. Scale bar, 2 μm.

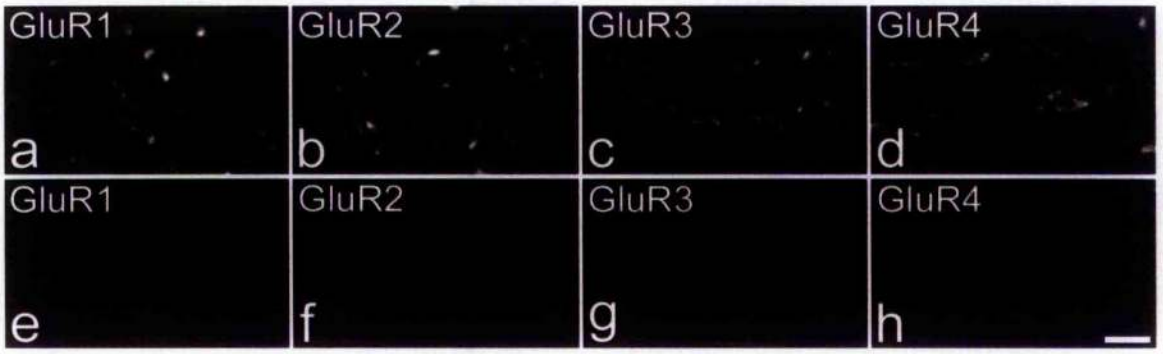
GluR1
a
GluR2
b
GluR3
c
GluR4
d
GluR1
e
GluR2
f
GluR3
g
GluR4
h

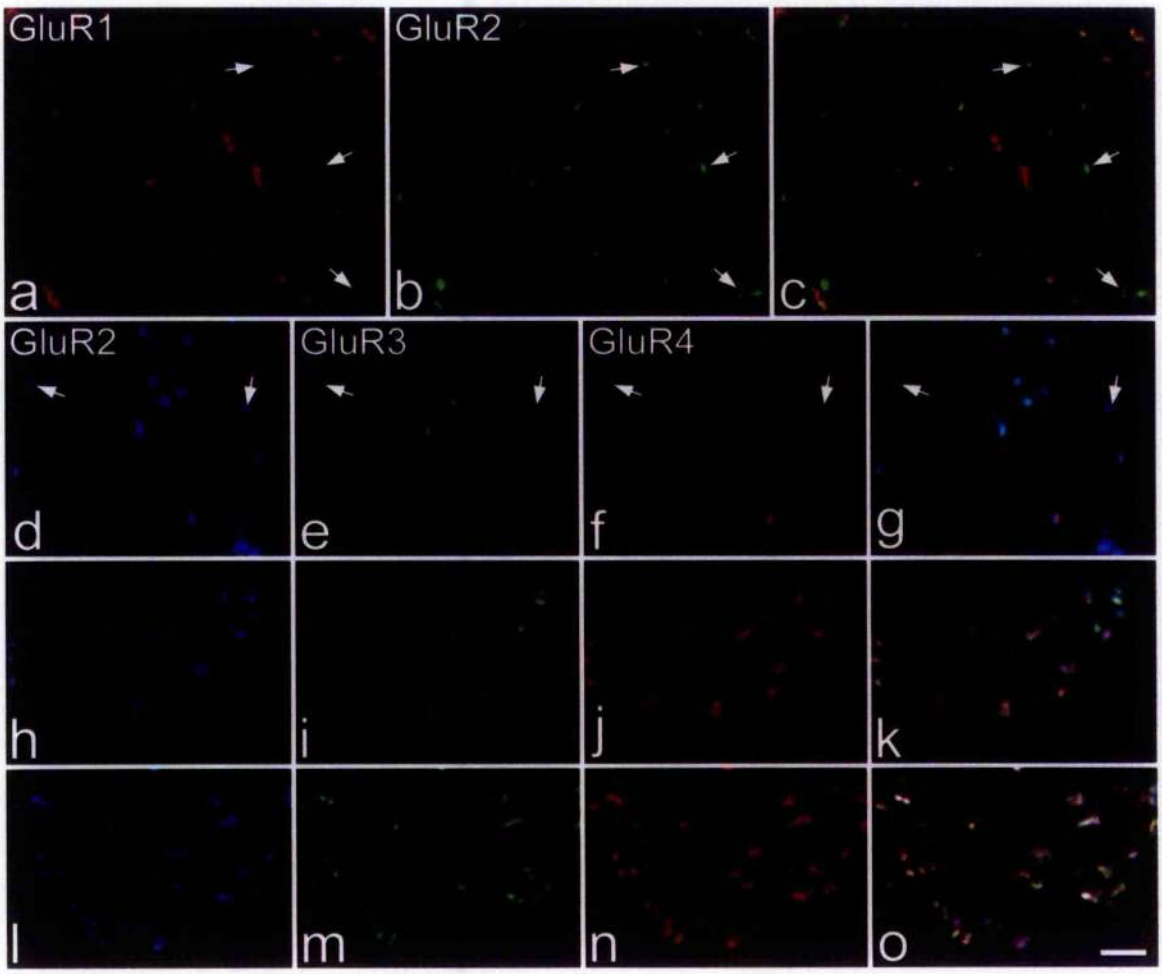
GluR1
a
GluR2
b
c
GluR2
d
GluR3
e
GluR4
f
g
h
i
j
k
l
m
n
o

	Subunit combination (%)							
Lamina	**2/3/4**	**2/3**	**2/4**	**3/4**	**2**	**3**	**4**	**GluR2+ (%)**
I/II	**36** (31-39)	**32.7** (28-35)	**7.3** (2-10)	**1** (0-2)	**22.3** (22-23)	**0.7** (0-1)	**0**	**98.3**
III	**82** (77-89)	**6.7** (4-9)	**6.3** (4-9)	**1.3** (0-3)	**3.3** (1-8)	**0.3** (0-1)	**0**	**98.3**
IV	**92** (91-93)	**0.7** (0-1)	**5** (3-7)	**0**	**0.7** (0-1)	**1.3** (1-3)	**0.3** (0-1)	**98.4**
V	**94.3** (92-96)	**2** (0-3)	**2** (1-3)	**0.3** (0-1)	**0.3** (0-1)	**0.7** (0-1)	**0.3** (0-1)	**98.6**
IX	**96** (95-98)	**0**	**1.3** (1-3)	**1.3** (0-2)	**0.7** (0-2)	**0.7** (0-1)	**0**	**98.0**

Table 5.1 Colocalization of GluR2, GluR3 and GluR4 subunits in various regions of the spinal cord. The subunit composition of one hundred immunoreactive puncta was examined for each region in each of three rats. Mean numbers show the different patterns of colocalization, while ranges are given in parentheses. The last column (blue) shows the proportion of puncta that were immunoreactive for GluR2.

horn and ventral horn, where the great majority of immunoreactive puncta were triple-labelled for all three subunits. The colocalization was analysed quantitatively in laminae: I/II, III-V and IX (Table 5.1). In laminae IV, V and IX the great majority (>90%) of labelled puncta were immunoreactive with all three antibodies. The proportions of puncta that were triple-labelled in lamina III and laminae I-II were 82% and 36%, respectively. In all areas, between 98% and 99% of the puncta that were analysed showed GluR2-immunoreactivity. The relative intensity of labelling for the three subunits also varied between individual puncta (Fig. 5.5d-o). In particular, labelling for GluR3 and GluR4 was usually much weaker in the superficial dorsal horn than that observed in other laminae. However, a few puncta with strong GluR3- or GluR4-immunoreactivity were seen in this region (Fig. 5.5d-g). In contrast, the intensity of GluR2-immunoreactivity in individual puncta was generally much higher in the superficial laminae than in other regions.

Relationship of GluR1 and GluR2 to glutamatergic axons

Detection of VGLUT1-, VGLUT2- and CGRP-immunoreactivity and IB4 binding with the TSA method prior to pepsin treatment, resulted in labelling patterns identical to those reported previously for these markers in the rat spinal cord (e.g. Sakamoto et al., 1999; Varoqui et al., 2002; Todd et al., 2003).

VGLUT1-immunoreactive boutons were sparse in laminae I and IIo and densely distributed throughout the remainder of the grey matter, whereas VGLUT2-positive boutons were numerous in all laminae. CGRP-immunoreactive axons formed a dense plexus in laminae I-IIo with scattered profiles deeper in the dorsal horn and IB4-labelled axons were present throughout laminae I-II, with many labelled boutons in the central part of lamina II. More than 90% of the labelled boutons in each of these populations were in contact with one or more GluR2-immunoreactive puncta (Figs. 5.6-5.8; Tables 5.2, 5.3), and of the 4,800 glutamatergic boutons analysed in this part of the study, 96.2% had at least one contact.

In all regions examined, generally more than one GluR2 punctum was apposed to each VGLUT1-immunoreactive bouton (Table 5.2). In laminae IIi and III, clusters of GluR2 puncta were seen surrounding several VGLUT1-immunoreactive boutons. The appearance of these clusters resembled a glomerular arrangement (Fig. 5.6a-c). In laminae IIi and III the mean numbers of GluR2 puncta associated with each VGLUT1 bouton were 4.2 and 3.7, respectively, while for lamina IX this figure was 5.5 (Table 5.2, Fig. 5.6). The mean numbers of GluR2 puncta associated with VGLUT1 boutons in the other laminae analysed varied from 1.9-2.8 (Table 5.2). VGLUT2 boutons were associated with fewer

Figure 5.6 GluR1 and GluR2 puncta associated with VGLUT1-immunoreactive boutons. Images are single optical sections obtained from laminae IIi (**a-c**), IV (**d-f**) or IX (**g-h**). In each case GluR2-immunostaining is shown in the left panel (green), GluR1 in the centre panel (blue) and these have been merged with VGLUT1-staining (red) in the right panel. In all cases, the VGLUT1 boutons contact several GluR2-immunoreactive puncta. In the dorsal horn, some of these puncta are also GluR1-immunoreactive, while there is no immunostaining for this subunit in the ventral horn. Again all GluR1 puncta are double labelled, while some of the puncta only show immunoreactivity for GluR2. In lamina IIi immunoreactive puncta often surround the VGLUT1 bouton, with an appearance that is suggestive of a glomerular arrangement (*arrows*). Scale bar, 2 μm.

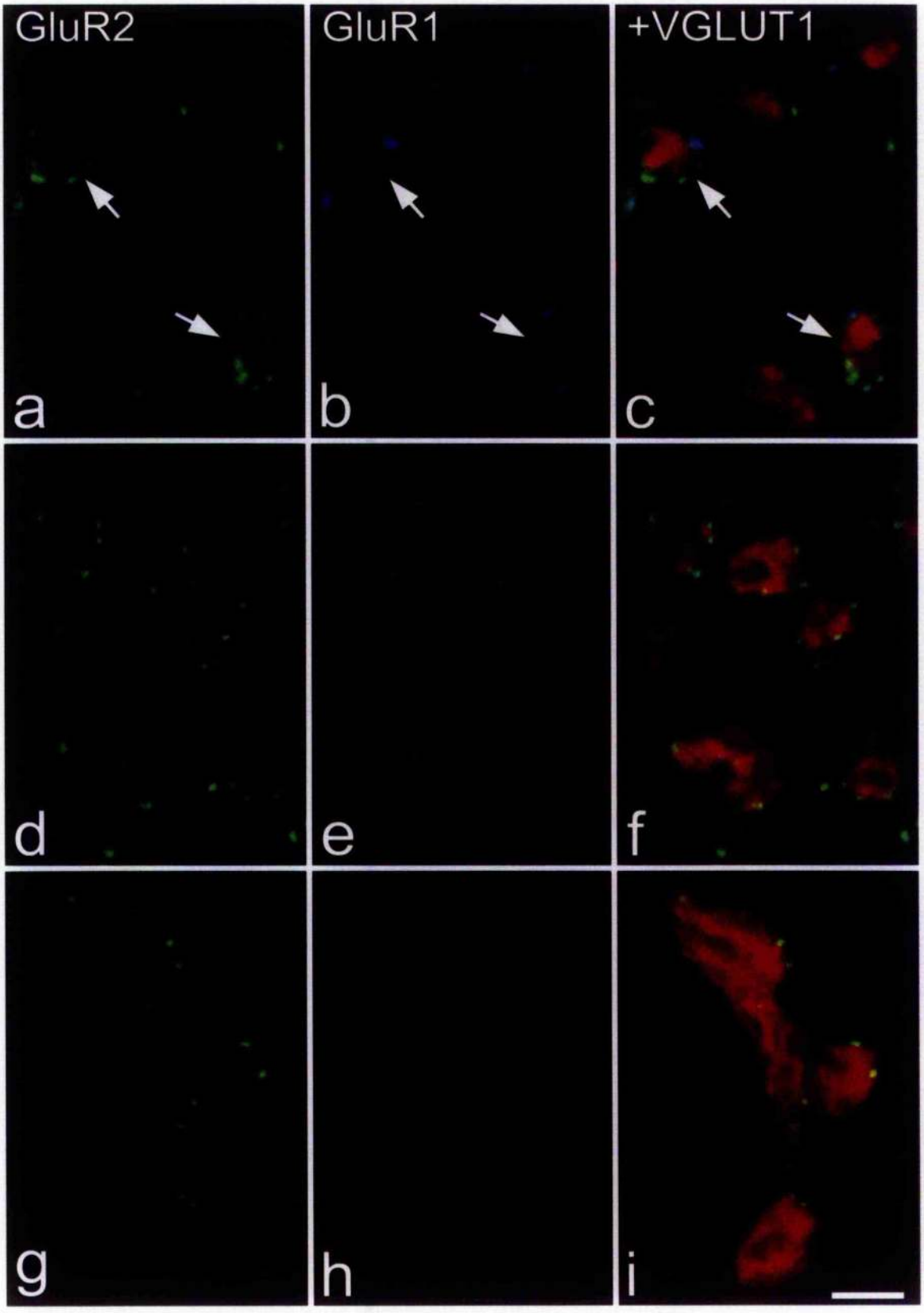
GluR2
GluR1
+VGLUT1
a
b
c
d
e
f
g
h
i

Figure 5.7 GluR1 and GluR2 puncta associated with VGLUT2-immunoreactive boutons. Images are single optical sections obtained from laminae I (**a-c**), V (**d-f**) or IX (**g-h**). In each case GluR2-immunostaining is shown in the left panel (green), GluR1 in the centre panel (blue) and these have been merged with VGLUT2-staining (red) in the right panel. In all cases, the VGLUT2 boutons contact GluR2-immunoreactive puncta. In the dorsal horn, some of these puncta are also GluR1-immunoreactive, while there is no immunostaining for this subunit it the ventral horn. Again all GluR1 puncta are double labelled, while some of the puncta only show immunoreactivity for GluR2. Individual VGLUT2-immunoreactive boutons are only associated with a few immunoreactive puncta. Scale bar, 2 μm.

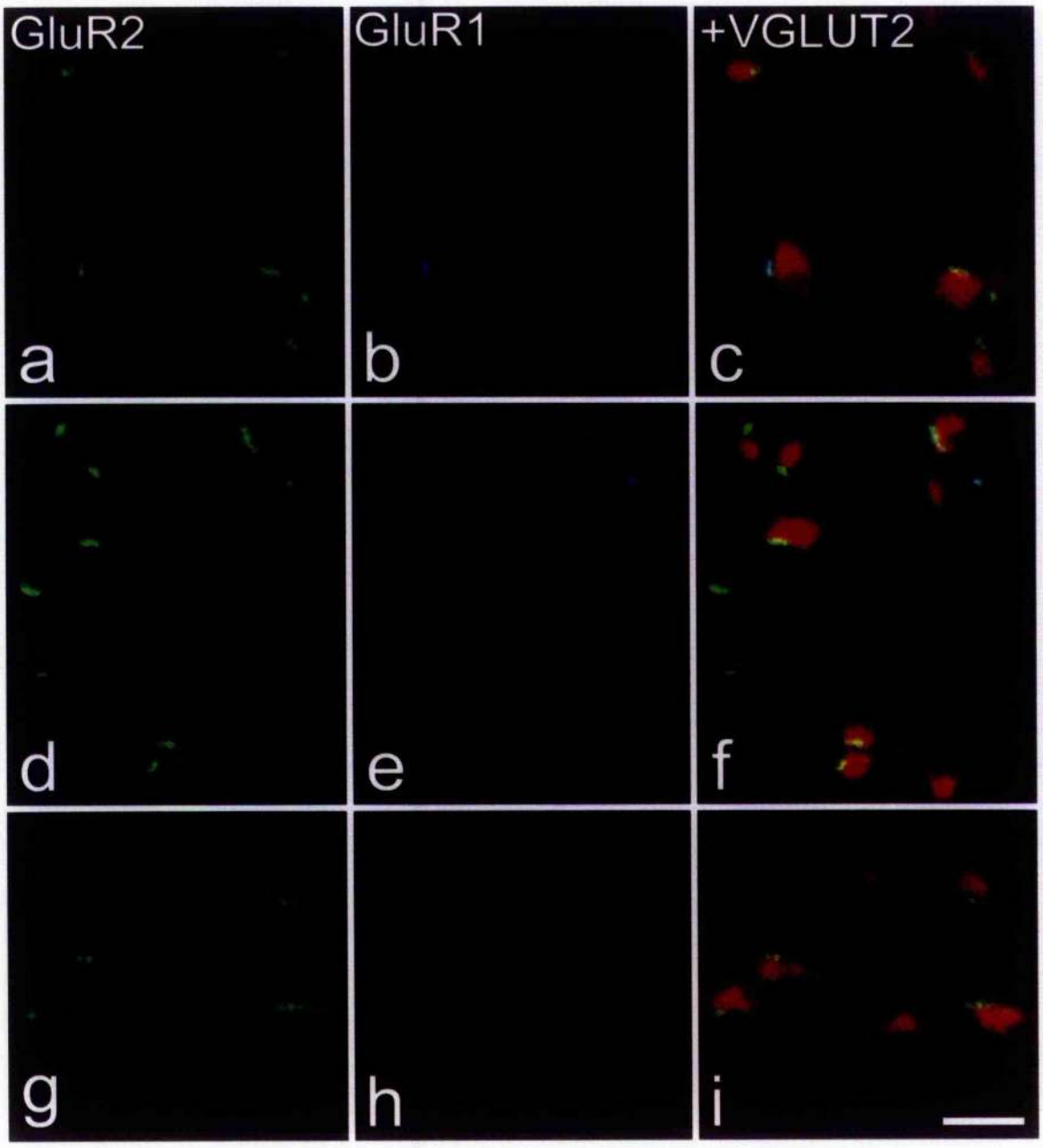
GluR2
GluR1
+VGLUT2
a
b
c
d
e
f
g
h
i

Figure 5.8 GluR1 and GluR2 puncta associated with peptidergic and non-peptidergic C-fibre terminals in lamina II. In each case GluR2-immunostaining (***a,d***) is shown in the left panel (green), GluR1 (***b,e***) in the centre panel (blue) and these have been merged with the axonal labelling (red) for IB4 (***c***) or CGRP (***f***) in the right panel. IB4- and CGRP-immunoreactive terminals are in contact with GluR2 puncta, some of which also show GluR1-immunostaining. Some of the IB4-labelled boutons are surrounded by GluR2-immunoreactive puncta with an appearance that was suggestive of a glomerular arrangement (*arrow*). All images were obtained from a single optical section. Scale bar, 2 μm.

Figure 5.9 Electron microscopic images of GluR1- and GluR2-immunoreactive synapses in the superficial laminae of the spinal cord after pepsin-treatment. (***a-c***) show GluR1 immunolabelling, while (***d-f***) show GluR2 immunolabelling. In all cases the immunoperoxidase reaction product is located inside postsynaptic profiles and associated with the postsynaptic density of synapses. (*arrows*). Scale bar, 0.5 μm.

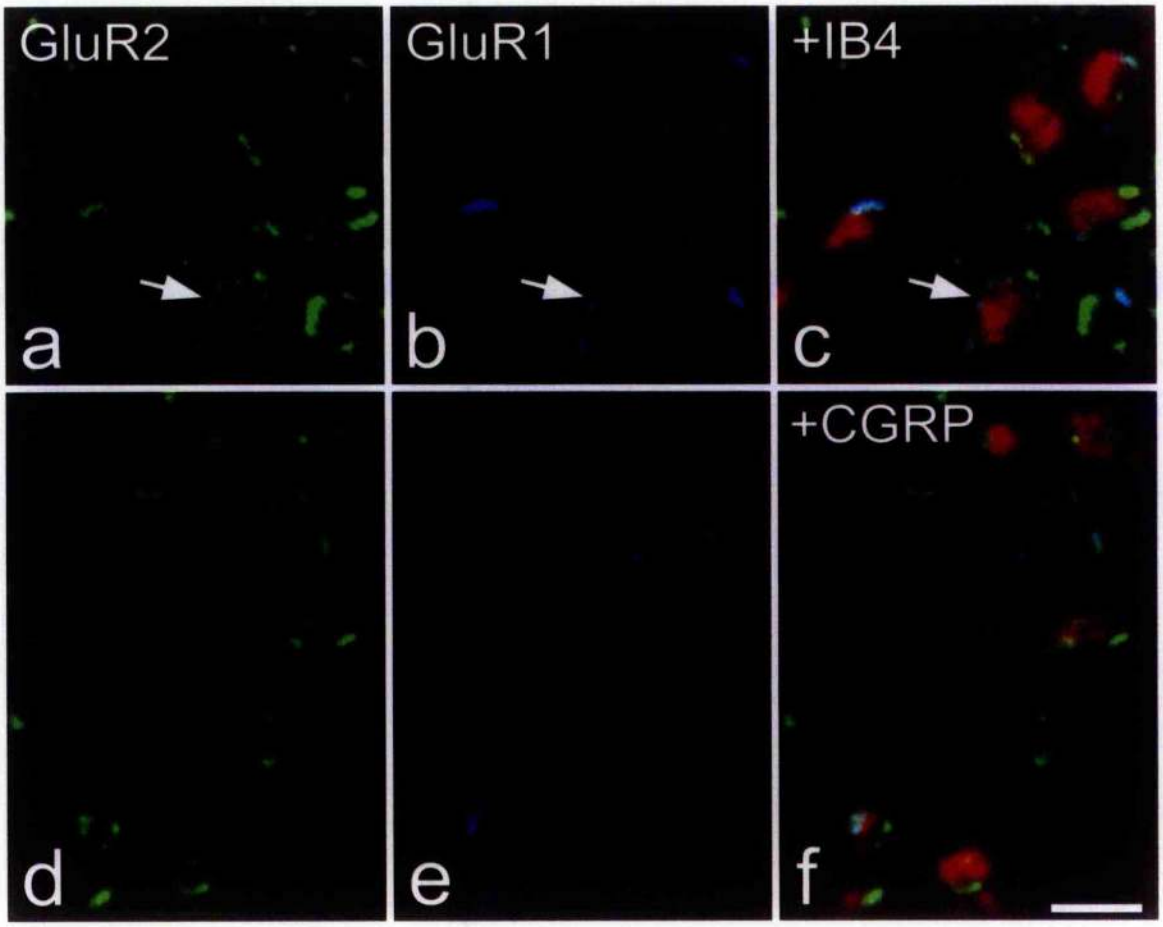
GluR2
GluR1
+IB4
a
b
c
d
e
+CGRP
f

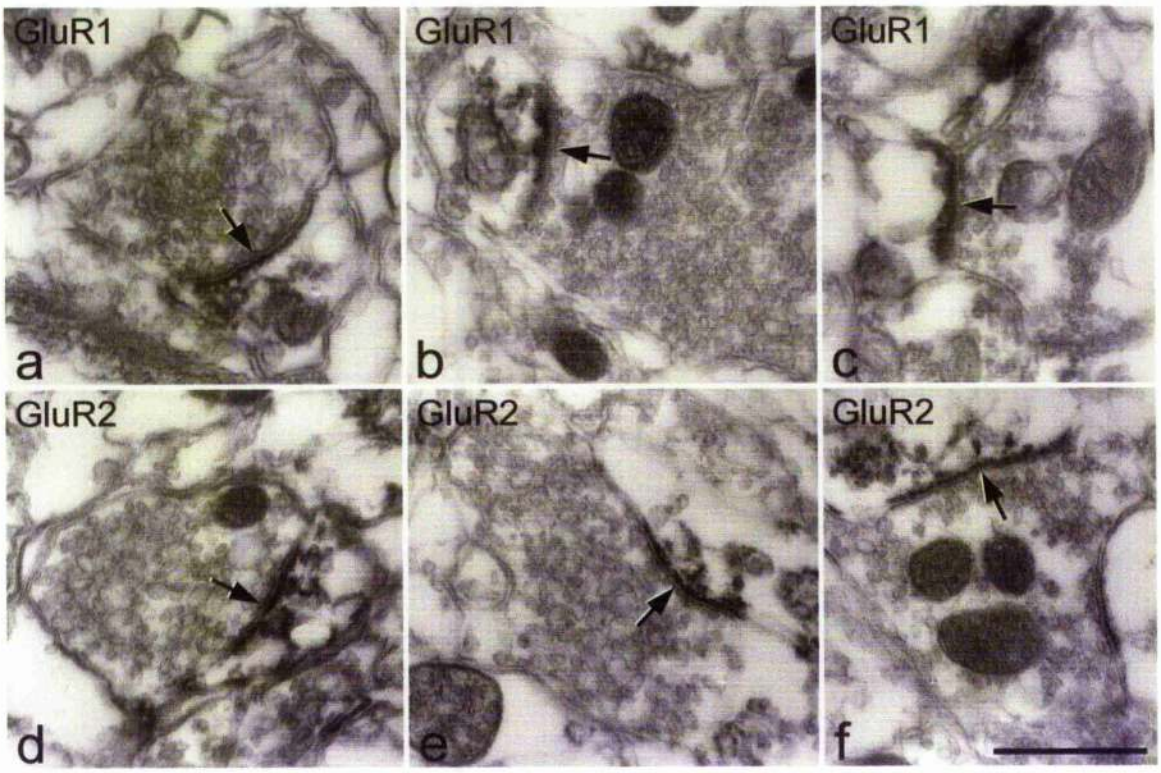
GluR1
GluR1
GluR1
a
b
c
GluR2
GluR2
GluR2
d
e
f

Lamina	VGLUT1				VGLUT2			
	% boutons with ≥ 1 GluR2 puncta	% boutons with ≥ 1 GluR1 puncta	Mean GluR2 puncta/bouton	% GluR2 puncta also GluR1	% boutons with ≥ 1 GluR2 puncta	% boutons with ≥ 1 GluR1 puncta	Mean GluR2 puncta/bouton	% GluR2 puncta also GluR1
I	91.7 (89-94)	40.3 (34-44)	1.9 (1.6-2.3)	29.8** (23.1-35.0)	92 (88-100)	16.7 (9-24)	1.4 (1.1-1.7)	12.9 (8.2-17.2)
IIo	95.0 (91-99)	64.3 (53-71)	2.8 (2.6-3.4)	40.2 (30.7-55.0)	97.3 (96-100)	24.7 (19-28)	1.6 (1.4-1.8)	17.0* (15.4-19.6)
IIi	98.3 (97-100)	76.3 (73-82)	4.2 (3.4-4.7)	38.1** (32.7-41.0)	96.7 (92-100)	24 (16-29)	1.6 (1.4-1.7)	16.9 (11.6-20.6)
III	96.0 (95-97)	44.3 (30-60)	3.7 (3.0-4.2)	19.0*** (15.5-24.0)	95 (90-100)	5 (4-7)	1.4 (1.3-1.5)	3.6 (2.7-4.9)
IV	93 (89-95)	31.7 (29-33)	2.6 (2.2-3.2)	19.4** (14.7-24.9)	96.7 (96-98)	4.3 (0-11)	1.6 (1.4-1.9)	1.9*** (0-4.3)
V	94 (91-99)	21 (16-26)	2.6 (2.4-2.9)	10.4** (7.3-14.0)	97.7 (95-100)	1.7 (0-4)	1.5 (1.2-1.7)	0.8* (0-1.9)
IX	97.3 (97-98)	4.3 (0-11)	5.5 (3.9-6.4)	0.8** (0-1.8)	97.7 (97-99)	0	1.9 (1.6-2.2)	0

Table 5.2 Association of GluR1- and GluR2-immunoreactive puncta with VGLUT-containing boutons. One hundred VGLUT-immunoreactive boutons were examined in each region in three rats. Ranges are given in parentheses. Asterisks indicate the number of GluR1-immunoreactive, but GluR2 lacking puncta in each region (*one, **two, ***three).

Lamina	CGRP				IB4			
	% boutons with ≥ 1 GluR2 puncta	% boutons with ≥ 1 GluR1 puncta	Mean GluR2 puncta/bouton	% GluR2 puncta also GluR1	% boutons with ≥ 1 GluR2 puncta	% boutons with ≥ 1 GluR1 puncta	Mean GluR2 puncta/bouton	% GluR2 puncta also GluR1
I	93.3	50.3	2.6	34.4				
IIo	(92-94)	(38-58)	(2.4-2.9)	(27.0-42.3)	100	77.3	4.8	30.7
IIi						(69-93)	(4.5-5.2)	(24.9-35.4)

Table 5.3 Association of GluR1- and GluR2-immunoreactive puncta with CGRP-immunoreactive and IB4-labelled boutons. One hundred boutons were examined in each region in three rats for each axonal marker. Ranges are given in parentheses. No GluR1-immunoreactive, but GluR2 lacking puncta were observed in this part of the study.

Rat	Left (ipsilateral to injection)			Right (contralateral to injection)		
	pSer845 GluR1 puncta	pSer845 GluR1 puncta/1000 μm^2	% GluR2	pSer845 GluR1 puncta	pSer845 GluR1 puncta/1000 μm^2	% GluR2
1	96	2.412	99	14	0.372	100
2	126	3.295	100	4	0.097	50
3	67	1.657	96	9	0.232	56

Table 5.4 pSer845 GluR1 immunoreactivity after capsaicin injection. The table shows the total number of puncta that had at least one pixel exceeding the threshold luminance value, the number of puncta per unit area, and the proportion of pSer845 GluR1 puncta that were also GluR2-immunoreactive.

GluR2 puncta (Fig. 5.7). The mean number of puncta per VGLUT2-immunoreactive bouton varied from 1.4-1.9 (Table 5.2). The difference between the number of GluR2 puncta associated with VGLUT1- and VGLUT2-immunoreactive boutons in each lamina was found to be significant (General Linear Model with Tukey's test *post-hoc*; $p<0.05$ for lamina I, $p<0.001$ for all other regions examined). IB4-labelled boutons in lamina II were also frequently surrounded by several GluR2-immunoreactive puncta (Fig. 5.8a-c) and the mean number of puncta per bouton was 4.8 (Table 5.3). The mean number of GluR2 puncta associated with CGRP-immunoreactive boutons in laminae I-IIo was 2.6 (Table 5.3, Fig. 5.8d-f).

Virtually all GluR1-immunoreactive puncta in the dorsal horn was also labelled for GluR2 (Figs 5.6-5.8; Tables 5.2, 5.3). Only 18 (0.14%) of the 12,493 puncta identified on the 4800 boutons examined in this part of the study showed GluR1- but not GluR2-immunoreactivity. Interestingly, in the dorsal horn, puncta with GluR1- and GluR2-immunoreactivity were less frequently associated with VGLUT2 boutons than with axon terminals immunoreactive for VGLUT1, CGRP or IB4. In laminae I and II, between 30 and 40% of the GluR2 puncta associated with VGLUT1 boutons were also GluR1-immunoreactive, whereas for VGLUT2 boutons the proportion was much lower, between 13 and 17% (Table 5.2). Similarly in laminae III and IV, 19% of puncta adjacent to VGLUT1 boutons were GluR1-immunoreactive, compared to 2-4% for VGLUT2 boutons in these laminae (Table 5.2). The proportion of puncta showing both GluR1- and GluR2-immunoreactivity was significantly higher for VGLUT1 than for VGLUT2 boutons in each of laminae I-IV (General Linear Model with Tukey's test *post-hoc*; $p<0.05$ for laminae I and III, $p<0.01$ for laminae IIo, IIi and IV). For the IB4 and CGRP boutons, the proportions of GluR2 puncta that were also GluR1-immunoreactive were 34 and 31%, respectively (Table 5.3), and these values were also significantly different from those for VGLUT2 boutons in the corresponding laminae (General Linear Model with Tukey's test *post-hoc*; $p<0.05$). These results suggest that GluR1-containing synapses are preferentially associated with primary afferent terminals.

To determine whether a significant proportion of the GluR2-immunoreactive puncta seen after pepsin treatment represented non-synaptic (e.g. cytoplasmic) receptors, sections that had been reacted with GluR2, VGLUT1 and VGLUT2 antibodies were analysed. Between 49-60% (mean 55.7) of GluR2-immunoreactive puncta in laminae I-II were associated with a bouton that was VGLUT1- and/or VGLUT2-immunoreactive. The corresponding values for laminae III-IV were 84-89% (mean 86.3) and for lamina IX they were 83-87% (mean 84.7). This suggests that for the deep dorsal horn and ventral horn, the

great majority (~ 85%) of puncta are associated with glutamatergic synapses, and since VGLUT1 and VGLUT2 do not stain all glutamatergic axons, this figure is probably an underestimate. Since boutons belonging to C fibres are often not labelled with VGLUT1 or VGLUT2 antibodies (Todd et al., 2003; Landry et al., 2004), these are likely to account for many of the GluR2 puncta that were not in contact with a VGLUT1/VGLUT2 containing bouton in laminae I and II (Fig. 5.8).

Electron microscopy

The penetration of immunoperoxidase reaction product in pepsin-treated sections prepared for electron microscopy was very limited, and therefore only ultrathin sections near the surface of the original Vibratome section were examined. In this region, the ultrastructural appearance was severely compromised by the pepsin treatment. Vesicles and other cell organelles were often distorted and membranes were disrupted. However, with both GluR1 and GluR2 antibodies it was frequently possible to identify immunoreactive synapses, and in all cases the reaction product was restricted to the postsynaptic profile, and was always associated with the postsynaptic density (Fig. 5.9). This staining pattern is consistent with a cytoplasmic location for the C terminal of these subunits, against which the antibodies were raised, and confirms that the puncta seen adjacent to glutamatergic boutons with confocal microscopy correspond to post-synaptic receptors.

With both antibodies, reaction product was occasionally seen in cell bodies, non-synaptic regions of dendrites and vesicle-containing profiles. While scanning an area that contained 50 immunoreactive synapses on each section, 3 immunoreactive vesicle-containing profiles were found in each of the 2 GluR1 sections analysed and only 1 was located in one of the GluR2 sections. One of these profiles (that found in the GluR2 section) was presynaptic at an asymmetrical synapse and was therefore presumably an axonal bouton. The reaction product in this profile was not associated with the presynaptic membrane, but was located in the centre of the bouton. The other 6 vesicle-containing profiles did not form synapses in these sections and it was therefore not possible to determine whether these were axons or vesicle-containing dendrites, which are relatively common in the superficial dorsal horn (Gobel et al., 1980), since distinguishing between these two types of profile can be difficult even in tissue with optimal ultrastructural preservation. In formaldehyde-fixed tissue treated with pepsin and viewed with confocal microscopy, GluR1-immunoreactive cell bodies were never seen, and GluR2-immunoreactive cell bodies were only observed in deeper parts of the section (see above).

Numerous synapses were seen in the sections that had been reacted with GluR1 and GluR2 antibodies without pepsin treatment, however none of these was immunoreactive with either antibody. This is consistent with our failure to see punctate staining for GluR1 and GluR2 with confocal microscopy on sections that had not been pepsin treated (Fig. 5.4e,f).

Detection of GluR1-pS845 following intra-plantar capsaicin injection

Immunostaining for phosphorylated GluR1 was abolished by pre-absorbing the antibody with the phosphopeptide, but not with the dephosphopeptide (Fig. 5.11g-i), indicating that it is specific for GluR1 subunits that had been phosphorylated at the S845 site. The antibody showed strong punctate immunostaining in the dorsal horn of rats which were subjected to noxious peripheral stimulation with an intradermal injection of capsaicin 10 minutes before fixation. The GluR1-pS845-immunoreactive puncta were largely restricted to the medial half of laminae I-II on the left (ipsilateral) side (Figs. 5.10, 5.11a-f). A small number of weakly immunoreactive puncta were also observed on the contralateral side and in the lateral part of the ipsilateral side. The distribution of strongly labelled puncta in the medial part of the ipsilateral superficial dorsal horn matches that of nociceptive afferents that innervate the plantar surface of the foot (Willis and Coggeshall, 1991). Strong labelling for phosphorylated GluR1 was not seen in the lateral part of the dorsal horn, which receives input from dorsal and proximal parts of the limb. The vast majority of GluR1-pS845-immunoreactive puncta were also labelled with the GluR2 antibody (Fig. 5.11a-c, Table 5.4). Between 67 and 126 puncta with pixels that exceeded the threshold luminance value (see Methods) were seen on the ipsilateral side in the medial half of laminae I-II in a single optical section (1.66-3.3/1000 μm^2), compared to between 4 and 14 puncta (0.1-0.37/1000 μm^2) in the corresponding part of the contralateral dorsal horn (Table 5.4), and this difference was found to be significant (Mann-Whitney, one-tailed U test, $p<0.05$).

In addition to the strongly labelled puncta, numerous very weakly immunoreactive puncta were seen throughout the superficial dorsal horn on both sides with the GluR1-pS845 antibody, and again these were generally also GluR2-immunoreactive. This weak staining, which is also seen in naïve rats (G. Nagy and A. Todd, unpublished observations), is likely to reflect a low basal level of phosphorylation of GluR1 subunits at glutamatergic synapses.

Figure 5.10 Distribution of GluR1-pS845-immunoreactive puncta in the lumbar spinal cord of a rat following noxious stimulation with an intradermal injection of capsaicin. Numerous immunoreactive puncta are present in the medial half of the superficial laminae on the ipsilateral side (***a***), while these are very sparse on the contralateral side (***b***). The dashed line marks the border between the gray and white matter. Each image was obtained from a projection of 11 optical sections at 0.5 μm z-separation. Scale bar, 100 μm.

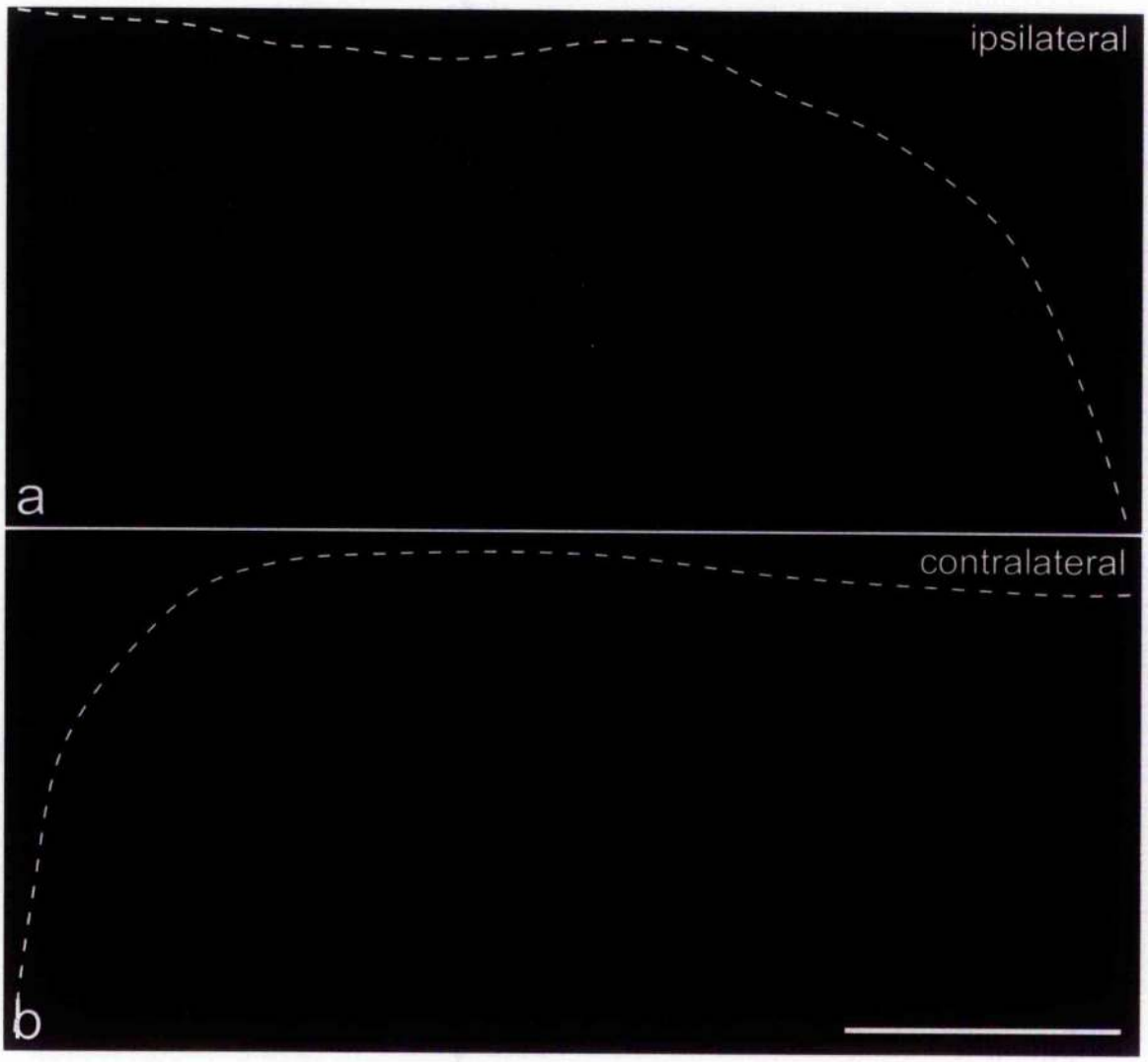
ipsilateral
a
contralateral
b

Figure 5.11 High magnification views of GluR1-pS845 immunostaining and pre-absorption controls. (*a-c*) show a region from laminae I and II ipsilateral to an intradermal capsaicin injection. Several pGluR1-immunoreactive puncta are visible (red) and these are also immunoreactive for GluR2 (green). Some of the double-labelled puncta are indicated with arrows. (*d-f*) show a similar region from the superficial dorsal horn on the contralateral side of the same section. Immunostaining for pGluR1 is much fainter. (*g-i*) show the superficial dorsal horn ipsilateral to capsaicin injection. For (*h*) and (*i*) the GluR1-pS845 antibody was pre-absorbed with the dephosphopeptide (*dp*) and the phosphopeptide (*pp*), respectively. Incubating the antibody with the phosphopeptide, but not with the dephosphopeptide abolished the staining. All images are from single optical sections. Scale bar, 20 μm.


pGluR1
a
GluR2
b
c
pGluR1
d
GluR2
e
f
pGluR1
g
pGluR1 + dp
h
pGluR1 + pp
i

DISCUSSION

The main finding of this study is that antigen unmasking with partial proteolytic digestion reveals punctate immunolabelling patterns in rat spinal cord using antibodies against GluR1-4 subunits. These puncta correspond to synapses, since a great majority of them were apposed to various types of glutamatergic axon and with electron microscopy on pepsin-treated sections the reaction product was associated with PSDs of asymmetrical synapses. There was extensive colocalization between different subunits, with GluR2 being present at virtually all AMPA receptor-immunoreactive puncta in all laminae examined. This suggests that GluR2 is almost universally expressed at AMPA-containing synapses throughout the spinal cord and that it can therefore serve as an immunocytochemical marker for these synapses. In addition, it was demonstrated that noxious stimulation with capsaicin results in phosphorylation of synaptic GluR1 subunits at the S845 residue in a somatotopically appropriate area of the superficial dorsal horn.

Technical considerations

The proteolytic method for antigen retrieval of iGluR subunits is thought to allow antibodies to gain access to epitopes that are normally masked by cross-linking due to fixation (Watanabe et al., 1998). The technique resulted in punctate labelling with both C- (GluR1, GluR3, polyclonal GluR2) and N-terminal antibodies (GluR4, monoclonal GluR2), and since the C-terminal of GluR subunits is intracellular and the N-terminal extracellular, this suggests that proteolytic digestion allows access to both the postsynaptic density and the synaptic cleft at glutamatergic synapses. It is important to point out that fixation has a dramatic effect on the quality of labelling after pepsin-treatment. Fixing for more than 8 hours resulted in a decreased intensity of punctate iGluR labelling, while if the tissue was fixed for a shorter time, sections had a tendency to disintegrate during the pepsin treatment. Postfixing at room temperature for 8 hours also reduced punctate iGluR immunostaining, suggesting that fixation is more efficient at elevated temperatures.

Conventional immunocytochemical techniques have revealed cytoplasmic staining for GluR subunits in spinal neurons (e.g. Tachibana et al., 1994; Jakowec et al., 1995a; Popratiloff et al., 1996, 1998a; Morrison et al., 1998; Spike et al., 1998), and this is thought to represent receptors that are in transit to the plasma membrane. Presumably the epitopes on these subunits are damaged by the proteolytic treatment, since cytoplasmic labelling was only seen with the GluR2 antibodies, and this was restricted to the deep parts of the section, where the pepsin digestion was presumably less effective as judged by the absence of punctate labelling. Synaptic receptors are presumably protected by the protein meshwork of the postsynaptic density and synaptic cleft.

Lu et al. (2002) found that following weak fixation, GluR2/3, GluR2/4 and GluR4 antibodies labelled central terminals of primary afferents in the dorsal horn, and concluded that this represented presynaptic receptors. A similar staining pattern was not seen with any of the GluR antibodies used in this study, suggesting that epitopes on these presynaptic receptors are either damaged or remain inaccessible following pepsin treatment in formaldehyde-fixed tissue.

The finding of occasional GluR1- and GluR2-immunoreactive cell bodies near the surface of pepsin-treated sections processed for electron microscopy suggests that glutaraldehyde (which was included in the fixative for this tissue) can protect non-synaptic AMPA receptor subunits from loss during pepsin digestion, presumably by limiting the extent of proteolysis. If the glutaraldehyde also preserves some presynaptic receptors in glutamatergic axons during pepsin treatment, this may account for some of the labelled vesicle-containing profiles seen with EM.

These findings with confocal and electron microscopy, taken together with the results of other studies that have revealed presynaptic receptors on lightly fixed material (Lu et al., 2002, 2003), suggest that receptor subunits located at different subcellular locations are affected differently by fixation and pepsin treatment. It is therefore likely that no single method can provide simultaneous labelling of iGluR subunits in all locations (i.e. postsynaptic, presynaptic and non-synaptic).

Another important technical finding of this study is, that the loss of labelling for various other antigens due to pepsin treatment can be prevented by the use of the tyramide signal amplification method. The TSA reaction carried out before the pepsin treatment covalently links the tyramide conjugated fluorescent dye to the tissue, therefore even if epitops are destroyed during the proteolytic digestion the labelling remains visible. This shows that the TSA reaction, which was initially developed to amplify weak signals during immunocytochemistry or fluorescent *in situ* hybridization, can also be used to preserve immunostaining for labile epitopes prior to antigen unmasking with pepsin.

Laminar distribution of AMPA subunits

Previous studies with *in situ* hybridization and conventional immunocytochemistry have suggested that GluR1 and GluR2 subunits are present throughout the dorsal horn, with highest levels in laminae I and II, that GluR2 is also present in the ventral horn and that GluR3 and GluR4 have high levels in the ventral horn, moderate levels in the deep dorsal horn and limited expression in laminae I-II (Furuyama et al., 1993; Tölle et al., 1993; Tachibana et al., 1994; Jakowec et al. 1995a,b; Popratiloff et al., 1996, 1998a;

Morrison et al., 1998; Spike et al., 1998; Shibata et al. 1999). The findings of this study on the laminar distribution of punctate staining following pepsin treatment are consistent with these previous investigations. However, there have been reports that motoneurons express GluR1 (Pellegrini-Giampietro et al., 1994; Virgo et al., 1996; Temkin et al., 1997; Williams et al., 1997; Bar-Peled et al., 1999; Shibata et al., 1999) or lack GluR2 subunits (Williams et al., 1997; Bar-Peled et al., 1999; Del Caño et al., 1999; Shaw et al., 1999). The results of this study are in disagreement with these suggestions, since it was found that in lamina IX there was virtually no punctate staining for GluR1, while GluR2 was expressed at virtually all puncta that were immunoreactive for any of the AMPA subunits.

Although the studies with *in situ* hybridization and conventional immunocytochemistry have provided information about the laminar distribution of neurons with different AMPA subunits, they are not suitable for determining the proportions of neurons that express a particular subunit, or the extent of colocalisation of subunits at individual synapses. Based on the assumption that all spinal neurons express AMPA receptors, the results of the present study suggest that all (or virtually all) dorsal horn neurons and motoneurons express the GluR2 subunit, that GluR1 is restricted to certain dorsal horn cells (particularly those in the superficial laminae) and is not expressed by motoneurons. GluR3 and GluR4 are expressed by all (or virtually all) motoneurons, by the great majority of neurons in the deep dorsal horn (laminae III-V) and by some of those in the superficial laminae. The extensive colocalisation of GluR2, GluR3 and GluR4 at puncta in laminae IV, V and IX (Table 5.1) suggests that neurons in these laminae have all three subunits at the great majority of synapses that possess AMPA receptors.

Although Morrison et al. (1998) found GluR2-immunoreactivity in many neuronal cell bodies throughout the spinal cord, most other studies with antibodies specific for GluR2 or GluR2/3 subunits have found a much more restricted distribution in the dorsal horn, with labelled neurons being highly concentrated in the superficial laminae but relatively sparse elsewhere (Jakowec et al., 1995a; Harris et al., 1996; Popratiloff et al., 1996, 1998a; Petralia et al., 1997; Spike et al., 1998; Engelman et al., 1999; Lu et al., 2002). Since the present study suggests that all dorsal horn express GluR2, this indicates that most conventional immunocytochemical techniques only detect a proportion of the neurons that use this subunit. It is not clear why some cells have relatively high levels of the protein in their cell bodies, but from their laminar distribution it is likely that these correspond to the neurons with the highest levels of GluR2 at their synapses.

Relation to glutamatergic axons

The GluR2 subunit was almost universally present at AMPA containing glutamatergic synapses in all laminae of the adult rat spinal cord, examined in this study. Therefore its relationship to various types of glutamatergic axon terminal was investigated. VGLUT1 boutons were surrounded by significantly more GluR2-immunoreactive puncta than those containing VGLUT2 (Table 5.2). VGLUT2-immunoreactive terminals in the spinal cord are thought to belong mainly to excitatory interneurons, while most of those with VGLUT1 are central terminals of myelinated primary afferents (Todd et al., 2003). The puncta seen with confocal microscopy do not necessarily represent individual synapses, but could correspond to active sites within a synapse. Many of the VGLUT1-immunoreactive boutons in lamina IX are terminals of Ia muscle-spindle afferents. Pierce and Mendell (1993) found that in cats these were presynaptic to a single profile and the mean number of active sites present at these synapses was 6.1. The mean number of GluR2 puncta apposed to VGLUT1-containing boutons in lamina IX was 5.5. This therefore suggests that the puncta observed with confocal microscopy after antigen unmasking correspond to active sites within individual synapses.

VGLUT1-immunoreactive boutons in laminae IIi and III were generally associated with more GluR2 puncta than those observed in other laminae of the dorsal horn. Aδ down-hair afferents terminate in this region, and some of these form central axons of type II synaptic glomeruli. GluR2-immunoreactive puncta were often seen in clusters surrounding VGLUT1-containing boutons in laminae IIi and III, and these presumably corresponded to synapses formed by type II glomeruli (Fig. 5.6a-c). Aβ primary afferent terminals usually terminate in laminae III-V and these form simpler synaptic arrangements (Maxwell and Réthelyi, 1987). This is consistent with the fact the number of GluR2-immunoreactive puncta associated with VGLUT1-containing boutons was lower in laminae IV and V. Less is known about the number of synapses formed by axons of excitatory interneurons, but the number of puncta associated with VGLUT2-immunoreactive boutons (1.4-1.9, Table 5.2) suggests that these have simpler arrangements, in many cases with only a single post-synaptic element. IB4-labelled boutons were also frequently surrounded by clusters of GluR2 puncta (Fig. 5.8) and these probably corresponded to type I synaptic glomeruli.

A very important finding of this study is that the proportions of GluR2-immunoreactive puncta that were also labelled with the GluR1 antibody were significantly higher for VGLUT1 boutons than for VGLUT2 boutons in laminae I-IV. Similarly, in the superficial laminae IB4- and CGRP-labelled boutons were also associated with

significantly more GluR1 puncta than were VGLUT2 boutons. This suggests that the GluR1 subunit is more often present at synapses formed by primary afferents than at those formed by excitatory interneurons and raises the possibility that GluR1 subunits are selectively targeted to those glutamatergic synapses which receive input from primary afferent terminals. An alternative explanation is that neurons with GluR1 have higher density of primary afferent input than those that lack this subunit. Rubio and Wenthold (1997) found evidence for the selective targeting of AMPA subunits in the dorsal cochlear nucleus. They reported that on fusiform neurons the GluR4 subunit was preferentially associated with synapses formed by auditory nerve terminals. In the spinal cord the presence of GluR1 at synapses formed by nociceptive afferents is important because GluR1- (and GluR4-) containing receptors are inserted into glutamatergic synapses in response to synaptic activity, unlike those that contain only GluR2 or GluR3, which are constitutively inserted (Bredt and Nicoll, 2003; see also Chapter 1). This suggests that insertion of new receptor subunits could contribute to activity-dependent plasticity at synapses formed by these afferents.

Popratiloff et al. (1996) reported that the GluR1 subunit was more frequently associated with synapses formed by type I synaptic glomeruli, while GluR2 was more commonly found at synapses formed by type II glomeruli. Although in this study it was not possible to distinguish the central axons of glomeruli from other boutons with confocal microscopy, the results obtained after the quantitative analysis of IB4-labelled and VGLUT1-immunoreactive boutons in laminae IIi-III (Tables 5.2, 5.3) suggest that there is a more even distribution of the GluR1 subunit at synapses formed by these different types of afferent. In addition, since the GluR2 subunit is present at most or all AMPA-containing synapses, it is unlikely that that GluR2 is more commonly associated with synapses formed by type II glomeruli. The discrepancies between these two studies are likely to result from the lower sensitivity of the post-embedding method. For example, it is likely that in the study carried out by Popratiloff et al. they detected a large number of false-negative synapses since many of the immunoreactive PSDs sampled in their study were labelled with only a single gold particle.

Baba et al. (2000) found that in adult rats silent synapses that express NMDA subunits, but lack AMPA receptors (see Chapter 1) are absent from lamina II and are extremely rare in lamina III. Although in this study only those synapses were examined which expressed AMPA receptors, the fact that out of the 3000 glutamatergic axon terminals analysed in laminae I-III fewer than 5% were not apposed to at least one GluR2

punctum (data from Tables 5.2, 5.3) supports the finding that silent synapses are not common in the dorsal horn.

Ca^{2+}-permeable AMPA receptors

Several authors have investigated the presence of Ca^{2+}-permeable AMPA receptors in the spinal cord (see Chapter 1). These have been detected in both the dorsal horn (Albuquerque et al., 1999; Engelman et al., 1999; Stanfa et al., 2000) and the ventral horn (e.g. Vandenberghe et al., 2000a, 2000b, 2001; van Damme et al., 2002). On dorsal horn neurons Ca^{2+}-permeable AMPA receptors are thought to play a role in tactile allodynia following noxious thermal stimulation or in carrageenan-induced acute inflammation (Sorkin et al., 1999, 2001). On motoneurons these receptors have been implicated in the excitotoxic cell death occurring in certain neurodegenerative disorders, such as amyotrophic lateral sclerosis. Ca^{2+}-permeability is prevented by the replacement of a single glutamine residue with an arginine in the channel pore (M_2 re-entrant membrane domain) at position 586 of the GluR2 subunit as a result of RNA editing (Burnashev et al., 1992). It has been demonstrated that a great majority of GluR2 subunits in the spinal cord are in the edited form (Greig et al., 2000; Vandenberghe et al., 2000b). Therefore AMPA receptors with Ca^{2+}-permeability are likely to lack this subunit. Several authors have demonstrated that Ca^{2+}-permeable and impermeable AMPA receptors can be co-expressed within the same cell (Goldstein et al., 1995, Gu et al., 1996, Vandenberghe et al., 2001; van Damme et al., 2002). In addition, the results of this study indicate that probably all spinal cord neurons express the GluR2 subunit. This raises the question whether the two receptor subtypes are spatially completely segregated at different synapses or whether AMPA complexes with and without Ca^{2+}-permeability are found together within the same synapses. Vandenberghe et al. (2001) reported that 8% of GluR4-immunoreactive clusters on cultured motoneurons lacked GluR2-immunoreactivity, suggesting that some synapses have solely Ca^{2+}-permeable AMPA receptors. There is evidence that different AMPA subunits in the dorsal cochlear nucleus can be selectively targeted to synapses formed by two distinct glutamatergic inputs (Rubio and Wenthold, 1997). However the findings of this study indicate, that *in vivo* a great majority of AMPA-containing synapses (>98%) in the spinal cord possess the GluR2 subunit, even though the relative concentrations of the different subunits can vary considerably. This makes it unlikely that there are synapses which express exclusively Ca^{2+}-permeable AMPA receptors. Instead, for neurons which have Ca^{2+}-permeable AMPA receptors, these are probably intermingled with GluR2-containing receptors within the same active sites. This is consistent with *in vitro*

experiments demonstrating that the co-expression of the edited form of GluR2 with other AMPA subunits results in a mosaic of receptors showing a wide range of Ca^{2+}-permeability (Burnashev et al., 1992, 1995; Washburn et al., 1997).

Phosphorylation of GluR1 subunits following noxious stimulation

Phosphorylation of different AMPA subunits in the CNS has been implicated in synaptic plasticity, including long-term potentiation and depression (Song and Huganir, 2002; Bredt and Nicoll, 2003). Roche et al. (1996) showed that the GluR1 subunit has two main phosphorylation sites, Ser-831 and Ser-845 and that in transfected HEK-293 cells phosphorylation of homomeric GluR1 channels at the Ser-845 site resulted in a 40% increase of peak current flow. This enhanced current flow resulted from an increase in the peak open channel probability (Banke et al., 2000). Lee et al. (2003) reported that preventing the phosphorylation of GluR1 by mutating the phosphorylation sites resulted in a loss of spatial memory retention and reduced hippocampal LTP. In addition, it is widely accepted, that phosphorylation of the Ser-845 residue is necessary for the recruitment of additional GluR1 subunit into the postsynaptic densities of excitatory synapses (Esteban et al., 2003). This phenomenon is thought to be involved in synaptic plasticity.

In the spinal cord AMPA receptor phosphorylation has been implicated in central sensitization and this is though to contribute to chronic pain states (Sandkuhler, 2000; Fang et al., 2002, 2003; Ji et al., 2003). This study shows that the basal phosphorylation of GluR1 at Ser-845 site in glutamatergic synapses of the dorsal horn is normally very low. Following noxious stimulation with intradermal injection of capsaicin, a stimulus know to cause central sensitization (Simone et al., 1991), this basal level of phosphorylation was rapidly and significantly increased at a proportion of glutamatergic synapses in a somatotopically appropriate location. The demonstration of phosphorylation at synapses is particularly important, since Chung et al. (2000) found that although there were relatively high levels of phosphorylated GluR2 in dendritic shafts of cultured hippocampal neurons, the level of phosphorylation at synapses remained very low.

This study apparently provides the first demonstration of phosphorylation of iGluRs at synapses *in vivo*. Noxious stimulation induces rapid phosphorylation of GluR1 subunits at glutamatergic synapses and provides a novel approach for investigating central sensitization and other forms of synaptic plasticity in specific neuronal circuits throughout the CNS.

Chapter 6

Distribution of the NMDA receptor NR1, NR2A and NR2B subunits at glutamatergic synapses in the rat spinal cord revealed with an antigen unmasking method

INTRODUCTION

In Chapter 5 it was shown that immunofluorescence following antigen unmasking with partial proteolytic digestion is suitable for revealing all four AMPA subunits at glutamatergic synapses in the spinal cord. In addition, it was demonstrated in Chapter 4 that pepsin-treatment can also be used to reveal punctate labelling for the NMDA NR2A subunit in mouse spinal cord and cerebellum and that this immunostaining disappears from transgenic animals in which the NR2A protein has been knocked out. This method therefore appears to be suitable for detecting synaptic NMDA receptors.

Heteromeric NMDA receptor channels containing different NR2 subunits have significantly different physiological, biophysical and pharmacological properties in terms of their sensitivity to magnesium block, desensitization kinetics, affinity for agonists and antagonists and the effects of phosphorylation (Monyer et al., 1994; Petrenko et al., 2003b). Therefore knowledge about which NR2 subunits are expressed at glutamatergic synapses in particular areas of the spinal gray matter is of great importance. In this study the antigen unmasking technique was used to provide the first description of the synaptic distribution of NR1, NR2A and NR2B subunits in the rat spinal cord. Since most previous studies have reported that NR2C and NR2D subunits are absent or present at very low levels in neurons of the adult rat spinal cord (Luque et al., 1994; Watanabe et al., 1994b; Yung et al., 1998; Shibata et al., 1999), these subunits were not investigated.

The GluR2 subunit is expressed at virtually all AMPA-containing excitatory synapses in the spinal cord, and therefore its relationship to NR1, NR2A and NR2B subunits was examined and quantitatively analysed. It is widely accepted that NMDA subunits do not form homomeric channels and NR1 must be assembled with at least one NR2 subunit to form functional receptors (Ishii et al., 1993). Therefore the colocalization of NR1 with NR2A or NR2B subunits was also investigated.

MATERIALS AND METHODS

Animals for immunocytochemistry

Nine adult male Wistar rats (210–310 g; Harlan, Loughborough, UK) were deeply anaesthetised with pentobarbitone (300 mg i.p.) and perfused through the left ventricle with a fixative consisting of 4% freshly de-polymerised formaldehyde. Lumbar spinal cord segments from all animals were removed and postfixed in the same fixative for 8 hours at 4°C, before being cut into transverse 60 μm thick sections with a Vibratome. Sections were immersed in 50% ethanol for 30 minutes prior to immunoreaction to enhance antibody penetration (Llewellyn-Smith and Minson, 1992).

Antibodies

Monoclonal mouse antibody against GluR2 and affinity purified rabbit antibodies against NR2B (N-terminal) and NR2A were described in Chapters 4 and 5. To detect NR1 subunits an affinity-purified guinea-pig antibody was used (kind gift from Dr. Masahiro Fukaya, Hokkaido University, Japan). It was raised against a synthetic peptide corresponding to the C_2'-cassette of the receptor. This antibody was chosen because it has been reported that approximately 90% of NR1 subunits in the adult rat spinal cord express the C_2'-cassette (Prybylowski et al., 2001). On Western blots prepared from cerebellar homogenates the NR1-C_2' antibody detected a protein band at 117 kDa, corresponding to the NR1 subunit of the NMDA receptor (Abe et al., 2004). On Western blots from HEK293 cells transfected with plasmid encoding NR1-1 (NR1 tailed with C_1- and C_2-cassettes) or NR1-4 (NR1 tailed with C_2'-cassette), the antibody selectively recognized a single protein band corresponding to NR1-4, and gave no immunosignal for NR1-1 (Abe et al., 2004). The pre-absorption of the antibody with C_2'-peptide, but not with C_2-peptide abolished this protein band and also immunostaining in the mouse brain (Abe et al., 2004). These results indicate that the NR1 antibody is specific to the C_2'-cassette and shows no cross-reactivity with C_1- or C_2-cassettes or with other NMDA subunits.

Immunofluorescent detection NMDA subunits

To demonstrate the distribution of the various NMDA subunits at synapses and to investigate their relationship to GluR2, double-labelling immunofluorescence was carried out. The colocalization between NMDA receptors and GluR2 was investigated for two reasons: (1) the punctate immunostaining for GluR2 has been shown to correspond to synapses, therefore an overlap between the two different types of iGluR would indicate that the punctate labelling seen with the NMDA antibodies (see below) also represented synaptic receptors; (2) GluR2 is present at virtually all AMPA-containing glutamatergic synapses. Therefore determining the proportion of GluR2 puncta that are also NR1-, NR2A-, or NR2B-immunoreactive in a particular spinal cord lamina would reveal whether NMDA receptors are always expressed together with AMPA receptors at synapses or are restricted to a subpopulation of glutamatergic synapses.

Mid-lumbar spinal cord sections from six rats were pepsin-treated to expose synaptic receptors (as described previously) and incubated for 72 hours at 4°C in the following antibody cocktails: (1) guinea-pig antibody against NR1 (1.5 μg/ml) and mouse antibody against GluR2 (Chemicon; cat. no. AB1768, 3.9 μg/ml), (2) rabbit antibody

against NR2A (0.11 μg/ml) and mouse antibody against GluR2, (3) rabbit antibody against NR2B (0.1 μg/ml) and mouse antibody against GluR2. Sections were rinsed in PBST and incubated for 2 hours at 21°C in a mixture of Alexa 488 conjugated donkey anti-mouse (Molecular Probes; diluted 1:500) and biotinylated donkey anti-guinea-pig or anti-rabbit (Jackson Immunoresearch; diluted 1:500) secondary antibodies. To reveal the NMDA receptors in this part of the study TSA reaction (tetramethylrhodamine, NEL 702; Perkin Elmer) was carried out as described in Chapter 4. Following rinsing in PBST sections were mounted with anti-fade medium (Vectashield) and stored at -20°C.

To investigate the extent of colocalization between NR1 and NR2A or NR2B, pepsin-treated mid-lumbar sections from three rats were incubated for 72 hours at 4°C in a mixture of guinea-pig anti-NR1 and rabbit anti-NR2A or anti-NR2B antibodies, followed by species specific secondary antibodies raised in donkey and conjugated to Rhodamine Red (Jackson Immunoresearch, diluted 1:100, for NR1) or Alexa 488 (for NR2A or NR2B). After the incubation sections were mounted with anti-fade medium (Vectashield) and stored at -20°C.

Analysis of immunofluorescence labelling

To determine the proportion of GluR2-immunoreactive puncta that were also labelled for NR1, NR2A or NR2B a representative section was scanned with the Bio-Rad Radiance 2100 confocal laser scanning microscope from each of the three animals, using a 60x oil immersion lens. Z-series were scanned at 0.3 μm separation and six spinal cord regions were analysed in each case: lamina I, II, III, IV, V and IX. Confocal image stacks were viewed with MetaMorph software. Initially only the green channel was viewed, and from each region 100 GluR2-immunoreactive puncta were randomly selected for analysis. The red channel (for the NMDA subunit) was then turned on to determine what proportion of GluR2-immunoreactive puncta were also labelled for NR1, NR2A or NR2B. To determine the proportion of NR1-, NR2A- or NR2B-immunoreactive puncta that also contained GluR2 a similar analysis was carried out, but a different optical section was used to select the NMDA receptor labelled puncta.

For each animal, the extent of colocalization between NR1 and NR2A or NR1 and NR2B was examined (as described above) in laminae I/II and III/IV for NR2A and laminae I/II for NR2B. Without signal amplification, the intensity of immunolabelling for NR2B was very weak in the deep dorsal horn and in the ventral horn, while lamina IX also showed weak immunoreactivity for the other two NMDA subunits. These regions were therefore not analysed quantitatively.

RESULTS

General appearance of immunostaining and distribution of synaptic NMDA subunits

Following antigen unmasking with pepsin, and tyramide signal amplification, punctate immunolabelling was observed throughout the gray matter for all NMDA subunits examined (Fig. 6.1). The general appearance of this punctate immunostaining was similar to that reported for AMPA subunits in Chapter 5. The penetration of immunolabelling was usually limited to the superficial parts of the Vibratome sections (≈20 μm), but it extended deeper into the tissue than that of GluR2. In addition to the punctate labelling, the NR2B antibody also labelled cell bodies, especially in the deep dorsal horn and ventral horn (Fig. 6.2). This labelling had a reticular appearance and occupied mainly the perikaryal cytoplasm, although occasionally proximal dendrites and axons were also immunoreactive. It was present in the entire depth of the sections, but weaker near the surface. The highest level of cytoplasmic labelling was observed in motoneurons. Although several authors have reported that NMDA receptors are present in DRG neurons and primary afferent axon terminals (Shigemoto et al., 1992; Sato et al., 1993; Liu et al., 1994; Watanabe et al., 1994a; Ma and Hargreaves, 2000; Marvizon et al., 2002; Lu et al., 2003), in this study no apparent immunostaining was observed inside profiles that appeared to be axonal boutons.

NR1-, NR2A- and NR2B-immunoreactive puncta were present in all laminae of the spinal cord, but their numbers and brightness varied considerably between different regions (Fig. 6.1). NR1-immunoreactive puncta were almost uniformly distributed in all laminae, but the immunostaining was weaker in the ventral horn than in the dorsal horn. NR2A and NR2B showed a differential distribution in the dorsal horn. Labelling with the NR2A antibody was strongest in lamina III and was present at lower levels elsewhere, with lamina IIo containing only very few, weakly immunoreactive puncta. Lamina I also contained a moderate number of puncta showing strong immunostaining for NR2A. NR2B-immunoreactive puncta were brightest and most numerous in laminae I-II and the intensity of the labelling gradually decreased towards the deeper laminae. Similarly to NR1, immunoreactivity for NR2A and NR2B was weaker in the ventral horn than in the dorsal horn.

Relationship of NR1, NR2A and NR2B subunits to GluR2

In the dorsal horn the great majority of NR1- or NR2A-immunoreactive puncta were also labelled for GluR2 (on average 87% for NR1 and 88% for NR2A; Fig. 6.3; Table

Figure 6.1 Confocal images of pepsin-treated spinal cord sections showing the distribution of NMDA NR1, NR2A and NR2B subunits. Pictures (***a-c***) correspond to the medial portion of laminae I-III, (***d-f***) to the medial part of laminae IV-V, while (***g-i***) represents lamina IX. NR1-immunoreactive puncta are widespread in all laminae (***a,d,g***), while NR2A (***b,e,h***) and NR2B (***c,f,i***) show a differential distribution. NR2A-immunoreactive puncta are brightest and most numerous in lamina III, while the immunostaining for this subunit is weakest in lamina IIo where only few, weakly immunoreactive puncta are visible. NR2B is present at high levels in laminae I-II, and these gradually decrease towards the ventral horn. The expression of all three subunits is much weaker in the ventral horn, than in the dorsal horn. All images are projections of three optical sections, scanned at 0.5 μm *z*-separation. Scale bar, 100 μm.

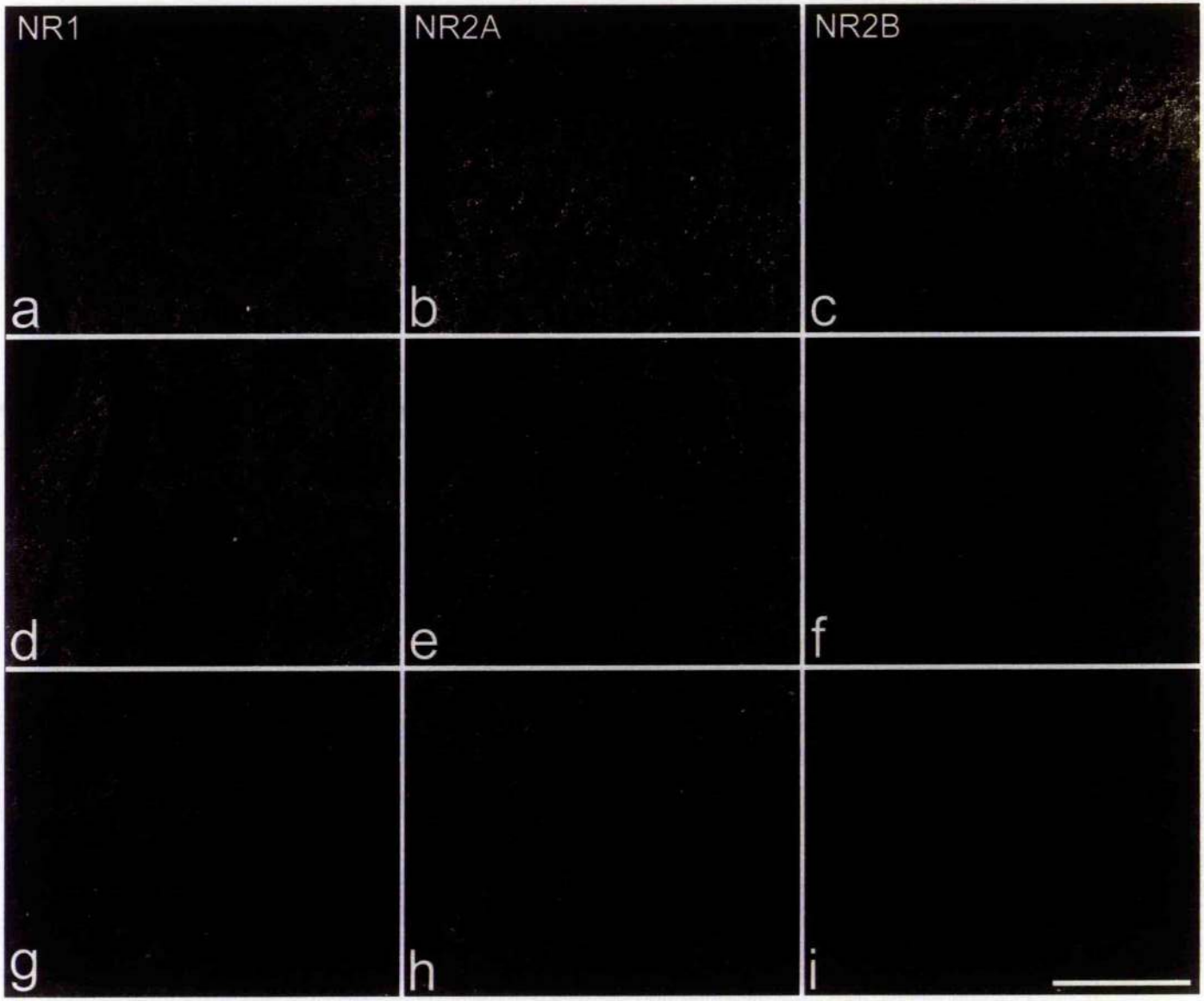
NR1
NR2A
NR2B
a
b
c
d
e
f
g
h
i

Figure 6.2 Cell body labelling with the NR2B antibody in the ventral horn following pepsin-treatment. The immunostaining has a reticular appearance and it extends into the axons and proximal dendrites. The nuclei are not labelled. Besides the cytoplasmic NR2B-labelling a faint punctate immunostaining is also visible. Images are projections of 10 optical sections, scanned at 0.5 μm z-separation from the middle portion of the sections. Scale bar, 20 μm.

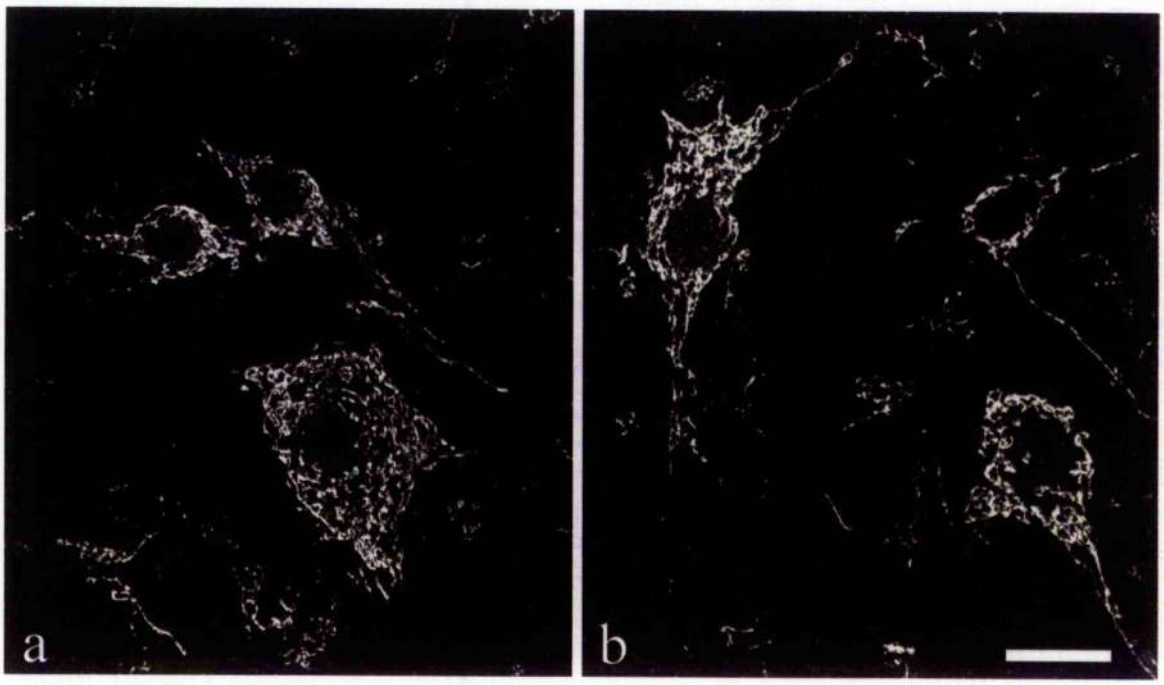
a
b

Figure 6.3 Confocal images showing the colocalization of NR1, NR2A or NR2B subunits with GluR2. (***a-c***) and (***g-i***) were obtained from the superficial laminae, while (***d-f***) show immunostaining in lamina III. In each case the vast majority of NR1-, NR2A- or NR2B-immunoreactive puncta (red) are also immunoreactive for GluR2 (green). There are numerous GluR2-immunoreactive puncta which lack NMDA subunits. All images are from single optical sections. Scale bar, 5μm.

Figure 6.4 Confocal images showing the colocalization of NR1 and NR2A (***a-c***) and NR1 and NR2B (***d-f***). (***a-c***) were obtained from lamina III, while (***d-f***) show the superficial laminae. There is extensive colocalization between NR1 and NR2A and NR1 and NR2B. All images are from single optical sections. Scale bar, 5μm.

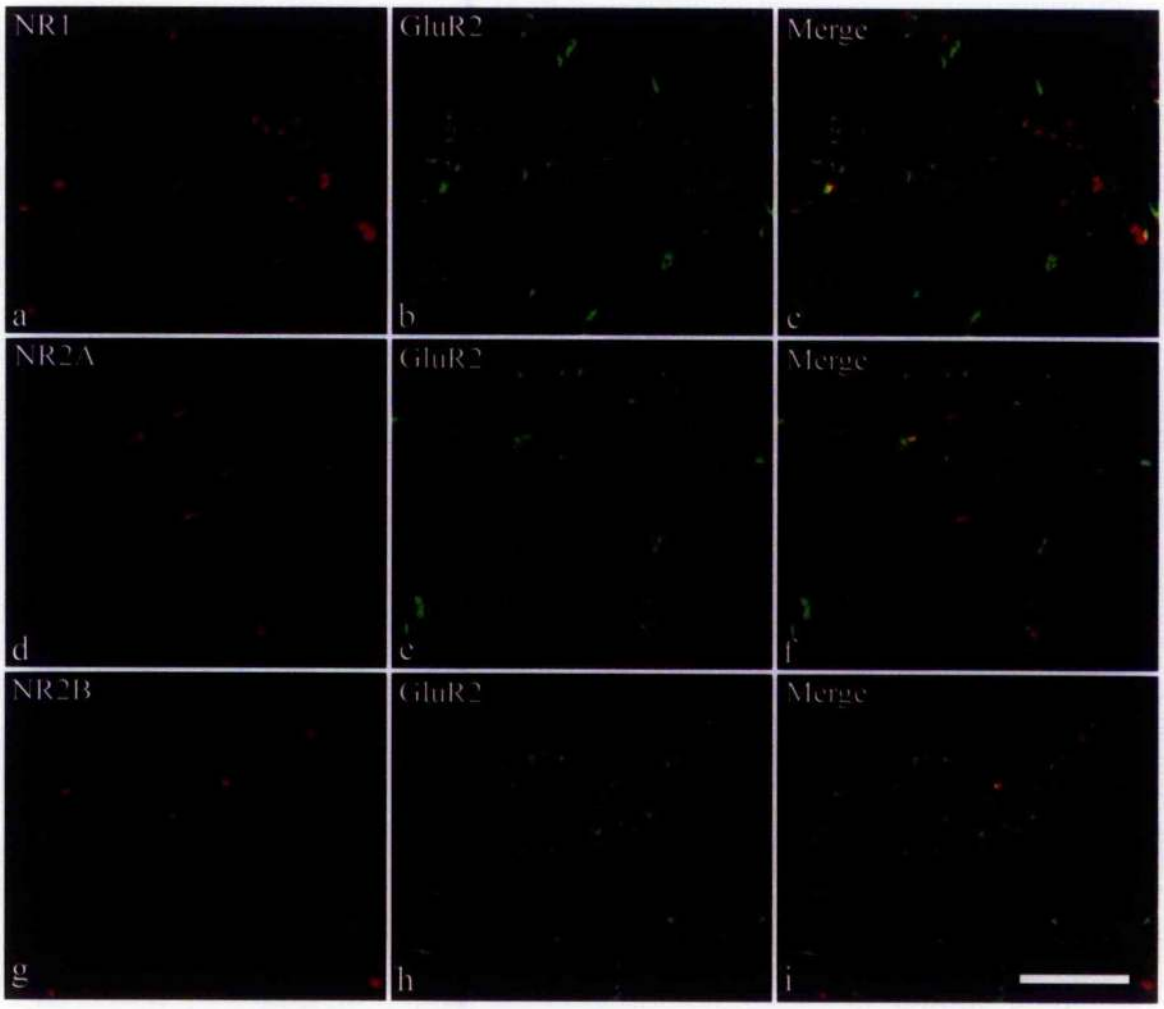
NR1
GluR2
Merge
a
b
c
NR2A
GluR2
Merge
d
e
f
NR2B
GluR2
Merge
g
h
i

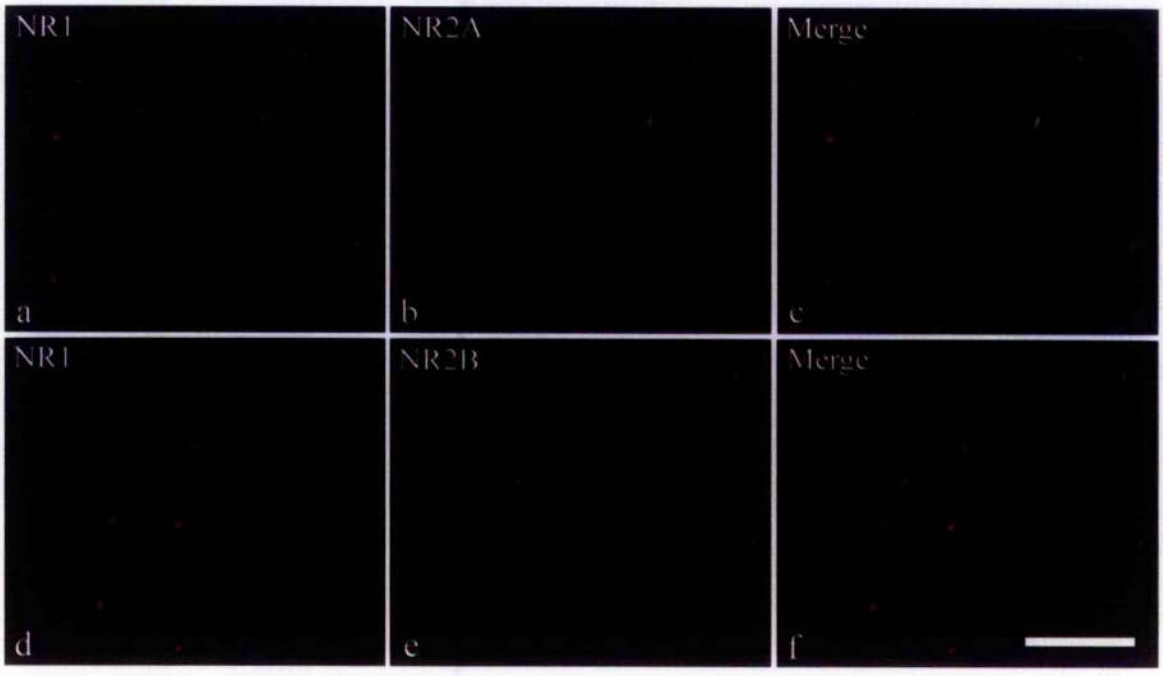
NR1
NR2A
Merge
a
b
c
NR1
NR2B
Merge
d
e
f

Lamina	% GluR2 puncta also NR1	% GluR2 puncta also NR2A	% GluR2 puncta also NR2B	% NR1 puncta also GluR2	% NR2A puncta also GluR2	% NR2B puncta also GluR2
I	58% (53-64%)	25% (18-29%)	36% (27-43%)	88% (87-89%)	88% (86-90%)	71% (60-78%)
II	47% (44-50%)	15% (7-20%)	39% (30-47%)	84% (81-86%)	79% (62-94%)	64% (55-78%)
III	60% (50-67%)	36% (30-40%)	35% (24-47%)	87% (85-89%)	92% (91-93%)	64% (62-69%)
IV	59% (56-67%)	40% (32-48%)	26% (24-28%)	90% (89-91%)	91% (90-93%)	77% (75-79%)
V	61% (56-64%)	36% (33-40%)	34% (26-41%)	87% (87-89%)	88% (80-93%)	82% (79-84%)
IX	31% (24-41%)	21% (11-27%)	23% (18-32%)	67% (66-69%)	75% (63-82%)	70% (69-72%)
Total				84% (66-91%)	86% (62-94%)	71% (55-84%)

Table 6.1 Colocalization of GluR2 with NR1, NR2A and NR2B in the spinal cord. In each of three rats one hundred immunoreactive puncta were examined for each region. Ranges are given in parentheses after the mean numbers.

Lamina	% NR2A puncta also NR1	% NR2B puncta also NR1	% NR1 puncta also NR2A	% NR1 puncta also NR2B
I-II	90.7% (84-94%)	93.3% (88-98%)	57.7% (50-63%)	89.3% (88-91%)
III-IV	93.3% (87-98%)		69.3% (54-82%)	

Table 6.2 Colocalization of NR1 with NR2A and NR2B in the spinal cord. In each of three rats one hundred immunoreactive puncta were examined for each region. Ranges are given in parentheses after the mean numbers.

6.1). The proportion of NR2B-immunoreactive puncta that were also immunostained for GluR2 was on average 72% in the dorsal horn. Corresponding numbers for lamina IX were slightly lower: 67% for NR1, 75% for NR2A and 70% for NR2B.

The proportion of GluR2-immunoreactive synapses that were also labelled for NR1 was very similar in laminae I, II, III, IV and V. Slightly more than half (on average 57%) of GluR2-immunoreactive synapses also showed labelling with the NR1 antibody in these laminae. As could be predicted from its distribution, the corresponding proportions for NR2A were lower in the superficial laminae (15% and 25% for lamina I and II) than in the deeper layers of the dorsal horn (on average 37% for laminae III-V). Surprisingly, although NR2B-immunoreactivity was strongest in the superficial dorsal horn, the proportion of GluR2-immunoreactive puncta that were also NR2B-immunoreactive was only slightly higher in this region (on average 38%) than in laminae III-V (on average 32%). Consistent with the lower levels of immunostaining for various NMDA subunits in the ventral horn, 31%, 21% and 23% of GluR2 expressing synapses in lamina IX were immunoreactive for NR1, NR2A or NR2B subunits, respectively. The brightness of NMDA-immunoreactive puncta was not uniform, but varied considerably within each region.

Colocalization between NR1 and NR2A or NR2B subunits

NR2A and NR2B showed extensive colocalization with NR1 in all of the laminae that were analysed (Fig. 6.4, Table 6.2). The immunoreaction without tyramide signal amplification was weak in the deep dorsal horn for NR2B and in the ventral horn for all three NMDA subunits. Therefore, the ventral horn was not analysed for either combination, and the deep dorsal horn was not examined for NR2B/NR1.

On average 92% (84-98%) of NR2A- and 93% (88-98%) of NR2B-immunoreactive puncta were also labelled with the NR1 antibody in the regions analysed (laminae I-II and III-IV for NR2A and laminae I-II for NR2B). In the superficial laminae on average 58% (50-63%) of puncta immunoreactive for NR1 were also stained for NR2A, while the corresponding value for the deep dorsal horn was 69% (54-82%). The proportion of NR1-immunoreactive synapses that were also labelled for NR2B was 89% (88-91%) in laminae I-II.

DISCUSSION

The main finding of this part of the study is that antigen unmasking with pepsin results in punctate immunolabelling for NR1, NR2A and NR2B subunits. A majority of these puncta are also immunoreactive for GluR2, a marker for AMPA containing synapses

(see Chapter 5). This indicates that pepsin-treatment is suitable for the detection of NR1, NR2A and NR2B subunits at glutamatergic synapses in the rat spinal cord. The great majority of NR2A- or NR2B-immunoreactive puncta were also immunoreactive for NR1, which is consistent with the current view that functional NMDA receptors are heteromers of NR1 and NR2 subunits.

Distribution of NR1, NR2A and NR2B subunits

Several authors have investigated the distribution of NMDA subunits in the spinal cord using *in situ* hybridization or conventional immunocytochemistry (see Chapter 1). However with *in situ* hybridization only the cell bodies of neurons that synthesize the subunits are labelled, while conventional immunocytochemistry generally failed to detect synaptic proteins (see Chapter 2, 4 and 5).

Moderate to high levels of NR1 subunit mRNAs have been found in cell bodies throughout the gray matter (Furuyama et al., 1993; Tölle et al., 1993; Luque et al., 1994; Shibata et al., 1999). The expression of mRNA for this subunit appeared to be higher in the ventral horn than in the dorsal horn (Furuyama et al., 1993; Kus et al., 1995; Stengenga and Kalb 2001). The results of the present study are partly consistent with these investigations, since following pepsin-treatment, punctate labelling for NR1 subunits at glutamatergic synapses was also present in all laminae, although it was much weaker in the ventral horn than in the dorsal horn. The relatively strong signal in the ventral horn with *in situ* hybridization probably resulted from the fact that motoneurons are large cells with active protein synthesis and well-developed rough endoplasmic reticulum.

In situ hybridization and immunocytochemical studies into the distribution of different NR2 subunits have yielded highly controversial results. Tölle et al. (1993) only detected mRNA for NR2C and NR2D subunits and claimed that NR2A and NR2B mRNAs were undetectable. Stengenga and Kalb (2001) reported that in adult rats the signal for NR2A was just above background with a slightly higher level in lamina II, while NR2B, NR2C and NR2D transcripts were undetectable. Watanabe et al. (1994b) on the other hand reported that mRNA for NR2A was present in all laminae except in lamina II and that transcript for NR2B was restricted to lamina II. Luque et al. (1994) detected NR2A mRNA throughout the gray matter, including lamina II and reported that mRNA for NR2B was only present in laminae II and IX. Shibata et al. (1999) also found NR2B mRNA in somatomotor neurons. Using immunocytochemistry Boyce et al. (1999) reported that NR2A-immunoreactive cell bodies were uniformly present in the rat spinal cord throughout the dorsal and ventral horn. Immunostaining with an NR2B antibody was more

restricted, with moderate labelling of fibres in laminae I-II, suggesting a presynaptic localization for this subunit. Yung (1998) found NR2B immunostaining in laminae I-III, but could not detect immunosignal for NR2A in this region.

The present study with antigen unmasking clearly shows that both NR2A and NR2B subunits are expressed at glutamatergic synapses in all laminae, but their levels vary considerably between different regions. NR2A is expressed at highest levels in lamina III and it has much lower levels elsewhere with the immunostaining being weakest in lamina IIo. NR2B is present at high levels in laminae I-II, these gradually decrease towards the ventral horn. The expression of both NR2A and NR2B at synapses is much weaker in the ventral horn than in the dorsal horn.

Colocalization of NR1, NR2A or NR2B with GluR2

A proportion of NR1-, NR2A- or NR2B-immunoreactive puncta did not show immunolabelling for GluR2. These puncta could correspond to (1) silent synapses, which lack AMPA receptors, but express NMDARs, (2) synapses at which GluR2 is present but at levels below the detection threshold (false-negatives), (3) synapses which lack GluR2, but express another AMPA subunit or (4) non-synaptic (i.e. cytoplasmic) labelling. The proportions of these GluR2-lacking puncta were similar for NR1 and NR2A, but higher for NR2B. This difference may result from the cytoplasmic labelling, which was clearly present with the NR2B antibody. During the random selection of puncta for analysis it was not possible to distinguish these immunoreactive cytoplasmic structures from puncta that are likely to correspond to synapses.

The finding that only a proportion (approximately half for NR1 and one-third for NR2A and NR2B) of GluR2-immunoreactive synapses express an NMDA subunit indicates that NMDA receptors are either selectively expressed by certain neurons or selectively targeted to particular synapses within individual neurons. Popratiloff et al. (1998b) used the postembedding immunogold method to investigate NR1 subunits at synapses formed by primary afferent terminals. They concluded that most primary afferent synapses in the superficial laminae express NR1. Since only about half of GluR2-containing synapses in laminae I-II were also immunoreactive for NR1, these findings raise the possibility that NMDA receptors a preferentially associated with synapses formed by primary afferent terminals. Further studies are needed to determine exactly which neuronal circuits express particular NMDA subunits in the spinal cord.

Colocalization of NR2A and NR2B with NR1

Studies using conventional immunocytochemistry or *in situ* hybridization only detected cell body labelling for NMDA receptors (e.g. Yung et al, 1998; Zhang et al., 1998; Boyce et al., 1999; Zou et al., 2002) and it was generally not possible to demonstrate that these subunits form functional receptors at synapses. There is evidence that certain neurons in the CNS can express a particular NMDA subunit, which is not present at their synapses, is thus not likely to form functional channels. For example NR1 subunits are highly expressed in adult rat Purkinje cells in the cerebellum, but they are not detectable at synapses (Yamada et al., 2001). In a recent study Abe et al. (2004) demonstrated that in the cerebellum NR2 subunits are essential for the postsynaptic localization of NR1. Indeed, Watanabe et al. (1994c) demonstrated that none of the NR2 subunits were transcribed by adult rat Purkinje cells, and this presumably explains the finding that NR1 subunits cannot be detected at their synapses. In addition, Fukaya et al. (2003) found that without NR1, NR2 subunits are retained in the endoplasmic-reticulum. These finding indicate that heteromer formation between NR1 and NR2 subunits is essential for their trafficking into PSDs and the formation of functional receptor channels. In the present study it was found that the great majority of NR2A or NR2B-immunoreactive puncta were also labelled for NR1, and this strongly suggests that immunoreactive puncta observed in the rat spinal cord after antigen unmasking correspond to functional NMDA receptors at glutamatergic synapses.

It was not possible to examine the relationship between the two NR2 subunits, because both antibodies used in this study were raised in rabbits. However the fact that the distribution of NR2A and NR2B subunits overlap throughout the gray matter (although their levels vary between different regions) and that in laminae I-II 58% and 89% of NR1-immunoreactive puncta were also immunoreactive for NR2A and NR2B, respectively, suggests that these subunits can be co-expressed at individual synapses. This is supported by Karlsson et al. (2002), who used single-cell RT PCR to show that single dorsal horn neurons can express mRNA for multiple NR2 subunits and that 84% of neurons investigated in their study had mRNA for both NR2A and NR2B. These finding raise the question whether NR2A and NR2B subunits within individual synapses form di- or tri-heteromer channels with NR1. In the rat cerebral cortex Luo et al. (1997) demonstrated that the dominant NMDA receptor complex contains at least three different subunits including NR1, NR2A and NR2B. There is also evidence that NMDA receptors in the superficial laminae of neonatal rats are not simply composed of NR1/NR2B or NR1/NR2D subunits, but are probably a combination of two different NR2 subunits together with NR1

(Green and Gibb, 2001). This is important, because NMDA complexes, containing more than two different subunits differ from those containing only two subunits in terms of their sensitivity to Mg^{2+}-block, channel-conductance and affinity for agonists and antagonists (Brimecombe et al., 1997; Kirson et al., 1999; Green and Gibb, 2001).

NMDA subunits in the dorsal horn

The high level of NR2B at synapses in the superficial laminae, where C and Aδ primary afferents are known to terminate, strongly suggest that this subunit may play an important role in nociceptive sensory processing and chronic pain states. In support of this suggestion, selective NR2B antagonists were shown to have an antinociceptive effect in capsaicin-induced acute pain, and attenuated carrageenan-induced mechanical hyperalgesia and mechanical allodynia following chronic nerve ligation (Taniguci et al., 1997; Boyce et al., 1999). Minami et al. (2001) reported that the NR2B antagonist CP-101,606 abolished the induction of allodynia evoked by the administration of PGE_2 or NMDA. In addition, NR2B antagonists were found to have an inhibitory effect on the windup of single spinal neurons in spinalized rats and rabbits *in vivo* (Boyce et al., 1999; Kovács et al., 2004). Further evidence for the role of NR2B subunits in nociceptive processing comes from the study of Guo et al. (2002). Using immunoprecipitation and an anti-phosphotyrosine antibody they reported that the tyrosine phosphorylation of this subunit correlated with the development of inflammation and hyperalgesia induced by intraplantar injection of complete Freund's adjuvant. The increase in NR2B phosphorylation was dependent on primary afferent activity suggesting that this subunit might be postsynaptic to nociceptive primary afferents.

Interestingly, Momiyama (2000) claimed that NR2B subunits in lamina II neurons of the adult rat spinal cord are extrasynaptic. She found that in somatic outside-out patches, presumably derived from the extrasynaptic membrane, ifenprodil, a selective NR2B antagonist, blocked high-conductance NMDA channels. Using a blind-patch technique applied to thick slices retaining dorsal roots, this antagonist was ineffective on NMDA-EPSCs. Results of the present study with immunofluorescence do not support Momiyama's interpretation. Although following antigen-unmasking it was not possible to detect extrasynaptic receptors, NR2B-immunoreactive puncta were common in lamina II. On average 64% (55-78%) of these puncta colocalized with GluR2 and 39% (30-47%) of GluR2-immunoreactive synapses were also labelled for NR2B in this region. These findings suggest that in pepsin-treated sections the majority of NR2B-immunoreactive puncta in lamina II represent synaptic NR2B subunits. A possible explanation for the

failure of ifenprodil to inhibit NMDA-EPSCs in the above mentioned study could lie in the pharmacological properties of the drug. Zhang et al. (2000) found that ifenprodil enhanced NMDA-induced currents in both cortical and subcortical areas. However, this enhancing effect was only observed at low NMDA concentrations. With increasing concentrations of NMDA, the effect of ifenprodil on NMDA-evoked currents changed from potentiation to inhibition (Kew et al., 1996). In her study, Momiyama used 0.1 Hz dorsal root stimulation for the patch-clamp recording of NMDA EPSCs, while NMDA receptors in the outside-out patches were activated with 50 μM NMDA. It is possible that dorsal root stimulation did not produce the same extent of NMDA receptor activation as the application of 50μm NMDA. If this was the case ifenprodil might not have inhibited synaptic NR2B subunits effectively. However, results from Brimecombe et al (1997) provide a more likely alternative explanation. They found that the presence of both NR2A and NR2B subunits within the same heteromer significantly alters its pharmacological attributes when compared with channels containing only a single type of NR2 subunit. The presence of NR2A in the triheteromer decreased the sensitivity of the receptor to ifenprodil analogues. These findings when taken together could further confirm the suggestion that at least a proportion of synaptic NMDA receptors in the spinal cord contain both NR2A and NR2B subunits together with NR1 (see above).

The distribution of strongly NR2A-immunoreactive puncta in the dorsal horn is similar to that of transganglionically transported CTb inside primary afferent terminals (Ganser et al., 1983). This suggests that NR2A could be postsynaptic to myelinated Aβ/Aδ low-threshold and Aδ nociceptive pimary afferents which are known to terminate mainly in laminae IIi-IV and lamina I, respectively. Preliminary studies confirm this hypothesis, since we have recently found that NR2A-immunoreactive puncta were apposed CTb-labelled primary afferent axon terminals in laminae I and III/IV (G. G. Nagy, D. Hughes and A. J. Todd, unpublished observations). This raises the possibility that NR2A subunits might be involved in mechanical allodynia. Indeed, evidence for this is provided by Minami et al. (2001), who found that NR2A knock-out mice did not develop prostaglandin E_2 (PGE_2)- or NMDA-induced mechanical allodynia. However they also found that after neonatal capsaicin treatment PGE_2 or NMDA could not induce allodynia and that capsaicin-treated, NR2A lacking mice did not show PGE_2-induced hyperalgesia (Minami et al., 1997). This suggests that in PGE_2-induced hyperalgesia and mechanical allodynia C-fibres are the most important contributing factor. However the synaptic expression of NR2A is the weakest in lamina IIo, where most (although clearly not all) of the nociceptive C-fibres terminate. In another study Petrenko et al. (2003a) reported that

formalin-induced acute pain, complete Freund's adjuvant-induced thermal hyperalgesia and mechanical allodynia following spared nerve injury (SNI) were all unaltered in NR2A knock-out mice. The apparent inconsistencies between behavioral, physiological and morphological investigations stress the need for further studies to determine which NR2 subunits are associated with particular neuronal circuits in the spinal cord.

NMDA subunits in the ventral horn

There has been great interest in which iGluRs are expressed by motoneurons, since Ca^{2+} entry through these channels has been implicated in the excitotoxic cell death occurring in certain pathological conditions, such as ALS. The increased intracellular Ca^{2+} concentration can lead to the generation of free radicals, the activation of proteases and the induction of apoptosis (Urushitani et al., 2001; Arundine and Tymianski, 2003). Several authors have suggested that Ca^{2+}-permeable AMPA receptors are the determining factor in the selective vulnerability of motoneurons to glutamate toxicity (Carriedo et al., 1996; Pellegrini-Giampietro et al., 1997; Williams et al., 1997; Shaw, 1999; van Den Bosch et al., 2000; van Damme et al., 2002). However, NMDA receptors also have Ca^{2+}-conductance and several authors have stressed their importance in the degeneration of ventral horn neurons (Wagey et al., 1997; Virgo et al., 2000; Urushitani et al., 2001; Sanelli et al., 2004). The present findings provide morphological evidence for the first time that NR1, NR2A and NR2B subunits are expressed at synapses in the ventral horn, although the intensity of immunostaining was very much weaker than in the dorsal horn.

The strong labelling for NR2B around the cell nucleus of motoneurons and the weak NR2B-immunoreactivity at synapses in the ventral horn suggests that these cells produce NR2B protein, but that it is not present in large amounts at their synapses. The shape and location of these NR2B-immunoreactive cytoplasmic structures resembles that of the Golgi-apparatus and endoplasmatic reticulum (ER). This is supported by the fact that in rats which received a CTb injection into the sciatic nerve the NR2B-immunoreactive cytoplasmic puncta colocalized with the tracer (G. G. Nagy, D. Hughes, A. J. Todd, unpublished observations). CTb is known to be transported to the Golgi-apparatus of motoneurons (Ragnarson et al., 1998). Using conventional immunofluorescence Marvizón et al. (2002) also reported a similar cytoplasmic labelling pattern for NR2A/B receptors in DRG neurons. In their study the cytoplasmic labelling for NR2A/B colocalized with CGRP, which is produced from its precursor protein in the Golgi-apparatus (Wimalawansa, 1996). The additional cytoplasmic labelling inside cellular processes might represent the intracellular trafficking of the receptor. It is possible

that NR2B subunits on motoneurons are constitutively inserted into the membrane, but are expressed mainly at extrasynaptic sites. Extrasynaptic receptors are lost during pepsin treatment (see Chapter 5), therefore during this study these NR2B subunits would have been undetectable following antigen unmasking. Evidence for the presence of extrasynaptic NR2B subunits in the dorsal horn was provided by Momiyama (2000), using patch clamping (see above). Alternatively, the Golgi-apparatus and/or ER in motoneurons could serve as a storage place for NR2B subunits, and these could be inserted into the membrane following certain type of cellular events, such as stimulation. Recruitment of NR2B subunits to the synaptic membrane could lead to an increase in NMDA mediated currents. NR2A or NR2B containing NDMA receptors have high-conductance channel openings (Petrenko et al., 2003b), while currents generated by NMDA receptors containing the NR2B subunit decay several times more slowly than those generated by NR2A containing NMDARs (Vicini et al., 1998). Ca^{2+} entry through newly inserted NMDA receptors could be involved in synaptic plasticity or in motoneuron degeneration occurring in amyotrophic lateral sclerosis or nerve injury. In a recent *in vitro* study Sanelli et al. (2004) found that spinal motoneurons from mice over-expressing the human low molecular weight neurofilament showed significant increases in intracellular Ca^{2+} following stimulation with NMDA and that this contributed to the cell death. In control animals only minimal alterations in Ca^{2+} levels were observed. Transgenic mice over-expressing neurofilaments develop motoneuron disease (Strong, 1999) and the intracellular trafficking of certain synaptic proteins is also impaired (Sanelli et al., 2004). Virgo et al. (2000) detected a significant upregulation of NR1 and NR2B mRNA in motoneurons following the crushing of the common peroneal nerve. They suggested that induction of these two NMDA subunits could contribute to excitotoxic cell death. Further studies are needed to examine whether cytoplasmic NR2B-immunostaining is translocated to the synaptic membrane during pathological conditions or following stimulation.

Chapter 7

Summation of the most important findings of the thesis

The most important findings of the investigations presented in this thesis are summarized below. Where appropriate, a brief interpretation of the results is also provided together with a short discussion of their functional significance.

1. The great majority (97.7%) of somatostatin-containing and CGRP-lacking boutons show immunoreactivity for VGLUT2. These terminals form asymmetrical synapses, the majority of which (87%) express AMPA subunits at their PSDs. These results suggest that somatostatin-containing interneurons in the dorsal horn are excitatory, and use glutamate as a neurotransmitter.
2. A majority (96.5%) of enkephalin-containing boutons form asymmetrical synapses, the majority of which (77%) express AMPA subunits at their PSDs. A small proportion (3.5%) of enkephalin-immunoreactive terminals form symmetrical synapses and these lack AMPA receptors. These results suggest that somatostatin-containing interneurons in the dorsal horn are excitatory, and use glutamate as a neurotransmitter.
3. Postembedding immunogold labelling on freeze-substituted spinal cord tissue can give non-specific synaptic labelling for NR2A, as judged by the presence of gold particles at asymmetrical synapses in the NR2A knock-out mice. This finding raises questions about the validity of the postembedding method for the detection of NMDA subunits and stress the need for the use of appropriate controls during immunocytochemistry.
4. Antigen unmasking with limited proteolytic digestion using pepsin is suitable to reveal AMPA and NMDA receptors at glutamatergic synapses in the spinal cord. This method probably allows antibodies to gain access to epitopes that are normally masked by cross-linking due to fixation. With immunofluorescence immunoreactive synapses appear as small puncta, while with electron microscopy the DAB reaction product is associated with PSDs.
5. Following pepsin-treatment GluR2-immunoreactive puncta are present throughout the gray matter, whereas GluR1-immunoreactive puncta are restricted to the dorsal horn and are most numerous in the superficial laminae. Punctate immunostaining for GluR3 and GluR4 is present in all laminae, but it is weak in the superficial dorsal horn.
6. GluR2 is present at virtually all (98%) puncta that are GluR1-, GluR3- or GluR4-immunoreactive. This subunit can therefore serve as a marker for glutamatergic synapses that contain AMPA receptors in the spinal cord. These results also suggest the all spinal cord neurons express GluR2. Since the presence or absence

of GluR2 determines the Ca^{2+}-permeability of AMPA complexes, it is likely that Ca^{2+}-permeable and impermeable AMPA receptors are intermingled within the same active sites.

7. GluR2- and GluR1-immunoreactive puncta are apposed to various types of glutamatergic axon terminal. Of the 4,800 glutamatergic boutons analysed, 96.2% formed at least one synapse where AMPA receptors were present.
8. GluR1 subunits are more often present at synapses formed by primary afferents than at those formed by excitatory interneurons. This is very important since GluR1 subunits have been implicated in activity-dependent synaptic plasticity both in the spinal cord and other parts of the CNS.
9. Intradermal injection of capsaicin leads to the rapid phosphorylation of GluR1 subunits at glutamatergic synapses in a somatotopically appropriate area of the superficial dorsal horn. Since phosphorylation of this subunit increases the open channel probability of the receptor complex, this could underlie the central sensitization of nociceptive neurons.
10. Following pepsin-treatment NR1-immunoreactive puncta are fairly evenly distributed throughout the gray matter. Punctate immunostaining for NR2A is strongest in the deep dorsal horn, with much lower levels elsewhere, except for lamina IIo, where it is virtually missing. NR2B is present at high levels in laminae I-II, and these gradually decrease towards the ventral horn. The laminar distribution of NR2B and NR2A subunits suggests that these might be associated preferentially with synapses formed by unmyelinated nociceptive C-fibres and myelinated Aβ/Aδ-fibres, respectively.
11. Only a proportion (approximately half for NR1 and one-third for NR2A and NR2B) of GluR2-immunoreactive synapses express an NMDA subunit and this indicates that NMDA receptors are either selectively expressed by certain neurons or selectively targeted to particular synapses within individual neurons. Further studies are needed to determine exactly which neuronal circuits express particular NMDA subunits.
12. The majority of NR2A- or NR2B-immunoreactive puncta are also labelled for NR1, and this strongly suggest that immunoreactive puncta observed after antigen unmasking correspond to functional NMDA receptors at glutamatergic synapses.

References

Aarli, J. A., Aparicio, S. R., Lumsden, C. E., and Tonder, O. (1975) Binding of normal human IgG to myelin sheaths, glia and neurons. *Immunology* **28,** 171-185.

Abbadie, C., Honore, P., Fournie-Zaluski, M. C., Roques, B. P., and Besson, J. M. (1994) Effects of opioids and non-opioids on c-Fos-like immunoreactivity induced in rat lumbar spinal cord neurons by noxious heat stimulation. *Eur. J. Pharmacol.* **258,** 215-227.

Abdrachmanova, G., Teisinger, J., Vlachova, V., and Vyklicky, L., Jr. (2000) Molecular and functional properties of synaptically activated NMDA receptors in neonatal motoneurons in rat spinal cord slices. *Eur. J. Neurosci.* **12,** 955-963.

Abe, M., Fukaya, M., Yagi, T., Mishina, M., Watanabe, M., and Sakimura, K. (2004) NMDA receptor GluRε/NR2 subunits are essential for postsynaptic localization and protein stability of GluRζ/NR1 subunit. *J. Neurosci.* in press.

Afrah, A. W., Fiska, A., Gjerstad, J., Gustafsson, H., Tjolsen, A., Olgart, L., Stiller, C. O., Hole, K., and Brodin, E. (2002) Spinal substance P release in vivo during the induction of long-term potentiation in dorsal horn neurons. *Pain* **96,** 49-55.

Agnati, L. F., Fuxe, K., Zoli, M., Ozini, I., Toffano, G., and Ferraguti, F. (1986) A correlation analysis of the regional distribution of central enkephalin and beta-endorphin immunoreactive terminals and of opiate receptors in adult and old male rats. Evidence for the existence of two main types of communication in the central nervous system: the volume transmission and the wiring transmission. *Acta Physiol. Scand.* **128,** 201-207.

Agnati, L. F., Tiengo, M., Ferraguti, F., Biagini, G., Benfenati, F., Benedetti, C., Rigoli, M., and Fuxe, K. (1991) Pain, analgesia, and stress: an integrated view. *Clin. J. Pain* **7 Suppl 1,** S23-S37.

Agnati, L. F., Bjelke, B., and Fuxe, K. (1995a) Volume versus wiring transmission in the brain: a new theoretical frame for neuropsychopharmacology. *Med. Res. Rev.* **15,** 33-45.

Agnati, L. F., Zoli, M., Stromberg, I., and Fuxe, K. (1995b) Intercellular communication in the brain: wiring versus volume transmission. *Neuroscience* **69,** 711-726.

Agrawal, S. G. and Evans, R. H. (1986) The primary afferent depolarizing action of kainate in the rat. *Br. J. Pharmacol.* **87,** 345-355.

Ahmadi, S., Muth-Selbach, U., Lauterbach, A., Lipfert, P., Neuhuber, W. L., and Zeilhofer, H. U. (2003) Facilitation of spinal NMDA receptor currents by spillover of synaptically released glycine. *Science* **300,** 2094-2097.

Aicher, S. A., Sharma, S., Cheng, P. Y., and Pickel, V. M. (1997) The N-methyl-D-aspartate (NMDA) receptor is postsynaptic to substance P-containing axon terminals in the rat superficial dorsal horn. *Brain Res.* **772,** 71-81.

Aihara, Y., Mashima, H., Onda, H., Hisano, S., Kasuya, H., Hori, T., Yamada, S., Tomura, H., Yamada, Y., Inoue, I., Kojima, I., and Takeda, J. (2000) Molecular cloning of a novel brain-type Na(+)-dependent inorganic phosphate cotransporter. *J. Neurochem.* **74,** 2622-2625.

Akil, H., Richardson, D. E., Hughes, J., and Barchas, J. D. (1978) Enkephalin-like material elevated in ventricular cerebrospinal fluid of pain patients after analgetic focal stimulation. *Science* **201,** 463-465.

Albuquerque, C., Lee, C. J., Jackson, A. C., and MacDermott, A. B. (1999) Subpopulations of GABAergic and non-GABAergic rat dorsal horn neurons express Ca2+-permeable AMPA receptors. *Eur. J. Neurosci.* **11,** 2758-2766.

Antal, M., Polgar, E., Chalmers, J., Minson, J. B., Llewellyn-Smith, I., Heizmann, C. W., and Somogyi, P. (1991) Different populations of parvalbumin- and calbindin-D28k-immunoreactive neurons contain GABA and accumulate 3H-D-aspartate in the dorsal horn of the rat spinal cord. *J. Comp. Neurol.* **314,** 114-124.

Aoki, C., Miko, I., Oviedo, H., Mikeladze-Dvali, T., Alexandre, L., Sweeney, N., and Bredt, D. S. (2001) Electron microscopic immunocytochemical detection of PSD-95, PSD-93, SAP-102, and SAP-97 at postsynaptic, presynaptic, and nonsynaptic sites of adult and neonatal rat visual cortex. *Synapse* **40,** 239-257.

Arundine, M. and Tymianski, M. (2003) Molecular mechanisms of calcium-dependent neurodegeneration in excitotoxicity. *Cell Calcium* **34,** 325-337.

Arvidsson, U., Riedl, M., Chakrabarti, S., Lee, J. H., Nakano, A. H., Dado, R. J., Loh, H. H., Law, P. Y., Wessendorf, M. W., and Elde, R. (1995) Distribution and targeting of a mu-opioid receptor (MOR1) in brain and spinal cord. *J. Neurosci.* **15,** 3328-3341.

Baba, H., Doubell, T. P., Moore, K. A., and Woolf, C. J. (2000) Silent NMDA receptor-mediated synapses are developmentally regulated in the dorsal horn of the rat spinal cord. *J. Neurophysiol.* **83,** 955-962.

Balcar, V. J. and Johnston, G. A. (1972) The structural specificity of the high affinity uptake of L-glutamate and L-aspartate by rat brain slices. *J. Neurochem.* **19,** 2657-2666.

Banke, T. G., Bowie, D., Lee, H., Huganir, R. L., Schousboe, A., and Traynelis, S. F. (2000) Control of GluR1 AMPA receptor function by cAMP-dependent protein kinase. *J. Neurosci.* **20,** 89-102.

Baranauskas, G. and Nistri, A. (1998) Sensitization of pain pathways in the spinal cord: cellular mechanisms. *Prog. Neurobiol.* **54,** 349-365.

Bardoni, R., Magherini, P. C., and MacDermott, A. B. (1998) NMDA EPSCs at glutamatergic synapses in the spinal cord dorsal horn of the postnatal rat. *J. Neurosci.* **18,** 6558-6567.

Bardoni, R., Torsney, C., Tong, C. K., Prandini, M., and MacDermott, A. B. (2004) Presynaptic NMDA receptors modulate glutamate release from primary sensory neurons in rat spinal cord dorsal horn. *J. Neurosci.* **24,** 2774-2781.

Bar-Peled, O., O'Brien, R. J., Morrison, J. H., and Rothstein, J. D. (1999) Cultured motor neurons possess calcium-permeable AMPA/kainate receptors. *Neuroreport* **10,** 855-859.

Baude, A., Nusser, Z., Molnar, E., McIlhinney, R. A., and Somogyi, P. (1995) High-resolution immunogold localization of AMPA type glutamate receptor subunits at synaptic and non-synaptic sites in rat hippocampus. *Neuroscience* **69,** 1031-1055.

Begon, S., Pickering, G., Eschalier, A., Mazur, A., Rayssiguier, Y., and Dubray, C. (2001) Role of spinal NMDA receptors, protein kinase C and nitric oxide synthase in the hyperalgesia induced by magnesium deficiency in rats. *Br. J. Pharmacol.* **134,** 1227-1236.

Beitz, A. J. and Ecklund, L. J. (1988) Colocalization of fixative-modified glutamate and glutaminase but not GAD in rubrospinal neurons. *J. Comp. Neurol.* **274,** 265-279.

Bellocchio, E. E., Hu, H., Pohorille, A., Chan, J., Pickel, V. M., and Edwards, R. H. (1998) The localization of the brain-specific inorganic phosphate transporter suggests a specific presynaptic role in glutamatergic transmission. *J. Neurosci.* **18,** 8648-8659.

Bellocchio, E. E., Reimer, R. J., Fremeau, R. T., Jr., and Edwards, R. H. (2000) Uptake of glutamate into synaptic vesicles by an inorganic phosphate transporter. *Science* **289,** 957-960.

Bennett, P. M. (1998) Structural changes in samples cryofixed by contact with a cold metal block. *J. Microsc.* **192 (Pt 3),** 259-268.

Bennett, G. J. (2000) Update on the neurophysiology of pain transmission and modulation: focus on the NMDA-receptor. *J. Pain Symptom Manage.* **19,** S2-S6.

Bergersen, L., Waerhaug, O., Helm, J., Thomas, M., Laake, P., Davies, A. J., Wilson, M. C., Halestrap, A. P., and Ottersen, O. P. (2001) A novel postsynaptic density protein:

the monocarboxylate transporter MCT2 is co-localized with delta-glutamate receptors in postsynaptic densities of parallel fiber-Purkinje cell synapses. *Exp. Brain Res.* **136,** 523-534.

Bernard, V., Somogyi, P., and Bolam, J. P. (1997) Cellular, subcellular, and subsynaptic distribution of AMPA-type glutamate receptor subunits in the neostriatum of the rat. *J. Neurosci.* **17,** 819-833.

Bernard, V. and Bolam, J. P. (1998) Subcellular and subsynaptic distribution of the NR1 subunit of the NMDA receptor in the neostriatum and globus pallidus of the rat: co-localization at synapses with the GluR2/3 subunit of the AMPA receptor. *Eur. J. Neurosci.* **10,** 3721-3736.

Bernardi, P. S., Valtschanoff, J. G., Weinberg, R. J., Schmidt, H. H., and Rustioni, A. (1995) Synaptic interactions between primary afferent terminals and GABA and nitric oxide-synthesizing neurons in superficial laminae of the rat spinal cord. *J. Neurosci.* **15,** 1363-1371.

Bigge, C. F. (1999) Ionotropic glutamate receptors. *Curr. Opin. Chem. Biol.* **3,** 441-447.

Biscoe, T. J., Headley, P. M., Lodge, D., Martin, M. R., and Watkins, J. C. (1976) The sensitivity of rat spinal interneurones and renshaw cells to L-glutamate and L-aspartate. *Exp. Brain Res.* **26,** 547-551.

Bohrmann, B. and Kellenberger, E. (2001) Cryosubstitution of frozen biological specimens in electron microscopy: use and application as an alternative to chemical fixation. *Micron* **32,** 11-19.

Bonanno, G. and Raiteri, M. (1994) Release-regulating presynaptic heterocarriers. *Prog. Neurobiol.* **44,** 451-462.

Boyce, S., Wyatt, A., Webb, J. K., O'Donnell, R., Mason, G., Rigby, M., Sirinathsinghji, D., Hill, R. G., and Rupniak, N. M. (1999) Selective NMDA NR2B antagonists induce antinociception without motor dysfunction: correlation with restricted localisation of NR2B subunit in dorsal horn. *Neuropharmacology* **38,** 611-623.

Bredt, D. S. and Nicoll, R. A. (2003) AMPA receptor trafficking at excitatory synapses. *Neuron* **40,** 361-379.

Brimecombe, J. C., Boeckman, F. A., and Aizenman, E. (1997) Functional consequences of NR2 subunit composition in single recombinant N-methyl-D-aspartate receptors. *Proc. Natl. Acad. Sci. U. S. A.* **94,** 11019-11024.

Brodin, L., Shupliakov, O., Pieribone, V. A., Hellgren, J., and Hill, R. H. (1994) The reticulospinal glutamate synapse in lamprey: plasticity and presynaptic variability. *J. Neurophysiol.* **72,** 592-604.

Broman, J., Anderson, S., and Ottersen, O. P. (1993) Enrichment of glutamate-like immunoreactivity in primary afferent terminals throughout the spinal cord dorsal horn. *Eur. J. Neurosci.* **5,** 1050-1061.

Broman, J. (1994a) Neurotransmitters in subcortical somatosensory pathways. *Anat. Embryol. (Berl.)* **189,** 181-214.

Broman, J. and Adahl, F. (1994b) Evidence for vesicular storage of glutamate in primary afferent terminals. *Neuroreport* **5,** 1801-1804.

Brorson, S. H. and Strom, E. H. (1998) A new immunoelectron microscopy approach for the detection of immunoglobulin and complement deposits in epoxy-embedded renal biopsies. *Ultrastruct. Pathol.* **22,** 449-457.

Brorson, S. H. (1999a) Comparison of the immunolabeling of heated and deplasticized epoxy sections on the electron microscopical level. *Micron* **30,** 319-324.

Brorson, S. H. (1999b) Fixative-dependent increase in immunogold labeling following antigen retrieval on acrylic and epoxy sections. *Biotech. Histochem.* **74,** 248-260.

Brorson, S. H. (2001) Heat-induced antigen retrieval of epoxy sections for electron microscopy. *Histol. Histopathol.* **16,** 923-930.

Brugger, F., Wicki, U., Nassenstein-Elton, D., Fagg, G. E., Olpe, H. R., and Pozza, M. F. (1990) Modulation of the NMDA receptor by D-serine in the cortex and the spinal cord, in vitro. *Eur. J. Pharmacol.* **191,** 29-38.

Budai, D. and Fields, H. L. (1998) Endogenous opioid peptides acting at mu-opioid receptors in the dorsal horn contribute to midbrain modulation of spinal nociceptive neurons. *J. Neurophysiol.* **79,** 677-687.

Burnashev, N., Khodorova, A., Jonas, P., Helm, P. J., Wisden, W., Monyer, H., Seeburg, P. H., and Sakmann, B. (1992) Calcium-permeable AMPA-kainate receptors in fusiform cerebellar glial cells. *Science* **256,** 1566-1570.

Burnashev, N., Zhou, Z., Neher, E., and Sakmann, B. (1995) Fractional calcium currents through recombinant GluR channels of the NMDA, AMPA and kainate receptor subtypes. *J. Physiol.* **485 (Pt 2),** 403-418.

Burnashev, N. and Rozov, A. (2000) Genomic control of receptor function. *Cell Mol. Life Sci.* **57,** 1499-1507.

Carriedo, S. G., Yin, H. Z., and Weiss, J. H. (1996) Motor neurons are selectively vulnerable to AMPA/kainate receptor-mediated injury in vitro. *J. Neurosci.* **16,** 4069-4079.

Carriedo, S. G., Sensi, S. L., Yin, H. Z., and Weiss, J. H. (2000) AMPA exposures induce mitochondrial Ca(2+) overload and ROS generation in spinal motor neurons in vitro. *J. Neurosci.* **20,** 240-250.

Carroll, R. C., Beattie, E. C., von Zastrow, M., and Malenka, R. C. (2001) Role of AMPA receptor endocytosis in synaptic plasticity. *Nat. Rev. Neurosci.* **2,** 315-324.

Chaplan, S. R., Malmberg, A. B., and Yaksh, T. L. (1997) Efficacy of spinal NMDA receptor antagonism in formalin hyperalgesia and nerve injury evoked allodynia in the rat. *J. Pharmacol. Exp. Ther.* **280,** 829-838.

Chapman, V. and Dickenson, A. H. (1992a) The combination of NMDA antagonism and morphine produces profound antinociception in the rat dorsal horn. *Brain Res.* **573,** 321-323.

Chapman, V. and Dickenson, A. H. (1992b) The effects of sandostatin and somatostatin on nociceptive transmission in the dorsal horn of the rat spinal cord. *Neuropeptides* **23,** 147-152.

Chatterton, J. E., Awobuluyi, M., Premkumar, L. S., Takahashi, H., Talantova, M., Shin, Y., Cui, J., Tu, S., Sevarino, K. A., Nakanishi, N., Tong, G., Lipton, S. A., and Zhang, D. (2002) Excitatory glycine receptors containing the NR3 family of NMDA receptor subunits. *Nature* **415,** 793-798.

Chazot, P. L. (2004) The NMDA receptor NR2B subunit: a valid therapeutic target for multiple CNS pathologies. *Curr. Med. Chem.* **11,** 389-396.

Chen, L. and Huang, L. Y. (1992) Protein kinase C reduces Mg2+ block of NMDA-receptor channels as a mechanism of modulation. *Nature* **356,** 521-523.

Chung, H. J., Xia, J., Scannevin, R. H., Zhang, X., and Huganir, R. L. (2000) Phosphorylation of the AMPA receptor subunit GluR2 differentially regulates its interaction with PDZ domain-containing proteins. *J. Neurosci.* **20,** 7258-7267.

Ciabarra, A. M., Sullivan, J. M., Gahn, L. G., Pecht, G., Heinemann, S., and Sevarino, K. A. (1995) Cloning and characterization of chi-1: a developmentally regulated member of a novel class of the ionotropic glutamate receptor family. *J. Neurosci.* **15,** 6498-6508.

Clarke, N. P. and Bolam, J. P. (1998) Distribution of glutamate receptor subunits at neurochemically characterized synapses in the entopeduncular nucleus and subthalamic nucleus of the rat. *J. Comp. Neurol.* **397,** 403-420.

Clements, J. D., Lester, R. A., Tong, G., Jahr, C. E., and Westbrook, G. L. (1992) The time course of glutamate in the synaptic cleft. *Science* **258,** 1498-1501.

Costa, O., Marion, C., Monier, J. C., and Roux, B. (1984) Non-specific binding of heat-aggregated IgG to histone detected by ELISA. *J. Immunol. Methods* **74,** 283-291.

Cull-Candy, S., Brickley, S., and Farrant, M., (2001) NMDA receptor subunits: diversity, development and disease. *Curr. Opinion Neurobiol.* **11,** 327-335.

Curtis, D. R., Phillis, J. W., and Watkins, J. C. (1959) Chemical excitation of spinal neurones. *Nature* **183,** 611-612.

Curtis, D. R., Phillis, J. W., and Watkins, J. C. (1960) The chemical excitation of spinal neurones by certain acidic amino acids. *J. Physiol.* **150,** 656-682.

Dai, W. M., Christensen, K. V., Egebjerg, J., Ebert, B., and Lambert, J. D. (2002) Correlation of the expression of kainate receptor subtypes to responses evoked in cultured cortical and spinal cord neurones. *Brain Res.* **926,** 94-107.

Danbolt, N. C. (2001) Glutamate uptake. *Prog. Neurobiol.* **65,** 1-105.

De Biasi, S. and Rustioni, A. (1988) Glutamate and substance P coexist in primary afferent terminals in the superficial laminae of spinal cord. *Proc. Natl. Acad. Sci. U. S. A.* **85,** 7820-7824.

De Blasi, A., Conn, P. J., Pin, J., and Nicoletti, F. (2001) Molecular determinants of metabotropic glutamate receptor signaling. *Trends Pharmacol. Sci.* **22,** 114-120.

Del Cano, G. G., Millan, L. M., Gerrikagoitia, I., Sarasa, M., and Matute, C. (1999) Ionotropic glutamate receptor subunit distribution on hypoglossal motoneuronal pools in the rat. *J. Neurocytol.* **28,** 455-468.

Dingledine, R., Borges, K., Bowie, D., and Traynelis, S. F. (1999) The glutamate receptor ion channels. *Pharmacol. Rev.* **51,** 7-61.

Dougherty, P. M. and Willis, W. D. (1991a) Enhancement of spinothalamic neuron responses to chemical and mechanical stimuli following combined micro-iontophoretic application of N-methyl-D-aspartic acid and substance P. *Pain* **47,** 85-93.

Dougherty, P. M. and Willis, W. D. (1991b) Modification of the responses of primate spinothalamic neurons to mechanical stimulation by excitatory amino acids and an N-methyl-D-aspartate antagonist. *Brain Res.* **542,** 15-22.

Dubner, R. and Ruda, M. A. (1992) Activity-dependent neuronal plasticity following tissue injury and inflammation. *Trends. Neurosci.* **15,** 96-103.

Dunah, A. W., Yasuda, R. P., Wang, Y. H., Luo, J., Davila-Garcia, M., Gbadegesin, M., Vicini, S., and Wolfe, B. B. (1996) Regional and ontogenic expression of the NMDA receptor subunit NR2D protein in rat brain using a subunit-specific antibody. *J. Neurochem.* **67,** 2335-2345.

Dusser De Barrene, J. G., (1933) The mode and site of action of strychine in the nervous system. *Physiol. Rev.* **13**, 325-335.

Eide, P. K., Jorum, E., Stubhaug, A., Bremnes, J., and Breivik, H. (1994) Relief of post-herpetic neuralgia with the N-methyl-D-aspartic acid receptor antagonist ketamine: a double-blind, cross-over comparison with morphine and placebo. *Pain* **58,** 347-354.

Eisenberg, E., LaCross, S., and Strassman, A. M. (1995) The clinically tested N-methyl-D-aspartate receptor antagonist memantine blocks and reverses thermal hyperalgesia in a rat model of painful mononeuropathy. *Neurosci. Lett.* **187,** 17-20.

Engelman, H. S., Albuquerque, C., Lee, C. J., Allen, T. B. and MacDermott, A. B. (1997) Calcium permeable AMPA receptors expressed in laminae I and II of the postnatal rat spinal cord. *Soc. Neurosci. Abstr.* **23,** 1754.

Engelman, H. S., Allen, T. B., and MacDermott, A. B. (1999) The distribution of neurons expressing calcium-permeable AMPA receptors in the superficial laminae of the spinal cord dorsal horn. *J. Neurosci.* **19,** 2081-2089.

Ericson, A. C., Blomqvist, A., Craig, A. D., Ottersen, O. P., and Broman, J. (1995) Evidence for glutamate as neurotransmitter in trigemino-and spinothalamic tract terminals in the nucleus submedius of cats. *Eur. J. Neurosci.* **7,** 305-317.

Esteban, J. A., Shi, S. H., Wilson, C., Nuriya, M., Huganir, R. L., and Malinow, R. (2003) PKA phosphorylation of AMPA receptor subunits controls synaptic trafficking underlying plasticity. *Nat. Neurosci.* **6,** 136-143.

Fang, L., Wu, J., Lin, Q., and Willis, W. D. (2002) Calcium-calmodulin-dependent protein kinase II contributes to spinal cord central sensitization. *J. Neurosci.* **22,** 4196-4204.

Fang, L., Wu, J., Zhang, X., Lin, Q., and Willis, W. D. (2003) Increased phosphorylation of the GluR1 subunit of spinal cord alpha-amino-3-hydroxy-5-methyl-4-isoxazole propionate receptor in rats following intradermal injection of capsaicin. *Neuroscience* **122,** 237-245.

Fitzpatrick-McElligott, S., Card, J. P., Lewis, M. E., and Baldino, F., Jr. (1988) Neuronal localization of prosomatostatin mRNA in the rat brain with in situ hybridization histochemistry. *J. Comp. Neurol.* **273,** 558-572.

Fonnum, F., Fykse, E. M., and Roseth, S. (1998) Uptake of glutamate into synaptic vesicles. *Prog. Brain Res.* **116,** 87-101.

Forrest, D., Yuzaki, M., Soares, H. D., Ng, L., Luk, D. C., Sheng, M., Stewart, C. L., Morgan, J. I., Connor, J. A., and Curran, T. (1994) Targeted disruption of NMDA receptor 1 gene abolishes NMDA response and results in neonatal death. *Neuron* **13,** 325-338.

Franciosi, S. (2001) AMPA receptors: potential implications in development and disease. *Cell. Mol. Life Sci.* **58,** 921-930.

Fremeau, R. T., Jr., Troyer, M. D., Pahner, I., Nygaard, G. O., Tran, C. H., Reimer, R. J., Bellocchio, E. E., Fortin, D., Storm-Mathisen, J., and Edwards, R. H. (2001) The expression of vesicular glutamate transporters defines two classes of excitatory synapse. *Neuron* **31,** 247-260.

Fukaya, M. and Watanabe, M. (2000) Improved immunohistochemical detection of postsynaptically located PSD-95/SAP90 protein family by protease section pretreatment: a study in the adult mouse brain. *J. Comp. Neurol.* **426,** 572-586.

Fukaya, M., Kato, A., Lovett, C., Tonegawa, S., and Watanabe, M. (2003) Retention of NMDA receptor NR2 subunits in the lumen of endoplasmic reticulum in targeted NR1 knockout mice. *Proc. Natl. Acad. Sci. U. S. A.* **100,** 4855-4860.

Fundytus, M. E. (2001) Glutamate receptors and nociception: implications for the drug treatment of pain. *CNS Drugs* **15,** 29-58.

Fung, S. J., Chan, J. Y., Manzoni, D., White, S. R., Lai, Y. Y., Strahlendorf, H. K., Zhuo, H., Liu, R. H., Reddy, V. K., and Barnes, C. D. (1994a) Cotransmitter-mediated locus coeruleus action on motoneurons. *Brain Res. Bull.* **35,** 423-432.

Fung, S. J., Reddy, V. K., Zhuo, H., Liu, R. H., Wang, Z., and Barnes, C. D. (1994b) Anatomical evidence for the presence of glutamate or enkephalin in noradrenergic projection neurons of the locus coeruleus. *Microsc. Res. Tech.* **29,** 219-225.

Furuyama, T., Kiyama, H., Sato, K., Park, H. T., Maeno, H., Takagi, H., and Tohyama, M. (1993) Region-specific expression of subunits of ionotropic glutamate receptors (AMPA-type, KA-type and NMDA receptors) in the rat spinal cord with special reference to nociception. *Brain Res Mol Brain Res.* **18,** 141-151.

Ganser, A. L., Kirschner, D. A., and Willinger, M. (1983) Ganglioside localization on myelinated nerve fibres by cholera toxin binding. *J. Neurocytol.* **12,** 921-938.

Garry, E. M., Moss, A., Rosie, R., Delaney, A., Mitchell, R., and Fleetwood-Walker, S. M. (2003) Specific involvement in neuropathic pain of AMPA receptors and adapter proteins for the GluR2 subunit. *Mol. Cell. Neurosci.* **24,** 10-22.

Garry, M. G., Miller, K. E., and Seybold, V. S. (1989) Lumbar dorsal root ganglia of the cat: a quantitative study of peptide immunoreactivity and cell size. *J. Comp. Neurol.* **284,** 36-47.

Garry, M. G., Malik, S., Yu, J., Davis, M. A., and Yang, J. (2000) Knock down of spinal NMDA receptors reduces NMDA and formalin evoked behaviors in rat. *Neuroreport* **11,** 49-55.

Gingrich, J. R., Pelkey, K. A., Fam, S. R., Huang, Y., Petralia, R. S., Wenthold, R. J., and Salter, M. W. (2004) Unique domain anchoring of Src to synaptic NMDA receptors via the mitochondrial protein NADH dehydrogenase subunit 2. *Proc. Natl. Acad. Sci. U. S. A.* **101,** 6237-6242.

Giuffrida, R. and Rustioni, A. (1989) Glutamate and aspartate immunoreactivity in corticospinal neurons of rats. *J. Comp. Neurol.* **288,** 154-164.

Glazer, E. J. and Basbaum, A. I. (1984) Axons which take up [3H]serotonin are presynaptic to enkephalin immunoreactive neurons in cat dorsal horn. *Brain Res.* **298,** 386-391.

Goldstein, P. A., Lee, C. J., and MacDermott, A. B. (1995) Variable distributions of Ca(2+)-permeable and Ca(2+)-impermeable AMPA receptors on embryonic rat dorsal horn neurons. *J. Neurophysiol.* **73,** 2522-2534.

Gras, C., Herzog, E., Bellenchi, G. C., Bernard, V., Ravassard, P., Pohl, M., Gasnier, B., Giros, B., and El Mestikawy, S. (2002) A third vesicular glutamate transporter expressed by cholinergic and serotoninergic neurons. *J. Neurosci.* **22,** 5442-5451.

Green, G. M. and Gibb, A. J. (2001) Characterization of the single-channel properties of NMDA receptors in laminae I and II of the dorsal horn of neonatal rat spinal cord. *Eur. J. Neurosci.* **14,** 1590-1602.

Greig, A., Donevan, S. D., Mujtaba, T. J., Parks, T. N., and Rao, M. S. (2000) Characterization of the AMPA-activated receptors present on motoneurons. *J. Neurochem.* **74,** 179-191.

Gross, A. J. and Sizer, I. W. (1959) The oxidation of tyramine, tyrosine, and related compounds by peroxidase. *J. Biol. Chem.* **234,** 1611-1614.

Gu, J. G., Albuquerque, C., Lee, C. J., and MacDermott, A. B. (1996) Synaptic strengthening through activation of Ca2+-permeable AMPA receptors. *Nature* **381,** 793-796.

Guo, W., Zou, S., Guan, Y., Ikeda, T., Tal, M., Dubner, R., and Ren, K. (2002) Tyrosine phosphorylation of the NR2B subunit of the NMDA receptor in the spinal cord during the development and maintenance of inflammatory hyperalgesia. *J. Neurosci.* **22,** 6208-6217.

Hainfeld, J. F. and Powell, R. D. (2000) New frontiers in gold labeling. *J. Histochem. Cytochem.* **48,** 471-480.

Harlan, R. E., Shivers, B. D., Romano, G. J., Howells, R. D., and Pfaff, D. W. (1987) Localization of preproenkephalin mRNA in the rat brain and spinal cord by in situ hybridization. *J. Comp. Neurol.* **258,** 159-184.

Harris, J. A., Corsi, M., Quartaroli, M., Arban, R., and Bentivoglio, M. (1996) Upregulation of spinal glutamate receptors in chronic pain. *Neuroscience* **74,** 7-12.

Hayat, M. A. (2001) *Microscopy, Immunohistochemistry and Antigen retrieval Methods For Light and Electron Microscopy*, New York: Kluwer Academic/Plenum Publishers.

He, Y., Janssen, W. G., and Morrison, J. H. (1998) Synaptic coexistence of AMPA and NMDA receptors in the rat hippocampus: a postembedding immunogold study. *J. Neurosci. Res.* **54,** 444-449.

He, Y., Hof, P. R., Janssen, W. G., Rothstein, J. D., and Morrison, J. H. (2001) Differential synaptic localization of GluR2 and EAAC1 in the macaque monkey entorhinal cortex: a postembedding immunogold study. *Neurosci. Lett.* **311,** 161-164.

Henley, J. M., Jenkins, R., and Hunt, S. P. (1993) Localisation of glutamate receptor binding sites and mRNAs to the dorsal horn of the rat spinal cord. *Neuropharmacology* **32,** 37-41.

Herrero, J. F., Laird, J. M., and Lopez-Garcia, J. A. (2000) Wind-up of spinal cord neurones and pain sensation: much ado about something? *Prog. Neurobiol.* **61,** 169-203.

Hertz, L., Dringen, R., Schousboe, A., and Robinson, S. R. (1999) Astrocytes: glutamate producers for neurons. *J. Neurosci. Res.* **57,** 417-428.

Herzog, E., Bellenchi, G. C., Gras, C., Bernard, V., Ravassard, P., Bedet, C., Gasnier, B., Giros, B., and El Mestikawy, S. (2001) The existence of a second vesicular glutamate transporter specifies subpopulations of glutamatergic neurons. *J. Neurosci.* **21,** RC181.

Hori, Y. and Kanda, K. (1994) Developmental alterations in NMDA receptor-mediated [Ca2+]i elevation in substantia gelatinosa neurons of neonatal rat spinal cord. *Brain Res. Dev. Brain Res.* **80,** 141-148.

Hökfelt, T., Efendic, S., Hellerstrom, C., Johansson, O., Luft, R., and Arimura, A. (1975) Cellular localization of somatostatin in endocrine-like cells and neurons of the rat with special references to the A1-cells of the pancreatic islets and to the hypothalamus. *Acta Endocrinol. Suppl. (Copenh)* **200,** 5-41.

Hökfelt, T., Ljungdahl, A., Terenius, L., Elde, R., and Nilsson, G. (1977) Immunohistochemical analysis of peptide pathways possibly related to pain and analgesia: enkephalin and substance P. *Proc. Natl. Acad. Sci. U. S. A.* **74,** 3081-3085.

Hökfelt, T., Terenius, L., Kuypers, H. G., and Dann, O. (1979) Evidence for enkephalin immunoreactive neurons in the medulla oblongata projecting to the spinal cord. *Neurosci Lett.* **14,** 55-60.

Hökfelt, T., Arvidsson, U., Cullheim, S., Millhorn, D., Nicholas, A. P., Pieribone, V., Seroogy, K., and Ulfhake, B. (2000a) Multiple messengers in descending serotonin neurons: localization and functional implications. *J. Chem. Neuroanat.* **18,** 75-86.

Hökfelt, T., Broberger, C., Xu, Z. Q., Sergeyev, V., Ubink, R., and Diez, M. (2000b) Neuropeptides--an overview. *Neuropharmacology* **39,** 1337-1356.

Huang, W. and Simpson, R. K., Jr. (1999a) Intrathecal treatment with MK-801 suppresses thermal nociceptive responses and prevents c-fos immunoreactivity induced in rat lumbar spinal cord neurons. *Neurol. Res.* **21,** 593-598.

Huang, W. and Simpson, R. K., Jr. (1999b) Noxious thermal stimulation of c-fos activity induced in rat lumbar spinal cord is reduced by AP-5 but not by glycine. *Neurosci Lett.* **259,** 1-4.

Huettner, J. E. (1990) Glutamate receptor channels in rat DRG neurons: activation by kainate and quisqualate and blockade of desensitization by Con A. *Neuron* **5,** 255-266.

Hughes, J., Smith, T., Morgan, B., and Fothergill, L. (1975a) Purification and properties of enkephalin - the possible endogenous ligand for the morphine receptor. *Life Sci.* **16,** 1753-1758.

Hughes, J., Smith, T. W., Kosterlitz, H. W., Fothergill, L. A., Morgan, B. A., and Morris, H. R. (1975b) Identification of two related pentapeptides from the brain with potent opiate agonist activity. *Nature* **258,** 577-580.

Hwang, S. J., Pagliardini, S., Rustioni, A., and Valtschanoff, J. G. (2001) Presynaptic kainate receptors in primary afferents to the superficial laminae of the rat spinal cord. *J. Comp. Neurol.* **436,** 275-289.

Ikeda, K., Nagasawa, M., Mori, H., Araki, K., Sakimura, K., Watanabe, M., Inoue, Y., and Mishina, M. (1992) Cloning and expression of the epsilon 4 subunit of the NMDA receptor channel. *FEBS Lett.* **313,** 34-38.

Iliakis, B., Anderson, N. L., Irish, P. S., Henry, M. A., and Westrum, L. E. (1996) Electron microscopy of immunoreactivity patterns for glutamate and gamma-aminobutyric acid in synaptic glomeruli of the feline spinal trigeminal nucleus (Subnucleus Caudalis). *J. Comp. Neurol.* **366,** 465-477.

Inoue, M., Mishina, M., and Ueda, H. (2000) Enhanced nociception by exogenous and endogenous substance P given into the spinal cord in mice lacking NR(2)A/epsilon(1), an NMDA receptor subunit. *Br. J. Pharmacol.* **129,** 239-241.

Isaac, J. T., Nicoll, R. A., and Malenka, R. C. (1995) Evidence for silent synapses: implications for the expression of LTP. *Neuron* **15,** 427-434.

Ishii, T., Moriyoshi, K., Sugihara, H., Sakurada, K., Kadotani, H., Yokoi, M., Akazawa, C., Shigemoto, R., Mizuno, N., Masu, M., and . (1993) Molecular characterization of the family of the N-methyl-D-aspartate receptor subunits. *J. Biol. Chem.* **268,** 2836-2843.

Iwasa, H. and Kondo, H. (1999) Differences in the width of the intercellular spaces in the epithelial basal infolding and the renal glomerular filtration site between freeze-substitution and conventional fixation. *J. Anat.* **194 (Pt 2),** 215-221.

Jakowec, M. W., Fox, A. J., Martin, L. J., and Kalb, R. G. (1995a) Quantitative and qualitative changes in AMPA receptor expression during spinal cord development. *Neuroscience* **67,** 893-907.

Jakowec, M. W., Yen, L., and Kalb, R. G. (1995b) In situ hybridization analysis of AMPA receptor subunit gene expression in the developing rat spinal cord. *Neuroscience* **67,** 909-920.

Jessell, T. M., Yoshioka, K., and Jahr, C. E. (1986) Amino acid receptor-mediated transmission at primary afferent synapses in rat spinal cord. *J. Exp. Biol.* **124,** 239-258.

Ji, R. R., Kohno, T., Moore, K. A., and Woolf, C. J. (2003) Central sensitization and LTP: do pain and memory share similar mechanisms? *Trends Neurosci.* **26,** 696-705.

Ji, Z. Q., Aas, J. E., Laake, J., Walberg, F., and Ottersen, O. P. (1991) An electron microscopic, immunogold analysis of glutamate and glutamine in terminals of rat spinocerebellar fibers. *J Comp Neurol* **307,** 296-310.

Jiang, N., Furue, H., Katafuchi, T., and Yoshimura, M. (2003) Somatostatin directly inhibits substantia gelatinosa neurons in adult rat spinal dorsal horn in vitro. *Neurosci Res.* **47,** 97-107.

Josephsen, K., Smith, C. E., and Nanci, A. (1999) Selective but nonspecific immunolabeling of enamel protein-associated compartments by a monoclonal antibody against vimentin. *J. Histochem. Cytochem.* **47,** 1237-1245.

Ju, G., Hökfelt, T., Brodin, E., Fahrenkrug, J., Fischer, J. A., Frey, P., Elde, R. P., and Brown, J. C. (1987) Primary sensory neurons of the rat showing calcitonin gene-related peptide immunoreactivity and their relation to substance P-, somatostatin-, galanin-, vasoactive intestinal polypeptide- and cholecystokinin-immunoreactive ganglion cells. *Cell Tissue Res.* **247,** 417-431.

Kalb, R. G. (1994) Regulation of motor neuron dendrite growth by NMDA receptor activation. *Development* **120,** 3063-3071.

Karlsson, U., Sjodin, J., Angeby, M. K., Johansson, S., Wikstrom, L., and Nasstrom, J. (2002) Glutamate-induced currents reveal three functionally distinct NMDA receptor

populations in rat dorsal horn - effects of peripheral nerve lesion and inflammation. *Neuroscience* **112,** 861-868.

Kawahara, Y., Kwak, S., Sun, H., Ito, K., Hashida, H., Aizawa, H., Jeong, S. Y., and Kanazawa, I. (2003) Human spinal motoneurons express low relative abundance of GluR2 mRNA: an implication for excitotoxicity in ALS. *J. Neurochem.* **85,** 680-689.

Kechagias, S. and Broman, J. (1995) Immunocytochemical evidence for vesicular storage of glutamate in cat spinocervical and cervicothalamic tract terminals. *Brain Res.* **675,** 316-320.

Kellenberger, E. (1991) The potential of cryofixation and freeze substitution: observations and theoretical considerations. *J. Microsc.* **161 (Pt 2),** 183-203.

Kellenberger, E., Johansen, R., Maeder, M., Bohrmann, B., Stauffer, E., and Villiger, W. (1992) Artefacts and morphological changes during chemical fixation. *J. Microsc.* **168 (Pt 2),** 181-201.

Kennedy, M. B. (1997) The postsynaptic density at glutamatergic synapses. *Trends Neurosci.* **20,** 264-268.

Kerchner, G. A., Wang, G. D., Qiu, C. S., Huettner, J. E., and Zhuo, M. (2001a) Direct presynaptic regulation of GABA/glycine release by kainate receptors in the dorsal horn: an ionotropic mechanism. *Neuron* **32,** 477-488.

Kerchner, G. A., Wilding, T. J., Li, P., Zhuo, M., and Huettner, J. E. (2001b) Presynaptic kainate receptors regulate spinal sensory transmission. *J. Neurosci.* **21,** 59-66.

Kew, J. N., Trube, G., and Kemp, J. A. (1996) A novel mechanism of activity-dependent NMDA receptor antagonism describes the effect of ifenprodil in rat cultured cortical neurones. *J. Physiol.* **497 (Pt 3),** 761-772.

Kharazia, V. N., Phend, K. D., Rustioni, A., and Weinberg, R. J. (1996) EM colocalization of AMPA and NMDA receptor subunits at synapses in rat cerebral cortex. *Neurosci. Lett.* **210,** 37-40.

Kharazia, V. N. and Weinberg, R. J. (1997) Tangential synaptic distribution of NMDA and AMPA receptors in rat neocortex. *Neurosci. Lett.* **238,** 41-44.

Kharazia, V. N. and Weinberg, R. J. (1999) Immunogold localization of AMPA and NMDA receptors in somatic sensory cortex of albino rat. *J. Comp. Neurol.* **412,** 292-302.

Kim, E., Cho, K. O., Rothschild, A., and Sheng, M. (1996) Heteromultimerization and NMDA receptor-clustering activity of Chapsyn-110, a member of the PSD-95 family of proteins. *Neuron* **17,** 103-113.

King, A. E. and Lopez-Garcia, J. A. (1993) Excitatory amino acid receptor-mediated neurotransmission from cutaneous afferents in rat dorsal horn in vitro. *J. Physiol.* **472,** 443-457.

Kirson, E. D., Schirra, C., Konnerth, A., and Yaari, Y. (1999) Early postnatal switch in magnesium sensitivity of NMDA receptors in rat CA1 pyramidal cells. *J. Physiol.* **521 Pt 1,** 99-111.

Kiss, J. Z. and McDonald, K. (1993) Electron microscopy immunocytochemistry following cryofixation and freeze substitution. *Methods Cell Biol.* **37,** 311-341.

Kiyama, H. and Emson, P. C. (1990) Distribution of somatostatin mRNA in the rat nervous system as visualized by a novel non-radioactive in situ hybridization histochemistry procedure. *Neuroscience* **38,** 223-244.

Kohr, G., Jensen, V., Koester, H. J., Mihaljevic, A. L., Utvik, J. K., Kvello, A., Ottersen, O. P., Seeburg, P. H., Sprengel, R., and Hvalby, O. (2003) Intracellular domains of NMDA receptor subtypes are determinants for long-term potentiation induction. *J. Neurosci.* **23,** 10791-10799.

Koistinaho, J., Hicks, K. J., and Sagar, S. M. (1993) Long-term induction of c-jun mRNA and Jun protein in rabbit retinal ganglion cells following axotomy or colchicine treatment. *J. Neurosci. Res.* **34,** 250-255.

Kolhekar, R., Meller, S. T., and Gebhart, G. F. (1993) Characterization of the role of spinal N-methyl-D-aspartate receptors in thermal nociception in the rat. *Neuroscience* **57,** 385-395.

Kontinen, V. K. and Meert, T. F. (2002) Vocalization responses after intrathecal administration of ionotropic glutamate receptor agonists in rats. *Anesth. Analg.* **95,** 997-1001, table.

Kornau, H. C., Schenker, L. T., Kennedy, M. B., and Seeburg, P. H. (1995) Domain interaction between NMDA receptor subunits and the postsynaptic density protein PSD-95. *Science* **269,** 1737-1740.

Kosaka, T., Nagatsu, I., Wu, J. Y., and Hama, K. (1986) Use of high concentrations of glutaraldehyde for immunocytochemistry of transmitter-synthesizing enzymes in the central nervous system. *Neuroscience* **18,** 975-990.

Kovács, G., Kocsis, P., Tarnawa, I., Horvath, C., Szombathelyi, Z., and Farkas, S. (2004) NR2B containing NMDA receptor dependent windup of single spinal neurons. *Neuropharmacology* **46,** 23-30.

Krebs, H. A. (1935a) Metabolism of amino acids. III. Deamination of amino acids. *Biochem. J.* **29,** 1620-1644.

Krebs, H. A., Eggleston, L. V., and Hems, R. (1949) Distribution of glutamin and glutamic acid in animal tissues. *Biochem. J.* **44,** 159-63.

Kullmann, D. M. (1994) Amplitude fluctuations of dual-component EPSCs in hippocampal pyramidal cells: implications for long-term potentiation. *Neuron* **12,** 1111-1120.

Kus, L., Saxon, D., and Beitz, A. J. (1995) NMDA R1 mRNA distribution in motor and thalamic-projecting sensory neurons in the rat spinal cord and brain stem. *Neurosci Lett.* **196,** 201-204.

Kutsuwada, T., Sakimura, K., Manabe, T., Takayama, C., Katakura, N., Kushiya, E., Natsume, R., Watanabe, M., Inoue, Y., Yagi, T., Aizawa, S., Arakawa, M., Takahashi, T., Nakamura, Y., Mori, H., and Mishina, M. (1996) Impairment of suckling response, trigeminal neuronal pattern formation, and hippocampal LTD in NMDA receptor epsilon 2 subunit mutant mice. *Neuron* **16,** 333-344.

Kvamme, E. (1998) Synthesis of glutamate and its regulation. *Prog. Brain Res.* **116,** 73-85.

Landry, M., Bouali-Benazzouz, R., El Mestikawy, S., Ravassard, P., and Nagy, F. (2004) Expression of vesicular glutamate transporters in rat lumbar spinal cord, with a note on dorsal root ganglia. *J. Comp. Neurol.* **468,** 380-394.

Landsend, A. S., Amiry-Moghaddam, M., Matsubara, A., Bergersen, L., Usami, S., Wenthold, R. J., and Ottersen, O. P. (1997) Differential localization of delta glutamate receptors in the rat cerebellum: coexpression with AMPA receptors in parallel fiber-spine synapses and absence from climbing fiber-spine synapses. *J. Neurosci.* **17,** 834-842.

Larson, A. A. and Beitz, A. J. (1988) Glycine potentiates strychnine-induced convulsions: role of NMDA receptors. *J. Neurosci.* **8,** 3822-3826.

Lee, C. J., Bardoni, R., Tong, C. K., Engelman, H. S., Joseph, D. J., Magherini, P. C., and MacDermott, A. B. (2002) Functional expression of AMPA receptors on central terminals of rat dorsal root ganglion neurons and presynaptic inhibition of glutamate release. *Neuron* **35,** 135-146.

Lee, H. K., Takamiya, K., Han, J. S., Man, H., Kim, C. H., Rumbaugh, G., Yu, S., Ding, L., He, C., Petralia, R. S., Wenthold, R. J., Gallagher, M., and Huganir, R. L. (2003) Phosphorylation of the AMPA receptor GluR1 subunit is required for synaptic plasticity and retention of spatial memory. *Cell* **112,** 631-643.

Lerma, J., Paternain, A. V., Rodriguez-Moreno, A., and Lopez-Garcia, J. C. (2001) Molecular physiology of kainate receptors. *Physiol. Rev.* **81,** 971-998.

Li, J., Simone, D. A., and Larson, A. A. (1999) Windup leads to characteristics of central sensitization. *Pain* **79,** 75-82.

Li, P. and Zhuo, M. (1998) Silent glutamatergic synapses and nociception in mammalian spinal cord. *Nature* **393,** 695-698.

Li, P., Wilding, T. J., Kim, S. J., Calejesan, A. A., Huettner, J. E., and Zhuo, M. (1999) Kainate-receptor-mediated sensory synaptic transmission in mammalian spinal cord. *Nature* **397,** 161-164.

Liao, D., Hessler, N. A., and Malinow, R. (1995) Activation of postsynaptically silent synapses during pairing-induced LTP in CA1 region of hippocampal slice. *Nature* **375,** 400-404.

Liu, H., Wang, H., Sheng, M., Jan, L. Y., Jan, Y. N., and Basbaum, A. I. (1994) Evidence for presynaptic N-methyl-D-aspartate autoreceptors in the spinal cord dorsal horn. *Proc. Natl. Acad. Sci. U. S. A.* **91,** 8383-8387.

Liu, H., Mantyh, P. W., and Basbaum, A. I. (1997) NMDA-receptor regulation of substance P release from primary afferent nociceptors. *Nature* **386,** 721-724.

Liu, X. G. and Sandkuhler, J. (1995) Long-term potentiation of C-fiber-evoked potentials in the rat spinal dorsal horn is prevented by spinal N-methyl-D-aspartic acid receptor blockage. *Neurosci Lett.* **191,** 43-46.

Llewellyn-Smith, I. J. and Minson, J. B. (1992) Complete penetration of antibodies into vibratome sections after glutaraldehyde fixation and ethanol treatment: light and electron microscopy for neuropeptides. *J. Histochem. Cytochem.* **40,** 1741-1749.

Lu, C. R., Hwang, S. J., Phend, K. D., Rustioni, A., and Valtschanoff, J. G. (2002) Primary afferent terminals in spinal cord express presynaptic AMPA receptors. *J. Neurosci.* **22,** 9522-9529.

Lu, C. R., Hwang, S. J., Phend, K. D., Rustioni, A., and Valtschanoff, J. G. (2003) Primary afferent terminals that express presynaptic NR1 in rats are mainly from myelinated, mechanosensitive fibers. *J. Comp. Neurol.* **460,** 191-202.

Lujan, R., Nusser, Z., Roberts, J. D., Shigemoto, R., and Somogyi, P. (1996) Perisynaptic location of metabotropic glutamate receptors mGluR1 and mGluR5 on dendrites and dendritic spines in the rat hippocampus. *Eur. J. Neurosci.* **8,** 1488-1500.

Luo, J., Wang, Y., Yasuda, R. P., Dunah, A. W., and Wolfe, B. B. (1997) The majority of N-methyl-D-aspartate receptor complexes in adult rat cerebral cortex contain at least three different subunits (NR1/NR2A/NR2B). *Mol. Pharmacol.* **51,** 79-86.

Luque, J. M., Bleuel, Z., Malherbe, P., and Richards, J. G. (1994) Alternatively spliced isoforms of the N-methyl-D-aspartate receptor subunit 1 are differentially distributed within the rat spinal cord. *Neuroscience* **63,** 629-635.

Lynn, B. and Carpenter, S. E. (1982) Primary afferent units from the hairy skin of the rat hind limb. *Brain Res.* **238,** 29-43.

Ma, Q. P. and Woolf, C. J. (1995) Noxious stimuli induce an N-methyl-D-aspartate receptor-dependent hypersensitivity of the flexion withdrawal reflex to touch: implications for the treatment of mechanical allodynia. *Pain* **61,** 383-390.

Ma, Q. P. and Hargreaves, R. J. (2000) Localization of N-methyl-D-aspartate NR2B subunits on primary sensory neurons that give rise to small-caliber sciatic nerve fibers in rats. *Neuroscience* **101,** 699-707.

MacDermott, A. B., Mayer, M. L., Westbrook, G. L., Smith, S. J., and Barker, J. L. (1986) NMDA-receptor activation increases cytoplasmic calcium concentration in cultured spinal cord neurones. *Nature* **321,** 519-522.

Malcangio, M., Fernandes, K., and Tomlinson, D. R. (1998) NMDA receptor activation modulates evoked release of substance P from rat spinal cord. *Br. J. Pharmacol.* **125,** 1625-1626.

Mao, J., Price, D. D., Hayes, R. L., Lu, J., and Mayer, D. J. (1992) Differential roles of NMDA and non-NMDA receptor activation in induction and maintenance of thermal hyperalgesia in rats with painful peripheral mononeuropathy. *Brain Res.* **598,** 271-278.

Marsh, D., Dickenson, A., Hatch, D., and Fitzgerald, M. (1999a) Epidural opioid analgesia in infant rats I: mechanical and heat responses. *Pain* **82,** 23-32.

Marsh, D., Dickenson, A., Hatch, D., and Fitzgerald, M. (1999b) Epidural opioid analgesia in infant rats II: responses to carrageenan and capsaicin. *Pain* **82,** 33-38.

Marvizon, J. C., McRoberts, J. A., Ennes, H. S., Song, B., Wang, X., Jinton, L., Corneliussen, B., and Mayer, E. A. (2002) Two N-methyl-D-aspartate receptors in rat dorsal root ganglia with different subunit composition and localization. *J. Comp. Neurol.* **446,** 325-341.

Mascias, P., Scheede, M., Bloms-Funke, P., and Chizh, B. (2002) Modulation of spinal nociception by GluR5 kainate receptor ligands in acute and hyperalgesic states and the role of gabaergic mechanisms. *Neuropharmacology* **43,** 327-339.

Matsubara, A., Laake, J. H., Davanger, S., Usami, S., and Ottersen, O. P. (1996) Organization of AMPA receptor subunits at a glutamate synapse: a quantitative immunogold analysis of hair cell synapses in the rat organ of Corti. *J. Neurosci.* **16,** 4457-4467.

Matsubara, A., Takumi, Y., Nakagawa, T., Usami, S., Shinkawa, H., and Ottersen, O. P. (1999) Immunoelectron microscopy of AMPA receptor subunits reveals three types of putative glutamatergic synapse in the rat vestibular end organs. *Brain Res.* **819,** 58-64.

Matsuda, K., Kamiya, Y., Matsuda, S., and Yuzaki, M. (2002) Cloning and characterization of a novel NMDA receptor subunit NR3B: a dominant subunit that reduces calcium permeability. *Brain Res. Mol Brain Res.* **100,** 43-52.

Matsuda, K., Fletcher, M., Kamiya, Y., and Yuzaki, M. (2003) Specific assembly with the NMDA receptor 3B subunit controls surface expression and calcium permeability of NMDA receptors. *J. Neurosci.* **23,** 10064-10073.

Maxwell, D.J., Réthelyi, M., (1987) Ultrastructure and synaptic connections of cutaneous afferent fibres in the spinal cord. *Trends. Neurosci.* **10,** 117-123.

Maxwell, D. J., Christie, W. M., Ottersen, O. P., and Storm-Mathisen, J. (1990a) Terminals of group Ia primary afferent fibres in Clarke's column are enriched with L-glutamate-like immunoreactivity. *Brain Res.* **510,** 346-350.

Maxwell, D. J., Christie, W. M., Short, A. D., Storm-Mathisen, J., and Ottersen, O. P. (1990b) Central boutons of glomeruli in the spinal cord of the cat are enriched with L-glutamate-like immunoreactivity. *Neuroscience* **36,** 83-104.

Mayer, M. L., Westbrook, G. L., and Guthrie, P. B. (1984) Voltage-dependent block by Mg2+ of NMDA responses in spinal cord neurones. *Nature* **309,** 261-263.

McCartney, C. J., Sinha, A., and Katz, J. (2004) A Qualitative Systematic Review of the Role of N-Methyl-D-Aspartate Receptor Antagonists in Preventive Analgesia. *Anesth. Analg.* **98,** 1385-1400.

McCauley, J. A., Theberge, C. R., Romano, J. J., Billings, S. B., Anderson, K. D., Claremon, D. A., Freidinger, R. M., Bednar, R. A., Mosser, S. D., Gaul, S. L., Connolly, T. M., Condra, C. L., Xia, M., Cunningham, M. E., Bednar, B., Stump, G. L., Lynch, J. J., Macaulay, A., Wafford, K. A., Koblan, K. S., and Liverton, N. J. (2004) NR2B-selective N-methyl-D-aspartate antagonists: synthesis and evaluation of 5-substituted benzimidazoles. *J. Med. Chem.* **47,** 2089-2096.

Meller, S. T., Dykstra, C., and Gebhart, G. F. (1992) Production of endogenous nitric oxide and activation of soluble guanylate cyclase are required for N-methyl-D-aspartate-produced facilitation of the nociceptive tail-flick reflex. *Eur. J. Pharmacol.* **214,** 93-96.

Mennini, T., Bigini, P., Ravizza, T., Vezzani, A., Calvaresi, N., Tortarolo, M., and Bendotti, C. (2002) Expression of glutamate receptor subtypes in the spinal cord of control and mnd mice, a model of motor neuron disorder. *J. Neurosci. Res.* **70,** 553-560.

Miller, K. E. and Salvatierra, A. T. (1998) Apposition of enkephalin- and neurotensin-immunoreactive neurons by serotonin-immunoreactive varicosities in the rat spinal cord. *Neuroscience* **85,** 837-846.

Minami, T., Sugatani, J., Sakimura, K., Abe, M., Mishina, M., and Ito, S. (1997) Absence of prostaglandin E2-induced hyperalgesia in NMDA receptor epsilon subunit knockout mice. *Br. J. Pharmacol.* **120,** 1522-1526.

Minami, T., Matsumura, S., Okuda-Ashitaka, E., Shimamoto, K., Sakimura, K., Mishina, M., Mori, H., and Ito, S. (2001) Characterization of the glutamatergic system for induction and maintenance of allodynia. *Brain Res.* **895,** 178-185.

Molander, C., Xu, Q., and Grant, G. (1984) The cytoarchitectonic organization of the spinal cord in the rat. I. The lower thoracic and lumbosacral cord. *J. Comp. Neurol.* **230,** 133-141.

Molander, C., Xu, Q., Rivero-Melian, C., and Grant, G. (1989) Cytoarchitectonic organization of the spinal cord in the rat: II. The cervical and upper thoracic cord. *J. Comp. Neurol.* **289,** 375-385.

Mollenholt, P., Post, C., Rawal, N., Freedman, J., Hokfelt, T., and Paulsson, I. (1988) Antinociceptive and 'neurotoxic' actions of somatostatin in rat spinal cord after intrathecal administration. *Pain* **32,** 95-105.

Momiyama, A. (2000) Distinct synaptic and extrasynaptic NMDA receptors identified in dorsal horn neurones of the adult rat spinal cord. *J. Physiol.* **523 Pt 3,** 621-628.

Monyer, H., Burnashev, N., Laurie, D. J., Sakmann, B., and Seeburg, P. H. (1994) Developmental and regional expression in the rat brain and functional properties of four NMDA receptors. *Neuron* **12,** 529-540.

Mooney, R. D., Bennett-Clarke, C. A., King, T. D., and Rhoades, R. W. (1990) Tectospinal neurons in hamster contain glutamate-like immunoreactivity. *Brain Res.* **537,** 375-380.

Mori, H., Manabe, T., Watanabe, M., Satoh, Y., Suzuki, N., Toki, S., Nakamura, K., Yagi, T., Kushiya, E., Takahashi, T., Inoue, Y., Sakimura, K., and Mishina, M. (1998) Role of the carboxy-terminal region of the GluR epsilon2 subunit in synaptic localization of the NMDA receptor channel. *Neuron* **21,** 571-580.

Morrison, B. M., Janssen, W. G., Gordon, J. W., and Morrison, J. H. (1998) Light and electron microscopic distribution of the AMPA receptor subunit, GluR2, in the spinal cord of control and G86R mutant superoxide dismutase transgenic mice. *J. Comp. Neurol.* **395,** 523-534.

Mosbacher, J., Schoepfer, R., Monyer, H., Burnashev, N., Seeburg, P. H., and Ruppersberg, J. P. (1994) A molecular determinant for submillisecond desensitization in glutamate receptors. *Science* **266,** 1059-1062.

Mullen, R. J., Buck, C. R., and Smith, A. M. (1992) NeuN, a neuronal specific nuclear protein in vertebrates. *Development* **116,** 201-211.

Murase, K., Nedeljkov, V., and Randic, M. (1982) The actions of neuropeptides on dorsal horn neurons in the rat spinal cord slice preparation: an intracellular study. *Brain Res.* **234,** 170-176.

Nagano, I., Murakami, T., Shiote, M., Abe, K., and Itoyama, Y. (2003) Ventral root avulsion leads to downregulation of GluR2 subunit in spinal motoneurons in adult rats. *Neuroscience* **117,** 139-146.

Nagelhus, E. A., Veruki, M. L., Torp, R., Haug, F. M., Laake, J. H., Nielsen, S., Agre, P., and Ottersen, O. P. (1998) Aquaporin-4 water channel protein in the rat retina and optic nerve: polarized expression in Muller cells and fibrous astrocytes. *J. Neurosci.* **18,** 2506-2519.

Nagy, G. G., Al Ayyan, M., Andrew, D., Fukaya, M., Watanabe, M., and Todd, A. J. (2004) Widespread expression of the AMPA receptor GluR2 subunit at glutamatergic synapses in the rat spinal cord and phosphorylation of GluR1 in response to noxious stimulation revealed with an antigen-unmasking method. *J. Neurosci.* **24,** 5766-5777.

Nagy, I., Woolf, C. J., Dray, A., and Urban, L. (1994) Cobalt accumulation in neurons expressing ionotropic excitatory amino acid receptors in young rat spinal cord: morphology and distribution. *J. Comp. Neurol.* **344,** 321-335.

Najlerahim, A., Harrison, P. J., Barton, A. J., Heffernan, J., and Pearson, R. C. (1990) Distribution of messenger RNAs encoding the enzymes glutaminase, aspartate aminotransferase and glutamic acid decarboxylase in rat brain. *Brain Res. Mol. Brain Res.* **7,** 317-333.

Neugebauer, V., Kornhuber, J., Lucke, T., and Schaible, H. G. (1993) The clinically available NMDA receptor antagonist memantine is antinociceptive on rat spinal neurones. *Neuroreport* **4,** 1259-1262.

Neugebauer, V., Lucke, T., Grubb, B., and Schaible, H. G. (1994) The involvement of N-methyl-D-aspartate (NMDA) and non-NMDA receptors in the responsiveness of rat spinal neurons with input from the chronically inflamed ankle. *Neurosci Lett.* **170,** 237-240.

Ni, B., Rosteck, P. R., Jr., Nadi, N. S., and Paul, S. M. (1994) Cloning and expression of a cDNA encoding a brain-specific Na(+)-dependent inorganic phosphate cotransporter. *Proc. Natl. Acad. Sci. U. S. A.* **91,** 5607-5611.

Nicholls, D. G., (1994) Mechanisms for exocytosis, Localized Ca^{2+} and the tirgger for SSV exocytosis in (ed.) Nicholls, D. G., *Proteins, Transmitters and Synapses*. Blackwell Scientific Publications, 119-121.

Nicholls, D. G. (1998) Presynaptic modulation of glutamate release. *Prog. Brain Res.* **116,** 15-22.

Nishi, M., Hinds, H., Lu, H. P., Kawata, M., and Hayashi, Y. (2001) Motoneuron-specific expression of NR3B, a novel NMDA-type glutamate receptor subunit that works in a dominant-negative manner. *J. Neurosci.* **21,** RC185.

Nishiyama, T., Yaksh, T. L., and Weber, E. (1998) Effects of intrathecal NMDA and non-NMDA antagonists on acute thermal nociception and their interaction with morphine. *Anesthesiology* **89,** 715-722.

Nüsser, Z., Mulvihill, E., Streit, P., and Somogyi, P. (1994) Subsynaptic segregation of metabotropic and ionotropic glutamate receptors as revealed by immunogold localization. *Neuroscience* **61,** 421-427.

Nüsser, Z., Roberts, J. D., Baude, A., Richards, J. G., and Somogyi, P. (1995) Relative densities of synaptic and extrasynaptic GABAA receptors on cerebellar granule cells as determined by a quantitative immunogold method. *J. Neurosci.* **15,** 2948-2960.

Nüsser, Z., Sieghart, W., Benke, D., Fritschy, J. M., and Somogyi, P. (1996) Differential synaptic localization of two major gamma-aminobutyric acid type A receptor alpha subunits on hippocampal pyramidal cells. *Proc. Natl. Acad. Sci. U. S. A.* **93,** 11939-11944.

Nüsser, Z., Lujan, R., Laube, G., Roberts, J. D., Molnar, E., and Somogyi, P. (1998) Cell type and pathway dependence of synaptic AMPA receptor number and variability in the hippocampus. *Neuron* **21,** 545-559.

Nyiri, G., Stephenson, F. A., Freund, T. F., and Somogyi, P. (2003) Large variability in synaptic N-methyl-D-aspartate receptor density on interneurons and a comparison with pyramidal-cell spines in the rat hippocampus. *Neuroscience* **119,** 347-363.

Olney, J. W. and Ho, O. L. (1970) Brain damage in infant mice following oral intake of glutamate, aspartate or cysteine. *Nature* **227,** 609-611.

Omkumar, R. V., Kiely, M. J., Rosenstein, A. J., Min, K. T., and Kennedy, M. B. (1996) Identification of a phosphorylation site for calcium/calmodulindependent protein kinase II in the NR2B subunit of the N-methyl-D-aspartate receptor. *J. Biol. Chem.* **271,** 31670-31678.

Otsuka, M. and Konishi, S. (1976) Release of substance P-like immunoreactivity from isolated spinal cord of newborn rat. *Nature* **264,** 83-84.

Ottersen, O. P. and Storm-Mathisen, J. (1984) Glutamate- and GABA-containing neurons in the mouse and rat brain, as demonstrated with a new immunocytochemical technique. *J. Comp. Neurol.* **229,** 374-392.

Ozawa, S., Kamiya, H., and Tsuzuki, K. (1998) Glutamate receptors in the mammalian central nervous system. *Prog. Neurobiol.* **54,** 581-618.

Ozkan, E. D. and Ueda, T. (1998) Glutamate transport and storage in synaptic vesicles. *Jpn. J. Pharmacol.* **77,** 1-10.

Parthasarathy, M. V. (1995) Freeze-substitution. *Methods. Cell. Biol.* **49,** 57-69.

Partin, K. M., Patneau, D. K., Winters, C. A., Mayer, M. L., and Buonanno, A. (1993) Selective modulation of desensitization at AMPA versus kainate receptors by cyclothiazide and concanavalin A. *Neuron* **11,** 1069-1082.

Passafaro, M., Piech, V., and Sheng, M. (2001) Subunit-specific temporal and spatial patterns of AMPA receptor exocytosis in hippocampal neurons. *Nat. Neurosci.* **4,** 917-926.

Paasivuo, R. and Saksela, E. (1983) Non-specific binding of mouse immunoglobulins by swollen-bodied astrocytes--a potential source of confusion in human brain immunohistochemistry. *Acta Neuropathol. (Berl.)* **59,** 103-108.

Pellegrini-Giampietro, D. E., Fan, S., Ault, B., Miller, B. E., and Zukin, R. S. (1994) Glutamate receptor gene expression in spinal cord of arthritic rats. *J. Neurosci.* **14,** 1576-1583.

Pellegrini-Giampietro, D. E., Gorter, J. A., Bennett, M. V., and Zukin, R. S. (1997) The GluR2 (GluR-B) hypothesis: Ca(2+)-permeable AMPA receptors in neurological disorders. *Trends Neurosci.* **20,** 464-470.

Penn, R. D., Paice, J. A., and Kroin, J. S. (1992) Octreotide: a potent new non-opiate analgesic for intrathecal infusion. *Pain* **49,** 13-19.

Perez-Otano, I., Schulteis, C. T., Contractor, A., Lipton, S. A., Trimmer, J. S., Sucher, N. J., and Heinemann, S. F. (2001) Assembly with the NR1 subunit is required for surface expression of NR3A-containing NMDA receptors. *J. Neurosci.* **21,** 1228-1237.

Petralia, R. S. and Wenthold, R. J. (1992) Light and electron immunocytochemical localization of AMPA-selective glutamate receptors in the rat brain. *J. Comp. Neurol.* **318,** 329-354.

Petralia, R. S., Wang, Y. X., and Wenthold, R. J. (1994a) Histological and ultrastructural localization of the kainate receptor subunits, KA2 and GluR6/7, in the rat nervous system using selective antipeptide antibodies. *J. Comp. Neurol.* **349,** 85-110.

Petralia, R. S., Wang, Y. X., and Wenthold, R. J. (1994b) The NMDA receptor subunits NR2A and NR2B show histological and ultrastructural localization patterns similar to those of NR1. *J. Neurosci.* **14,** 6102-6120.

Petralia, R. S., Yokotani, N., and Wenthold, R. J. (1994c) Light and electron microscope distribution of the NMDA receptor subunit NMDAR1 in the rat nervous system using a selective anti-peptide antibody. *J. Neurosci.* **14,** 667-696.

Petralia, R. S., Wang, Y. X., Mayat, E., and Wenthold, R. J. (1997) Glutamate receptor subunit 2-selective antibody shows a differential distribution of calcium-impermeable AMPA receptors among populations of neurons. *J. Comp. Neurol.* **385,** 456-476.

Petrenko, A. B., Yamakura, T., Baba, H., and Sakimura, K. (2003a) Unaltered pain-related behavior in mice lacking NMDA receptor GluRepsilon 1 subunit. *Neurosci. Res.* **46,** 199-204.

Petrenko, A. B., Yamakura, T., Baba, H., and Shimoji, K. (2003b) The role of N-methyl-D-aspartate (NMDA) receptors in pain: a review. *Anesth. Analg.* **97,** 1108-1116.

Phend, K. D., Rustioni, A., and Weinberg, R. J. (1995) An osmium-free method of epon embedment that preserves both ultrastructure and antigenicity for post-embedding immunocytochemistry. *J. Histochem. Cytochem.* **43,** 283-292.

Piehl, F., Tabar, G., and Cullheim, S. (1995) Expression of NMDA receptor mRNAs in rat motoneurons is down-regulated after axotomy. *Eur. J. Neurosci.* **7,** 2101-2110.

Pierce, J. P. and Mendell, L. M. (1993) Quantitative ultrastructure of Ia boutons in the ventral horn: scaling and positional relationships. *J. Neurosci.* **13,** 4748-4763.

Platenik, J., Kuramoto, N., and Yoneda, Y. (2000) Molecular mechanisms associated with long-term consolidation of the NMDA signals. *Life Sci.* **67,** 335-364.

Pomeranz, B. and Gurevich, N. (1979) Effects of enkephalin analogue and naloxone on cat spinal cord dorsal root potentials. *Eur. J. Pharmacol.* **60,** 307-313.

Popratiloff, A., Weinberg, R. J., and Rustioni, A. (1996) AMPA receptor subunits underlying terminals of fine-caliber primary afferent fibers. *J. Neurosci.* **16,** 3363-3372.

Popratiloff, A., Weinberg, R. J., and Rustioni, A. (1998a) AMPA receptors at primary afferent synapses in substantia gelatinosa after sciatic nerve section. *Eur. J. Neurosci.* **10,** 3220-3230.

Popratiloff, S. A., Weinberg, J. R., and Rustioni, A. (1998b) NMDAR1 and primary afferent terminals in the superficial spinal cord. *Neuroreport* **9,** 2423-2429.

Procter, M. J., Houghton, A. K., Faber, E. S., Chizh, B. A., Ornstein, P. L., Lodge, D., and Headley, P. M. (1998) Actions of kainate and AMPA selective glutamate receptor

ligands on nociceptive processing in the spinal cord. *Neuropharmacology* **37,** 1287-1297.

Proudlock, F., Spike, R. C., and Todd, A. J. (1993) Immunocytochemical study of somatostatin, neurotensin, GABA, and glycine in rat spinal dorsal horn. *J. Comp. Neurol.* **327,** 289-297.

Prybylowski, K. L., Grossman, S. D., Wrathall, J. R., and Wolfe, B. B. (2001) Expression of splice variants of the NR1 subunit of the N-methyl-D-aspartate receptor in the normal and injured rat spinal cord. *J. Neurochem.* **76,** 797-805.

Racca, C., Stephenson, F. A., Streit, P., Roberts, J. D., and Somogyi, P. (2000) NMDA receptor content of synapses in stratum radiatum of the hippocampal CA1 area. *J. Neurosci.* **20,** 2512-2522.

Ragnarson, B., Ornung, G., Grant, G., Ottersen, O. P., and Ulfhake, B. (2003) Glutamate and AMPA receptor immunoreactivity in Ia synapses with motoneurons and neurons of the central cervical nucleus. *Exp. Brain Res.* **149,** 447-457.

Raigorodsky, G., and Urca, G. (1990) Spinal antinociceptive effects of excitatory amino acid antagonists: quisqualate modulates the action of N-methyl-D-aspartate. *Eur. J. Pharmacol.* **182,** 37-47.

Reichling, D. B., and MacDermott, A. B. (1993) Brief calcium transients evoked by glutamate receptor agonists in rat dorsal horn neurons: fast kinetics and mechanisms. *J. Physiol.* **469,** 67-88.

Ren, K., Hylden, J. L., Williams, G. M., Ruda, M. A., and Dubner, R. (1992a) The effects of a non-competitive NMDA receptor antagonist, MK-801, on behavioral hyperalgesia and dorsal horn neuronal activity in rats with unilateral inflammation. *Pain* **50,** 331-344.

Ren, K., Williams, G. M., Hylden, J. L., Ruda, M. A., and Dubner, R. (1992b) The intrathecal administration of excitatory amino acid receptor antagonists selectively attenuated carrageenan-induced behavioral hyperalgesia in rats. *Eur. J. Pharmacol.* **219,** 235-243.

Ren, K. and Dubner, R. (1993) NMDA receptor antagonists attenuate mechanical hyperalgesia in rats with unilateral inflammation of the hindpaw. *Neurosci. Lett.* **163,** 22-26.

Réthelyi M., Light, A. R., and Perl, E. R. (1982) Synaptic complexes formed by functionally defined primary sensory afferent units with fine myelinated fibers. *J. Comp. Neurol.* **207,** 381-393.

Réthelyi, M., Mohapatra, N. K., Metz, C. B., Petrusz, P., and Lund, P. K. (1991) Colchicine enhances mRNAs encoding the precursor of calcitonin gene-related peptide in brainstem motoneurons. *Neuroscience* **42,** 531-539.

Rexed, B. (1952) The cytoarchitectonic organization of the spinal cord in the cat. *J. Comp. Neurol.* **96,** 414-495.

Rexed, B. (1954) A cytoarchitectonic atlas of the spinal cord in the cat. *J. Comp. Neurol.* **100,** 297-379.

Rexed, B. (1964) Some aspects of the cytoarchitectonics and synaptology of the spinal cord. *Prog. Brain Res.* **11,** 58-92.

Ribeiro-Da-Silva, A. and Coimbra, A. (1982) Two types of synaptic glomeruli and their distribution in laminae I-III of the rat spinal cord. *J. Comp. Neurol.* **209,** 176-186.

Ribeiro-da-Silva, A. (1994) Substantia gelatinosa of spinal cord. In: G. Paxinos, ed. *The rat nervous system.* Sydney: Academic, 47-59.

Ribeiro-Da-Silva, A. (1995) Ultrastructural features of the colocalization of calcitonin gene related peptide with substance P or somatostatin in the dorsal horn of the spinal cord. *Can. J. Physiol. Pharmacol.* **73,** 940-944.

Ribeiro-da-Silva, A. (2003) Substantia gelatinosa of the spinal cord. In: G Paxinos, ed. *The Rat Nervous System.* Academic Press, Sydney.

Roche, K. W., O'Brien, R. J., Mammen, A. L., Bernhardt, J., and Huganir, R. L. (1996) Characterization of multiple phosphorylation sites on the AMPA receptor GluR1 subunit. *Neuron* **16,** 1179-1188.

Rossi, P., Sola, E., Taglietti, V., Borchardt, T., Steigerwald, F., Utvik, J. K., Ottersen, O. P., Kohr, G., and D'Angelo, E. (2002) NMDA receptor 2 (NR2) C-terminal control of NR open probability regulates synaptic transmission and plasticity at a cerebellar synapse. *J. Neurosci.* **22,** 9687-9697.

Ruan, H. Z., Li, X. C., and Cai, W. Q. (1997) [Somatostatin inhibited pain modulation action of substance P in spinal cord]. *Sheng Li Xue Bao* **49,** 13-17.

Rubio, M. E. and Wenthold, R. J. (1997) Glutamate receptors are selectively targeted to postsynaptic sites in neurons. *Neuron* **18,** 939-950.

Ruda, M. A. (1982) Opiates and pain pathways: demonstration of enkephalin synapses on dorsal horn projection neurons. *Science* **215,** 1523-1525.

Ruscheweyh, R. and Sandkuhler, J. (2002) Role of kainate receptors in nociception. *Brain Res. Brain Res. Rev.* **40,** 215-222.

Rustioni, A. and Cuenod, M. (1982) Selective retrograde transport of D-aspartate in spinal interneurons and cortical neurons of rats. *Brain Res.* **236,** 143-155.

Rustioni, A. and Weinberg, R. J. (1989). The somatosensory system. In: Bjorklund, A., Hökfelt, T., Swanson, L. W. (Eds.), *Handbook of Chemical Neuroanatomy*, Vol. 7: Integrated System of the CNS, Part II. Amsterda: Elsevier, pp. 219-321.

Safferling, M., Tichelaar, W., Kummerle, G., Jouppila, A., Kuusinen, A., Keinanen, K., and Madden, D. R. (2001) First images of a glutamate receptor ion channel: oligomeric state and molecular dimensions of GluRB homomers. *Biochemistry* **40,** 13948-13953.

Sakamoto, H., Spike, R. C., and Todd, A. J. (1999) Neurons in laminae III and IV of the rat spinal cord with the neurokinin-1 receptor receive few contacts from unmyelinated primary afferents which do not contain substance P. *Neuroscience* **94,** 903-908.

Sakimura, K., Kutsuwada, T., Ito, I., Manabe, T., Takayama, C., Kushiya, E., Yagi, T., Aizawa, S., Inoue, Y., Sugiyama, H., and . (1995) Reduced hippocampal LTP and spatial learning in mice lacking NMDA receptor epsilon 1 subunit. *Nature* **373,** 151-155.

Sakurada, T., Wako, K., Sugiyama, A., Sakurada, C., Tan-No, K., and Kisara, K. (1998) Involvement of spinal NMDA receptors in capsaicin-induced nociception. *Pharmacol. Biochem. Behav.* **59,** 339-345.

Samarasinghe, S., Virgo, L., and de Belleroche, J. (1996) Distribution of the N-methyl-D-aspartate glutamate receptor subunit NR2A in control and amyotrophic lateral sclerosis spinal cord. *Brain Res.* **727,** 233-237.

Sandkühler, J. (2000) Learning and memory in pain pathways. *Pain* **88,** 113-118.

Sang, C. N., Hostetter, M. P., Gracely, R. H., Chappell, A. S., Schoepp, D. D., Lee, G., Whitcup, S., Caruso, R., and Max, M. B. (1998) AMPA/kainate antagonist LY293558 reduces capsaicin-evoked hyperalgesia but not pain in normal skin in humans. *Anesthesiology* **89,** 1060-1067.

Sanelli, T. R., Sopper, M. M., and Strong, M. J. (2004) Sequestration of nNOS in neurofilamentous aggregate bearing neurons in vitro leads to enhanced NMDA-mediated calcium influx. *Brain Res.* **1004,** 8-17.

Sassoe-Pognetto, M. and Ottersen, O. P. (2000) Organization of ionotropic glutamate receptors at dendrodendritic synapses in the rat olfactory bulb. *J. Neurosci.* **20,** 2192-2201.

Sassoe-Pognetto, M., Utvik, J. K., Camoletto, P., Watanabe, M., Stephenson, F. A., Bredt, D. S., and Ottersen, O. P. (2003) Organization of postsynaptic density proteins and glutamate receptors in axodendritic and dendrodendritic synapses of the rat olfactory bulb. *J. Comp. Neurol.* **463,** 237-248.

Sato, K., Kiyama, H., Park, H. T., and Tohyama, M. (1993) AMPA, KA and NMDA receptors are expressed in the rat DRG neurones. *Neuroreport* **4,** 1263-1265.

Senba, E., Yanaihara, C., Yanaihara, N., and Tohyama, M. (1988) Co-localization of substance P and Met-enkephalin-Arg6-Gly7-Leu8 in the intraspinal neurons of the rat, with special reference to the neurons in the substantia gelatinosa. *Brain Res.* **453,** 110-116.

Shaw, P. J., Williams, T. L., Slade, J. Y., Eggett, C. J., and Ince, P. G. (1999) Low expression of GluR2 AMPA receptor subunit protein by human motor neurons. *Neuroreport* **10,** 261-265.

Shen, S., Bian, J. T., Tian, J. B., and Han, J. S. (1996) [Frequency dependence of substance P release by electroacupuncture in rat spinal cord]. *Sheng Li Xue Bao* **48,** 89-93.

Shi, SR., Gu J., Taylor, C. R. (2000) *Antigen Retrieval Techniques: Immunohistochemistry and Molecular Morphology*, BioTechniques Books Publication, Eaton Publishing.

Shibata, T., Watanabe, M., Ichikawa, R., Inoue, Y., and Koyanagi, T. (1999) Different expressions of alpha-amino-3-hydroxy-5-methyl-4-isoxazole propionic acid and N-methyl-D-aspartate receptor subunit mRNAs between visceromotor and somatomotor neurons of the rat lumbosacral spinal cord. *J. Comp. Neurol.* **404,** 172-182.

Shigemoto, R., Ohishi, H., Nakanishi, S., and Mizuno, N. (1992) Expression of the mRNA for the rat NMDA receptor (NMDAR1) in the sensory and autonomic ganglion neurons. *Neurosci Lett.* **144,** 229-232.

Shigemoto, R. and Mizuno, N. (2000) Metabotropic glutamate receptors, In: *Glutamate* (eds: Ottersen, O. P.) 64-98.

Shiurba, R. (2001) Freeze-substitution: origins and applications. *Int. Rev. Cytol.* **206,** 45-96.

Silverman, J. D. and Kruger, L. (1990) Selective neuronal glycoconjugate expression in sensory and autonomic ganglia: relation of lectin reactivity to peptide and enzyme markers. *J. Neurocytol.* **19,** 789-801.

Simone, D. A., Sorkin, L. S., Oh, U., Chung, J. M., Owens, C., LaMotte, R. H., and Willis, W. D. (1991) Neurogenic hyperalgesia: central neural correlates in responses of spinothalamic tract neurons. *J. Neurophysiol.* **66,** 228-246.

Skerry, T. M. and Genever, P. G. (2001) Glutamate signalling in non-neuronal tissues. *Trends Pharmacol. Sci.* **22,** 174-181.

Sommer, B., Keinanen, K., Verdoorn, T. A., Wisden, W., Burnashev, N., Herb, A., Kohler, M., Takagi, T., Sakmann, B., and Seeburg, P. H. (1990) Flip and flop: a cell-specific functional switch in glutamate-operated channels of the CNS. *Science* **249,** 1580-1585.

Somogyi, P. and Takagi, H. (1982) A note on the use of picric acid-paraformaldehyde-glutaraldehyde fixative for correlated light and electron microscopic immunocytochemistry. *Neuroscience* **7,** 1779-1783.

Song, I. and Huganir, R. L. (2002) Regulation of AMPA receptors during synaptic plasticity. *Trends. Neurosci.* **25,** 578-588.

Song, P., Hu, J. Y., and Zhao, Z. Q. (2002) Spinal somatostatin SSTR2A receptors are preferentially up-regulated and involved in thermonociception but not mechanonociception. *Exp. Neurol.* **178,** 280-287.

Sorkin, L. S., McAdoo, D. J., and Willis, W. D. (1993) Raphe magnus stimulation-induced antinociception in the cat is associated with release of amino acids as well as serotonin in the lumbar dorsal horn. *Brain Res.* **618,** 95-108.

Sorkin, L. S., Yaksh, T. L., and Doom, C. M. (1999) Mechanical allodynia in rats is blocked by a Ca2+ permeable AMPA receptor antagonist. *Neuroreport* **10,** 3523-3526.

Sorkin, L. S., Yaksh, T. L., and Doom, C. M. (2001) Pain models display differential sensitivity to Ca2+-permeable non-NMDA glutamate receptor antagonists. *Anesthesiology* **95,** 965-973.

South, S. M., Kohno, T., Kaspar, B. K., Hegarty, D., Vissel, B., Drake, C. T., Ohata, M., Jenab, S., Sailer, A. W., Malkmus, S., Masuyama, T., Horner, P., Bogulavsky, J., Gage, F. H., Yaksh, T. L., Woolf, C. J., Heinemann, S. F., and Inturrisi, C. E. (2003) A conditional deletion of the NR1 subunit of the NMDA receptor in adult spinal cord dorsal horn reduces NMDA currents and injury-induced pain. *J. Neurosci.* **23,** 5031-5040.

Spike, R. C., Kerr, R., Maxwell, D. J., and Todd, A. J. (1998) GluR1 and GluR2/3 subunits of the AMPA-type glutamate receptor are associated with particular types of neurone in laminae I-III of the spinal dorsal horn of the rat. *Eur. J. Neurosci.* **10,** 324-333.

Spraggins, D. S., Turnbach, M. E., and Randich, A. (2001) Effects of glutamate receptor antagonists on spinal dorsal horn neurons during zymosan-induced inflammation in rats. *J. Pain* **2,** 12-24.

Sprengel, R., Suchanek, B., Amico, C., Brusa, R., Burnashev, N., Rozov, A., Hvalby, O., Jensen, V., Paulsen, O., Andersen, P., Kim, J. J., Thompson, R. F., Sun, W., Webster, L. C., Grant, S. G., Eilers, J., Konnerth, A., Li, J., McNamara, J. O., and Seeburg, P. H. (1998) Importance of the intracellular domain of NR2 subunits for NMDA receptor function in vivo. *Cell* **92,** 279-289.

Stanfa, L. C. and Dickenson, A. H. (1999) The role of non-N-methyl-D-aspartate ionotropic glutamate receptors in the spinal transmission of nociception in normal animals and animals with carrageenan inflammation. *Neuroscience* **93,** 1391-1398.

Stanfa, L. C., Hampton, D. W., and Dickenson, A. H. (2000) Role of Ca2+-permeable non-NMDA glutamate receptors in spinal nociceptive transmission. *Neuroreport* **11,** 3199-3202.

Stegenga, S. L. and Kalb, R. G. (2001) Developmental regulation of N-methyl-D-aspartate- and kainate-type glutamate receptor expression in the rat spinal cord. *Neuroscience* **105,** 499-507.

Stirling, J. W. and Graff, P. S. (1995) Antigen unmasking for immunoelectron microscopy: labeling is improved by treating with sodium ethoxide or sodium metaperiodate, then heating on retrieval medium. *J. Histochem. Cytochem.* **43,** 115-123.

Strong, M. J. (1999) Neurofilament metabolism in sporadic amyotrophic lateral sclerosis. *J. Neurol. Sci.* **169,** 170-177.

Strong, M. and Rosenfeld, J. (2003) Amyotrophic lateral sclerosis: a review of current concepts. *Amyotroph. Lateral Scler. Other Motor Neuron Disord.* **4,** 136-143.

Sucher, N. J., Awobuluyi, M., Choi, Y. B., and Lipton, S. A. (1996) NMDA receptors: from genes to channels. *Trends Pharmacol. Sci.* **17,** 348-355.

Tachibana, M., Wenthold, R. J., Morioka, H., and Petralia, R. S. (1994) Light and electron microscopic immunocytochemical localization of AMPA-selective glutamate receptors in the rat spinal cord. *J. Comp. Neurol.* **344,** 431-454.

Takamori, S., Rhee, J. S., Rosenmund, C., and Jahn, R. (2000) Identification of a vesicular glutamate transporter that defines a glutamatergic phenotype in neurons. *Nature* **407,** 189-194.

Takamori, S., Rhee, J. S., Rosenmund, C., and Jahn, R. (2001) Identification of differentiation-associated brain-specific phosphate transporter as a second vesicular glutamate transporter (VGLUT2). *J. Neurosci.* **21,** RC182.

Takamori, S., Malherbe, P., Broger, C., and Jahn, R. (2002) Molecular cloning and functional characterization of human vesicular glutamate transporter 3. *EMBO Rep.* **3,** 798-803.

Takumi, Y., Ramirez-Leon, V., Laake, P., Rinvik, E., and Ottersen, O. P. (1999) Different modes of expression of AMPA and NMDA receptors in hippocampal synapses. *Nat. Neurosci.* **2,** 618-624.

Taniguchi, K., Shinjo, K., Mizutani, M., Shimada, K., Ishikawa, T., Menniti, F. S., and Nagahisa, A. (1997) Antinociceptive activity of CP-101,606, an NMDA receptor NR2B subunit antagonist. *Br. J. Pharmacol.* **122,** 809-812.

Temkin, R., Lowe, D., Jensen, P., Hatt, H., and Smith, D. O. (1997) Expression of glutamate receptor subunits in alpha-motoneurons. *Brain Res. Mol. Brain Res.* **52,** 38-45.

Terman, G. W., Eastman, C. L., and Chavkin, C. (2001) Mu opiates inhibit long-term potentiation induction in the spinal cord slice. *J. Neurophysiol.* **85,** 485-494.

Todd, A. J. and Sullivan, A. C. (1990) Light microscope study of the coexistence of GABA-like and glycine-like immunoreactivities in the spinal cord of the rat. *J. Comp. Neurol.* **296,** 496-505.

Todd, A. J., Maxwell, D. J., and Brown, A. G. (1991) Relationships between hair-follicle afferent axons and glycine-immunoreactive profiles in cat spinal dorsal horn. *Brain Res.* **564,** 132-137.

Todd, A. J. and Spike, R. C. (1992a) Co-localization of Met-enkephalin and somatostatin in the spinal cord of the rat. *Neurosci Lett.* **145,** 71-74.

Todd, A. J., Spike, R. C., Russell, G., and Johnston, H. M. (1992b) Immunohistochemical evidence that Met-enkephalin and GABA coexist in some neurones in rat dorsal horn. *Brain Res.* **584,** 149-156.

Todd, A. J. and Spike, R. C. (1993) The localization of classical transmitters and neuropeptides within neurons in laminae I-III of the mammalian spinal dorsal horn. *Prog. Neurobiol.* **41,** 609-645.

Todd, A. J., Spike, R. C., Price, R. F., and Neilson, M. (1994) Immunocytochemical evidence that neurotensin is present in glutamatergic neurons in the superficial dorsal horn of the rat. *J. Neurosci.* **14,** 774-784.

Todd, A. J. (1996) GABA and glycine in synaptic glomeruli of the rat spinal dorsal horn. *Eur. J. Neurosci.* **8,** 2492-2498.

Todd, A. J., Spike, R. C., and Polgar, E. (1998) A quantitative study of neurons which express neurokinin-1 or somatostatin sst2a receptor in rat spinal dorsal horn. *Neuroscience* **85,** 459-473.

Todd, A. J. (2002) Anatomy of primary afferents and projection neurones in the rat spinal dorsal horn with particular emphasis on substance P and the neurokinin 1 receptor. *Exp. Physiol.* **87,** 245-249.

Todd, A. J., Hughes, D. I., Polgar, E., Nagy, G. G., Mackie, M., Ottersen, O. P., and Maxwell, D. J. (2003) The expression of vesicular glutamate transporters VGLUT1 and

VGLUT2 in neurochemically defined axonal populations in the rat spinal cord with emphasis on the dorsal horn. *Eur. J. Neurosci.* **17,** 13-27.

Tölle, T. R., Berthele, A., Zieglgansberger, W., Seeburg, P. H., and Wisden, W. (1993) The differential expression of 16 NMDA and non-NMDA receptor subunits in the rat spinal cord and in periaqueductal gray. *J. Neurosci.* **13,** 5009-5028.

Tölle, T. R., Berthele, A., Laurie, D. J., Seeburg, P. H., and Zieglgansberger, W. (1995a) Cellular and subcellular distribution of NMDAR1 splice variant mRNA in the rat lumbar spinal cord. *Eur J Neurosci* **7,** 1235-1244.

Tölle, T. R., Berthele, A., Zieglgansberger, W., Seeburg, P. H., and Wisden, W. (1995b) Flip and Flop variants of AMPA receptors in the rat lumbar spinal cord. *Eur. J. Neurosci.* **7,** 1414-1419.

Tsunoda, S., Sierralta, J., Sun, Y., Bodner, R., Suzuki, E., Becker, A., Socolich, M., and Zuker, C. S. (1997) A multivalent PDZ-domain protein assembles signalling complexes in a G-protein-coupled cascade. *Nature* **388,** 243-249.

Tung, A. S. and Yaksh, T. L. (1982) In vivo evidence for multiple opiate receptors mediating analgesia in the rat spinal cord. *Brain Res.* **247,** 75-83.

Turner, T. J. (1998) Calcium channels coupled to glutamate release. *Prog. Brain Res.* **116,** 3-14.

Urushitani, M., Nakamizo, T., Inoue, R., Sawada, H., Kihara, T., Honda, K., Akaike, A., and Shimohama, S. (2001) N-methyl-D-aspartate receptor-mediated mitochondrial Ca(2−) overload in acute excitotoxic motor neuron death: a mechanism distinct from chronic neurotoxicity after Ca(2+) influx. *J. Neurosci. Res.* **63,** 377-387.

Valtschanoff, J. G., Burette, A., Wenthold, R. J., and Weinberg, R. J. (1999) Expression of NR2 receptor subunit in rat somatic sensory cortex: synaptic distribution and colocalization with NR1 and PSD-95. *J. Comp. Neurol.* **410,** 599-611.

van Damme, P., Van Den, B. L., Van Houtte, E., Callewaert, G., and Robberecht, W. (2002) GluR2-dependent properties of AMPA receptors determine the selective vulnerability of motor neurons to excitotoxicity. *J. Neurophysiol.* **88,** 1279-1287.

Vandenberghe, W., Ihle, E. C., Patneau, D. K., Robberecht, W., and Brorson, J. R. (2000a) AMPA receptor current density, not desensitization, predicts selective motoneuron vulnerability. *J. Neurosci.* **20,** 7158-7166.

Vandenberghe, W., Robberecht, W., and Brorson, J. R. (2000b) AMPA receptor calcium permeability, GluR2 expression, and selective motoneuron vulnerability. *J. Neurosci.* **20,** 123-132.

Vandenberghe, W., Bindokas, V. P., Miller, R. J., Robberecht, W., and Brorson, J. R. (2001) Subcellular localization of calcium-permeable AMPA receptors in spinal motoneurons. *Eur. J. Neurosci.* **14,** 305-314.

van Den Bosch,. L. and Robberecht, W. (2000) Different receptors mediate motor neuron death induced by short and long exposures to excitotoxicity. *Brain Res. Bull.* **53,** 383-388.

van Lookeren, C. M., Oestreicher, A. B., van der Krift, T. P., Gispen, W. H., and Verkleij, A. J. (1991) Freeze-substitution and Lowicryl HM20 embedding of fixed rat brain: suitability for immunogold ultrastructural localization of neural antigens. *J. Histochem. Cytochem.* **39,** 1267-1279.

Varoqui, H., Schafer, M. K., Zhu, H., Weihe, E., and Erickson, J. D. (2002) Identification of the differentiation-associated Na+/PI transporter as a novel vesicular glutamate transporter expressed in a distinct set of glutamatergic synapses. *J. Neurosci.* **22,** 142-155.

Verhage, M., McMahon, H. T., Ghijsen, W. E., Boomsma, F., Scholten, G., Wiegant, V. M., and Nicholls, D. G. (1991) Differential release of amino acids, neuropeptides, and catecholamines from isolated nerve terminals. *Neuron* **6,** 517-524.

Verkhratsky, A., and Steinhauser, C. (2000) Ion channels in glial cells. *Brain Res. Rev.* **32,** 380-412.

Vicini, S., Wang, J. F., Li, J. H., Zhu, W. J., Wang, Y. H., Luo, J. H., Wolfe, B. B., and Grayson, D. R. (1998) Functional and pharmacological differences between recombinant N-methyl-D-aspartate receptors. *J. Neurophysiol.* **79,** 555-566.

Virgo, L. and de Belleroche, J. (1995) Induction of the immediate early gene c-jun in human spinal cord in amyotrophic lateral sclerosis with concomitant loss of NMDA receptor NR-1 and glycine transporter mRNA. *Brain Res.* **676,** 196-204.

Virgo, L., Samarasinghe, S., and de Belleroche, J. (1996) Analysis of AMPA receptor subunit mRNA expression in control and ALS spinal cord. *Neuroreport* **7,** 2507-2511.

Virgo, L., Dekkers, J., Mentis, G. Z., Navarrete, R., and de Belleroche, J. (2000) Changes in expression of NMDA receptor subunits in the rat lumbar spinal cord following neonatal nerve injury. *Neuropathol. Appl. Neurobiol.* **26,** 258-272.

Vissavajjhala, P., Janssen, W. G., Hu, Y., Gazzaley, A. H., Moran, T., Hof, P. R., and Morrison, J. H. (1996) Synaptic distribution of the AMPA-GluR2 subunit and its colocalization with calcium-binding proteins in rat cerebral cortex: an immunohistochemical study using a GluR2-specific monoclonal antibody. *Exp. Neurol.* **142,** 296-312.

Voitenko, N., Gerber, G., Youn, D., and Randic, M. (2004) Peripheral inflammation-induced increase of AMPA-mediated currents and Ca^{2+} transients in the presence of cyclothiazide in the rat substantia gelationosa neurons. *Cell Calcium* **35,** 461-469.

Wagey, R., Krieger, C., and Shaw, C. A. (1997) Abnormal dephosphorylation effect on NMDA receptor regulation in ALS spinal cord. *Neurobiol. Dis.* **4,** 350-355.

Walberg, F., Ottersen, O. P., and Rinvik, E. (1990) GABA, glycine, aspartate, glutamate and taurine in the vestibular nuclei: an immunocytochemical investigation in the cat. *Exp. Brain Res.* **79,** 547-563.

Wanaka, A., Shiotani, Y., Kiyama, H., Matsuyama, T., Kamada, T., Shiosaka, S., and Tohyama, M. (1987) Glutamate-like immunoreactive structures in primary sensory neurons in the rat detected by a specific antiserum against glutamate. *Exp. Brain Res.* **65,** 691-694.

Washburn, M. S., Numberger, M., Zhang, S., and Dingledine, R. (1997) Differential dependence on GluR2 expression of three characteristic features of AMPA receptors. *J. Neurosci.* **17,** 9393-9406.

Watanabe, M., Mishina, M., and Inoue, Y. (1994a) Distinct gene expression of the N-methyl-D-aspartate receptor channel subunit in peripheral neurons of the mouse sensory ganglia and adrenal gland. *Neurosci Lett.* **165,** 183-186.

Watanabe, M., Mishina, M., and Inoue, Y. (1994b) Distinct spatiotemporal distributions of the N-methyl-D-aspartate receptor channel subunit mRNAs in the mouse cervical cord. *J. Comp. Neurol.* **345,** 314-319.

Watanabe, M., Mishina, M., and Inoue, Y. (1994c) Distinct spatiotemporal expressions of five NMDA receptor channel subunit mRNAs in the cerebellum. *J. Comp. Neurol.* **343,** 513-519.

Watanabe, M., Fukaya, M., Sakimura, K., Manabe, T., Mishina, M., and Inoue, Y. (1998) Selective scarcity of NMDA receptor channel subunits in the stratum lucidum (mossy fibre-recipient layer) of the mouse hippocampal CA3 subfield. *Eur. J. Neurosci.* **10,** 478-487.

Wenthold, R. J., Petralia, R. S., Blahos, J., II, and Niedzielski, A. S. (1996) Evidence for multiple AMPA receptor complexes in hippocampal CA1/CA2 neurons. *J. Neurosci.* **16,** 1982-1989.

Williams, T. L., Day, N. C., Ince, P. G., Kamboj, R. K., and Shaw, P. J. (1997) Calcium-permeable alpha-amino-3-hydroxy-5-methyl-4-isoxazole propionic acid receptors: a molecular determinant of selective vulnerability in amyotrophic lateral sclerosis. *Ann. Neurol.* **42,** 200-207.

Willis, W. D. and Coggeshall, R. E. (1991) *Sensory Mechanisms of the Spinal Cord*, 2nd ed. New York: Plenum Press.

Willis, W. D. (2002) Long-term potentiation in spinothalamic neurons. *Brain Res. Brain Res. Rev.* **40,** 202-214.

Wimalawansa, S. J. (1996) Calcitonin gene-related peptide and its receptors: molecular genetics, physiology, pathophysiology, and therapeutic potentials. *Endocr. Rev.* **17,** 533-585.

Wong, H. K., Liu, X. B., Matos, M. F., Chan, S. F., Perez-Otano, I., Boysen, M., Cui, J., Nakanishi, N., Trimmer, J. S., Jones, E. G., Lipton, S. A., and Sucher, N. J. (2002) Temporal and regional expression of NMDA receptor subunit NR3A in the mammalian brain. *J. Comp. Neurol.* **450,** 303-317.

Woolf, C. J. (1996) Windup and central sensitization are not equivalent. *Pain* **66,** 105-108.

Woolf, C. J. and Costigan, M. (1999) Transcriptional and posttranslational plasticity and the generation of inflammatory pain. *Proc. Natl. Acad. Sci. U. S. A.* **96,** 7723-7730.

Yamada, K., Fukaya, M., Shimizu, H., Sakimura, K., and Watanabe, M. (2001) NMDA receptor subunits GluRepsilon1, GluRepsilon3 and GluRzeta1 are enriched at the mossy fibre-granule cell synapse in the adult mouse cerebellum. *Eur. J. Neurosci.* **13,** 2025-2036.

Yamamoto, T. and Yaksh, T. L. (1992a) Comparison of the antinociceptive effects of pre- and posttreatment with intrathecal morphine and MK801, an NMDA antagonist, on the formalin test in the rat. *Anesthesiology* **77,** 757-763.

Yamamoto, T. and Yaksh, T. L. (1992b) Studies on the spinal interaction of morphine and the NMDA antagonist MK-801 on the hyperesthesia observed in a rat model of sciatic mononeuropathy. *Neurosci. Lett.* **135,** 67-70.

Yashpal, K., Fisher, K., Chabot, J. G., and Coderre, T. J. (2001) Differential effects of NMDA and group I mGluR antagonists on both nociception and spinal cord protein kinase C translocation in the formalin test and a model of neuropathic pain in rats. *Pain* **94,** 17-29.

Yingcharoen, K., Rinvik, E., Storm-Mathisen, J., and Ottersen, O. P. (1989) GABA, glycine, glutamate, aspartate and taurine in the perihypoglossal nuclei: an immunocytochemical investigation in the cat with particular reference to the issue of amino acid colocalization. *Exp. Brain Res.* **78,** 345-357.

Yukhananov, R., Guan, J., and Crosby, G. (2002) Antisense oligonucleotides to N-methyl-D-aspartate receptor subunits attenuate formalin-induced nociception in the rat. *Brain Res.* **930,** 163-169.

Yung, K. K. (1998) Localization of glutamate receptors in dorsal horn of rat spinal cord. *Neuroreport* **9,** 1639-1644.

Zhang, X., Nicholas, A. P., and Hökfelt, T. (1993) Ultrastructural studies on peptides in the dorsal horn of the spinal cord--I. Co-existence of galanin with other peptides in primary afferents in normal rats. *Neuroscience* **57,** 365-384.

Zhang, R. X., Wang, H., Ruda, M., Iadarola, M. J., and Qiao, J. T. (1998) c-Fos expression in NMDA receptor-contained neurons in spinal cord in a rat model of inflammation: a double immunocytochemical study. *Brain. Res.* **795,** 282-286.

Zhang, X., Bao, L., Arvidsson, U., Elde, R., and Hökfelt, T. (1998) Localization and regulation of the delta-opioid receptor in dorsal root ganglia and spinal cord of the rat and monkey: evidence for association with the membrane of large dense-core vesicles. *Neuroscience* **82,** 1225-1242.

Zhang, X. X., Bunney, B. S., and Shi, W. X. (2000) Enhancement of NMDA-induced current by the putative NR2B selective antagonist ifenprodil. *Synapse* **37,** 56-63.

Zou, X., Lin, Q., and Willis, W. D. (2000) Enhanced phosphorylation of NMDA receptor 1 subunits in spinal cord dorsal horn and spinothalamic tract neurons after intradermal injection of capsaicin in rats. *J. Neurosci.* **20,** 6989-6997.

Zou, X., Lin, Q., and Willis, W. D. (2001) NMDA or non-NMDA receptor antagonists attenuate increased Fos expression in spinal dorsal horn GABAergic neurons after intradermal injection of capsaicin in rats. *Neuroscience* **106,** 171-182.

Zou, X., Lin, Q., and Willis, W. D. (2002) Role of protein kinase A in phosphorylation of NMDA receptor 1 subunits in dorsal horn and spinothalamic tract neurons after intradermal injection of capsaicin in rats. *Neuroscience* **115,** 775-786.

Zukin, R. S. and Bennett, M. V. (1995) Alternatively spliced isoforms of the NMDARI receptor subunit. *Trends Neurosci.* **18,** 306-313.

Appendix

0.1 M PHOSPHATE BUFFER (PB)

- NaH_2PO_4 x (2 H_2O) 37.44 g in 1200 ml H_2O → Solution A
- Na_2HPO_4 84.9 g in 3000 ml H_2O → Solution B

Mix 1120 ml of Solution A and 2880 ml of solution B.

Adjust pH to 7.4 with HCl or NaOH.

Add 3000 ml distilled water.

PHOSPHATE BUFFER WITH 0.3 M SALINE (PBS)

- 0.2 M PB 200 ml
- NaCl 72 g
- distilled water 3800 ml

TRIS-BUFFERED SALINE WITH TRITON X-100 (TBST)

- 0.05 M Tris pH 7.4 100 ml
- distilled water 900 ml
- NaCl 3-9 g
- Triton X-100 1 g

MAMMALIAN RINGER (MR)

- NaCl 45 g
- KCl 2 g
- $CaCl_2$ 1,25 g
- $MgCl_2$ 0.025 g
- $NaHCO_3$ 2.5 g
- NaH_2PO_4 0.25 g
- glucose 5 g
- distilled water 5000 ml

0.2 M BICARBONATE BUFFER (pH 10.5)

- $NaHCO_3$ 16.8 g
- 0.1 M NaOH 175 ml
- distilled water make up to 1000 ml

02. M SODIUM ACETATE BUFFER (pH 6.0)

- sodium acetate 16.4 g
- 0.2 M acetic acid 3 ml
- distilled water make up to 1000 ml

URANYL ACETATE FOR CONTRASTING

- saturated solution of uranyl acetate in ultra pure water

LEAD ACETATE FOR CONTRASTING

- lead acetate 39 g
- distilled water 100 ml → saturated lead acetate

- saturated lead acetate 100 ml
- ammonium acetate 18.5 g

LEAD CITRATE FOR CONTRASTING

- lead nitrate 1.33 g
- sodium citrate 1.76 g
- distilled water 30 ml
- 1 M NaOH 8 ml
- distilled water make up to 50 ml